The Diurnal Cycle of Air Pollution In the Kathmandu Valley, Nepal

by

Arnico K. Panday

A.B. in Environmental Science and Public Policy
Harvard University, 1997

M.S. at the Institute for Environmental Studies
University of Wisconsin – Madison, 1999

Submitted to the
Department of Earth, Atmospheric and Planetary Sciences
in partial fulfillment of the requirements
for the degree of

Doctor of Science in Atmospheric Science

at the
Massachusetts Institute of Technology
June, 2006

Signature of the Author: _____
Department of Earth, Atmospheric, and Planetary Sciences
May 5, 2006

Certified by: _____
Ronald Prinn
TEPCO Professor of Atmospheric Chemistry
Thesis Supervisor

Accepted by: _____
Maria Zuber
Head, Department of Earth, Atmospheric, and Planetary Sciences

THE DIURNAL CYCLE OF AIR POLLUTION IN THE KATHMANDU VALLEY, NEPAL

by Arnico K. Panday

Submitted to the Department of Earth, Atmospheric and Planetary Sciences
on May 5, 2006, in Partial Fulfillment of the Requirements for the Degree of
Doctor of Science in Atmospheric Science

ABSTRACT

This dissertation describes the most comprehensive study to date of the diurnal cycle of air pollution in the Kathmandu Valley, Nepal – a bowl-shaped mountain valley of two million people with a growing air pollution problem but little past research. Field measurements and computer simulations were used to study the interplay of emissions and ventilation.

From September 2004 through June 2005, CO (carbon monoxide), ozone, PM_{10} (particles smaller than 10 micrometers), wind speed and direction, solar radiation, temperature, and humidity were continuously measured east of Kathmandu. Sensors towers and mountains measured the diurnal cycle of the vertical temperature structure and stability. A sodar measured the mixed layer height and upper-level winds. Bag sampling provided the diurnal cycle of CO on mountains, passes and around the valley. Winds were measured on a mountain pass and ozone on a mountaintop. Patterns of air pollution and meteorology in the valley showed remarkable day-to-day similarity, with daily twin peaks of CO and PM_{10}, a noon ozone maximum, afternoon westerly winds, and a stagnant cold pool at night. On mountaintops at night, ozone remained high, while CO dropped to regional background levels.

The meso-scale meteorological model MM5 was adapted to the Kathmandu Valley for days in February and May 2005. It was able to capture the essential features of the valley's meteorology and was used to address three specific questions: The break-up of the valley's temperature inversion was found to be dominated in February by up-slope winds on the valley rim, plus subsidence over the valley center; in May surface heating of the valley bottom also played a major role. The pathways of pollutant transport out of the valley were found to be up the valley rim slopes in the morning, but out the eastern and southern passes in the afternoons. At night pollutants remained within the valley except

near the river outlet. They were lifted off the ground at night and re-circulated in the morning.

The eulerian chemistry transport model CAMx, was used in tracer mode, with MM5 meteorology to simulate the emission, transport and removal of CO from the Kathmandu Valley. The simulations were limited by the accuracy of Kathmandu's emissions inventory, especially the spatial distribution of emissions.

Thesis Supervisor: Ronald G. Prinn
Title: TEPCO Professor of Atmospheric Chemistry

CONTENTS

ACKNOWLEDGEMENTS

First and foremost, I would like to thank my advisor Ron Prinn for making this dissertation possible. Ron you have gone beyond my wildest hopes in providing financial and logistical support for an ambitious research project, in providing me with the right mix of patience and guidance to maximize learning, and in providing me with understanding, flexibility and trust that made it possible to pursue graduate studies while navigating a roller-coaster of unexpected events during the past seven years.

I would like to thank my committee members Steve Wofsy, Christoph Schär, Greg McRae and Mario Molina for guiding me during the past four and a half years. I would like to extend a special thank you to Christoph for hosting me in his group and helping me get started with meso-scale modeling, to Steve for detailed advice about instrumentation and field measurement set-up, and to Greg for many thought provoking conversations. I would like to thank Karl Schroff at ETH Zürich for lending me two temperature loggers. The planning of the field project benefited greatly from face-to-face conversations with Bill Munger at Harvard, Johannes Stähelin at ETH Zürich, André Prévôt and Joseph Dommen at the Paul Scherrer Institut inVilligen, Valentin Simeonov and Erika Zárate at EPF Lausanne, Ram Shrestha and Kim Oanh at AIT Bangkok, as well as from correspondence with Joseph Egger at the University of Munich, Edward Hindman at City College of New York, and C. David Whiteman at Pacific Northwest National Laboratory.

The field research in Kathmandu could not have happened without the assistance of several key individuals, and it benefited from the goodwill of countless more. Professor Ram Regmi at Purbanchal University made it his mission to have me succeed. He convinced the administration of his university to write countless letters requesting assistance from various government offices. Professor Regmi also helped me find and evaluate instrument sites, introduced me to key people at Tribhuvan University and Nepal Television, and kindly provided me with his unpublished CO emissions inventory, thereby saving me months of labor.

I would like to thank the entire management and staff of the Hyatt Regency Hotel in Kathmandu, and especially Mr. Suman Shrestha and the engineering department, for letting me use their facilities to set up the main laboratory in Kathmandu, and for providing me with any assistance I could ask for. I would like to thank the management, staff, and students of CTEVT Sano Thimi for allowing me to install the sodar on their roof, and for putting up with

its noise for months. I would like to thank the engineering department at Nepal Television for making it possible to install temperature sensors on the NTV Metro tower. Similarly I would like to thank the management and staff at Dharahara tower, Hattiban Resort, Hotel Viewpoint in Nagarkot, and Pullahari Monastery for making it possible to use their facilities to collect bag samples and install temperature sensors. Finally I would like to thank the soldiers guarding Bhimdhunga Pass for the opportunity to install a weather station and collect air samples within a restricted area.

I have much to thank my assistants in Kathmandu. Raju Gharti made sure the laboratory instruments were running every morning, designed and wired a back-up power supply system for the sodar, and managed the transportation logistics for bag sampling. Ajay Rana downloaded and maintained the data in my absence and handled food and camping logistics for the bag sampling. Raju and Ajay also took care of much of the bag sample analysis and bag flushing between bag sampling campaigns. Kabindra Shakya helped calibrate the CO instrument in my absence, and arranged permission letters from the Ministry of Population and Environment.

I would like to thank Professor Kedar Rijal and his colleagues at Tribhuvan University's Central Department of Environmental Science for making it possible to work with his students. Naresh Neupane, Khadak Singh Mahata, Avishesh Neupane, Raviram Pokharel, Santosh Gaire as well as several of their classmates enthusiastically participated in 24 hour bag sampling expeditions with contagious humor and untiring enthusiasm to learn.

At MIT I would like to extend a special thank you to my current officemates: to Elke Hodson for her readiness to listen and give advice, for joining me in the January 2003 field campaign in Nepal, for the long distance administrative and equipment help, and for feedback on dissertation drafts; and to Matthew Alvarado for his ever cheerful presence in the office, and for the mega-effort of packing and shipping my instrumentation to Nepal. I would also like to thank past officemates for their friendship, inspiration, and encouragement: Donnan Steele, Donald Lucas, Annica Ekman, Vallerio Luccarini, and Kazuyuki Saito. Other past and current students and researchers in the department deserving thanks include Gary Kleiman and Stephanie Shaw for teaching me the necessary laboratory skills, Ben de Foy for helping me get started with MM5, Jason Cohen for helping me get started with CAMx, Chien Wang for access to and emergency help with the computer cluster in 54-1325, and Chris Forest for providing access to the computer cluster in Building E40. Other members of the research group provided valuable feedback and advice over the years. I would also like to particularly thank Frances

Goldstein, Leontyne Bynoe, Gwendolyn Wong, Veronica Lupampa, Rosemary Hanlon, Mark Pendleton, Anne Slinn, Carol Sprague, Vicky McKenna, Lisa McFarren and Mary Elliff for administrative assistance, encouragement and good wishes over the years. At MIT Medical, I would like to thank Simon Lejeune and Para Ambardar for making sure that I recovered quickly from a depression.

I would like to thank my friends who filled the year of field research in Nepal with fun and learning: Swarnim Waglé, Manju Karki, Pradeep Paudel, Srijana Sapkota, and Retika Rajbhandari frequently visited me in the lab, taught me Nepali history and politics, kept me in good spirits, accompanied me on data-collection visits to temperature loggers. In Singapore I would like to thank Irving Johnson and Felix Chang for emergency help with data recovery from a damaged laptop hard drive.

I would like to convey special thanks and hugs to my wife Prista Ratanapruck for her unyielding support over the past seven years, for always believing in me and encouraging me, for enduring personal sacrifices and separations so that I could pursue my research, and for making sure that I learned more about the world beyond my thesis than I ever expected. I would like to thank my parents and sister for their best wishes. I would like to thank my mom, Rosmarie Panday-Schaffner, for her continuous support and for her making sure that I always had the latest travel advisories while navigating Kathmandu's rapidly changing situation. I would like to thank my dad Krishnakumar Panday for sparking my enthusiasm for field measurements by taking me along on his agronomy dissertation research travels while I was still in elementary school, teaching me about temperature, humidity, sensors, and strip-chart recorders.

My doctoral studies and dissertation research were supported by an MIT Presidential Fellowship, the Martin Fellowship for Sustainability, a pilot research project grant from the Alliance for Global Sustainability, the PAOC Houghton Fund, the TEPCO Chair account, NSF Grant ATM-0120468 to MIT, NASA grants NAG5-12099 and NAG5-12669 to MIT, as well as by federal and industrial sponsors of the MIT Joint Program on the Science and Policy of Global Change.

CHAPTER 1: DISSERTATION INTRODUCTION

1.1 Chapter Introduction

Mountains influence the accumulation of air pollution in nearby cities. They block or reroute prevailing winds, alter the atmosphere's thermal structure, and create local wind systems. Mountains also create large changes in local meteorology over short distances [*Lang and Barros*, 2002]. In recent years, extensive research has been carried out in several cities where air pollution is influenced by nearby or surrounding mountains, including in Los Angeles, Mexico City, Phoenix, and Santiago de Chile. In each city the accumulation and dispersion of pollutants was found to be influenced by a complex and time-varying interplay of local and regional winds with spatial and temporal patterns of emissions. Predicting how the topography influences air pollution in a new place requires detailed understanding of the specifics of the place.

The Kathmandu Valley in Nepal is a rapidly urbanizing mountain basin in the Himalayan foothills that is experiencing a growing air pollution problem, but has seen scant past research. This dissertation presents the results of multi-month *in situ* chemical and meteorological field measurements in the Kathmandu Valley, and of meteorological and transport modeling, which focused on studying carbon monoxide (CO) as a tracer of urban emissions. The overall goal guiding the research was to understand how meteorology and emission patterns interact to determine the concentration of air pollutants in the valley over time, exploring the causes of observed diurnal pattern of pollutants. The dissertation achieves this by interpreting new field data and using meso-scale modeling to study in detail the processes responsible for the observed daily twin peaks of CO and PM_{10}, the growth of the mixed layer in the morning, the pathways of pollutant transport out of the Kathmandu Valley, and the causes of a night-time minimum in CO, and the sensitivity of ambient CO to changes in emissions.

Chapter 2 describes the methodology and the field set up of the measurement campaign carried out in Kathmandu from September 2004 through June 2005. Chapter 3 presents

the results of the field measurements. Discussing these results, Chapter 4, introduces research questions that arise from the data, followed by hypotheses and ways to address the questions with modeling. Chapter 5 describes meso-scale meteorological modeling using the MM5 model, validates MM5 results with field observations, and then uses the model results to address the specific questions raised in Chapter 4. Chapter 6 describes the CAMx eulerian chemistry transport model that that was used in tracer mode, with MM5 meteorology, to simulated observed CO concentrations in the Kathmandu Valley. The chapter also describes the available emissions inventory and its uncertainties. Finally, Chapter 7 concludes the dissertation. The rest of Chapter 1 is organized as follows: Section 1.2 describes why the Kathmandu Valley was chosen as a study site, while introducing key features of the valley. Section 1.4 reviews the literature of past research in the Kathmandu Valley. Section 1.5 explains the decision to focus on carbon monoxide.

1.2 Why Study the Kathmandu Valley?

The Kathmandu Valley provides a case study of urban air pollution in a mountainous basin of a developing country. Kathmandu shares features with many other inadequately understood cities in developing countries. These include its subtropical location and vegetation, large amounts of biomass combustion, a poorly maintained vehicle fleet, and a monsoon-induced seasonal cycle in aerosol loads. Recent decades have seen much progress in the scientific understanding and modeling capability of ozone and other components of urban air pollution in mid-latitude regions in high-income countries. For example, six different models in use today are able to reproduce observed ozone peaks in Los Angeles to within a few percentage points [*Russell and Dennis*, 2000]; air pollution research in conditions found in developing countries lags far behind.

Meanwhile, most past research on air pollution problems in complex terrain has focused upon a small number of places with large data sets: Los Angeles [*Harley et al.*, 1993; *Jacobson*, 1998; *Lee et al.*, 2003a; *Lu and Turco*, 1996; *McRae et al.*, 1982; *Milford et al.*, 1989; *Moore et al.*, 1991; *Mulholland and Seinfeld*, 1995; *Qin et al.*, 2004; *Sillman et*

al., 1997; *Ulrickson*, 1990; *Ulrickson and Mass*, 1990], Mexico City [*Baumgardner et al.*, 2000; *Bossert*, 1997; *Doran et al.*, 1998; *Fernandez-Bremauntz and Ashmore*, 1995; *Molina and Molina*, 2002; *Raga et al.*, 2001; *Whiteman et al.*, 2000b], Phoenix [*Berkowitz et al.*, 2005; *Doran et al.*, 2003; *Fast et al.*, 2000; *Fernando et al.*, 2001; *Idso et al.*, 2002; *Kleinman et al.*, 2003; *Lee et al.*, 2003b; *Shaw et al.*, 2005], and Santiago de Chile [*Chen et al.*, 1999; *Horvath et al.*, 1997; *Jorquera et al.*, 1998; *Morel et al.*, 1999; *Perez and Trier*, 2001; *Rappenglück et al.*, 2000; *Rappenglück et al.*, 2005; *Romero et al.*, 1999; *Schmitz*, 2005; *Silva and Quiroz*, 2003]., as well as the Rhine Valley, the Swiss Plateau, Alps, and northern Italy [*Baumbach and Vogt*, 1999; *Dommen et al.*, 1999; *Frioud et al.*, 2003; *Furger et al.*, 2000; *Henne et al.*, 2004; *Kalthoff et al.*, 2000; *Martilli and Graziani*, 1998; *Pachart et al.*, 1999; *Prévôt*, 1994; *Prévôt et al.*, 2000a; *Prévôt et al.*, 2000b; *Prévôt et al.*, 1997; *Röösli et al.*, 2001; *Seibert et al.*, 1998; *Staehelin et al.*, 2001; *Staffelbach et al.*, 1997]. Large numbers of specialists, using data from networks of expensive instruments, along with sophisticated computer models, have succeeded in greatly improving the scientific understanding of the interplay among various factors that control air quality in these well studied places. Much less is known about the processes controlling air pollutants in mountain regions in developing countries [*Lal*, 2000], especially ones in mountain regions where the shape of the topography has strong influences. In fact, during the planning stages of the research described in this dissertation, it was determined that without local field data, theory and findings from elsewhere would not adequately be able to explain the diurnal cycle of air pollution in the complex situation of the Kathmandu Valley.

Not only do cities in developing countries have emissions mixtures that are different from those in more affluent cities, but resources constraints severely limit the scientific understanding of their air pollution problems. There are little past data, few local experts, and limited infrastructure to carry out measurements. For example, in Kathmandu, forecasts at the Department of Hydrology and Meteorology's weather forecasting office are still done by hand-drawing geopotential height contours onto large charts [*Rosoff*, 2003]. Cities in developing countries also often do not have access to effective policy: the systems of translating science into policy and regulations tend to be ineffective, few

resources are available for enforcement, pollution reduction competes for money with other urgent needs, and the public usually has few means of reducing its exposure to pollution. To give one example, the only routine measurements carried out in Kathmandu prior to the work described in this thesis (24-hour average measurements of particles smaller than 10 microns (PM_{10}) at six sites) does not tell anything about the diurnal variations of pollution in the valley. As this dissertation will show, the timing of emissions and the locations where they take place are both crucial in determining the peak concentrations to which the pollutants will rise in populated areas surrounded by mountains. To understand the spatial and temporal dynamics of air pollution in a city, especially one surrounded by mountains, and to create the scientific knowledge necessary to effectively address its air pollution problem, it is important to gather data of high temporal and spatial resolution. The field measurements described in this dissertation are significant not only because of the logistical, bureaucratic, and security complications that had to be overcome to make them possible, but also because they allow the verification of numerous theoretical modeling investigations in the future, and because they provide an extensive new dataset in a place that urgently needs such data – a place where there is a real chance that the results can have a significant impact on the health of two million people.

The Kathmandu Valley is located in the Middle Hills of the Nepal Himalaya, between the Ganges Plains and the peaks of the High Himalaya which line the southern edge of the Tibetan Plateau. It is thus embedded in extremely complex terrain, whose effects on atmospheric circulation and pollution transport are hard to predict. It is also located between the two most populous countries in the world, India and China, which are projected to play increasingly large roles in the global budget of greenhouse gases and air pollutants [*Brasseur et al.*, 1998].

Geographically Kathmandu shares many similarities with Mexico City. Both are rapidly growing capital cities in flat basins that are surrounded by tall mountains, but are connected via passes to lower-elevation valleys nearby. Both basins experience temperature inversions that restrict the ventilation of locally emitted pollutants from the

cities. The transportation systems in both cities have a strong reliance on buses, para-transit vehicles and taxis. However there are also significant differences. As shown in Table 1.1, the Kathmandu Valley is an order of magnitude smaller in both area and population. It has no rail-based public transportation alternative. Compared to Mexico City, it sits at a lower elevation, lies further north, and is situated in a basin that is more completely enclosed by mountains. The Kathmandu Valley is influenced by the South Asian monsoon, with a three-month long annual wet season. Air pollution in the Kathmandu Valley also has not received as much international media attention as it has in Mexico City. In recent years the Massachusetts Institute of Technology has led a major interdisciplinary collaborative air pollution research project in Mexico City; a study of the Kathmandu Valley thus provides interesting comparisons.

	Kathmandu Valley	**Valley of Mexico City**
Latitude	27º 43' N	19º 25' N
Area of flat basin floor	340 km^2	5000 km^2
Approximate Population	2 million	19 million
Altitude of basin floor	~ 1300 m.a.s.l.	~ 2240 m.a.s.l.
Average basin depth	~ 600-800 m	800-1000 m
Elevation of highest peak above basin floor	~ 1565 m	~ 3212 m

Table 1.1: Comparison of Kathmandu [various sources] and Mexico City [*Molina and Molina*, 2002].

1.3 The Kathmandu Valley's Geography, Climate, and Meteorology

The Kathmandu valley is an enclosed basin with a watershed area of about 660 km^2. A former lake bed, the flat basin floor at an altitude of 1300 m has an area of about 340 km^2 [*NESS*, 1999]. It is located between 27°36' and 27°48' North, between 85°12' and 85°31' East. No river flows into the valley; the only surface run-off is from the streams originating at the valley rim. It is surrounded by mountains that are 1900-2800 meters tall, except for a narrow winding outlet of the Bagmati River towards the south, three mountain passes of about 1500 m altitude each on the west side, and two more on the east side. Although there are valleys immediately east and southwest of the Kathmandu Valley's rim, which sit at a higher elevation than the Kathmandu Valley floor, most of the terrain beyond the valley rim is significantly lower. Thus the Kathmandu Valley can

be pictured not just as a bowl-shaped depression, but as an elevated basin, a plateau with a rim. It is commonly referred to as the Kathmandu "Valley"; however, its circular shape and flat center make the word "basin" a more accurate descriptor. The dissertation text refers to it as the Kathmandu Valley when identifying it by name, but uses the word basin when reference to its shape is important. Figure 1.1 introduces key geographical features of the Kathmandu Valley by showing composites of satellite imagery and digital elevation data plotted using Google Earth®. The following labels are used throughout the images:

Cities (red labels):

Label	Name	Population (approx.)
K	Kathmandu	1,050,000
L	Lalitpur	260,000
B	Bhaktapur	110,000
T	Thimi	60,000
D	Dhulikhel-Banepa	30,000
P	Panauti	30,000

Note that an additional half a million people live within the valley, but outside of the city municipalities.

Peaks and Ridges (orange labels):

Label	Name	Altitude
hb	Hattiban ridge	1800-1900 m
cg	Chandragiri Peak	2561m
dc	Dahachok Peak	1885 m
nj	Nagarjun Peak	2095 m
kk	Kakani Ridge	2066 m
sp	Shivapuri Peak	2725 m
nk	Nagarkot Peak	2166 m
pc	Phulchoki Peak	2765 m

Passes and Outlets (yellow labels):

Label	Name	Altitude
nd	Nagdhunga Pass	1480 m
bd	Bhimdhunga Pass	1500 m
mk	Mudku Pass	1480 m
na	Nala Pass	1530 m
Sa	Sanga Pass	1530 m
Bv	Bagmati Valley outflow	< 1250 m

The top image shows a vertical view, while the bottom imageshows oblique views from the south showing the Bagmati outlet valley in the foreground, and the Tibetan Plateau in the background.

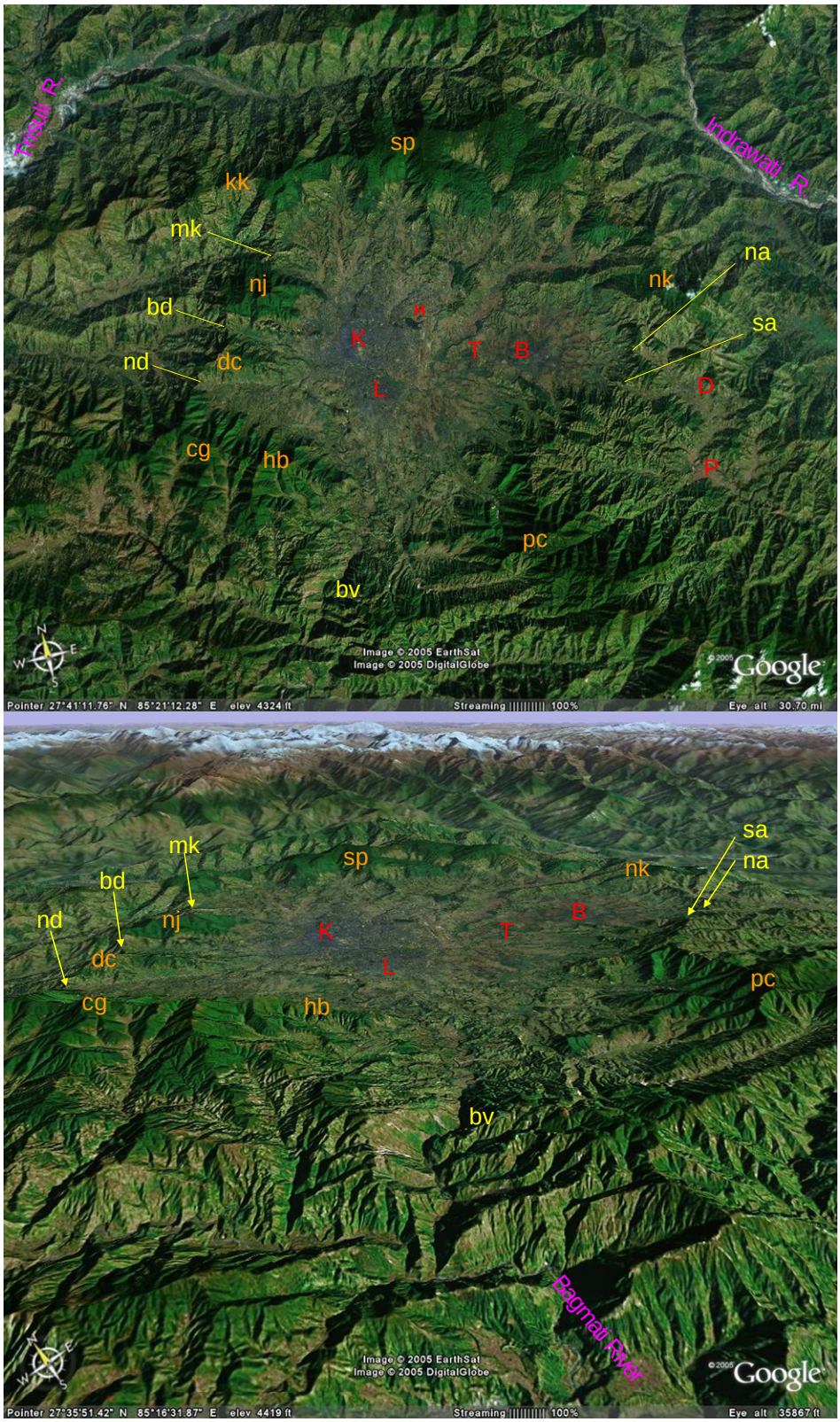

Figure 1.1: The Kathmandu Valley from space (above) and from the south (below) :

The climate of the Kathmandu Valley is influenced by a number of factors. The South Asian monsoon strongly affects precipitation and wind direction. The valley receives more than 80% of its annual rainfall during the summer monsoon, from mid-June through mid-September [*NESS*, 1999]. This is followed by a clear, sunny fall, a dry, cold winter, and warm, dry spring and early summer. The annual average temperature in the valley is 18.1°C, with a July-August maximum monthly average of 23.8°C and a January minimum monthly average of 9.9°C [*Sharma*, 1997]. The annual temperature range is from around -2º C in January mornings to 34º C in May afternoons. During non-monsoon months the valley is often cloud-free, allowing large daytime heating and nighttime cooling that gives it a diurnal temperature range of around 15º C [*NESS*, 1999].

During the winter, the Kathmandu Valley is dry, dusty, and cold enough to require residential heating. A strong temperature inversion isolates the basin bottom air from surrounding air masses, with visibly heavy pollution build-up near the ground. During spring, the Kathmandu Valley is down-wind of the deserts in western India, Pakistan and Iran. Occasionally dust storms in these places blanket the Kathmandu alley for weeks in fine layers of dust. No such dust episode was recorded during Spring 2005. The amount of dust received from the deserts increases as one goes west within Nepal [*Shrestha et al.*, 1997]. Spring is the driest time of the year, with frequent forest and brush fires on the surrounding hills. Monsoon rains vary by location even within the basin. The basin center receives less rainfall than its edges. Annual rainfall varies between about 1.22 meters at Khumaltar near the valley center, to 2.74 meters at Kakani, on the northern valley rim. [*Sharma*, 1997]. At the airport, just 3 km north of Khumaltar the annual rainfall is 1.38 meters, at Godavari, at the base of Mt. Phulchoki it is 1.87 meters, and at Thankot, near the western end of the basin it is 1.99 meters [*Sharma*, 1997].

During the summer monsoon the synoptic winds blow from the southeast, from the Bay of Bengal, passing over Bangladesh, West Bengal and Bihar. At this time there is a strong low pressure over India, and the ITCZ is shifted far north in this region of the world. In contrast, during the rest of the year, Nepal is more influenced by mid-latitude synoptic conditions marked by strong upper-level westerly winds. Often the midlatitude

jet-stream travels along the southern edge of the Tibetan Plateau, with mean wind speeds at 300 mb of 43 m s^{-1} [*Moore*, 2004]. During the winter seasons low pressure systems propagate eastwards from the Caspian Sea region 3-5 times a month, often bringing snow to higher mountains [*Rao*, 2003].

1.4 Existing Data and Past Research in the Kathmandu Valley.

The next few pages summarize the existing data and past research activities around the Kathmandu Valley, focusing first upon meteorology, and then upon air pollution. The Department of Hydrology and Meteorology maintains four surface weather stations are within the Kathmandu Valley, and two on the valley rim [*Shrestha et al.*, 1999]. Very little upper air meteorological data is available for the Kathmandu Valley. A currently inoperable radiosonde launch station still sits at the airport, but its only soundings took place in 1978-1979. The data quality was poor. Figure 1.2 contains all the 1978-1979 temperature data points from all radiosonde launches in Kathmandu during the seasons shown.

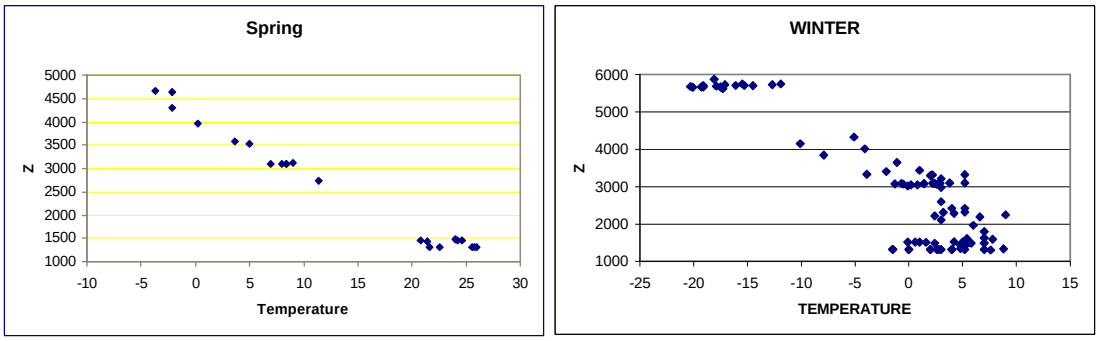

Figure 1.2: Combined plot of all temperature data available from radiosondes launches in 1978-79.

Visual observations of the Kathmandu sky [*Hindman*, 1999] showed frequent afternoon cumulus clouds over the valley center in October, with soaring birds underneath the clouds indicating rising air.

Wind speed and direction are recorded every hour at the airport; the surface wind speeds have been found to be less than 1 m/s about 70% of the time. Nepal Environmental and Scientific Services (NESS) did a field study [*NESS*, 1999] of the general surface wind patterns during the dry season by moving a single anemometer around the southern half of the valley. During the nights and early mornings, the conditions were generally calm. In the late morning there was a south-easterly wind, usually reaching 2 m/s, but as fast as 5-7 m/s in March through May. Progressing into the afternoon, the wind rotated, through the south, and southwesterly directions to finally become westerly. Wind speeds were generally around 5 m/s at 2 pm, but at times were as high as 15 m/s in late Spring. The change from winter to spring was marked by increases in both daytime temperature and wind speed [*NESS*, 1999].

Visibility is often restricted during the winter months by fog that covers the basin bottom until 10 or 11 am [*Sharma*, 1997]. Hourly observations of visibility made at the airport are available since 1969 [*Larssen et al.*, 1997]. In recent decades winter fog has increased and visibility has decreased. *Larssen et al.* [1997] report that the average annual number of foggy mornings between November and February recorded at the airport has increased from 40 to 60 between 1969 and 1993, and that the number of days in January with greater than 8 km visibility at 11 a.m. had dropped from 23 in 1969 to 1 in 1993. The number of days in January with greater than 8 km visibility at noon shrank from 25 in 1970 to 5 in 1993. [*Larssen et al.*, 1997]. This is illustrated in Figure 1.3.

The number of days per year with fog at 9 am increased from around 40 in 1969 to more than 60 in the early 1990s. The number of days with good visibility at noon has remained high from March through October. Starting in the early- to mid- 1980s, visibility has been declining during November through February, with the largest decrease taking place in December and January [*Larssen et al.*, 1997]. The authors attribute the decrease in visibility to the increased concentration of hygroscopic aerosols in the valley air, including both sulfate and organic aerosols. In southern Nepal northern India, a large increase in foggy days has been recorded in recent years [*Lal*, 2002].

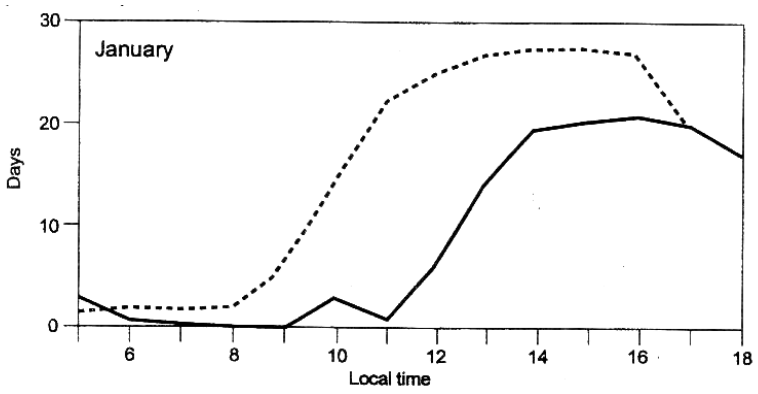

Figure 1.3: Number of January days with visibility exceeding 8 km at specific times of day. (dashed = 1969, solid = 1993). From [*Larssen et al.*, 1997].

Elsewhere in Nepal, a small number of more intensive field campaigns have tried to quantify meteorological phenomena in greater detail. In September and October 1998, a team from the University of Munich measured vertical profiles of diurnal winds in the Kali Gandaki Valley, 200 km northwest of Kathmandu [*Egger et al.*, 2000]. Using double theodolites to track ascending helium-filled balloons at a dozen locations along the valley, they collected wind data in the valley of a river that originates on the Tibetan Plateau and cuts through the Himalaya through the deepest gorge in the World (6 km depth) to the Middle Hills of Nepal and on to the Ganges Plains. They confirmed the anecdotal findings of very strong (15-20 m/s) daytime up-valley winds and weak nighttime drainage winds. Their 1998 field research formed the basis for a meso-scale modeling study using MM5 [*Zängl et al.*, 2001], as well as a second field study in 2001 that used remotely piloted aircraft to conduct vertical soundings [*Egger et al.*, 2002]. They found that the strong up-valley winds were generated by heating of the arid Mustang basin at the upper end of the valley, and that these winds were confined within a neutrally stratified turbulent layer topped by stable layers.

In 1999-2001 the onset of the Summer monsoon in Nepal was studied with a network of 20 automated weather stations on the ridges flanking the Marsyangdi Valley, 140 km west of Kathmandu [*Barros and Lang*, 2003; *Gehrman*, 2001; *Lang and Barros*, 2002]. In June 2001, radiosondes were launched five times a day from two sites west of Kathmandu as part of the same study [*Barros and Lang*, 2003]. Here too the daytime up-

slope/up-valley winds were stronger than the nighttime down-slope/down-valley winds. The authors found that the monsoon onset coincided with a gradual increase in total column moisture and convective instability, and found that the diurnal cycles of moisture and instability supported the observations of nighttime maxima in rainfall. An analysis of TRMM satellite data showed that, along most of the Himalaya range, monsoon rainfall is concentrated during evening hours [*Bhatt and Nakamura*, 2005].

Aerosol and snow chemistry in Nepal were studied by researchers of the Climate Change Research Center at the University of New Hampshire during the 1990's [*Shrestha et al.*, 1997; *Shrestha et al.*, 2000; *Wake et al.*, 1994]. They assessed the suitability of high Himalayan locations for the measurement of free tropospheric air, and explained the observed aerosol composition variations in terms of air mass origin. The team also looked at the recent surface maximum temperature record of Nepal and found evidence for an amplification of both cooling and warming trends at higher elevation locations [*Shrestha et al.*, 1999].

One of the earliest published studies of air pollution in Kathmandu took place during winter 1982-83, with the sampling of indoor and outdoor pollutants in the Kathmandu Valley and in the remote Khumbu region near Mt. Everest [*Davidson*, 1986]. In addition to laboratory chemical analysis of aerosols collected on filters, and of the gases CO, CO_2, methane, nitrous oxide, methyl-chloride, CFC-11, CFC-12, and several hydrocarbons collected in flasks, the researchers used an Ecolyzer instrument to make 50 CO spot measurements. They found indoor CO concentrations in houses with firewood stoves in the range of 11 to 37 ppm, and outdoor concentrations on a ridge near Kathmandu of 0.21 ppm.[1] Three days of continuous measurements in Kathmandu city yielded CO concentrations around 2 ppm, with a range of <1 ppm to 2.5 ppm [*Davidson*, 1986].

A World Bank project [*Larssen et al.*, 1997] coordinated and summarized studies conducted by several agencies measuring air pollutants around the Kathmandu Valley in winter 1992-1993. They measured total suspended particulates (TSP), PM_{10}, SO_2, NO_2,

[1] The paper does not state at what time of day those spot measurements were made.

CO, and lead. 8 or 24 hour average passive samples were collected on filters, followed by wet-chemical analysis. NO_2 concentrations were found to be generally low, while near roads with heaby traffic, very high concentrations of particulates were found, exceeding WHO health guidelines by several factors. Sulfur dioxide was generally low except in places with heavy traffic dominated by trucks and buses [*Larssen et al.*, 1997]. Very high particulate levels were measured from January through May; they decreased significantly after the onset of monsoon rains. SO_2 measurements ranged from 5 to 70 ppb, and NO_2 from 7 to 50 ppb.

Further ambient air pollution monitoring in Kathmandu was carried out in December 1998 by a joint NESS-Ministry of Population and Environment project [*NESS*, 1999]. Twice monthly measurements of wind, temperature, and daily average values of PM_{10}, SO_2, NO_2, CO as well as Pb, Ca and SiO_2 in TSP were conducted at 11 sites around the valley. Because a single weather station and set of samplers was moved daily to a new location (through six cycles), and the study found large variations in concentrations both between different days at the same station, and between stations making it difficult to establish clear spatial patterns. The highest pollutant concentrations were found in winter, in the urban and residential regions of the valley [*NESS*, 1999]. With few exceptions, SO_2, NO_2, Pb and CO concentrations were found to be within the WHO guidelines, but TSP and PM_{10} to be far in excess, especially in central city locations. Stations near the Himal Cement Factory[2] showed high particulate levels whenever the factory was in operation [*NESS*, 1999]. The authors also found that SO_2, NO_2, and CO concentrations decreased from winter into spring, while TSP and PM_{10} concentrations increased.

Flask sampling and GC analysis of non-methane hydrocarbons (NMHC) was conducted by Usha Sharma as part of her dissertation research supervised by H. Akimoto at the University of Tokyo [*Sharma*, 2000]. A total of 38 flask samples were collected in downtown Kathmandu and at Nagarkot (on the valley rim) in November 1998, and transported to a laboratory in Tokyo for analysis of 28 hydrocarbons. Figure 1.4 shows

[2] Permanently closed since several years.

the results for three hydrocarbons in 22 samples collected over four days on busy Putalisadak Road in Kathmandu. Note the low nocturnal values, and the low weekend day-time values. All the samples collected by Sharma were dominated by high mixing ratios of ethene, acetylene, and C_4-C_5 hydrocarbons. The first two are characteristic internal combustion engine products while the C_4-C_5 hydrocarbons come from incompletely burned vehicle exhaust, as well as leaked gasoline vapors and liquefied petroleum gas (LPG) [*Sharma*, 2000]. Within Kathmandu city, *Sharma* [2000] found strong influences of automobile emissions in signature species such as ethene and acetylene. In Nagarkot, many alkanes still showed signs of urban emissions, but isoprene did not correlate with the other species, suggesting local biogenic sources [*Sharma*, 2000].

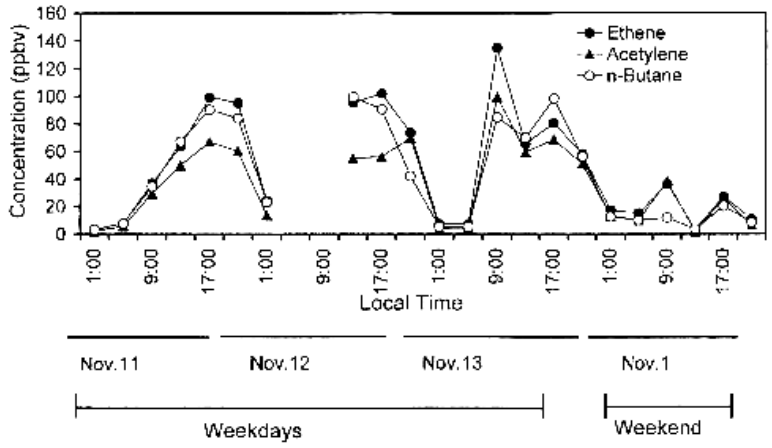

Figure 1.4: Three NMHC's measured by Sharma [2000] at Putalisadak, Kathmandu in 1998.

In Spring 1999 a sun photometer and a nephelometer were used to study the aerosol extinction coefficient and ångstrom coefficient above the Kathmandu Valley for 21 days [*Sapkota and Dhaubadel*, 2002]. The researchers found the coefficients to be high in the morning, decreasing during the day, and increasing again in the late afternoon, consistent with a higher day-time mixed layer and the flushing out of pollutants from the valley.

A field study in 1995-1996 used two and later three sets of a surface weather station and a condensation nuclei (CN) particle counter that were moved around. Observations were

gathered at two sites in Kathmandu, on Nagarkot peak, as well as at three sites south of and one site north of Mount Everest [*Hindman and Upadhyay*, 2002]. CN and weather parameters were measured in Kathmandu from October 18 to 23, 1995; weather measurements were also conducted in Kathmandu and Nagarkot between April 4 and 6, 1996. Within these time periods, several patterns were found. Within Kathmandu, condensation nuclei showed a morning peak between 6 and 10 am, a trough in the afternoon, and a second broader peak after about 6 pm that gradually decreased to a minimum at 5 am (Figure 1.5).

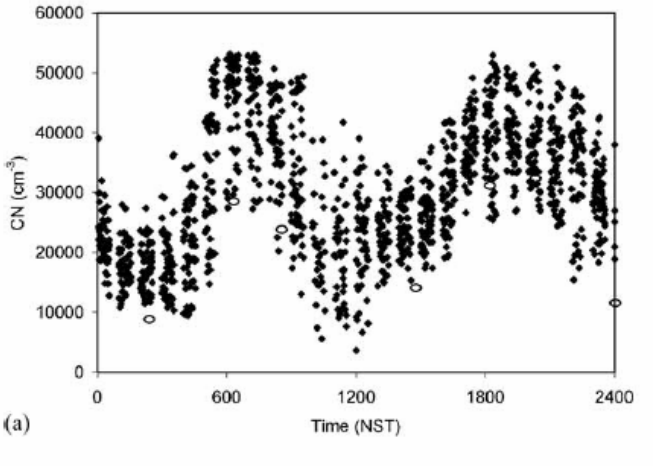

Figure 1.5: Diurnal cycle of CN measured between October 18 and 23, 1995 [*Hindman and Upadhyay*, 2002]

The authors found wind speeds to be calm at night, rising rapidly from about 10 am onwards, reaching peak values in the mid afternoon, and decreasing again by nightfall. Weak winds in the morning blew from the southeast, while there were strong afternoon winds from the west. During the afternoon the dew point dropped to lower values than at other times. In Nagarkot the wind switched back and forth between easterly and westerly during the morning, and in the afternoon the site received strong southwesterly winds from the Kathmandu Valley.

Between February and April 2001, samples of SO_2 and NO_2 were measured using passive sampling at 22 sites around the Kathmandu Valley, a sodar was operated for a week in

April 2001, smoke plumes were frequently photographed, and emissions maps on a 1 km grid were prepared [*Kitada and Regmi,* 2003; *Regmi et al.*, 2003]. This data formed the basis for comparison to the first MM5 simulation of the Kathmandu Valley conducted for the four day period of March 4 – 8, 2001, using an inner-most grid spacing of 1 km. The authors used their simulation to explain the observations of strong afternoon westerly winds at the airport in terms of up-valley winds penetrating into the Kathmandu Valley basin from the western passes and the Bagmati valley. They found a front between the cooler Bagmati valley air and the warmer air entering through the passes. The MM5 simulation was also used to drive a chemistry-transport model that tried to reproduce the observed SO_2 and NO_2 concentrations [*Kitada and Regmi,* 2003] as well as to create air pollution exposure maps based on census data [*Regmi and Kitada,* 2003]. One of the researchers, Ram P. Regmi, has provided to us unpublished CO emissions maps at 1 km resolution, which formed the starting point for an emissions database described in Chapter 6.

In January – February 2003, a pilot field measurement campaign funded by the Alliance for Global Sustainability (AGS) was carried out in Kathmandu by Elke Hodson and Arnico Panday from MIT, together with Yong Yu and Bo Galle from Chalmers University. The measurement campaign included *in-situ* measurements of ozone, NOx, PM_{10} and weather variables at the Hyatt Regency Hotel in Bouddha, Kathmandu, as well as long-path DOAS (differential optical absorption spectroscopy) measurements of ozone, NO_2, HONO, formaldehyde, SO_2 and aromatics along a 1 km light path in the Bouddha region. Carbon monoxide measurements as well as upper air soundings with a sodar were unsuccessful due to instrument failures. While all the data from the field campaign remains unpublished[3], some of it has been written up in the form of an MIT general examination paper. Figure 1.6 shows ozone, nitric oxide (NO) and nitrogen dioxide (NO_2) measurements from 24 hour period. Ozone exhibited a diurnal cycle similar to what was measured in the field campaign described in this dissertation. NO showed morning and evening peaks. NO_2 had its highest values in the late morning, after the NO peak declined, as well as in the evening. One interesting finding was that the

[3] But it formed the basis for several poster presentations.

DOAS was unable to carry out measurements for several hours each morning due to fog blocking its optical path.

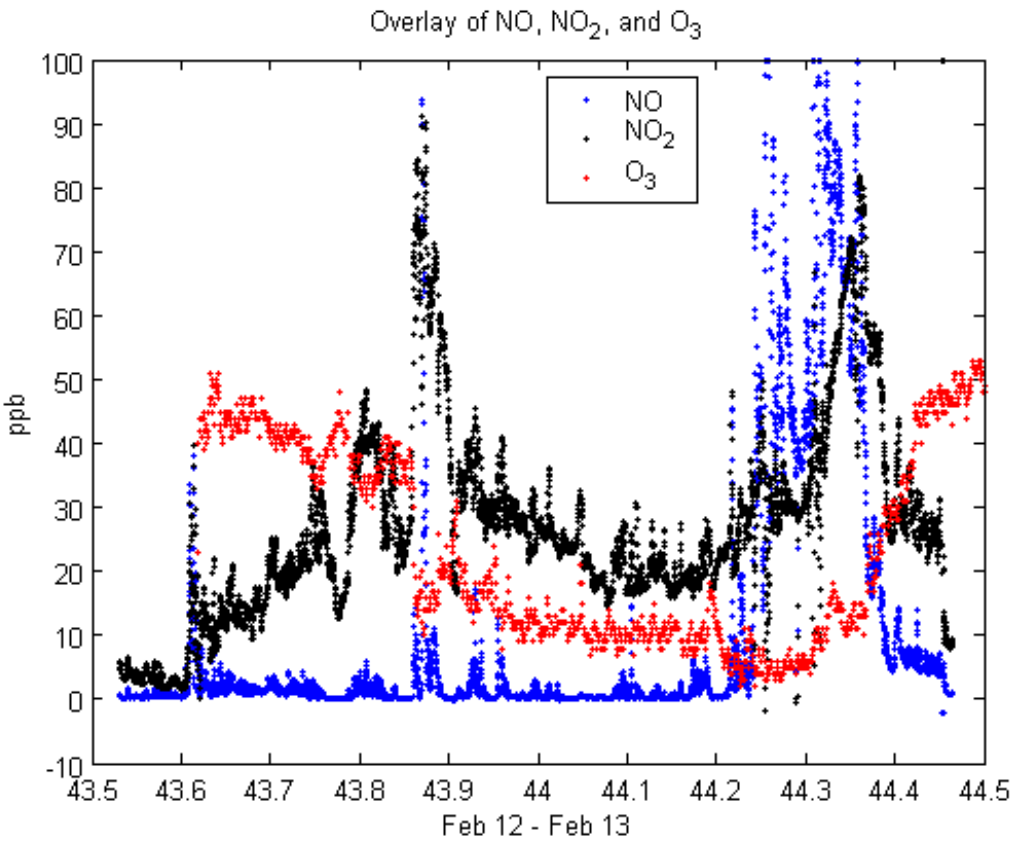

Figure 1.6: NO, NO_2 and ozone measurements from noon on February 12 through noon on February 13, 2003, during the AGS pilot study. (Figure © Elke Hodson)

As a part of the Atmospheric Brown Cloud (formerly Asian Brown Cloud) project (http://www-abc-asia.ucsd.edu), one measurement station was set up on Nagarkot peak and one in Godavari (base of Mt. Fulchoki at the eastern end of the Kathmandu Valley) to measure aerosol absorption and scattering properties with nephelometers and pyranometers. During the set-up phase of the stations from February 9 to 17, 2003, a high-resolution micro-pulse lidar was run in Kathmandu to measure the vertical aerosol extinction profile [*Ramana et al.*, 2004]. Analyzing 24-hour average data (Figure 1.7Figure 1.1), the authors found that a 300 meter thick layer near the surface experienced a maximum in light extinction by aerosols, followed by a minimum from 300-600 meters above ground, and a second extinction maximum around 1.3 km above

ground, with the upper aerosol layer ending at around 2 km above ground [*Ramana et al.*, 2004]. Unfortunately their analysis does not provide any glimpse into the diurnal cycle. They attributed the lower aerosol layer to local sources and the higher layer to long-distance transport from far-away sources [*Ramana et al.*, 2004]. As a part of the Atmospheric Brown Cloud research, haze layers were also photographed over eastern Nepal [*Ramanathan and Ramana*, 2003].

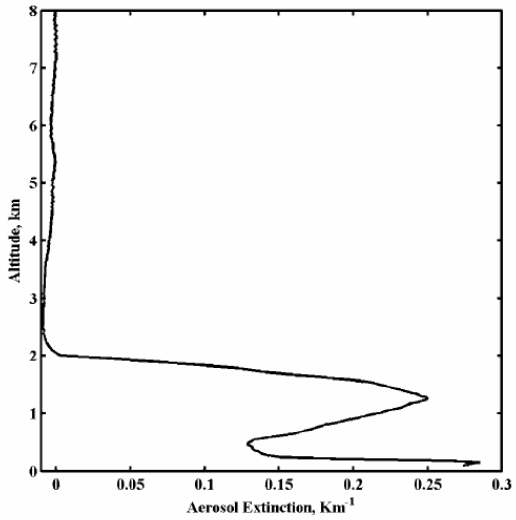

Figure 1.7: 24-hour average aerosol extinction profile measured in Kathmandu on February 10, 2003 with a micro-pulse lidar [*Ramana et al.*, 2004]

Finally, since Fall 2002, the Nepali Ministry of Population and Environment (MoPE) has been carrying out 24 hour-average passive sampling of PM10 at six sites around the valley. The data is available on the ministry's website (http://www.mope.gov.np); plots of it are displayed in Figure 1.8 and Figure 1.9. The Putalisadak and Patan Hospital sites are located on busy roads and, not surprisingly showed the highest pollution levels. Thamel is within the old city core, with little road traffic. Mastyagaon is located at the base of the Chandragiri Peak, on the southern valley rim; it had the least PM_{10} pollution. The Kirtipur station is on the roof of a college building surrounded by green space, half-way between Matsyagaon and the city. Bhaktapur is a separate city east of and downwind from Kathmandu. Figure 1.10 zooms in to the January-February 2005 period; we see the same ranking among the stations as in the seasonal plots. We also see weak signals of weekend minima in some of the data.

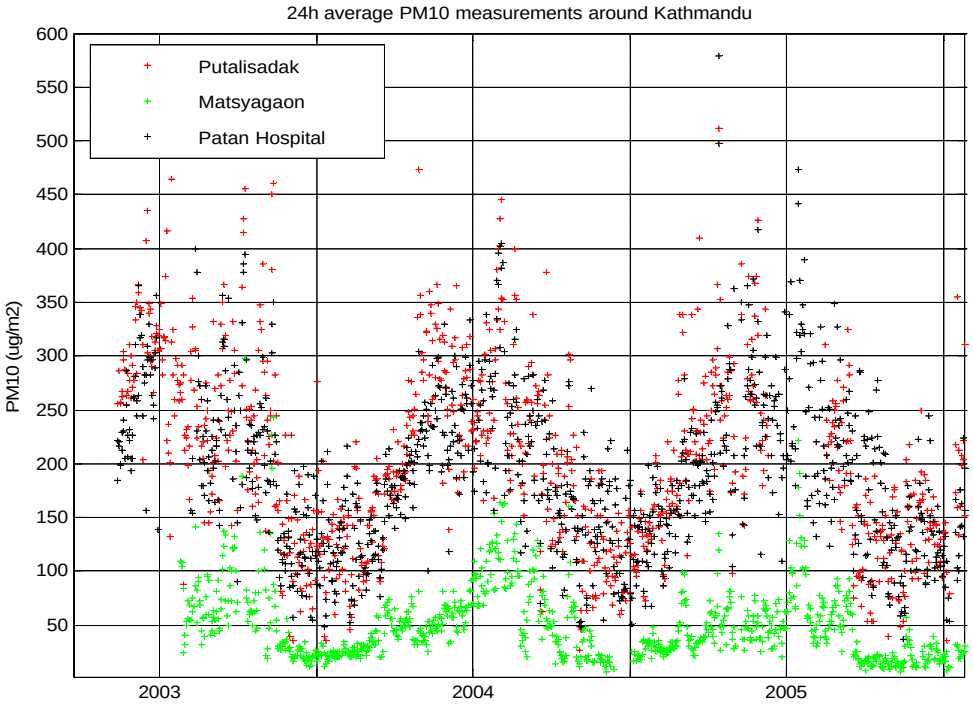

Figure 1.8: Daily average PM_{10} values at three sites around the Valley (MoPE).

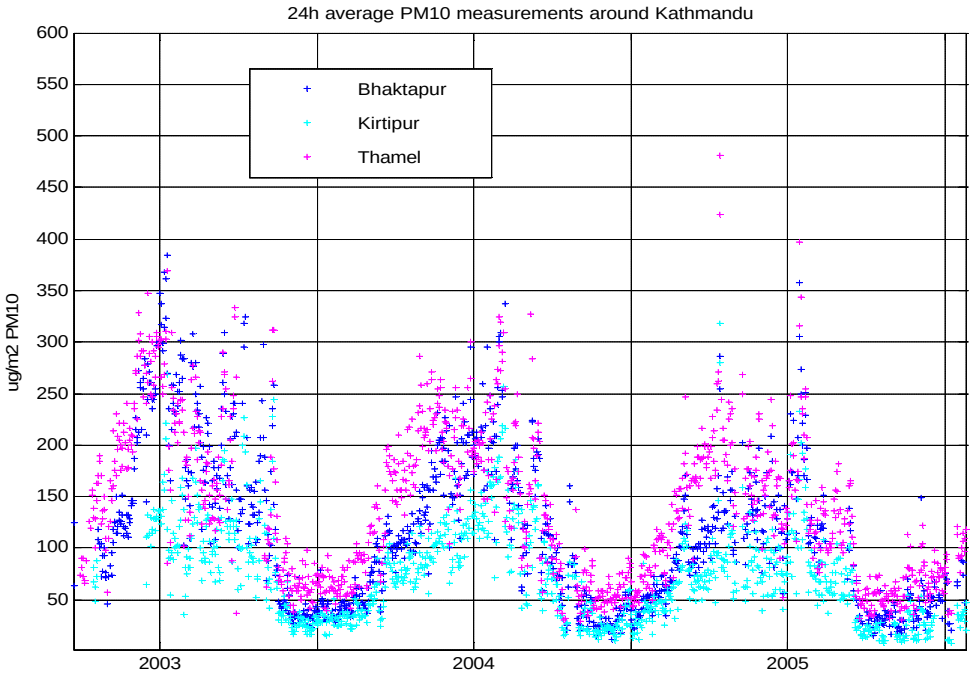

Figure 1.9: Daily average PM_{10} values at three sites around the Valley (MoPE).

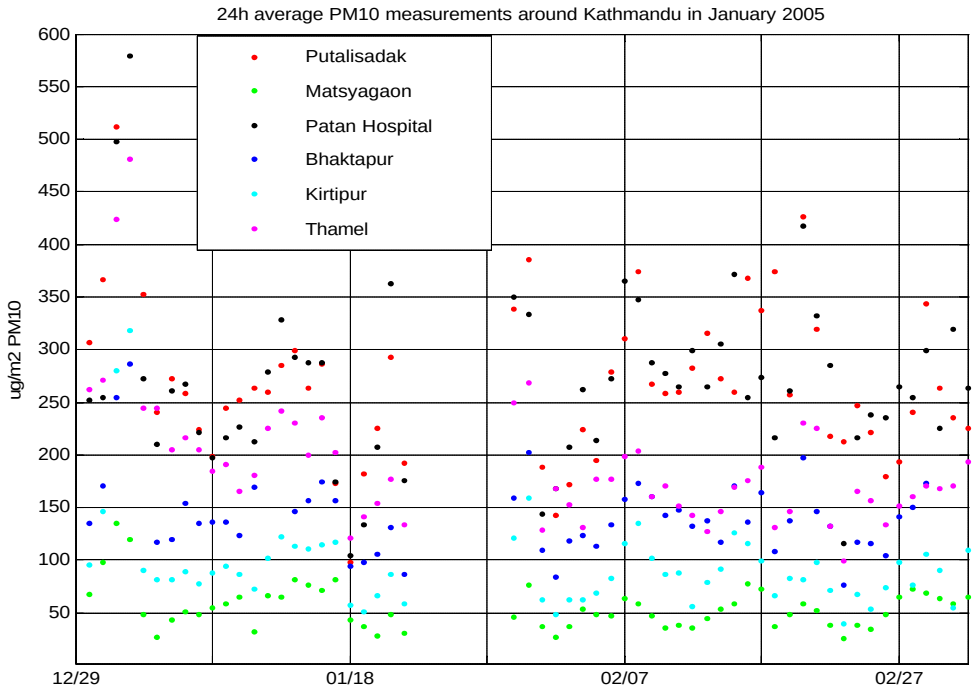

Figure 1.10: PM_{10} in January – February 2005 (MoPE).

The PM_{10} data clearly shows a seasonal cycle, with minima during the summer monsoon months. Not surprisingly, the busy road-side locations had pollution levels that were several times higher than at rural locations. Interestingly, the post-monsoon rebound of particulate pollution happened first in the urban locations of Putalisadak, Thamel, and Patan Hospital, and followed much more slowly at the more rural locations. The cause might be that urban air experienced high particulate loading from local traffic sources as soon as the monsoon rains stopped regularly washing the particulates out, whereas rural areas only started to see higher particulate loads of local origin once fields were harvested and soils dried.

Apart from MoPE's ongoing PM_{10} monitoring, we are not aware of any other research-grade air pollution measurements in the Kathmandu Valley during our 2004-2005 measurement period. The next section explains why the field observations for this dissertation were centered around measuring carbon monoxide.

1.5 Why Focus on Carbon Monoxide?

Carbon monoxide (CO) is both a common threat to public health in polluted urban environments, and a common indicator pollutant for resource-limited field studies. The major urban source of carbon monoxide is incomplete combustion: in motor vehicles, industries and cooking (especially with biofuels, but also with kerosene and LPG, the common cooking fuels in Kathmandu). Gasoline (petrol) powered vehicles produce almost ten times as much CO per liter of fuel burned as diesel powered vehicles. Two stroke motorcycles have been found to produce 1.5 times as much CO as four-stroke motorcycles [*Han and Naeher*, 2005]. CO is also produced during the photochemical break-down of short-lived hydrocarbon and other organic species [*Kanakidou and Crutzen*, 1999], many of which are emitted during incomplete combustion.

Significant quantities of CO are also produced photochemically in rural areas during the breakdown of methane and isoprene [*Kanakidou and Crutzen*, 1999]. These photochemical sources, as well as transport from polluted regions, contribute to the significant CO concentrations observed in remote regions of the world. "Background" CO concentrations vary seasonally (with spring maxima and summer minima) and with latitude: from a range of 60-80 ppb in Samoa, to 100-200 ppb in Alaska [*Novelli et al.*, 1992], 100-150 ppb in Mace Head, Ireland [*Derwent et al.*, 1998] and 150-250 ppb in remote rural Japan [*Narita et al.*, 1999]. The background concentration of CO varies little within the southern hemisphere, but north of the equator it increase rapidly with latitude [*Brasseur et al.*, 2003]. For three decades starting around 1960, the global background CO concentrations grew at a rate of 1-2% a year, but in the early 1990s the trend had leveled off and started to show signs of reversing [*Khalil and Rasmussen*, 1994; *Novelli et al.*, 1994], as a result of several changes in sources (decreasing anthropogenic emissions) and sinks [*Law*, 1999]. However the changes have not been monotonic: for example, in 1998-99 the global mean CO concentration temporarily increased 16% due to a large numbers of forest fires [*Mészáros et al.*, 2005].

On a global scale, the primary sink of CO is reaction with hydroxyl radicals (OH), responsible for 85% of CO loss; uptake by soils is responsible for about 10% of the loss [*Badr and Probert*, 1995], mostly through consumption by fungi and other microbes. While temperate soils have been found to be a net sink for CO, some arid as well as water-saturated soils have been found to be sources of CO [*King*, 1999]. The CO that is not removed by OH or soils is transported to and destroyed in the Stratosphere [*Badr and Probert*, 1995]. Although the reaction of carbon monoxide with OH is slow, about 60% of the atmosphere's OH molecules end up reacting with CO [*Zhang et al.*, 2001]. CO's abundance thus affects the global OH budget, and thus the atmosphere's oxidation capacity. Observed reductions in global atmospheric CO have been shown to significantly increase atmospheric OH, thereby decreasing the growth rate of atmospheric methane [*Brühl and Crutzen*, 1999].

Carbon monoxide is also a toxic gas, joining onto hemoglobin in red blood cells to reduce their delivery of oxygen to body tissues. Each ppm of ambient CO inactivates 0.17% of the blood's hemoglobin [*Badr and Probert*, 1995]. More than a few percent of hemoglobin tied to CO can affect the functioning of the heart, lungs, brain, and other body parts [*Raub*, 1999]. At concentrations exceeding a few hundred ppm (such as in unvented rooms with combustion sources) CO can cause loss of consciousness and even death [*Badr and Probert*, 1995]. Outdoor levels of CO are often far below the United States (US) 8 hour standard of 9 ppm or the 1 hour standard of 35 ppm [*Raub*, 1999] as well as the World Health Organization (WHO) 8 hour standard of 10 ppm and 1 hour standard of 25 ppm [*Badr and Probert*, 1995]; however short-duration road-side measurements exceeding 50 ppm have been found in Ankara [*Atimtay et al.*, 2000], Mexico City [*Han and Naeher*, 2005], and Kathmandu [*Larssen et al.*, 1997]. Traffic policemen and other people who spend long hours on busy streets, especially ones who also smoke, may be at risk of CO poisoning [*Atimtay et al.*, 2000]. During free-flow traffic condition, road-side CO concentrations tend to be linearly correlated to traffic volume [*Boddy et al.*, 2005].

Carbon monoxide is a useful indicator of urban air pollution. It has many of the same combustion sources as fine particulate matter and other urban primary pollutants (for example it is well correlated with NMHC from combustion sources [*Kuebler et al.*, 1996; *Möllman-Coers et al.*, 2002]). However, CO tends to show greater spatial homogeneity [*Holmes et al.*, 2005] than many shorter lived pollutants whose concentration is strongly affected by local sources. Compared to ozone, nitrogen oxides, many VOCs and other gaseous urban air pollutants, carbon monoxide has a long atmospheric lifetime, from 1.1 to 2.4 months in the tropical boundary layer, and from 2.2 to 3 months in the midlatitude lower troposphere [*Martin et al.*, 2003]. Due to its long life time, CO has often been studied as a tracer of long distance and intercontinental pollution transport [*Bertschi and Jaffe*, 2005; *Guttikunda et al.*, 2005; *Lobert and Harris*, 2002; *Stohl et al.*, 2002]. On the timescale of its emission and ventilation from urban areas (hours to a day), carbon monoxide can be treated as an almost inert tracer: the difference in CO measured in an air parcel before and after it passes over a city directly reveals the CO added to the parcel by the city, and there is no need to take into account significant chemical loss enroute. CO enhancement in air parcels traveling over an urban region has been used to verify the emission inventory of the region [*Barnes et al.*, 2003][4].

To contrast, quantifying the budget of urban ozone requires not just detailed measurements of meteorological variables, but also of the concentration of dozens of gases whose photochemical reactions are responsible for the production and loss of ozone. Ozone also has significant dry deposition rates onto surfaces that are highly dependent on vegetation types. A detailed study of of the ozone budget, while desirable, would have been beyond the scope of the resources available for this dissertation. The understanding pollution transport and ventilation from the Kathmandu valley gained through the study of CO in this dissertation helps pave the way for future studies of pollutants that are influenced by the same transport as well as by chemistry.

[4] That was one of the initial goals of this dissertation, but was unrealized due to windflow complexity.

1.6 Chapter Conclusion

The literature and past data from the Kathmandu Valley that were summarized in this chapter provide some glimpses into air pollution in the Kathmandu Valley at certain times. They suggest that the biggest known air pollution problem in the valley is fine particles. They also suggest that the Kathmandu Valley has cleaner air during the summer monsoon period than during the rest of the year. The few studies that show a diurnal cycle suggest that, at the time of studies, the valley experienced stagnant conditions at night, but was better ventilated during the day by strong westerly winds. They suggest that pollution levels were lower during the afternoon than in the morning and evening, and that they were lower on weekends than on weekdays.

There are gaping holes in the understanding provided by the available data and by the past research. Most of the data was only collected over a few days and it is not clear how representative those days were. In addition, the past data leaves many important questions unanswered. For example, what controls the diurnal cycle of pollutants in the Kathmandu Valley? Does the timing and location of emissions matter? How are pollutants transported out of the valley? Do they get lifted vertically by convection, move up the slopes of valley-rim mountains, or get blown out through mountain passes? Once removed from near the surface, are they permanently gone, or do they return? Are the strong afternoon winds a result of the arrival of up-valley winds from surrounding valleys, or are they synoptic winds aloft that have penetrated down to the ground level? Does the air mass in the Kathmandu Valley behave like air masses in narrow river valleys, in flat basins, or over elevated plateaus? What is the mechanism of the morning mixed layer growth? Is it affected by the winter fog in the valley bottom? Does the air pollution in the Kathmandu Valley originate within the valley, or come from afar? Answering questions such as these requires detailed field measurements as well as computer modeling. These two approaches form the backbone of this dissertation. Because past research left too many unknowns to even generate plausible hypotheses, the dissertation first focuses exclusively on describing the set-up and results of new field measurements. This generates questions addressed with model simulations.

CHAPTER 2: THE FIELD OBSERVATIONS

2.1 Chapter Introduction

This chapter describes the set up of field measurements of air pollutants and meteorology that were carried out in Kathmandu during an entire dry season spanning from September 2004 through June 2005. As described in Chapter 1, the Kathmandu Valley is influenced by the South Asian Summer Monsoon, which brings three very wet summer months during which the valley's atmospheric conditions are distinctly different from the dry "season" during the rest of the year. Not only does the dry season get much less precipitation (only 10-20% of the annual total during 9 months), but its wind patterns, cloud formation, valley ventilation, visibility, and air pollution accumulation are also distinctly different from the wet season. The valley's air pollution problem is far more severe during the dry season.

The field measurements were designed to fulfill several objectives. First, they had to establish a continuous multi-month record of ambient air quality and meteorology at a representative site on the valley floor, which would reveal diurnal, day-to-day, and seasonal patterns. Second, the measurements were to reveal the effects of urban emissions upon air masses passing over the city. Third, the measurements had to provide glimpses into the physical mechanisms responsible for the accumulation of air pollutants at the valley bottom and their ventilation out of the valley. These objectives had to be fulfilled within the scope of limited resource availability.

The rest of this chapter describes the sites for long-term measurement, the instruments at those sites, as well as short campaigns that were designed to gather additional information. Section 2.2 provides an overview of the instruments, while section 2.3 provides a timeline of their deployment in the field. Section 2.4 describes the measurements of CO, ozone, and PM_{10} and the set-up of the main lab where those measurements were carried out. Section 2.5 describes the weather station, section 2.6

the sodar, and section 2.7 the temperature loggers. Section 2.8 describes the bag sampling and analysis, and section 2.9 describes the time-lapse photography of morning fog.

2.2 The Instruments

In addition to carbon monoxide, several other chemical and meteorological parameters were measured in the Kathmandu Valley. PM_{10} was measured because it shares many combustion sources with CO, yet usually has a shorter atmospheric life time, helping identify spikes In the CO data caused by local sources[5]. Ozone was measured to help understand the morning breakup of nocturnal inversions: while ozone aloft was expected to remain unchanged during the night, near the surface it was expected be depleted by surface deposition and by reaction with NO. At the time of the inversion break-up, ozone from aloft was expected to rapidly mix down to the surface. Horizontal wind speed and direction were measured using both an automated weather station and an acoustic sounder (SODAR).[6] The weather station also measured rainfall, solar radiation and relative humidity (helpful for reconstructing fog and cloud events), as well as pressure, temperature, and due point temperature (helpful for distinguishing air masses). The sodar measured the mixed layer height immediately overhead. The temperature profile of the boundary layer, including the existence and strength of temperature inversions was measured by temperature loggers that were installed at the top and bottom of a mountain, at 4 elevations on a 72 meter tall TV tower in the valley center, near the top of another 50 m tower, and on a hill overlooking the lab site's weather station.[7]

---

[5] The source overlap is not complete: Far more CO is emitted by gasoline vehicles than by diesel vehicles, while PM_{10} has a larger source among Diesel vehicles, and also some soil dust sources. However, PM_{10} peaks do indicate local pollution sources, such as nearby road traffic or garbage incineration.

[6] As mentioned elsewhere, the sodar was, unfortunately, only available during a short period of time.

[7] Having pressure and relative humidity in addition to temperature at each location would have allowed straight-forward computation of potential temperature and virtual potential temperature profiles. Unfortunately we were limited by the availability of sensors. However, temperature measurements at different elevations still allow computing average lapse rates assuming horizontal homogeneity between the sensors at different altitudes.

Table 2.1 summarizes the specifications of the instruments used for field measurements in Nepal. All of the instrumentation used were commercially built, but research-grade. The measurement principles, as well as the site setups are described in individual subsections below. Also available for field observation were six model 222-2301 Grab Air bag sampler pumps (SKC Inc., Pennsylvania) running on 9V batteries, as well as 190 five-liter foil bags with polypropylene fittings (SKC model 245-25). In addition, a GPS receiver (Garmin map60cs, Garmin, Taipei) was used to keep track of locations and travel paths, and a digital sound meter (Model 322, Center Technology, Taipei) was used to evaluate ambient noise levels at potential sodar sites.

Manufacturer and model	No. Units	Properties measured	Accuracy	Logging Precision	Averaging & logging Interval	Measurement range
Teledyne API 300EU	1	CO (and internal diagnostics)	5 ppb	1 ppb	1– 5 min	10 ppb – 1000 ppm
2B Techonologies Model 202	1	Ozone (and internal diagnostics)	1.5 ppb	1 ppb	1 minute	0 - 100 ppm
TSI Dusttrak	1	PM_{10}	0.1 %	1 $\mu g/m^3$	10 - 60sec	1 – 100,000 $\mu g/m^3$
Rainwise Portlog weatherstation	1	Wind speed Wind direction Temperature Pressure Rel.humidity Solar radiation Rainfall	1.3 m/s 5 º 1 ºC 1.69 mb 2 % 3 %	1 m/s 10 º 1 ºC 0.01 mb 1 % 1 W/m^2 0.01 mm	1-60 min 1-60 min 1-60 min 1-60 min 1-60 min 1-60 min 1-60 min	0.5 – 67 m/s 0 – 360 º - 54 – +65ºC 551 – 1084 mb 0 – 100% 0 – 2000 W/m^2
Onset Hobo H08-031-08 with solar radiation shield	7	Temperature (with external sensor inside shield)	0.2 ºC	0.01 ºC	1 minute	- 40 – +100 ºC
Gemini Tinytag	2	Temperature	0.4 ºC	0.01 ºC	1 minute	- 40 – +125 ºC
Remtech PA0 sodar	1	Mixed layer height Wind speed Wind direction	n / a 3 % 10 º	1 m 0.1 m/s 1 º	15 minute 15 minutes @ 50 m vert. resol.	50 m – 1200 m 50-500 m altitude 50-500 m altitude

Table 2.1 Summary of the instruments used in the field campaign in Kathmandu.

2.3 Timeline of the Field Deployment of the Instruments

The CO, ozone and PM_{10} instruments as well as one Hobo temperature logger and a GPS were available from the start of the field measurements. The weather station and sodar were shipped to Nepal at the same time, but stopped functioning shortly after field deployment and had to be sent back to their manufacturers for repair. The weather station arrived back to Kathmandu in late December 2004, along with 6 new Hobo temperature loggers. These were joined by 2 Gemini temperature loggers borrowed from ETH Zürich in January 2005. The sodar only returned to Nepal in April 2005 and was operational from late April into June 2005. To facilitate discussion later in the thesis, we divide the field deployment period into six phases.

Phase 1, from mid-July 2004 through the end of August 2005 prepared the groundwork field measurements in Kathmandu. This included the establishment of collaboration with local institutions including the signing of a memorandum of understanding between MIT and Purbanchal University as well as the preparation of customs release letters and permission request letters. Phase 1 also involved the search for, and evaluation of, possible sites for a small laboratory for continuous measurements using the CO, ozone and PM10 instruments. This would serve as a base of operation, computers and storage. At this time we also searched for a site suitable for the sodar. Access to the chosen sites was negotiated, and a laboratory enclosure was built to receive the instrumentation arriving from MIT.

During Phase 2, from early September 2005 through late December 2005, continuous measurements by the CO, ozone, and PM_{10} instruments were carried out at the main laboratory site. During this phase the weather station and the sodar were set up, tested, then sent back to their manufacturers for repairs. Daily laboratory record keeping forms were created, and regular instrument calibration protocols were established. Laboratory maintenance schedules, such as for particle filter changes, were created. Bag sampling and analysis protocols were set up and tested. A small four-wheel-drive vehicle (a 1989 Suzuki Samurai) was rented and used for the exploration of sampling sites around the

valley rim mountains. Three part-time local research assistants were hired and trained, and they maintained the laboratory during Arnico Panday's trip to MIT and ETH in November - December 2004. Also during this phase a temperature logger was installed on the automobile for GPS-tracked drives up and down valley rim mountain roads in order to test a method of recording vertical temperature profiles [*Mayr et al.*, 2002; *Saitoh et al.*, 1996]. Six new temperature loggers were purchased, and permission was negotiated for their installation on the tallest structure near the center of the valley: the 72 meter tall NTV Metro transmission tower. The weather station arrived back in Kathmandu in late December.

Phase 3, from late December 2004 to late January 2005 saw the measurement of CO, ozone, and PM10 by instruments at the main laboratory site, as well as of meteorological parameters using the repaired weather station on a nearby roof. Four temperature loggers were installed on a television tower near the center of the valley, and two were installed at the top and base of a valley rim mountain. Two temperature loggers borrowed from ETH arrived, and were installed on a second tower and on a small hill. On two occasions the ozone and PM10 instruments were moved to the top of Nagarkot peak (See Figure 1.1) for periods of 24 -72 hours, while additional data about the formation and breakup of nocturnal temperature inversions was collected using the temperature logger and GPS on the car, driving up and down mountain roads. In the mean time, student volunteers from the Central Department of Environmental Science at Tribhuvan University were trained to correctly fill air sampling bags, with a full-scale trial run conducted in late January.

Phase 4, from February 1 through late April 2005 saw the continuation of measurements at the main laboratory site, as well as the monitoring of temperature by eight loggers at fixed sites. Following the royal coup d'etat and accompanying telecommunication shut-down in Nepal on February 1, 2005, temperature logger and bag sampling site access permissions as well as security clearances had to be re-negotiated; and bag sampling logistics had to be redesigned. Sampling compromises due to site access problems during field measurements are not unique to Kathmandu [*Rotach et al.*, 2004]. But in this case,

since sites had already been chosen and sensors had already been installed, the best strategy was to renegotiate permissions in the new situation. Once the system was back on track, every 1-3 weeks student volunteers collected 24 hours of simultaneous hourly/half-hourly CO bag samples at up to six sites around the valley, followed by analysis and flushing of the bags in the lab.

Phase 5, from late April through early June 2005, continued the activities of Phase 4, with the addition of having the SODAR reinstalled and running. One temperature logger was moved from the second city-center tower to the top of a ridge overlooking the south side of the valley. Also, on several days the student volunteers measured CO, PM_{10} and noise, and counted traffic at important road intersections in Kathmandu. On one occasion, the ozone and PM_{10} instruments and temperature logger/GPS were taken on a 250 km drive west of Kathmandu. Unfortunately, the bag samples taken on that trip did not produce reliable data.

During Phase 6, from early June 2005 through mid July 2006, while the wet season started off, temperature loggers were removed from towers and mountains, the SODAR and of the instruments at the Hyatt lab were dismantled, MIT owned equipment was packed, cleared through customs, and shipped back to MIT, while the laboratory housing was dismantled and the rented vehicle was returned.

Table 2.2 summarizes the times and durations of successful data collection with continuous measurement instruments, while Table 2.3 summarizes the short-term sampling.

Continuous Measurements	From	To	Notes:
CO continuous measurements (1 or 2 minute logging) at the main lab	Mid Sept. 2004	Early June 2005	Very few data gaps
Ozone continuous measurements (1 minute logging) at the main lab	Late Aug. 2004	Early May 2005	Some gaps in May-June when the instrument was moved around
PM_{10} continuous measurements (10 sec or 1 min logging at the main lab)	Late Sept. 2004	Early June 2004	Some data gaps in May
Weather station (T, P, RH, wind speed, wind direction, total solar radiation, rainfall) at the main lab	Early Nov. 2004	Mid Nov. 2005	Faulty solar radiation and rainfall sensor
Weather station (T, P, RH, wind speed, wind direction, total solar radiation, rainfall) at the main lab	Late Dec. 2004	Mid June 2005	Repaired. Some logging errors in May/June.
Sodar measurements of mixed layer height and vertical wind profile at CTEVT (east of the city)	Early May 2004	Mid June 2005	Also worked for 2 days in Sept. 2004
Temperature loggers at 5, 25, 47, 62 m height up TV tower in valley center	Early Jan 2005	Mid June 2005	Some gaps of 1-2 weeks
Temperature loggers at top (1970 masl) and base of Nagarkot peak, on the eastern valley rim	Mid Jan 2005	Mid June 2005	Very few data gaps
Temperature logger at Pullahari, 1550 masl, north of the main lab.	Early Feb 2005	Late May 2005	Some gaps of 1 week
Temperature logger on 50 m Dharahara tower in city center	Mid Jan 2005	Late Mar. 2005	Few data gaps
Temperature logger at Hattiban, 1800 masl, south side of valley	Late Mar. 2005	Late Apr. 2005	Moved from Dharahara

Table 2.2 Summary of data collected by continuous measurement instruments.

Short campaign Measurements	**When?**
Ozone continous measurements on Nagarkot peak (eastern valley rim)	1 day in December, 2004 2 days in January, 2005 10 days in April, 2005
PM10 continous measurements on Nagarkot peak (eastern valley rim)	1 day in December, 2004 3 days in January, 2005
Weather station (T, P, RH, wind speed, wind dir, total solar radiation, rainfall) at Bhimdhunga pass (west entrance)	2 x 3 days each in April, 2005
24 hour CO bag sampling at Nagarkot Peak, eastern valley rim	2 x in February, 2005 1 x in March, 2005 3 x in April, 2005 1 x in May, 2005
24 hour CO bag sampling at Hattiban, on the southern valley rim	1 x in February, 2005 1 x in March, 2005 1 x in April, 2005
24 hour CO bag sampling at the top and bottom of Dharahara tower in the city center	2 x in February, 2005 2 x in March, 2005 1 x in April, 2005
24 hour CO bag sampling at CTEVT, east of the city (sodar site)	1 x in February, 2005 2 x in March, 2005 1 x in April, 2005 1 x in May, 2005
24 hour bag sampling at Bhimdhunga Pass (western valley entrance)	2 x in April, 2005 1 x in May, 2005
CO bag sampling in other locations	1 x in March, 2005 1 x in April, 2005 1 x in May, 2005
Time-lapse photography of valley fog/smog from Hattiban	2 mornings in February, 2005 from ~5:30 am to ~ 10 am
CO and PM_{10} sampling from morning till evening in a bus circling the city ring road	1 x in May, 2005
CO bag sampling, PM_{10} and noise measurement, plus traffic counting at major intersections	5 x in May, 2005
Continuous trace of temperature and GPS tracking on the car from February to May 2005	Multiple times and places

Table 2.3: Summary of the short-term sampling data.

2.4 The CO, Ozone, and PM_{10} Measurements at the Main Laboratory

This subsection describes selection of a site for the main laboratory in Kathmandu, the instruments and the internal set-up of laboratory, and the instrument calibration procedures.

2.4.1. Site selection for the main laboratory in Kathmandu

It was decided in advance that the continuous measurement instruments should operate at a site east of Kathmandu City, which would place them usually, but not always, downwind of the city. Potential sites were searched in the region extending eastward from the Kathmandu Ring Road between the Sankhu and the Godavari roads. Additional criteria for the site selection included good security, generator back-up power supply, and public transportation access. The site also had to be surrounded by open space, to be as far as possible from local pollution sources, and to be exposed to ambient winds without being blocked by nearby trees and buildings. Six sites were short-listed. The owners of the first-choice site (the Agricultural Bank Training Center in Bode) rejected us, and we settled for the second choice site: The Hyatt Regency Hotel in Bouddha. It was slightly further north than preferred, but met other criteria well. This site also happens to be located almost exactly at the midpoint of a straight line connecting Bhimdhunga Pass (the westernmost bag sampling site) to Nagarkot Peak (the easternmost bag sampling site).

The Hyatt Regency is a 270 room 5-star hotel with adjoining conference center and casino, sprawling over 37 acres of landscaped gardens (see Figure 2.1). The hotel drive-way approaches from the west, and is flanked by a sprawling surface parking lots. The main building forms a north-south wall of five sections. West of the central section are the entrance and lobby, and north of that is the casino and conference center. On the southern and northern most ends of the hotel building are two “towers” containing fire escape staircases and utility rooms, topped by their own roofs and joined to the main building by bridges on each floor. On the top (fifth) floor of these fire escape towers

there are large landings and some open space surrounded by a short wall and railings, covered by a tall roof. A lease was negotiated for the empty space at the top of the southern fire escape tower and a metal-frame-and-wood-panel enclosure was built to fit into a 7 by 11 ft corner to serve as our main laboratory in Kathmandu (See Figure 2.2).

Figure 2.1: The Hyatt Regency Hotel from the air in 2001. North is towards the lower right of the picture. The laboratory was set up at the southern-most end of the main building (light blue arrow). Downtown Kathmandu is beyond the top edge of the photo.

Figure 2.2: Location and construction of the laboratory enclosure on the Hyatt fire escape tower.

The laboratory room was provided with electricity (including back-up generator power) from the hotel, a thermostat-controlled air conditioner and heater, a telephone line, and a broadband internet connection. It housed the CO and ozone instruments (the PM_{10} instrument sat outdoors in its own environmental enclosure), computers, spare parts and tools, calibration gases, field sampling equipment, and, after each bag sampling campaign, duffel bags filled with sampling bags (Figure 2.4).

2.4.2 The measurement of carbon monoxide

Carbon monoxide measurements in Kathmandu were carried out using gas filter correlation. Ambient carbon monoxide is usually measured by one of three common methods[8]. The first, tunable diode laser absorption spectroscopy (TDLAS) provides the best combination of high precision and time resolution (± 1.5 ppb, 1 second) [*Sachse et al.*, 1987]. It uses a laser to generate wavelength resolved infrared light traveling along a multi-pass beam, whose absorption by CO is measured [*Parrish and Fehsenfeld,* 2000]. This method was unaffordable and unavailable for the field measurements in Kathmandu. It is commonly used for *in-situ* measurements aboard research aircraft (for example [*Waibel et al.*, 1999])

The second method uses gas chromatography to separate CO, which then reacts with hot mercury oxide (HgO) to release mercury vapor. CO is quantified by measuring the absorption of light from a mercury lamp by the vapor [*Finlayson-Pitts and Pitts*, 2000]. This method has been used at numerous permanent monitoring sites in remote as well as urban locations around the world [*Derwent et al.*, 2001; *Greenberg et al.*, 1996; *Gros et al.*, 1999; *Moxley and Smith*, 1998; *Novelli et al.*, 1992; *Rappenglück et al.*, 2005; *Scheel et al.*, 1998; *Seiler and Fishman*, 1981; *Seiler and Junge*, 1970; *Simmonds et al.*, 1997; *Zahn et al.*, 2002], as well as for the analysis of airborne flask samples [*Zahn et al.*, 2002]. Operated in stable, temperature controlled laboratory conditions, the method

[8] Other methods have also been used to measure CO, including differential absorption CO measurement (DACOM), which, like TDLAS requires wavelength resolved IR beams produced by a laser [*Parrish and Fehsenfeld*, 2000]. Attempts have also been made to use other gas chromatographic methods as well as Fourier transform infrared radiometry (FTIR) and UV resonance fluorescence (RF) to measure CO [*Novelli et al.*, 1999], but these methods are much less common than the ones described here.

achieves precisions of 1-2 ppb, but its major down-side is the low time resolution (2-3 samples per hour, with loss of data in between) due to the time required for chromatographic separation of each sample. Use of the HgO method to measure carbon monoxide in Kathmandu was attempted during winter 2002-2003, but as predicted by a committee member [Steve Wofsy, personal communication, November 2002], the method failed to measure CO under the field conditions. It was too complex (too many parts that had to be reassembled to function independently and together) for field shipment conditions, and too sensitive to calibration errors due to the detector's nonlinear response at typical ambient CO concentrations [*Novelli et al.*, 1998].

Most routine air pollution monitoring of carbon monoxide is carried out by the third common method: non-dispersive infrared gas filter correlation (referred to as either NDIR or GFC). This method does have a linear response over a large range of CO concentrations [*Novelli et al.*, 1998], thus allowing simpler zero-span calibration. The method uses the Beer-Lambert law to take advantage of carbon monoxide's 4.67 μm infrared absorption band. Because other gases also absorb at this wavelength, the instrument uses a gas-filter-correlation wheel between the infrared source and the sample cell. The wheel has one chamber filled with pure N_2 (called the measurement cell) and one filled with N_2 and high concentrations of CO (called the reference cell). As the wheel spins, the infrared beam passes through alternating chambers. The chamber filled with CO strips the beam of all IR that CO can absorb. The sample CO concentration is computed from the ratio of IR absorption between measurements through the two chambers of the GFC wheel [*Novelli*, 1999; *Teledyne_API*, 2003].

Commercial GFC instruments are commonly used for regulatory CO monitoring as well as in scientific research, with a small number of models by American and Japanese manufacturers dominating the literature: Thermo Environment Instruments model 48 [*Mühle et al.*, 2002; *Parrish et al.*, 1991; *Röckmann et al.*, 1999], Teledyne API model 300 [*Wang and Kwok*, 2003; *Wang et al.*, 2003; *Zhang and Oanh*, 2002], Monitor Labs model 48 [*Bogo et al.*, 1999], Dasibi model 3008 [*Paino*, 1993], Kimoto model 541 [*Pochanart et al.*, 2003], and Horiba model APMA-350E [*Staffelbach et al.*, 1997].

Until the late 1980's, off-the-shelf GFC instruments had difficulty measuring CO in non-polluted environments due to their high detection limit of around ~90 ppb caused by water vapor in the air sample. They also tended to suffer from a zero drift of up to 200 ppb per day [*Dickerson and Delaney*, 1988]. These problems have been addressed with slight changes to the optics, the addition of a water trap [*Dickerson and Delaney*, 1988], and frequent zeroing of the instrument by periodically diverting the sample stream through a catalytic CO scrubber [*Parrish et al.*, 1994]. Many researchers have themselves modified their GFC instruments this way, including some Teledyne API 300's [*Lobert and Harris*, 2002; *Wang and Kwok*, 2003] a Kimoto [*Pochanart et al.*, 2003], and several TEI 48's [*Parrish and Fehsenfeld*, 2000; *Prévôt et al.*, 1997; *Stehr et al.*, 2002; *Wang et al.*, 2001]. After studying this solution on a TEI 48 at the Wofsy laboratory at Harvard Forest, it was decided in Fall 2003 that a GFC instrument would provide the best solution for CO measurements in Kathmandu. The modifications would make its detection limit and precision acceptable; the instrument's rugged single-box construction would be more suitable for field conditions than the HgO method; and its high temporal resolution would make it suitable for the questions to be investigated in the field. As we prepared to order the instrument, we learned of the new Teledyne API 300EU (Teledyne Advanced Pollution Instrumentation, San Diego, California), which is the first instrument with the modifications already built-in. It included an automatic zeroing function (hourly diversion of the flow through a heated scrubber), and an internal Permapure dryer. The new instrument was purchased in February 2004, tested at MIT, and shipped to Kathmandu.

2.4.3 The measurement of ozone

Ozone measurements were carried out using a Model 202 instrument (2B Technology, Golden, Colorado), which had already been field-tested in Nepal during Winter 2002-2003 [*Hodson*, 2003]. It uses the standard ozone measurement method of UV-absorption. That is, the air sample passes through a chamber of fixed length (the absorption cell); on one end of the chamber is a UV light source, while on the other end a

detector measures the UV absorption at 254 nm. Using the Beer-Lambert law, the instrument calculates the amount of absorbing ozone present. The 2B Model 202 was the most portable high-precision ozone instrument available (weighing only 2.1 kg), designed for mobile measurements (12V DC power). It has even been carried on tethersondes for vertical profiles [*Lee et al.*, 2003b]. Because tube connections inside the instrument used clamps rather than Swagelok fittings, the instrument needed periodic leak-checking by pressurizing it with zero air and watching for leaks on a pressure gauge.

2.4.4 The measurement of fine particles

The mass density of particles smaller than 10 micrometers (PM_{10}) is often measured using gravimetric techniques: a pump draws ambient air through a size-separator, and then through filter paper of precisely known weight, which collects particles for a fixed duration (typically 6, 8 or 24 hours). The filter paper is weighed again and the difference provides the mass of particles collected [*Sharma and Maloo*, 2005]. The pump's flow rate plus the duration of the collection provides the volume of air from which the particles were collected. This method can be very accurate (if the pump flow rate is constant and the weighing scale accurate), and its results can be useful for assessments. As mentioned in Chapter 1, Nepal's Ministry of Environment has been operating gravimetric PM_{10} sampling at six sites around the valley collecting 24 hour average samples since October 2002,. For the purpose of this research project however, where PM_{10} was to be used to help interpret CO measurements, gravimetry lacked the required temporal resolution.

We measured PM_{10} in Kathmandu using the portable TSI Dusttrak (TSI Inc, Shoreview, MN), which had been previously field tested in Kathmandu in Winter 2002-2003, as well as by other researchers [*Gillies et al.*, 2005]. The instrument inlet orifice determines the particle size cut-off with a choice of 1.0, 2.5 or 10 μm. We chose to measure PM_{10} rather than finer particles because we wanted measurements that were compatible with the ongoing MoPE measurements and because we intended to catch local pollution sources. Coarser particles have shorter atmospheric lifetimes and more spatial heterogeneity

compared to finer particles [*Wilson et al.*, 2005]. The particle quantity is computed from the amount of light scattered at a 90 degree angle from a light beam inside the instrument's measurement chamber. The Dusttrak was chosen for the high temporal resolution of its measurements (as frequent as every second, although we usually ran it at 10 second or 1 minute logging intervals) and its portability: it is lightweight, rugged, and can run on 4 C-size batteries. It served the additional purpose of being easy to lend to local university students for their class projects in exchange for their invaluable help with bag sampling.

2.4.5 The laboratory set-up

The air sample inlet (described below) for the CO and ozone instruments was attached to the end of a metal rod extending out 6 feet southwards beyond the railing of the fire escape tower, to be suspended about 12.5 meters above ground. It overlooked the hotel's gardens and tennis courts and was exposed to strong winds. Both the Hyatt parking lot on the west, and the Bouddha Road on the south were more than 60 meters away. From the location of the inlet tower, the view extended to the valley-rim mountains on the east, south and west sides of the Kathmandu Valley. Figure 2.3 shows a schematic diagram of the laboratory at the Hyatt; all fittings were ¼" stainless steel Swagelok. We used ¼" (3/16" interior diameter) FEP tubing, with the exception of some ¼" stainless steel tubing between the valves at the CO instrument inlet.

The sample inlet consisted of an upside-down clear funnel, with wire-mesh protecting the inlet from insects. Sample air entering the inlet first passed through a particle filter (Teflon #1131 by Savillex) before traveling along a straight tube into the lab. A T-junction branched off some air to the ozone instrument, through a toggle valve (Swagelok SS-43x54), and then through a second, identical, particle filter at the instrument inlet. According to its manual, the ozone instrument should have an inlet tube nolonger than 120 cm. Due to the instrument's weak pump, longer tubing would create too long a residence time in the tubing, with a risk of ozone loss during transit. The toggle valve provided the option of supplying the ozone instrument with air through a short tube

directly from outside the lab enclosure. However, finding no discernible difference in measurements, we preferred setting the toggle valve to supply the ozone instrument with air through the same inlet as for the CO instrument.

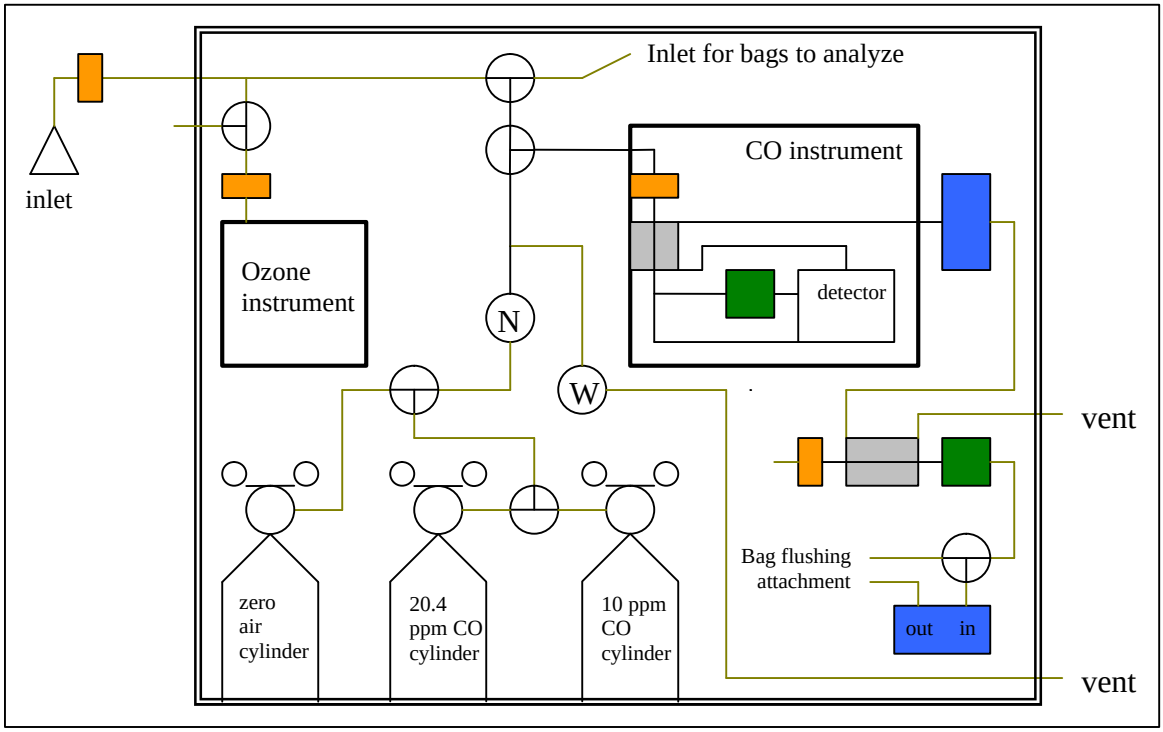

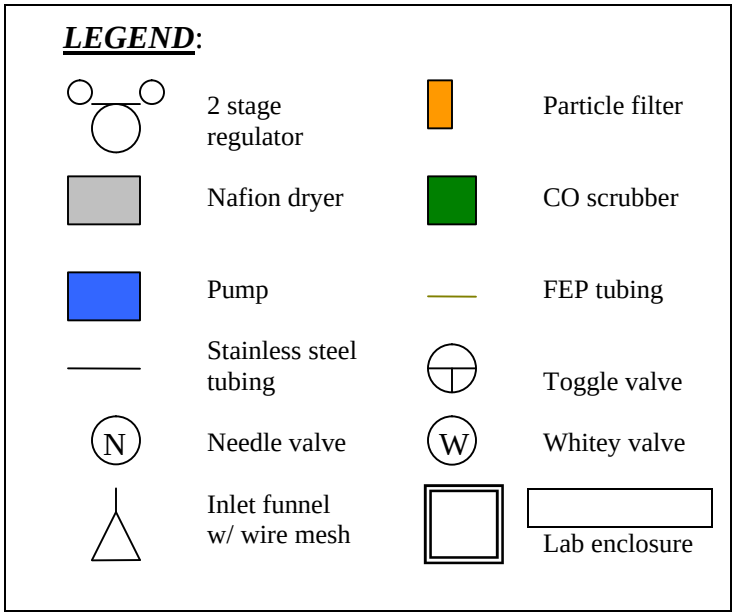

Figure 2.3: Schematic diagram of the laboratory set-up.

The tube length was ~ 3.5 meters from the inlet to the T-junction, and another 60 cm from the T-junction to the ozone instrument. The reason no ozone loss in the long tubing was found with the that from the inlet to the T-junction, air was pulled in very fast by the CO instrument's powerful 1.7 liter/minute pump. The ozone instrument's weak pump only had to pull the sample from the T-junction. We did check to make sure that the CO instrument's pump was not pulling air in the reverse direction through the ozone instrument.

From the T-junction, the rest of the sample continued towards the CO instrument, passing through a toggle valve (Swagelok SS-43x54) that gave a choice of supplying ambient or bag sample air to the instrument. A second toggle valve gave a choice of sample air or calibration gas. Calibration gas supply from a choice of three cylinders (zero air, 10 ppm CO standard and 20.4 ppm CO standard) was controlled by two toggle valves. The flow of calibration gas from the pressurized cylinders was fine-tuned using both the pressure valve on the cylinders' two-stage regulators, as well as a needle valve (Nupro SS-4BMG) to make sure that there was slight outward flow through a vent regulated by a Whitey (SS-1KS4) valve. This ensured that the instrument was not supplied with calibration gas at pressures higher than ambient.

The dry, warm vented air from the CO instrument was used for counter-flow drying of the air that was used to flush sampling bags. Due to the limited supply of zero air in Kathmandu, but the availability of a spare CO scrubber, we decided to flush bags with CO-scrubbed air rather than with bottled zero air. The bag flushing set-up was built as follows: ambient lab air was pulled through a particle filter (Teflon #1131 by Savillex), followed by a Nafion dryer (to improve the effectiveness of the CO scrubber) followed by a heated CO scrubber (Teledyne API part # 010370300). The air then passed through a toggle valve into a metal bellows pump; at the pump outlet we connected the bag to be filled for flushing. To empty, the bag was connected to an inlet on the other side of the toggle valve. Then the toggle valve was switched, and the bag was emptied by the metal bellows pump. Testing indicated that the scrubbed air did not contain detectable amounts of CO, and was thus appropriate for flushing the bags (without needing to deplete the

limited supply of bottled zero air). Further testing indicated that three rounds of filling and emptying were sufficient to clean each bag between bag sampling campaigns.

Figure 2.4: The laboratory on a normal day, and after the return of dufflebags filled with sampling bags.

On several occasions (December 2004, January 2005, and April 2005) the ozone instrument and Dusttrak were moved from the Hyatt lab to the top of Nagarkot's Viewpoint Peak (1975m), with the hope of capturing longer-lived background ozone concentrations at a site above the nocturnal boundary layer. Studies in Phoenix, Arizona, and Doi Inthanon, Thailand had indicated that mountain tops, even near cities, show very little diurnal variation in ozone mixing ratios, reflecting the regional background levels instead [*Fast et al.*, 2000; *Pochanart et al.*, 2001]. The ozone instrument and Dusttrak were also taken on a drive as far as Parbat District, 250 km west of Kathmandu, and run for several days in Pokhara City in May 2005.

2.4.6 Calibration procedures

The CO instrument was calibrated weekly, following the manufacturer's instructions. This involved supplying zero air for 10 minutes, resetting the instrument's zero memory, supplying span air[9] (in our case the 20.4 ppm standard) for an additional ten minutes, and resetting the instrument's span memory. Zero air was used from two cylinders by Scott

[9] Span air is a standard containing the pollutant of interest at a precisely known concentration that is near the upper limit of what is expected to be measured in the field.

Marrin, shipped to Nepal in December 2002. The 20.4 ppm standard was purchased from BOC Gases in Spring 2004, and shipped to Nepal in August 2004. The calibration was occasionally tested by sending the older 10 ppm standard (Scott-Marrin, December 2002) through the instrument.

The ozone instrument was zeroed every week with factory-provided scrubber; it showed very little zero drift. Unfortunately, no calibrated ozone source for span check of the instrument was available to take to the field. The manufacturer certified the instrument to be accurate with regular zeroing, even without regular span calibration[10]. Even if there were an undetected non-unity slope between actual and measured ozone values, the ratios between ozone values at different times can be trusted.

A similar uncertainty exists in the accuracy of the PM_{10} measurements. Without the facility to calibrate the Dusttrak instrument in the field (except for regular zeroing), it was used at factory re-calibrated settings. Plans were made to check the calibration in the field by running it for 24 hour periods at Ministry of Environment 24-hour gravimetric PM_{10} sampling sites. However, staff rearrangements in the ministry following the February 1 coup prevented us from carrying out the plan.

2.5 The Weather station

An automated weather station (Portlog by Rainwise Inc., Bar Harbor, ME) was installed on roof of the Hyatt hotel, approximately 20 meters above the ground. It was installed at a corner of the north-south running gable of the hotel's sloping roof, 6ft above the top of the gable, using its own tripod mast and support ropes (Figure 2.5). During Fall 2004 several of its sensors malfunctioned, while its sealed lead acid battery had to be replaced every few days, so it was shipped back to the manufacturer for repairs. It returned to Kathmandu at the end of December 2004 and was reinstalled on the Hyatt roof.

[10] In fact the instrument is not set up to allow span calibration by the user.

Figure 2.5: The weather station on The Hyatt roof.

The weather station ran reliably until March 2005, after which it occasionally lost power, or the desired data logging protocols (resetting itself to default English units and 1 hour logging intervals). During April, May and June it was coaxed into action again every few days, and was able to be deployed on the Bhimdhunga Pass, on the western entrance to the valley on two occasions. At the Bhimdhunga Pass the weather station was set up on a grassy ridge at the watershed of the valley, south of and about 15 meters higher than where the local road crossed the pass. Plans to run it for a few days at the Bagmati river outlet at the southern end of the valley to measure nocturnal down-valley flows were unfortunately not realized due to security concerns.[11]

2.6 The Sodar

The most accurate method of detecting the mixed layer height is through the use of rawinsondes or tethersondes, which provide a continuous track of temperature, pressure and relative humidity as they rise through the atmosphere [*Emeis et al.*, 2004; *Marsik et al.*, 1995; *Reid*, 2003]. In most places worldwide radiosondes are only launched twice a day [*Seibert et al.*, 2000]. There are no regular launches in Nepal. The last launches in Kathmandu were done in 1978. The last launches in Nepal were done during a precipitation study in western Nepal in 2001 [*Barros and Lang*, 2003]. It thus was essential for us to make new measurements of the mixed layer height in Kathmandu for this project. The tallest mast in the valley center that could be instrumented was only 72 meters tall (see Section 2.7), while other sophisticated methods of boundary layer

[11] There were kidnappings by the Maoist rebels, followed by an army crackdown close to our chosen measurement site.

determination, such as lidars, radar wind profilers, radio-acoustic sounding systems, or instrumented aircraft [*Seibert et al.*, 2000] were not available. A Remtech PA-0 minisodar (Remtech S.A., Velizy Cedex, France) purchased for the 2002-2003 pilot project was still available. Sodars are simpler to operate than the more expensive alternatives, but they are both noisy and sensitive to ambient noise.

Over the past three decades, sodars have been widely used to study boundary layer phenomena in many places, and are now considered a "respectable operational technique" [*Kallistratova and Coulter*, 2004]. For example, sodars have been used to detect the mixed layer height during field campaigns in Utah [*Coulter et al.*, 2004], in Japan [*Kataoka et al.*, 2001], and during studies of stratus dissipation in northern Switzerland [*Hünerbein and Richner*, 2002]. Remtech sodars have been used in field campaigns to measure vertical wind profiles routinely on hilltops in New Zealand [*Reid*, 2003], and during a field campaign in Marseille France [*Mestayer et al.*, 1005]. In Marseille and in the Czech Republic[*Keder et al.*, 2004] sodars were used to track winds transport of pollutants viewed with a lidar. Other sodars have been used to measured day-time upslope flows in British Columbia [*Reuten et al.*, 2005], to measure nocturnal downdrafts at the top of the boundary layer in Italy [*Martano et al.*, 2005], and to measure boundary layer winds in Mexico City [*Doran et al.*, 1998] and the Swiss Alps [*Desiato et al.*, 1998].

A sodar works by emitting sounds of known frequencies into the atmosphere, and listening to the backscatter. It measures when and with what kind of frequency shifts, the sounds are reflected back by the atmosphere. Backscatter is affected by the atmosphere's acoustic refractive index, which characterizes the thermal turbulence that scatters sodar signals [*Remtech*, 2003; *Seibert et al.*, 2000]. There are several ways for sodars to detect the mixed layer height [*Argentini*, 2004; *Asimakopoulos et al.*, 2004]. Inversion layers capping mixed layers have stronger backscatter than the mixed layer below; for example, early sodars detected the mixed layer height simply by noting the height (based on sound travel time) of a sharp change in backscatter intensity [*Asimakopoulos et al.*, 2004]. Remtech sodars use an automated algorithm that analyzes vertical wind velocity changes

over short time intervals, detecting the most energetic eddies. Because the mixed layer height calculation requires only a few data points of vertical velocity at a few specific layers, Remtech sodars are able to calculate the mixed layer height to altitudes exceeding their range for measuring other variables [*Asimakopoulos et al.*, 2004]. Generally sodars perform best during the day when there is a convective boundary layer topped by an inversion; they are less able to detect nocturnal boundary layer heights when the inversion extends down close to the ground [*Beyrich*, 1997; *Venkatesan et al.*, 1995]. Comparisons to direct measurements (tethersondes and rawinsonde) showed that the Remtech method performed very well during the day, but that at night it is unreliable, with a tendency to over-predict the mixed layer height [*Asimakopoulos et al.*, 2004]. Early Remtech algorithms were even more error-prone than newer ones [*Emeis et al.*, 2004], such as the one used in the PA-0.

Doppler sodars can compute wind velocities from the frequency shift of the returning sound signals that were sent out along at least three beams. The altitude bins for the velocities at different heights are determined by the time lag between the emission and return of the sound. The Remtech PA-0 sodar uses nine frequencies centered at 3500Hz, with 52 piezo-electric transducers of 1 W acoustic power, which emit sounds in one vertical beam and 4 oblique beams (tilted 30 degrees from vertical) [*Remtech*, 2003]. Using multiple frequencies provides multiple pieces of information for each altitude. Such phased array sodars with computer controlled, digitally switched, beams date back to the early 1990's. The PA-0 was Remtech's newest model at the time of purchase in 2002; we used the second unit ever built. Today there are twenty units in use worldwide, owned by fourteen institutions (www.remtechinc.com/customers5.htm).

Choosing a sodar site requires special considerations. Ambient noise must be low for the instrument to hear its backscatter from increasingly higher altitudes. Rain drops, rustling tree leaves, air conditioners, and automobile sounds can adversely affect the sodar's range. At the same time, the sodar produces significant noise pollution during the day and night that imposes restrictions on its siting. The sodar antenna also must have a completely clear sky view down to large zenith angles to avoid beam reflection and

modification by nearby buildings, trees, mountains, and powerlines. Finding a suitable sodar site in Kathmandu was harder than finding a laboratory site. Together with Professor Ram Regmi from Purbanchal University, we visited more than 12 sites. At many we were turned away simply because of the sodar's noise. Conversely, any sites near roads were too noisy for the sodar. We were finally able to choose and use the roof of the Council for Technical Education and Vocational Training (CTEVT) in Sano Thimi, due east of the airport, and close to valley's geographic center (see Figure 2.6).

Figure 2.6 : The sodar antenna on the CTEVT roof.

Figure 2.7: The power supply and computer controlling the sodar (on a shelf inside CTEVT).

The antenna (on a 5ft tripod) was set up on CTEVT's fourth floor roof, about 10 meters off the ground; the computer controlling it was kept in a small storeroom at the top of the stair landing, connected by a 50 m data cable (see Figure 2.7). The height and shape of the low roof and railing were such that they did not reflect the sodar beam, yet protected the offices and classrooms downstairs from noise pollution.

As mentioned earlier, the sodar malfunctioned shortly after it was installed in September, 2004. Correspondence with the manufacturer for warranty repair approval, plus preparation of export and import papers took till November, 2004, before the instrument was shipped back to Remtech. It returned to Nepal in April, 2005. From late April through early June it ran reliably. We had planned to move the sodar around to a variety of sites in the valley. In particular we were interested in measuring the airflow through the western mountain passes and the Bagmati river outflow at night. However, due to the limited time that the sodar was operational in Kathmandu, plus security concerns at the sites we had intended to use it, we were unable to do so.

2.7 The Temperature Loggers

A well functioning sodar can measure the mixed layer height and a vertical profile of wind velocities, providing reliable measurements during the day. We were also interested in understanding the night time temperature inversions. Inversions in basins have been studied by measuring the evolution of the vertical temperature profiles, for example by frequent up-and-down flights of tethered balloons (tethersondes) [*Whiteman et al.*, 2004b]. Using a commercial tethersonde or launching radiosondes were both beyond our budget. We explored building our own tethersonde based on an EPFL design, but two difficulties stopped us: obtaining helium locally in Kathmandu, and obtaining civil aviation permission to fly a tethersonde in a valley that has an airport with a few hundred daily take-offs and landings that circle over the valley.

An alternative approach was suggested by the work of [*Whiteman et al.*, 2004a], who carried out a detailed field campaign to study the temperature profile in a small basin in Austria, inter-comparing a tethersonde in the basin center with lines of temperature loggers strung up the basin side-walls. They found that inexpensive temperature loggers on basin side-walls provided good proxies for temperature soundings in the basin's free air during times of low wind speeds and stable night-time conditions. Rigorous testing showed that the Hobo H8 Pro loggers (Onset Computers of Bourne, MA), with an external thermistor in an epoxy-potted cylinder, provided very reliable temperature

measurements as long as the thermistor was installed in a radiation shield protecting it from sunlight and IR radiation [*Whiteman et al.*, 2000a]. The same authors also rigorously tested the Hobo Shuttle that can be used to transfer data and reset loggers without taking a laptop to the logger locations. Meanwhile, Hobo temperature loggers have been successfully used to study cold pools in the Columbia basin over horizontal scales of tens of kilometers [*Whiteman et al.*, 2001] as well as on a tower in the US mid-west while studying drainage flows in gullies [*Mahrt et al.*, 2001]. An urban temperature profile study in Tokyo also used temperature sensors on a tower [*Kanda et al.*, 2005].

As mentioned earlier, a total of nine temperature loggers with radiation shields were available starting in Phase 3, including seven Hobo H8 Pro's. One was set aside for mobile measurements, and the other eight loggers were installed at fixed locations at the valley center and valley rim. Four Hobo temperature loggers were installed on the 72 meter tall Nepal Television (NTV) Metro transmission tower, at the heavily fortified Singha Durbar government compound in the valley center (Figure 2.8). The top 10 meters (red-and-white part on Figure 2.9) containing the TV transmitters was inaccessible; the top logger was thus installed at the upper platform, at 62 meters above ground, others at 48m, 26m, and 5m. Another temperature logger was installed at 48 meters elevation on Bhimsen Stambha (commonly known as Dharahara) at Sundhara in central Kathmandu: a 19th century monument that had recently been renovated. (This logger was moved to Hattiban ridge (1785m) starting in early April). Compared to NTV Metro tower's caged ladder, the Dharahara had a comfortable spiral staircase inside and thus provided a suitable location not just for an accessible temperature logger, but also to collect bag samples 48 meters above ground, as described in Section 2.2.7.[12]

[12] The only other structures in the valley of comparable height are two industrial chimneys east of the city, and a radio mast to the south. Both have only unprotected vertical ladders and were thus not considered.

Figure 2.8: Arrows point at the four temperature loggers on the NTV Metro tower. From the bottom up, the loggers were mounted at 5m, 26m, 48m, and 62m above ground level. The bottom two were mounted on the ladder cage, and the top two on platform railings.

Figure 2.9: On the left: NTV Metro, on the right the Dharahara.

Other temperature loggers were installed at an elevation of 1975 meters above sea level, at the Hotel View Point in Nagarkot (at the end of a 3m horizontal pipe reaching out from hotel's roof level), on a tree at Kharipati at an elevation of 1375 meters at the base of Nagarkot, and at Pullahari Monastery (1500 meters), on a hilltop overlooking the Bouddha area (Figure 2.10).

Figure 2.10: Temperature loggers on a pipe extending from the roof of Hotel Viewpoint, Nagarkot (left), on a tree at Kharipati and on a bamboo pole at Pullahari monastery, on a little hill.

A ninth temperature logger (in its radiation shield) was often attached to the rental car roof, and its travels were automatically tracked by a GPS. During Phase 2 and 3, several attempts were made to sample the evolution of the vertical profile in the mornings and evenings by repeatedly driving up and down the Nagarkot road from 4 pm to 8 pm, and from 5 am to 10 am. Attempts were also made at assessing the horizontal temperature gradient across the city (and detecting potential urban heat island effects) by driving night-time cross sections through town. Using a temperature logger on a car tracked by GPS is a well established method for assessing urban heat islands [*Saitoh et al.*, 1996; *Straka et al.*, 1996]. The method has even been tested driving over the Brenner Pass in Austria; it was found that driving speeds had little effect on temperature measurement accuracy [*Mayr et al.*, 2002].

2.8 Bag Sampling and Analysis

We had only one functioning CO instrument in Kathmandu, yet were interested in understanding the spatial heterogeneity of the gas – especially its concentrations upwind of the city, and on mountain tops surrounding the valley. The standard method for studying long-lived trace gases at locations without *in-situ* instrumentation is to use a pump to collect pressurized air samples in evacuated stainless-steel or glass flasks, ship the flasks to a laboratory, and analyze them within 1 week to 6 months [*Altuzar et al.*,

2005; *Gros et al.*, 1999; *Khalil and Rasmussen*, 1994; *Novelli et al.*, 1994; *Novelli et al.*, 1992; *Tyler et al.*, 1999]. Spatial heterogeneity of CO in an urban area was studied in Santiago de Chile by [*Chen et al.*, 1999] with the help of 30 university students and faculty spread around the city, who simultaneously filled 45 flasks at 5:00 am and 43 flasks at 9:00 am of the same day; these flasks were subsequently analyzed at a laboratory in UC Irvine, providing contour maps of CO around the city, as well as methodological inspiration to us.

Our objective was to do a weekly collection of at least hourly samples at several locations, over the full 24 hour diurnal cycle, and then to analyze the samples within days at our lab in Kathmandu. Had we used stainless steel flasks, the expense and transportation hassles would have severely limited the number of samples we could collect. We thus chose to collect samples in inflatable gas sampling bags. In the past, [*Paino*, 1993] had done a study in Boston collecting air samples in 5-liter tedlar bags, analyzing their contents on a gas filter correlation CO instrument. Tedlar bags (SKC, Inc., Pennsylvania) have previously been used for CO sampling by [*Fan and Zhang*, 2001], and by [*Baek et al.*, 1997], who analyzed the samples with a GFC instrument.

In Spring 2004, we tested a variety of SKC bags with sizes of 1 L, 3 L, 5 L, and 10 L, with stainless-steel and polypropylene fittings, and made of tedlar or foil. We chose to use the 4-ply FlexFoil bags (SKC model 245-25), which were stronger than tedlar bags. Opaque foil bags keep CO samples more stable; they specifically prevent CO formation by photochemical breakdown of other VOCs in the sample [*Novelli et al.*, 1992]. They were certified to keep CO, CO_2 and methane samples stable for 5 days. Given the ~ 1 minute lag time for the 300EU CO instrument to show a stable reading, and given it's pump's 1.7 L/min flow rate, the 1 L bags were far too small. The 3 L bags were often unable to provide a stable reading before running out of sample, while 10 L bags were bigger than necessary, appeared fragile, and would have doubled the analysis and flushing time. Hence we settled on 5 L bags and purchased 190 of them, along with 6 battery-powered pumps capable of pumping a liter a minute (SKC GrabAir). The objective was to have 144 bags (for 6 x 24 hourly samples) plus spares. Given the loss

rate of bags (torn, leaking), the number of spares turned out to be barely adequate. By the last sampling campaign, almost half the bags were either leaking, or had to be prevented from tearing by having their seams clamped with jumbo clips and cardboard strips.

On several occasions we decided to have fewer than 6 sites but instead to collect more frequent samples, especially during morning and evening transitions. Bag sampling campaigns were carried out 2-3 times a month during Spring 2005, with the help of the local research assistants as well as several student volunteers from the Department of Environmental Science at Tribhuvan University in Kirtipur, Kathmandu. Managing the sampling campaigns was learned from short-term testing in Kathmandu plus a full-scale 24 hour trial run in January 2005 that was followed by a detailed feed-back questionnaire filled out by all participants. The lessons that were incorporated included shifting the start and end times to the late morning, renting warmer sleeping bags, having at least two people per site, packing more spare pump batteries, improving the record-keeping forms to be filled out when each bag was filled, adding flushing start and end times on the form to ensure that pumps were properly flushed before each use, and adding visibility and wind direction onto the forms. Also, a wooden frame, designed through a competition among the students, was built for each pump to protect the pump's fragile inlets, outlets and particle filters, and to ensure that sample collection happened sufficiently high above ground.

Typically, by the evening before a bag sampling campaign, the following tasks would be completed: all bags triple-flushed, leak-checked, and inventoried, with leaking bags removed; expected number of students and sampling locations determined; sleeping bags and tents rented from a camping store; bottled water and cookies stocked; permissions obtained for the planned sampling sites; and reservations made for a car with driver. On the morning of a sampling campaign, the students, assistants, and the author would meet at the laboratory at 7 am, and after a brief discussion of objectives, would pack duffel bags destined for each site according to checklists,[13] making sure to have packed tents,

[13] The king's closing of mobile phone services made it harder to report missing items from the field, making detailed pre-departure checks essential.

sleeping bags, flash lights, drinking water, food, clipboards, bag sampling forms, sampling schedules, enough sampling bags including spares, pumps with clean particle filters, thermo-hygrometers, spare batteries, and, for some sites, security clearance letters. By 8:30 or 9 am the downtown bound students would leave by taxi; the ones bound for Nagarkot, up a paved road to the eastern valley rim, and to places enroute, would leave by rental car; and the author would drive the students bound up dirt roads to the southern or western valley rim.

Bags were usually filled hourly during the day and night, and half-hourly or more frequently during evening and morning transitions. Filling a bag involved the following procedure: flushing the pump with ambient air for 5 minutes, making sure that the inlet tube was projecting at least 2 feet off the ground (usually higher) and that the tube connections were tight; recording filler name, date, pump number, and bag number; connecting the bag to the pump outlet; noting the time, turning on the pump, and opening the bag valve; recording the temperature, humidity, wind direction, and wind speed (Beaufort scale); looking through a site-specific visibility table, checking off which landmarks were clearly visible, which were barely visible through haze, and which were blocked by fog or clouds; watching the bag as it inflated, making sure it did not over-inflate; shutting the bag valve, noting the time, turning off the pump, and recording once again the temperature, humidity, wind direction, and wind speed Beaufort scale; disconnecting the inflated bag from the pump, and packing it in one of the duffel bags. Students also noted what happened during bag filling, such as passing vehicles, arrival of smoke from a barbeque restaurant at Dharahara, or observations of valley fog from Nagarkot and Hattiban. This procedure would be repeated throughout the day and night for each bag sample. Figure 2.11 shows bag filling in progress.

The following day, in the early afternoon, the students, assistants, sampling equipment, and 12-15 duffel bags filled with inflated sampling bags would return to the lab. The duffel bags would be labeled and hung up (see Figure 2.4, right), inventories checked, and everyone would go home and rest. Over the next three days the bag contents would be sent through the API 300EU CO instrument (via the valve switching described in

Section 2.3). The instrument's display screen (updating frequency 1 Hz) would be watched for a stable reading, which would be manually recorded, while the time would be recorded for future cross-checking with the instrument's data logger. Failure to reach a stable reading would also be recorded and such a sample would be excluded from analysis.

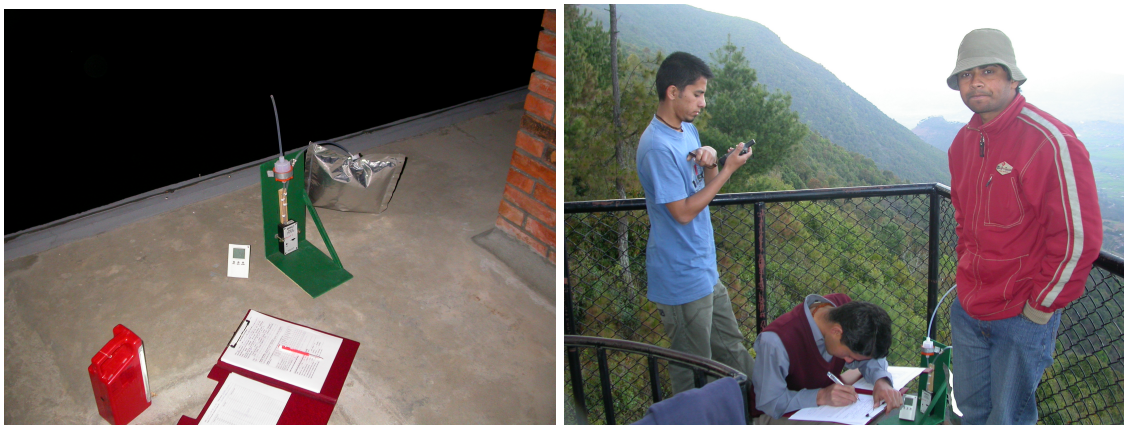

Figure 2.11: Bag sampling on the Pullahari monastery roof (left) and Hattiban viewtower (right). Note the green wooden frame holding the pump and filter.

Successful bag sampling campaigns were carried out eight times between February and May 2005, with a variety of site combinations. Sampling was done seven times on the roof of the Hotel Viewpoint, at the top of Nagarkot Peak on the eastern valley rim, next to our temperature logger, at the site of occasional ozone measurements. Bag samples were collected three times on the view tower on Hattiban ridge (1785 m, south of the valley) to compare to the Nagarkot measurements.

Samples were collected five times at Dharahara tower in Sundhara, at the edge of Kathmandu inner city. Each time bags were simultaneously filled at the terrace/window at the top of the tower, and on the steps or in the little park at the base of the tower. On February 17-18, samples were collected simultaneously at up to five locations on and around the tower. Three times bag samples were collected at the army base on Bhimdhunga Pass (1500 meters), one of the western entrances to the valley; on two occasions the weather station was operated on the pass at the same time, while sampling frequency was raised to 2-4 samples per hour. Bag samples were collected five times at

CTEVT, the sodar site east of the airport, to compare to the east-of-the city measurements at the Hyatt lab. Single-day bag samplings were carried out at Tribhuvan University in Kirtipur (at the base of Hattiban), at Pullahari monastery hilltop (1500 meters), and at Lubhu, in the brick-factory region southeast of the city.

2.9 Time-lapse photography of morning fog

Stable atmospheric conditions suppress vertical mixing of smoke plumes, fog, and elevated pollution layers. Inversion-trapped fog at a valley bottom often has a flat top. The evolution of fog and trapped pollution layers can be observed and filmed from a mountain top [*Rakovec et al.*, 2002]. During the mornings of February 10, 2005 and February 26, 2005, a tripod and a high quality digital camera (Nikon D70, with Nikkor lenses covering a zoom range from 18mm to 210mm, Nikon, Japan) were set up on the view tower on Hattiban ridge between 5 and 6 am (Figure 2.12).

Figure 2.12: The digital camera on the Hattiban view tower overlooking the Kathmandu Valley.

The evolution of the valley fog was photographed repeatedly over several hours. Three wide-angle framings were repeated every few minutes (generating a time-lapse sequence) while in between, the camera was rotated to zoom in on specific smoke plumes and fog edges. On December 3, 2005, another round of time-lapse photography was carried out from the same location from 5 am until 11:30 am, taking photos at a higher frequency, with a wider angle lens (Tokina 12-24 mm, THK, Japan). The camera angle was kept

constant, while each time a picture was taken at both 12 mm and 24 mm focal lengths (18 mm and 36 mm equivalent on 35 mm film cameras), thereby capturing one frame covering the entire valley, and one focusing on the urban central region.

2.10 Chapter Summary and Conclusion

This chapter provided an overview of the field measurements carried out in Nepal during the dry season 2004-2005. Figure 2.13 provides a visual overview of all fixed instrument sites around the Kathmandu Valley. The Hyatt lab and the sodar at CTEVT are marked by yellow and red squares, respectively, while the temperature logger and temporary weather station sites are marked by colored circles. Many of the bag sampling sites coincided with temperature logger sites. The coverage of the valley was better in the east-west direction than in the north-south direction. We would have liked to set up the weather station and collect bag samples in the Bagmati river outflow valley (foreground), but were hindered by safety concerns.

Location	Description	Longitude	Latitude	Altitude
Hyatt lab	Enclosure on Hyatt fire-escape	27°43.295'N	85°21.424'E	1350 m
Hyatt roof	Weather station above top gable	27°43.275'N	85°21.422'E	1363 m
Nagarkot	Pipe from roof of Hotel Viewpoint	27°43.422'N	85°31.527'E	1972 m
Kharipati	Tree among fields	27°42.453'N	85°28.226'E	1372 m
TV tower	62 meter tall metal tower	27°41.771'N	85°19.603'E	1300 m (base)
Dharahara	City-center 52m tower with park at base	27°42.015'N	85°18.705'E	1294 m (base)
CTEVT	Roof of technical college building	27°40.929'N	85°22.477'E	1321 m
Hattiban	10m view tower overlooking valley	27°37.737'N	85°16.419'E	1784 m
Pullahari	Pole on 7storey tall monastery roof	27°44.741'N	85°22.495'E	1476 m
Bhimdhunga	Grassy ridge, 50 m from pass	27°43.582'N	85°13.838'E	1496 m

Table 2.4 Coordinates of the measurement sites.

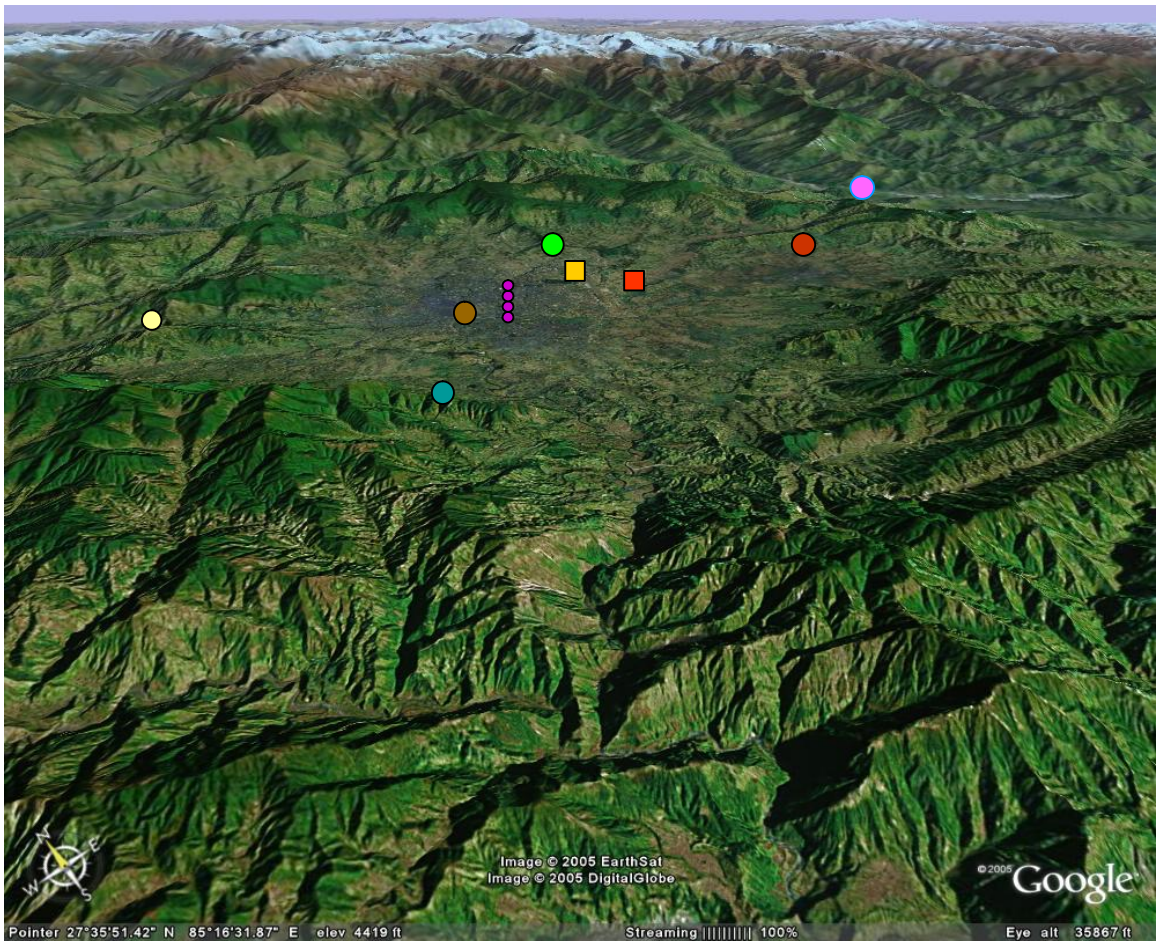

Figure 2.13: Locations of the instrument and temperature logger sites super-imposed on a Google Earth image, looking at the valley from the south. From left to right, we see: Bhimdhunga (light yellow circle), Hattiban (blue circle), Dharahara (brown circle), NTV tower (four purple circles), Pullahari (green circle), Hyatt lab (yellow square), CTEVT sodar site (red square), Kharipati logger (red circle) and Nagarkot (pink circle).

CHAPTER 3: THE FIELD RESULTS

3.1 Chapter Introduction

This chapter describes results of the dry season 2004-2005 field measurements in the Kathmandu Valley, focusing on data from interesting time periods. Section 3.2 presents data from a week in October 2004, at a time when just the CO, ozone, and PM_{10} instruments were working (Phase 2). Section 3.3 contrasts this to data from a month later, during a week in November 2004. Sections 3.4 and 3.5 describe data collected during a week each in January and early February, at a time when when additional data from the weather station and then from the temperature loggers were also available. Section 3.6 takes a closer look at a 48 hour period centered around February 10, 2005, when there was interruption-free data from most instruments, plus a bag sampling campaign and time-lapse photography. Section 3.7 examines data from a six day period in late February, and Section 3.8 from a week in April. Section 3.9 describes late spring data from the repaired sodar, while Section 3.10 focuses in upon a second 48 hour period with good data, centered around May 10, 2005.

After that, several sections describe results of short-term measurements at other locations around the valley. Section 3.12 returns to the spatial distribution of CO by describing the bag sampling campaigns conducted during the rest of Spring 2005. Section 3.13 examines at what was learned by moving the weather station to Bhimdhunga Pass while collecting bag samples there. Section 3.14 presents the results of running the ozone instrument on Nagarkot peak. The chapter thus provides an overview of what was learned directly from the field measurements. Discussion of questions and hypotheses arising from the data follows in Chapter 4.

3.2 A Week in October

Figure 3.1 shows CO, PM_{10}, and ozone measurements at the Hyatt lab during the week starting Monday, October 18, 2004. The figure illustrates several key points. First, there

were clearly repeating diurnal patterns, especially for CO and ozone[14]. This suggests that conditions responsible for the pollutant fluctuations did not vary much from day to day. It suggests local forcings; remote places exposed to a variety of air masses arriving from different directions do not exhibit this kind of regularity [*Cheung and Wang*, 2001; *Simmonds et al.*, 1997].

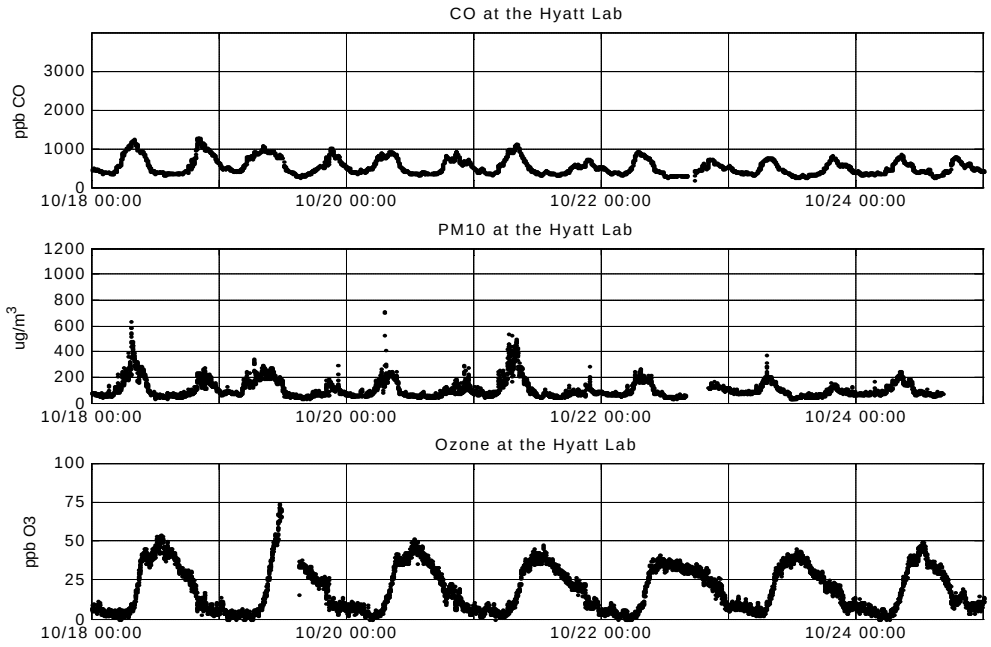

Figure 3.1: Measurements of CO, PM_{10} and ozone during a week at the Hyatt lab in October 2004. October 18 was a Monday. Vertical scales chosen for consistency with later figures.

Every day CO showed a peak in the morning and a peak in the evening. Morning and evening peaks in urban CO records have been found elsewhere, before, including in Bangkok [*Zhang and Oanh*, 2002], Santiago de Chile [*Rappenglück et al.*, 2000; *Rappenglück et al.*, 2005; *Schmitz*, 2005], Buenos Aires [*Bogo et al.*, 2001b], Greece [*Gros et al.*, 2002], and, at times in Hongkong [*Wang and Kwok*, 2003]. In southern California [*Qin et al.*, 2004] and in Brisbane [*Morawska et al.*, 2002] morning and evening CO peaks were found to be stronger on weekdays than on weekends. Often the

[14] Ozone shows a higher peak on October 19 just before a power failure; we cannot exclude the possibility that this may have been produced locally by faulty electrical equipment.

peaks were a direct result of the local rush-hour traffic emissions; for example in Buenos Aires and Santiago de Chile they correlated very well with traffic volumes. Does that mean the morning and evening CO peaks in Kathmandu were just a result of morning and evening peaks in emissions?

This particular week was deliberately chosen not only because it had almost interruption-free data, but because it led up to a major festival, thus covering a variety of emission patterns. Monday and Tuesday (October 18-19) were regular weekdays for people going to work, but schools were already closed. Wednesday through Friday were official holidays. Several hundreds thousands of people traveled out of the valley to their ancestral homes to celebrate the *Dashain* festival, creating heavy traffic on roads leaving the valley throughout the day on Wednesday and Thursday. Saturday was *Tika*, the main day of *Dashain*, when most people stayed home, and Sunday was a day when a lot of people went to visit nearby relatives. Only Monday and Tuesday had relatively normal traffic patterns with morning and evening rush hours.

Looking more closely at the subplot of CO data, one sees that CO peaks *were* slightly lower during the holidays in the later parts of the week. But the fact that we still found morning and evening peaks every day, including on days with no rush hours, indicates that the peaks were not simply caused by the timing of traffic emissions, even if traffic intensity might have an effect on peak amplitude. Local CO emissions are not the only factors that affect the diurnal cycle of atmospheric CO concentrations near the ground. For example in rural Thailand, CO from biomass combustion was found to have night-time highs and day-time lows due to reduced night-time ventilation caused by inversions [*Pochanart et al.*, 2003].

Another major finding is that the Kathmandu Valley's air was polluted during the entire week. The morning and evening CO peaks regularly approached or exceeded 1 ppm on the work-days. Night-time and afternoon values, although lower, were still far higher than typical northern hemispheric clean air. In clean areas at Nepal's latitude, tropospheric CO mixing ratios are usuallyl around 150 ppb [*Novelli et al.*, 1992]. During

the entire dry season CO levels rarely dropped below 350 ppb. Even at its cleanest, the Kathmandu Valley air still showed significant pollution.

The figure also shows that CO and PM_{10} were highly correlated, with PM_{10} showing two daily peaks at the same times and of the same durations as the CO peaks. For example we find the same broad peak appearing on Tuesday morning, a narrow peak on Tuesday evening, and a tall peak on Thursday morning. During the second half of the week (the holidays) PM_{10} showed far smaller but still distinct peaks, consistent with the reduced holiday traffic. We can interpret this as an indication that the festival may have shut down PM_{10} sources to a greater degree than it shut down CO sources. Cooking exhausts (from LGP and kerosene) can be a significant source of CO. However, if morning and evening cooking[15] were to be the main source of the morning and evening CO peaks, we would expect to see a big difference in the timing of the peaks between the work days (Monday-Tuesday), and some of the later festival days that would have had significant late-morning and mid-day cooking. We do *not* see such a temporal shift in peaks; we only see slight differences in peak amplitudes. We thus do not have a way of explaining the regularity of CO or PM_{10} peaks observed during this week on the basis of emissions patterns alone. As we shall see in Chapter Four and beyond, the diurnal variations in ventilation, as determined by the dynamics of the valley's atmospheric boundary layer, play a major role in shaping the diurnal cycle of pollutant concentrations in the Kathmandu Valley.

Ozone had daily maximum concentrations around 40-50 ppb, and night-time values near zero throughout the week. The night-time depletion of ozone in valley-bottom air comes as no surprise: there are no night-time local sources of ozone, but two possible loss pathways: dry deposition to surfaces [*Warneck*, 2000] and reaction with NO to form NO_2, which cannot photolize until after sunrise. In fact even in areas outside of, but near cities, ozone has been found to be depleted by NO at night [*Güsten et al.*, 1998; *Wang et al.*, 2003]. We see in Figure 3.1 that ozone levels rose every morning at about the same time.

[15] Most people in the Kathmandu Valley follow a meal pattern consisting of a large warm meal in the morning, before work or school, followed by light snacks in the afternoon and a second large warm meal at night. On weekends, festivals and other holidays, the morning meal is often delayed until noon or later.

Ground-level ozone in urban areas rises in the morning due to two possible processes: the photochemical formation of ozone after sunrise, and the downward-mixing of ozone from aloft. The rapid growth from minimum to maximum daily ozone levels suggests a strong contribution by the second process.

3.3 A Week in November

Figure 3.2 shows CO, PM_{10}, and ozone four weeks later, on the same vertical and horizontal scales as Figure 3.1. CO and PM_{10} still showed matching daily peaks in the mornings and evenings, but now the CO peak values were much higher, frequently exceeding 2 ppm. Ozone showed a very similar pattern to the one in October, with mid-day values around 50 ppb and night time values near zero. We see that CO and PM_{10} peak and trough values fluctuated from day to day to a greater extent than they did a month earlier. For example, during the night of November 16-17 they never dropped down to their usual lows. Very likely this was a result of some unusual weather patterns. Only starting late December 2004 was reliable weather station data available to help interpret the chemistry measurements.

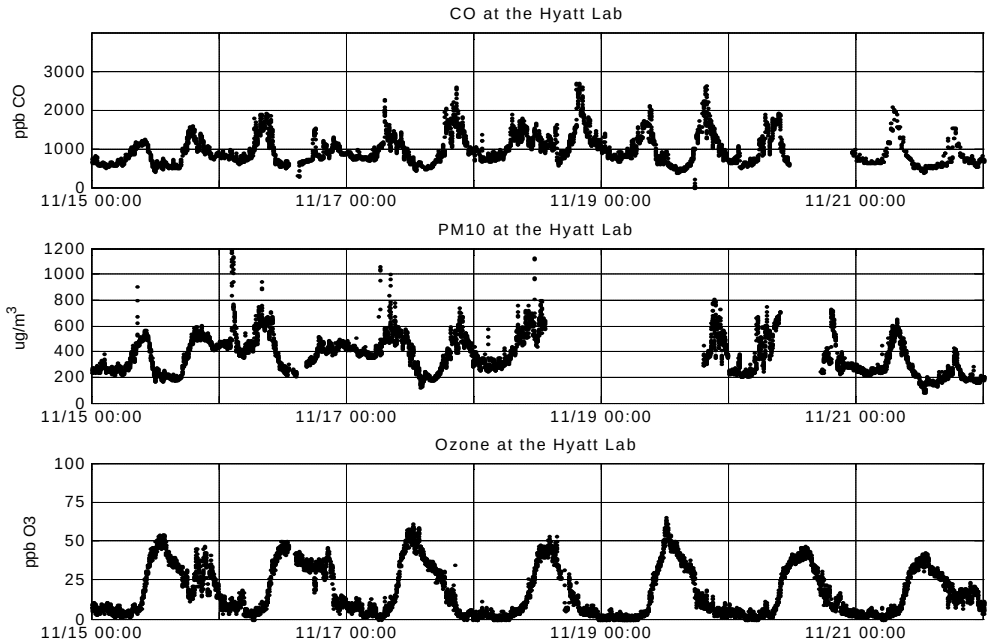

Figure 3.2: Measurements of CO, PM_{10} and ozone during a week at the Hyatt lab in November 2004.

3.4 A Week in January

Figure 3.3 presents data collected during a winter week in early January. At this time there is additional information provided by the surface weather station; unfortunately, the PM_{10} data was lost during the first half of the week. Many of the same patterns seen before are again visible. CO values during the afternoons and nights were similar to what was observed in October, but the morning and afternoon peaks were 2-3 times higher. The weekend (last 2 days) had lower CO peaks than many of the weekdays.

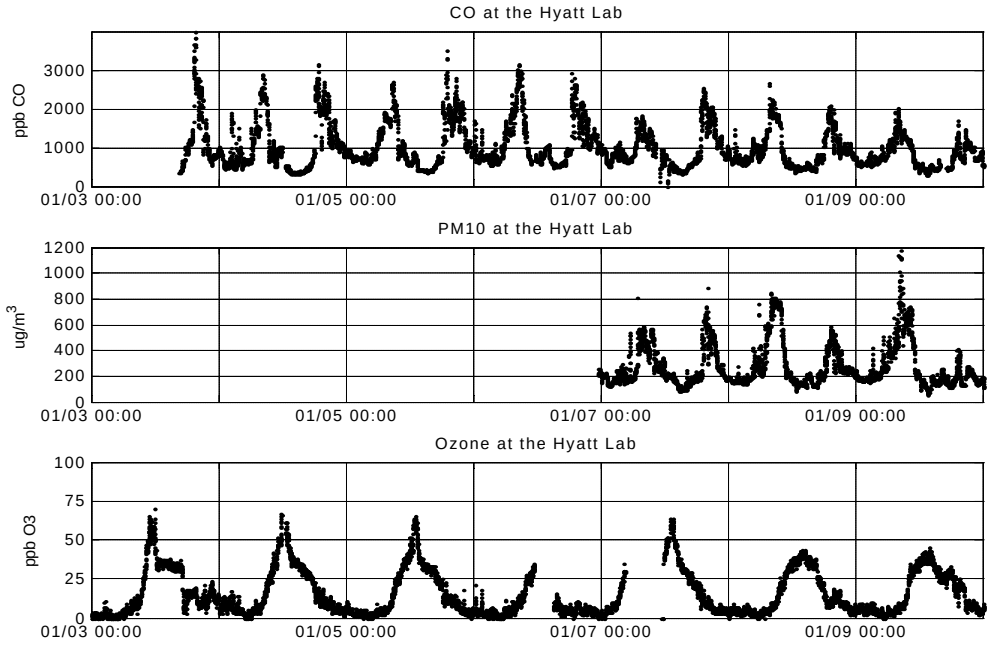

Figure 3.3: CO, PM_{10}, and ozone measurements at the Hyatt lab during a week in January 2005.

From the relative humidity data, as well as from the temperature and dew-point data (Figure 3.5), we see that there was fog on several mornings, but that the fog only lasted for a few hours. This matches with observations made during the AGS project in January 2003, when the DOAS would quit working between 5 am and 10 am because fog obscured its light path. In Figure 3.5 fog can be identified not only by the 100% relative humidity, but also by noting that once the temperature reached the dew point, both the temperature and the dew point kept decreasing (as water condensed out). This is clearly visible on January 3, 5, 7, 8, and 9. The barometer data from the weather station shows a late-morning peak and an afternoon trough in pressure every day.

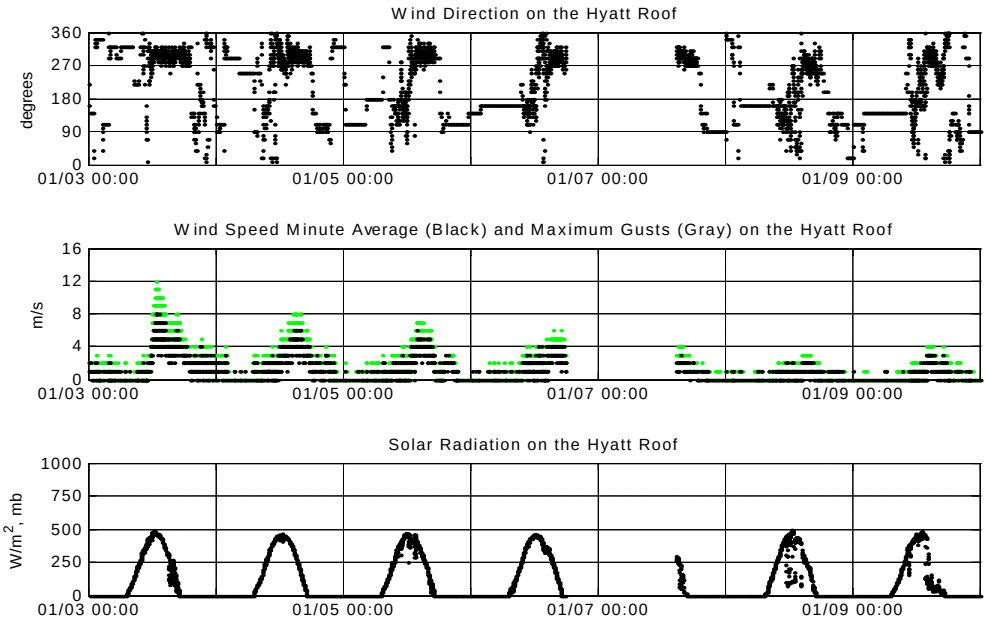

Figure 3.4: Wind direction, wind speed and solar radiation from the weather station on the Hyatt roof during the same week in January 2005.

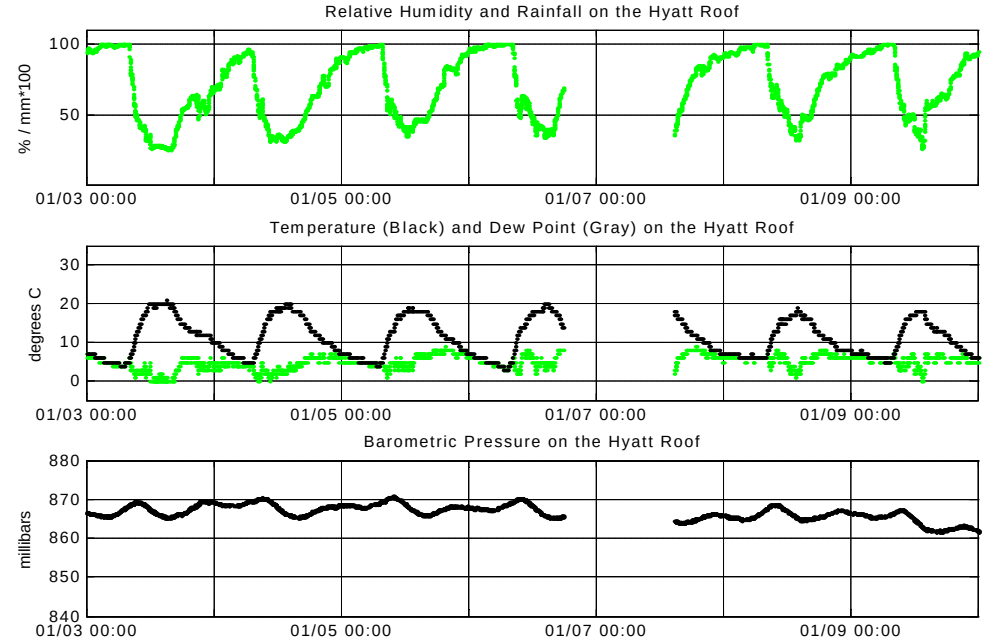

Figure 3.5: Relative humidity, temperature, dew point, and barometric pressure from the weather station on the Hyatt roof during the same week. There was no rainfall that week.

From the wind and solar radiation data in Figure 3.4, we can see that winds were the weakest at night, reaching the highest speeds during mid-afternoon when they were westerly. The weather station on the Hyatt roof was located about 22 meters above ground. Conditions might have been more stagnant near the ground, but wind speed measurements above the roof level give a better indication of pollution transport than at the ground.

Mountain basins often experience a sharp increase in wind speed at the point in time when the nocturnal inversion has completed dissipating [*Banta and Cotton,* 1981; *Whiteman,* 1982]. The timing of the onset of the fast westerly winds is discussed again again later in the dissertation. Figure 3.4 also shows that on sunny days (January 3-6) the strong westerly (or northwesterly) winds in the afternoons were sometimes preceded by weaker easterly (or southeasterly) winds. It is interesting to examine the findings of an earlier study that used MM5 to simulate the Kathmandu Valley over a four day period in March 2001 [*Regmi et al.*, 2003]. They found each day that the valley first experienced southerly flows coming up the Bagmati Valley, which were subsequently pushed aside by a much stronger westerly flow entering the valley through the western valley rim passes. In addition we also see that on cloudy days (January 8, 9) the afternoon wind speeds were less, while wind directions showed less distinct westerlies.

3.5 A Week in February

This section presents a week in early February that exhibited a wider range of weather conditions including rainy and cloudy days. By this time temperature loggers were operating at Nagarkot peak, Kharipati (Nagarkot base) and on the TV tower at the valley center supplementing the data recorded at the Hyatt. This provided additional information about the diurnal cycle of the valley's vertical temperature profile and horizontal temperature gradients. The TV tower data for the second half of the week was lost when the loggers could not be accessed in time while we were still re-negotiating tower access with the army following Nepal's military coup on February 1, 2005.

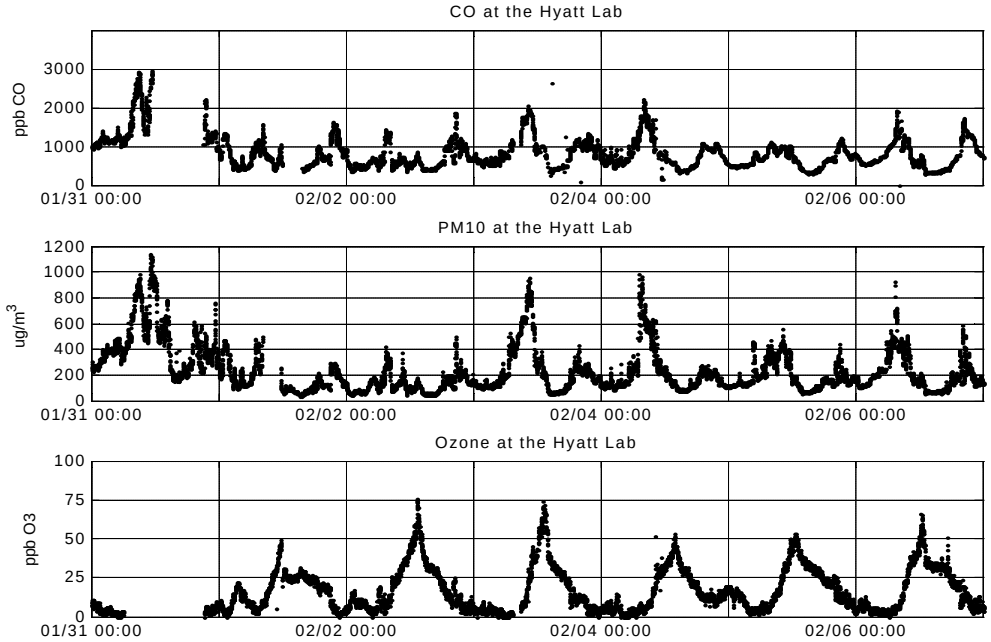

Figure 3.6: CO, PM_{10}, and ozone measurements at the Hyatt lab during a week in January 2005.

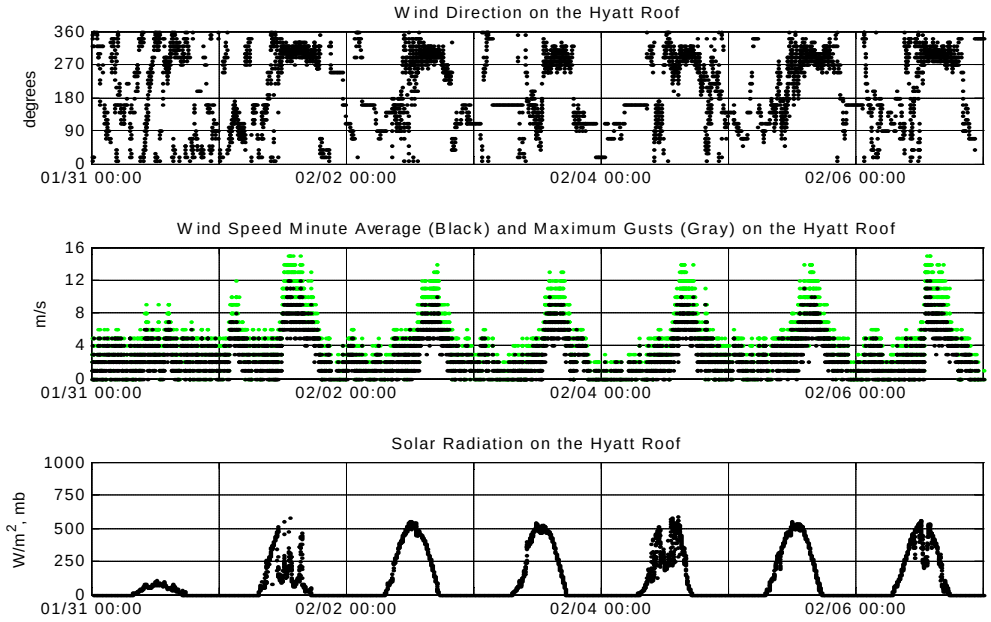

Figure 3.7: Wind direction, wind speed and solar radiation measured by the weather station on the Hyatt roof during the first week of February 2005.

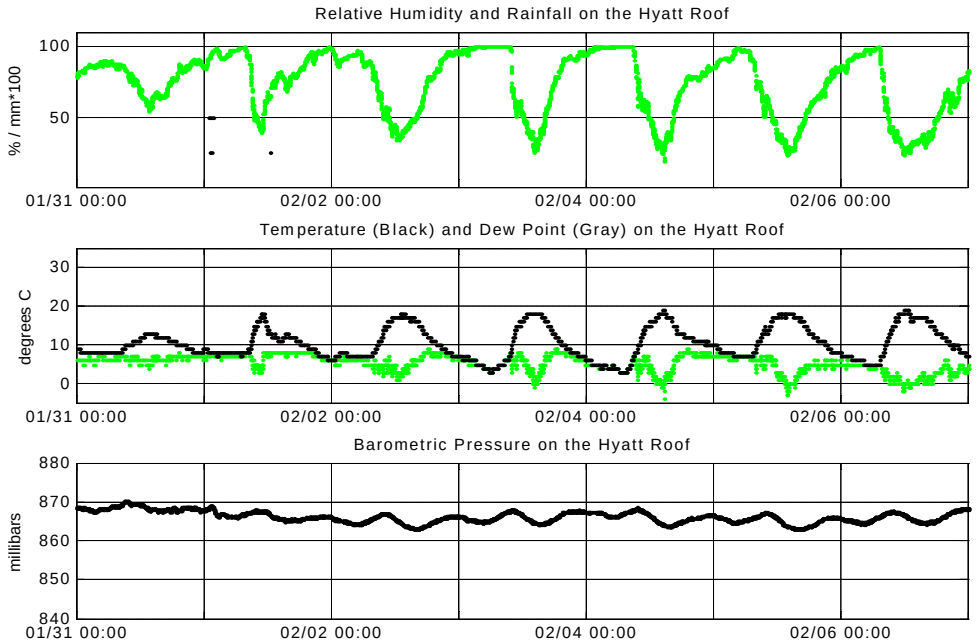

Figure 3.8: Relative humidity and rainfall, temperature and dew point, and the barometric pressure measured by the weather station on the Hyatt roof during the same week.

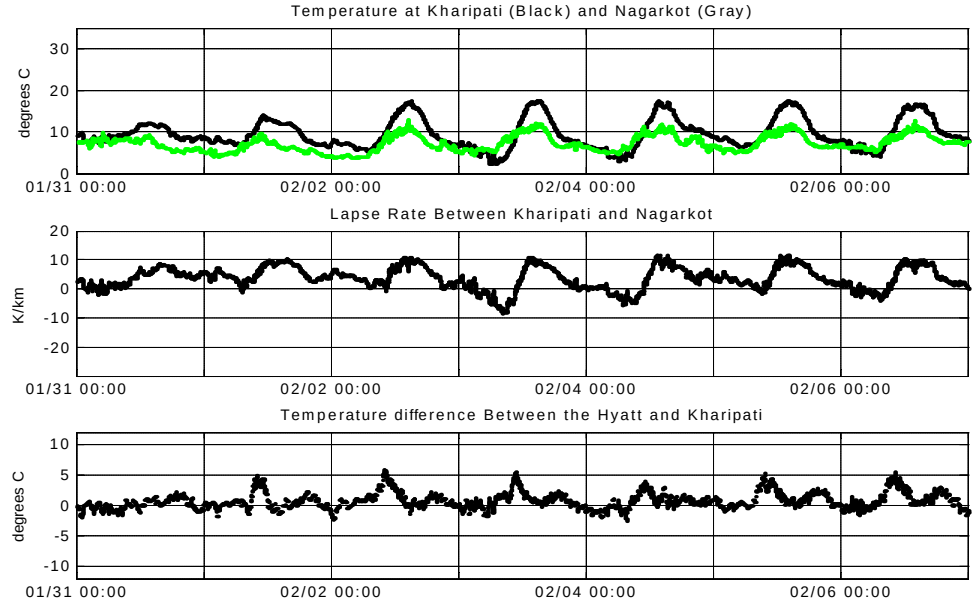

Figure 3.9: Temperature logger data from Nagarkot and Kharipati during the same week. The top panel shows the actual temperatures in degrees C, while the middle one shows the lapse rate in degrees K/km. The bottom panel shows the temperature difference between the Hyatt weather station and Kharipati.

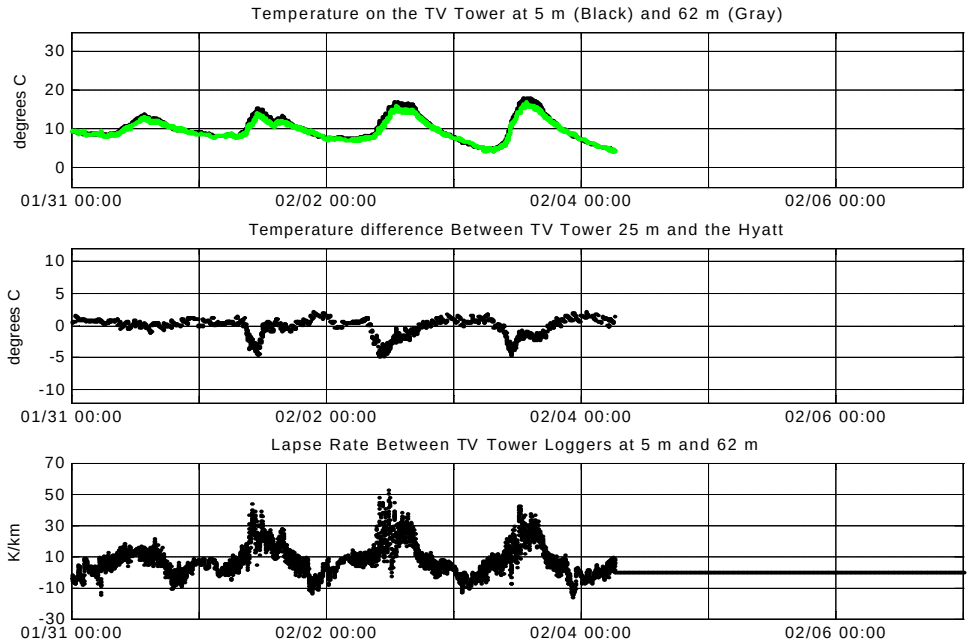

Figure 3.10: Temperature logger data from the TV tower during the same week. The top panel shows the actual temperatures at the tower top (black) and bottom (gray), the middle panel shows the horizontal temperature difference between the tower and the Hyatt weather station, while the bottom panel shows the lapse rate between the tower top and bottom.

The weather station data shows that January 31 (Monday) was a cold, sunless day followed by rain during the night. Tuesday, Friday and Sunday had patches of clouds, while Wednesday, Thursday, and Saturday were sunny. We see that on the rainy days there were gusty winds with rapidly changing directions during the day and night. The rest of the days (which were sunny) exhibited many of the same patterns already discussed. Wednesday and Thursday morning had particularly high CO and PM_{10} peaks.

The temperature logger data and lapse rate calculations show that a temperature inversion formed on many nights (especially on February 3rd), but that the air was well mixed during the day. The inversion extended almost down to the ground, suggesting that vertical mixing was strongly suppressed at the elevations where most of the pollution emissions took place. The temperature inversion was much weaker on Monday and Tuesday nights following the two almost sun-less days. On all sunny days the air was least stable during the afternoon, a time corresponding to the time of high wind speeds.

This is not surprising: day-time convective boundary layers allow winds to penetrate down to the bottom of basins [*Banta and Cotton*, 1981; *Whiteman et al.*, 1999; *Whiteman and Doran*, 1993; *Zhong et al.*, 2001]. Near the surface, measured by the TV tower, we see rapid fluctuations with some very unstable thermals (lapse rate exceeding 40 K/km). Over the 600 meter altitude difference between Kharipati and Nagarkot the temperature difference produced a lapse rate close to the dry adiabatic lapse rate (9.8 K/km) every afternoon.

The formation of a nocturnal cold pool in the valley is evident in Figure 3.9 (top); except during overcast or rainy conditions, air in the valley bottom was colder than on Nagarkot peak during the night. Over the depth of the valley the stability increased throughout the night (Figure 3.9 middle), while at the TV tower the strongest inversion was already reached around midnight (Figure 3.10 bottom). Looking at the horizontal temperature gradients (Figure 3.9 bottom) and (Figure 3.10 middle), one sees that the temperature on the Hyatt roof was very similar to the temperature at the same elevation on the TV tower and in Kharipati, except during the late morning, when it was warmer than both.

3.6 Zooming in to a 48 Hour Period

The previous four sections provided an overview of day-to-day and seasonal patterns in the Kathmandu Valley by looking at a week each. On days without unusual weather conditions or unusual human activities, the patterns of air pollution and meteorology showed remarkable day-to-day similarity, with daily twin peaks of CO and PM_{10}, a day-time maximum of ozone, afternoon westerly winds, and a stable stagnant cold pool at night. To better understand the typical diurnal patterns, this section focuses in upon a representative 48 hour period that had some of the best data available: noon on February 9, 2005 through noon on February 11, 2005. In addition to perfectly functioning CO, ozone, PM_{10} and weather station sensors at the Hyatt plus 8 temperature loggers, this time period also included 24 hours of bag sampling at five locations (late morning of February 9 through late morning of February 10), as well as time-lapse photography of the morning fog from Hattiban ridge.

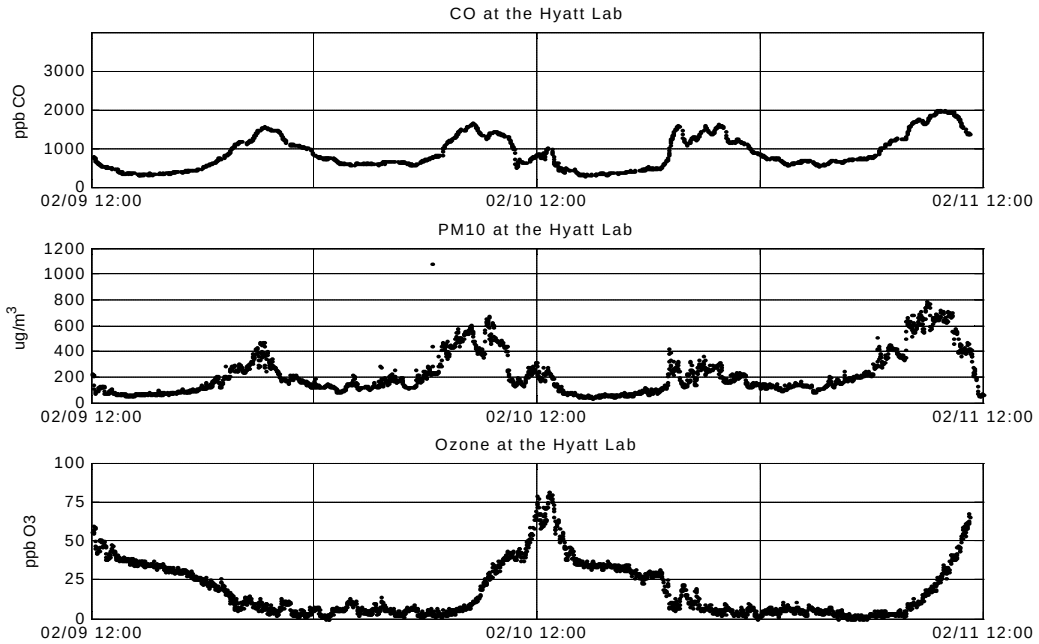

Figure 3.11: CO, PM_{10}, and ozone measurements at the Hyatt lab from noon on February 9, 2004 through noon on February 11, 2004.

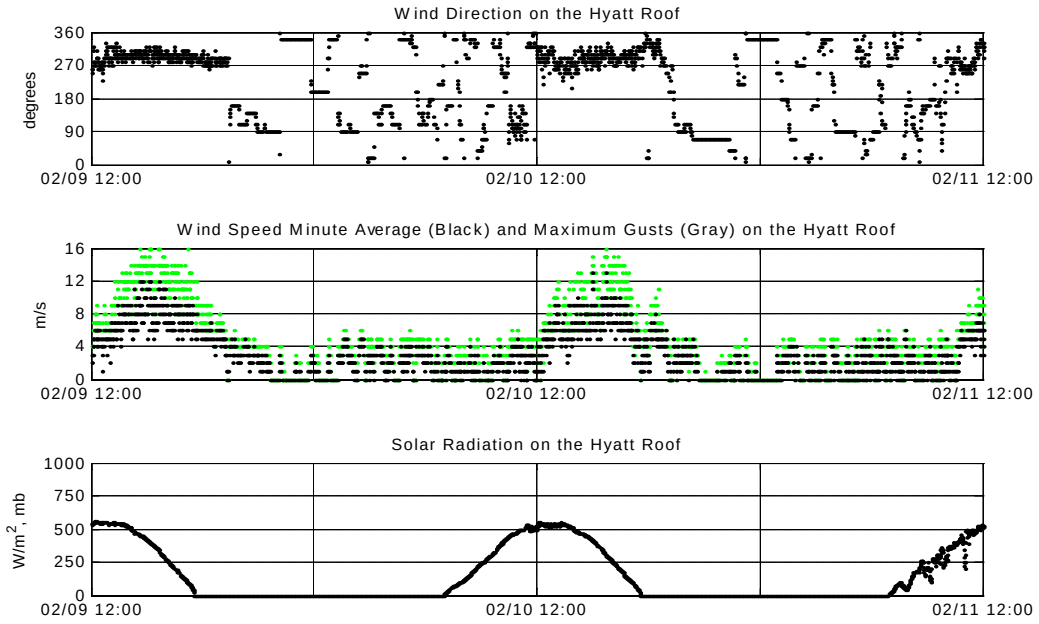

Figure 3.12: Wind direction, wind speed and solar radiation measured by the weather station on the Hyatt roof from noon on February 9, 2004 through noon on February 11, 2004.

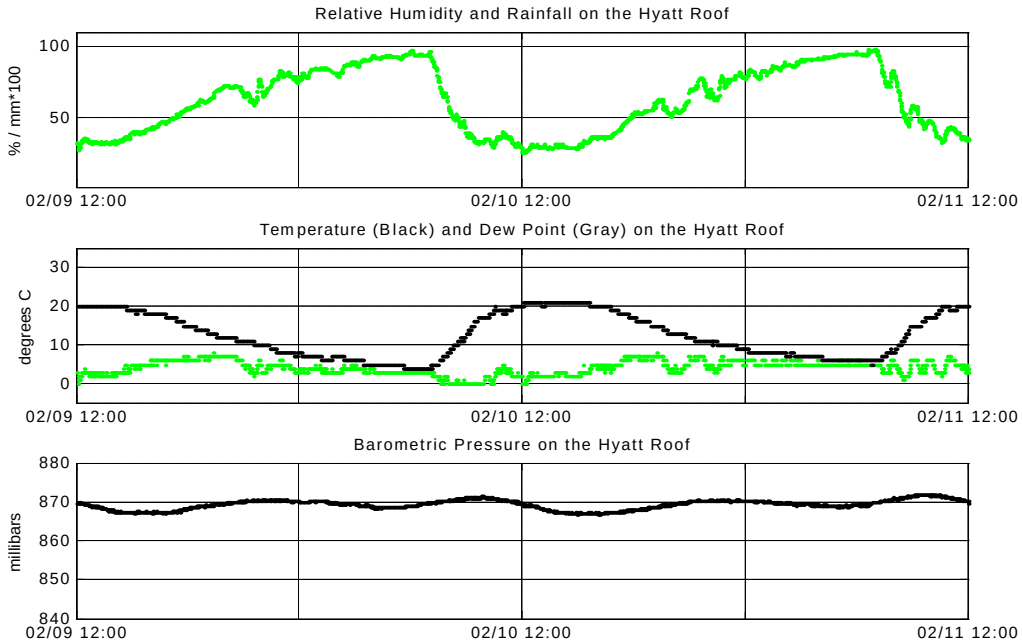

Figure 3.13: Relative humidity, temperature, dew point, and barometric pressure at the weather station on the Hyatt roof during the same 48 hour period. There was no rain.

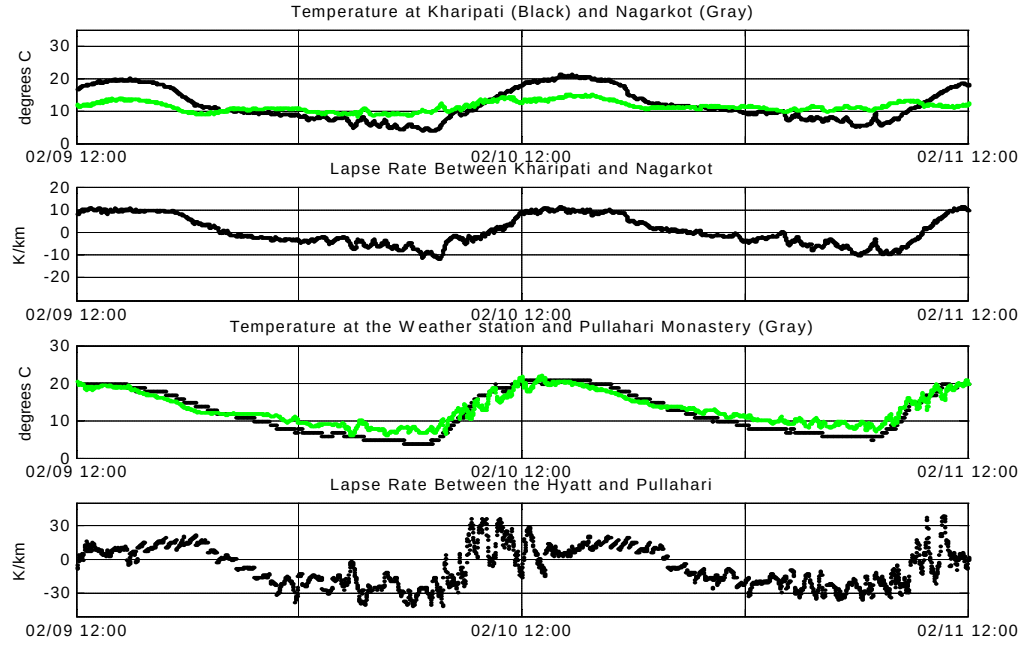

Figure 3.14: (From top to bottom): Temperature at Kharipati and Nagarkot; lapse rate between Kharipati and Nagarkot; temperature at the Hyatt weather station and at Pullahari monastery; lapse rate between the Hyatt and Pullahari.

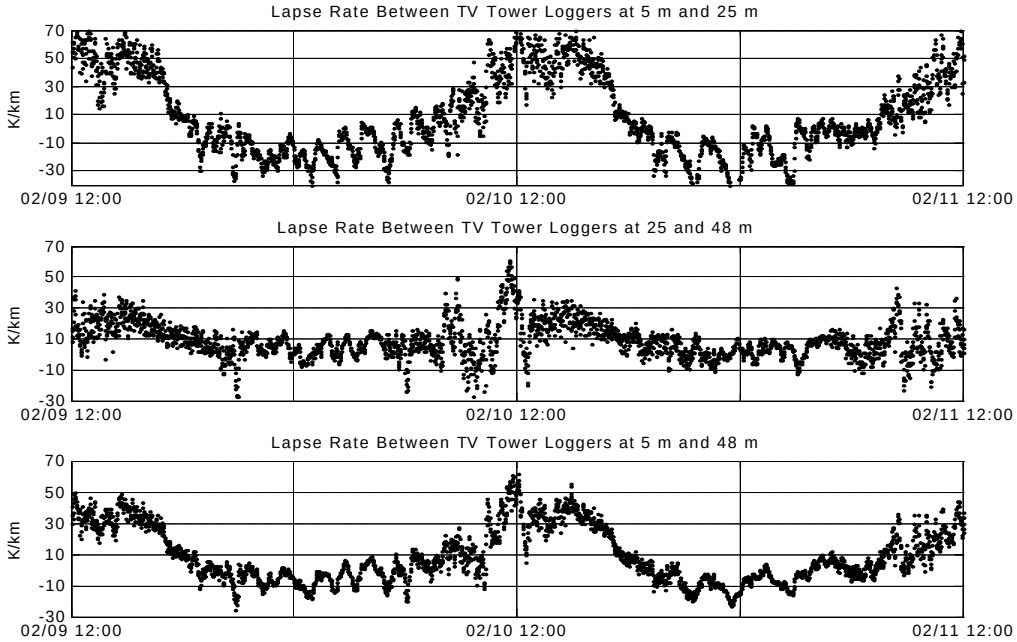

Figure 3.15: Lapse rates between different temperature loggers on the TV tower.

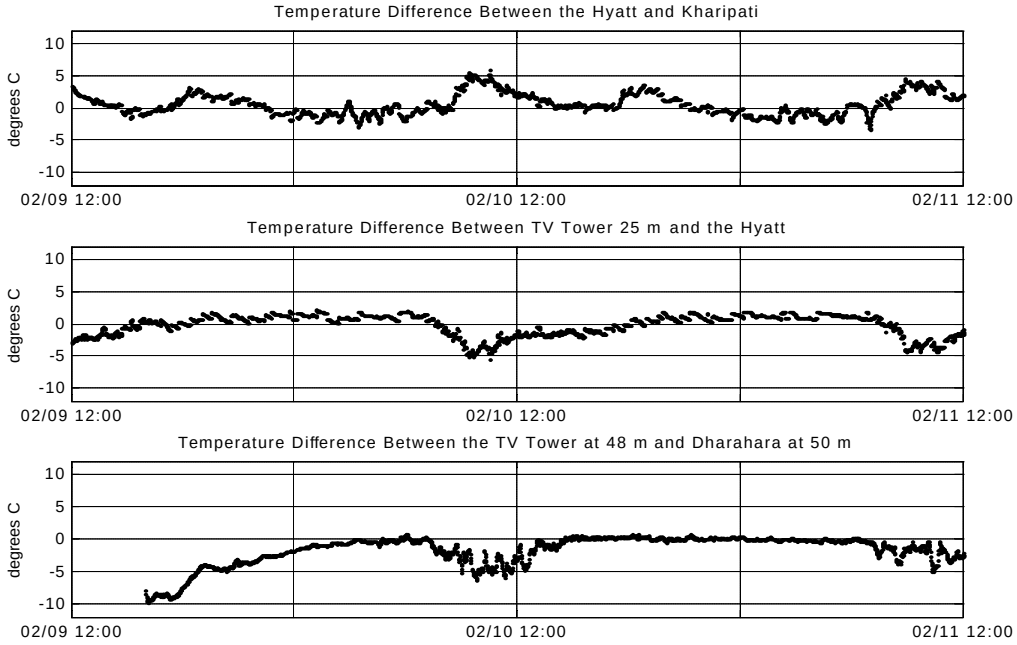

Figure 3.16: Horizontal temperature gradients: temperature difference between the Hyatt and Kharipati, between same elevations on the TV tower and the Hyatt, and between the same elevations on the TV tower and Dharahara.

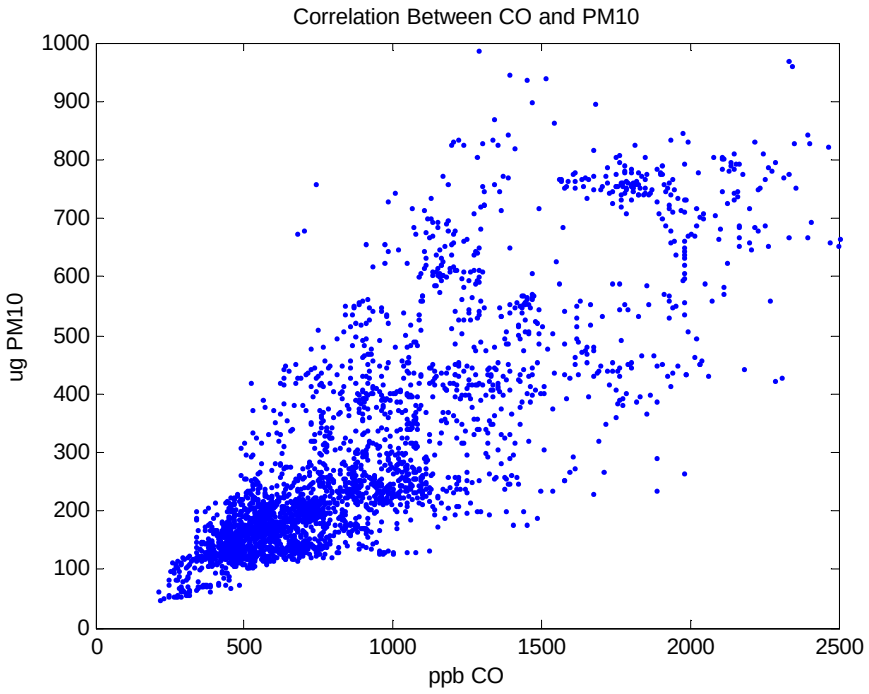

Figure 3.17: Scatterplot of simultaneous CO (ppb, horizontal axis) and PM_{10} ($\mu g/m^3$, vertical axis) measurements at the Hyatt during the same 48 hour period.

The figures above show consistency with previously mentioned patterns of CO and PM_{10} twin-peaks, nocturnal ozone depletion, morning fog, day-time drop in relative humidity and afternoon westerly winds. Figure 3.17 confirms the high degree of correlation (R = 0.8812) between CO and PM_{10} during this 48 hour period. Returning to Figure 3.11 and Figure 3.12, we note that the ozone spike at noon corresponded to the onset of westerly winds (coming from over the city) as well as to times of spikes in CO and PM_{10} concentrations.

Figure 3.18 zooms in further to confirm that the increase in westerly wind speed at 12:18 pm initiated a little peak in ozone and in CO that were then followed by a larger broader peak in both from 12:30 to about 12:52 pm. The average wind speed from 11:30 am to 12:17 pm was only 2.0 m/s, but from 12:18 to12:52 pm it was 4.9 m/s. After 12:52 pm it was even faster. We can hypothesize what happened: as the stronger westerly winds arrived, they blew the polluted air mass that had previously been stationary over the city

towards the east, past our measurement station. The initial spike marked the arrival of pollution from the nearby Chabahil Ring Road intersection, followed by a trough from the residential area immediately west of there, and then the broad peak from the main city further west. The distance from the Hyatt to the western edge of the city is 10 kilometers. At 4.9 m/s, it would take 34 minutes to cross the city: that was almost exactly the duration of the ozone and CO spikes! We thus have confirmation that the spikes in pollution corresponded to transport past our sensors, upon commencement of higher wind speeds, of the air mass that had been almost stagnant over the city during the morning. The drop in pollution concentrations after 12:52 pm happened once the tail-end of that air mass had gone past the measurement station. From that moment onwards, throughout the afternoon, the sensors were measuring air that had initially been upwind of the city (including outside of the western passes), and that had traversed the city quickly (transported by the fast afternoon westerly winds). Later we shall see that the low pollution levels in the Kathmandu Valley during the afternoons are not just due to dilution by faster wind speeds, but also due to dilution into a taller mixed layer.

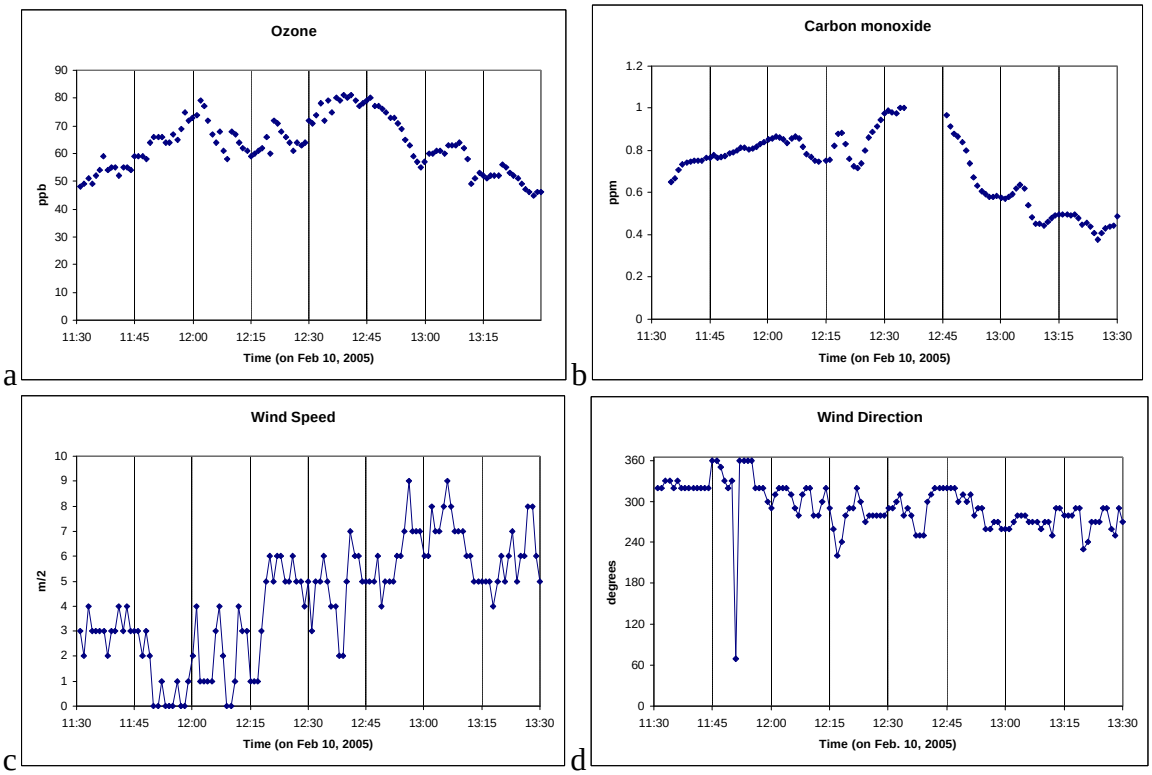

Figure 3.18: Close-up look at ozone, CO, wind speed and wind direction, mid-day, Feb. 10, 2005.

Looking at the temperature logger data in Figure 3.14, we see that again, the diurnal amplitude of temperature at Nagarkot peak was less than within the valley, with lower day-time maxima and higher night-time minima. Lower night-time minima within the valley compared to the valley rim suggests night-time cold-air pooling [*Whiteman et al.*, 2001]. The temperature dropped more rapidly at dusk at Kharipati than on loggers closer to the center of the valley: it appears that the evening cooling of the valley started from the edges and moved in towards the center, in the same direction as we would expect down-slope katabatic winds to travel once they reached the bottom of the valley rim slopes. The night-time surface cooling rate at Kharipati was almost linear, with a rate of approximately 1°C/hour. We also see in Figure 3.14 that the nocturnal temperature inversion was strongest at dawn, but took until late morning to be eliminated. Between the Hyatt and Pullahari monastery, 100 meters higher, we find that the unstable mixed conditions started earlier in the morning (consistent with an inversion break-up from the bottom).

From noon to 6:00 pm, the lapse rate between Kharipati and Nagarkot hovered very close to the dry adiabatic lapse rate of 9.8 K/km, indicating a mixed layer over the valley that extended from the surface to at least 600 m height. Air parcels at the altitude of Kharipati could convect vertically to the altitude of Nagarkot. It might be questioned whether basin-edge measurements are sufficiently representative of conditions over the basin center to draw such a conclusion. Air temperature on sunny days tends to be higher over mountains than over nearby low-land. We know from measurements that afternoon temperatures at Kharipati and at the Hyatt were similar. Now suppose that 600 meters above the Hyatt, it was indeed colder than at Nagarkot, as expected from theory. That would give a lapse rate above the Hyatt that was larger than above Kharipati: larger than 9.8 K/km, implying unstable conditions. This supports rather than negates the conclusion that the mixed layer was at least 600 meters thick. Not having had the opportunity to install and frequently visit sensors on the taller Shivapuri peak (5 hour hike to the top), we do not have a means of determining how much thicker than 600 meters the mixed layer really was.

Figure 3.15 presents the lapse rate between pairs of loggers on the TV Tower. Unfortunately the ground temperature was not monitored concurrently[16]. We see that the nocturnal temperature inversion was present throughout the night even in the 5-25m layer. We also see that its strength oscillated on the time scale of 2 hours. At this point the cause of these oscillations is unclear; they might be due to some internal gravity waves within the cold air pool. The nocturnal temperature inversion was stronger between the lowest (5-25 m) layer than between the 25-48 meter layer. This is consistent with radiative cooling of the surface [*Arya*, 1999]. During the afternoons, the strongest instability due to thermals was recorded in the bottom-most layer as well (with the largest positive lapse rates).

The conclusion from the vertical temperature profiles is that during this time period, air parcels (and pollutants) starting at the valley bottom were able to rise to the height of Nagarkot (600m above valley floor) or higher during the afternoon, but not even 25 meters during the night. Linking this the much stronger horizontal wind speed during the afternoon and the almost stagnant condition at other times, we can see why in the mornings and evenings emitted pollutants remained in the city, while the afternoons had the cleanest air quality.

Figure 3.16 shows the horizontal temperature profile between loggers at similar heights. We see that in the late morning and at dusk the Hyatt was warmer than Kharipati. It was also warmer than 25 m on the TV tower in the late morning. The TV tower had the same temperature as Dharahara, 1 km away, throughout the day, except in the late morning when it was colder. Likely the late morning temperature differences were caused by fog thickness variations affecting the amount of solar radiation in the morning. The colder dusk at Kharipati suggests the earlier arrival of Katabatic winds, as already mentioned.

[16] The bottom logger was placed at 5 meters to keep away from a 1 storey building below the tower.

6:22am, towards NW

6:43am, towards NW

10:13am.towards NW

6:25am, towards east

10:13am.towards east

Figure 3.19: Photos from Hattiban on February 10, 2005, looking towards the northwest (city is in the fog in the right middle-ground) , and towards the east (city in the fog in the left middle-ground).

Figure 3.19 shows some samples of the early morning photography of fog from Hattiban. From the full photo record we were able to determine that the fog only started forming between 5:30 and 6:00 am. At 6:00 am every city light was visible through light fog. By 6:30 am nothing in the city was visible from above anymore. Close examination of the hills and slopes intersected by the fog shows that the top of the fog level was between 1500 and 1580 meters above sea level, with a slight increase over time. The sun rose at 7 am. By 10 am the fog had disappeared on the western side of the valley (visible in the photo at 10:13 am). Over the city it had acquired a more brownish tone, and its top had started to ablate away. This suggests that, by 10 am, the polluted surface mixed layer had grown through the depth of the fog layer, making the fog uniformly polluted. Other elevated haze layers, some originating from smoke plumes on the slopes, were visible against mountain sides from about 6:25 am continuously until after 10 am.

Figure 3.20: Photos of a lone smokestack near the Bagmati Valley exit, taken from Hattiban looking east on the morning of February 10, 2005, at 6:12 am (a), 6:23 am(b), 6:25 am(c), and 6:35 am(d).

One large smokestack near the Bagmati outlet, at the southern end of the valley, provided a tracer of changing wind direction (Figure 3.20). Until 6:20 am it was observed to rise slightly and then travel south in a straight narrow plume, down the Bagmati river outlet, indicating stable air but strong winds [*Scorer*, 2002]. At 6:23 and 6:25 am, the smoke plume was photographed rising vertically to a fixed level, and then spreading horizontally (visible in the center of the picture at 6:25 am): this indicates that the horizontal winds stopped, and the smoke was trapped at the altitude of neutral buoyancy by the stable atmosphere. At 6:31 am the smoke plume started to travel towards the north, and by 6:34 am it was traveling northward (in a mirror image to what it was doing at 6:20 am), in a straight narrow plume indicative of smoke in a stable but windy situation.

Figure 3.21 shows the CO contents of bag samples collected from late morning on February 9 through late morning on February 10, 2004, along with a repetition of the CO record at the Hyatt over the same time period (yellow line). The blue and the red dots show the CO mixing ratios at Nagarkot and Hattiban on the valley-rim mountains. Green dots show data at CTEVT -- the sodar site east of the city, and southeast of the Hyatt. Black dots show CO mixing ratios at the base of the Dharahara tower in downtown Kathmandu, at the edge of the old city, near the geographic center of the urban area, and near a busy major road, shopping center and outdoor market. Purple dots show CO sampled at the top of Dharahara tower.

At Hattiban and Nagarkot, mountains on opposite sides of the valley, CO levels stayed almost constant during the night, at around 450 ppb, suggesting the absence of local sources as well as horizontal homogeneity at that altitude at night. The night-time levels were similar to ones experienced in Kathmandu during well-ventilated afternoons, suggesting that this the sites were measuring the effective background level in Nepal at the time – in a large polluted region downwind of the Ganges Plains.

Unfortunately on this day the first half of the CTEVT data was lost due to bag leakages. The available data shows CO at CTEVT (green dots) with a similar pattern to that found

at the Hyatt, with a night-time low, morning high, and afternoon low. The black dots show CO values at the base of the Dharahara. Some of the measurements were conducted at the little park at the base, 30 meters from the bottom of the tower, and some on the doorstep of the tower. We see an amplified version of the twin-peak pattern, with a morning high, an afternoon low (though still mostly at and above 1 ppm), an evening highs (3 ppm and more), and then a decline through the first half of the night until about 3:00 am, followed by a slower decline until 6:00 am, and a rapid rise in the morning back to 3 ppm levels. The student volunteers filling the bags noted that the 8-9 pm peak of CO corresponded not with local traffic (which was quite light then), but with smoke drifting over from a barbeque restaurant. The morning rise coincided with the city's stoves and traffic waking up.

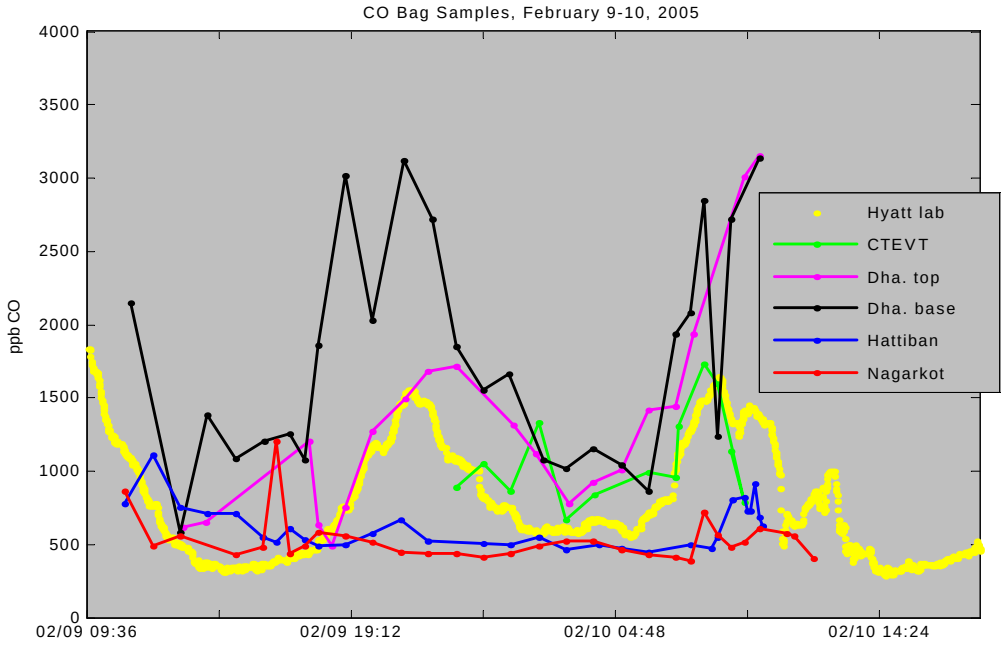

Figure 3.21: Bag sampling results from February 9 – 10, 2005. The yellow line shows CO measurements at the Hyatt lab during the same time period.

In contrast, the samples collected at the top of the Dharahara tower show a somewhat different pattern. During the afternoon, CO values were slightly lower than at the base.

At 7 pm, when the base reached its first CO peak, the top of the tower experienced a minimum of 488 ppb, corresponding to background levels seen at Hattiban and Nagarkot at the same time (and throughout the night). This suggest that at 7 pm, about an hour after sunset, the top of the tower received unpolluted background air, while being cut off from the traffic emissions taking place at its base. From 7 pm to 11 pm the CO concentration grew steadily, almost reaching the same levels as the now falling CO concentrations at the tower base. It is likely that the slow rise seen is due to upward transport of near-surface air via turbulent diffusion or other means of traveling vertically through stably stratified air. Although care was taken to sample away from the tower, we cannot exclude the possibility that the open door at the base, and the flow of students up and down the tower's staircase may have contributed to the enhanced turbulent transport of polluted air to the tower top during stable conditions.

From 11 pm to 3 am CO mixing ratios at the top of the tower decreased, staying barely lower than at the base. From 3 am to 7 am they slowly grew again, momentarily exceeding the levels observed at the tower base. After 7 am, and definitely by 8 am, CO at the top and bottom of the tower were almost the same, with both growing rapidly, suggesting a mixed layer of at least the height of the Dharahara tower.

3.7 Six Days at the End of February

The next set of figures shows a six day period at the end of February and in early March, with mostly sunny days. Please note that unlike all figures showing a seven day week, this set of figures does *not* begin on a Monday. Many of the same patterns that we noted in Section 3.6 and earlier are seen again. Figure 3.24 and Figure 3.23 show that fog formed every morning, and that winds showed a regularly repeating pattern, with strong afternoon westerlies. Figure 3.22 shows that ozone maintained the same pattern each day that we had seen in Section 3.6, with a short-lived peak around noon. CO and PM_{10} had twin peaks, but we notice that on most days the morning peak was significantly larger than the evening peak. Very similar patterns as discussed earlier (nocturnal

inversions, afternoon instabilities at the tower and dry adiabatic lapse rate up to Nagarkot) were also found in the temperature logger data in Figure 3.25 and Figure 3.26.

Another round of time-lapse photography was carried out on February 26th. The only difference to Figure 3.19 was a denser fog over the Bagmati river in the foreground in the early morning. An additional round of time-lapse photography on December 3, 2005 caught the fog in this area disappearing earlier than over the city, at the time of the onset of up-slope winds.

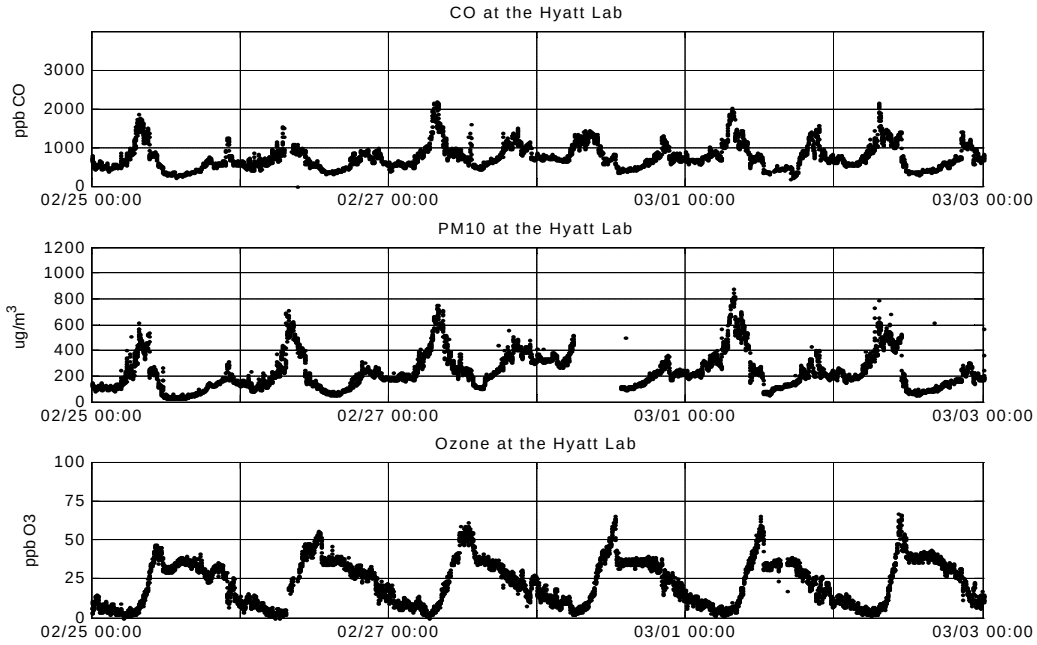

Figure 3.22: CO, PM_{10}, and ozone measurements at the Hyatt lab from February 25 through the end of the day on March 2, 2005.

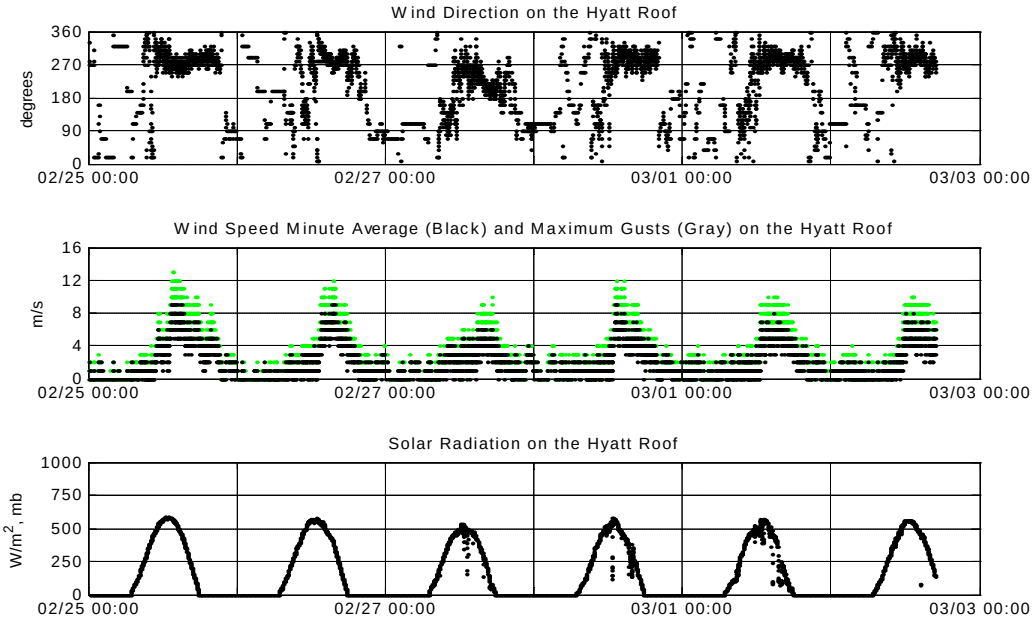

Figure 3.23: Wind direction, wind speed and solar radiation measured by the weather station on the Hyatt roof from February 25 through the end of the day on March 2, 2005.

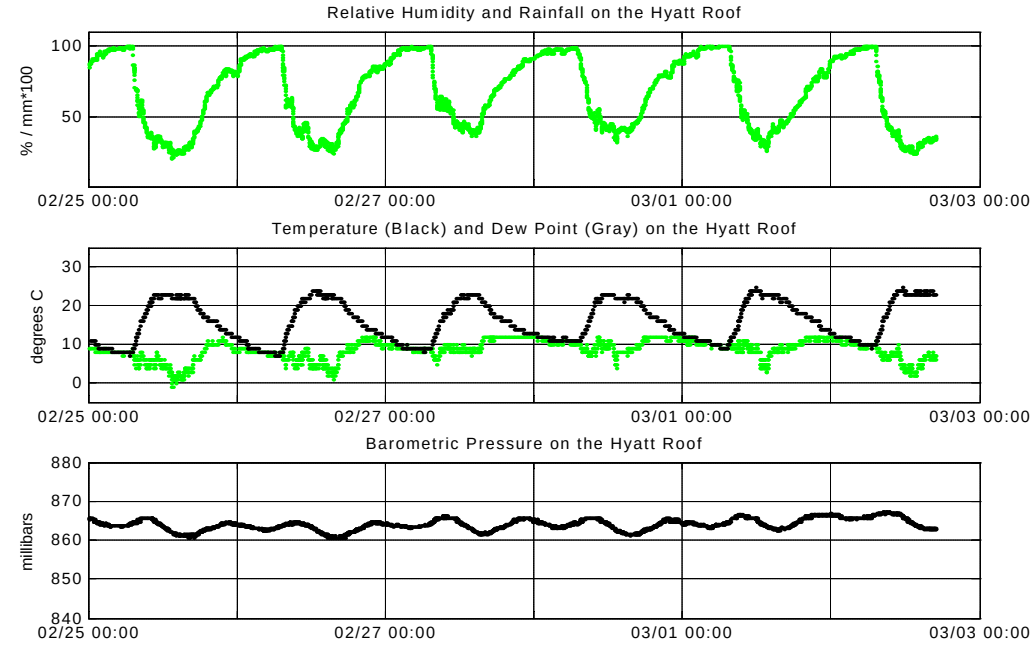

Figure 3.24: Relative humidity, temperature, dew point, and barometric pressure from the weather station on the Hyatt roof during the same time period.

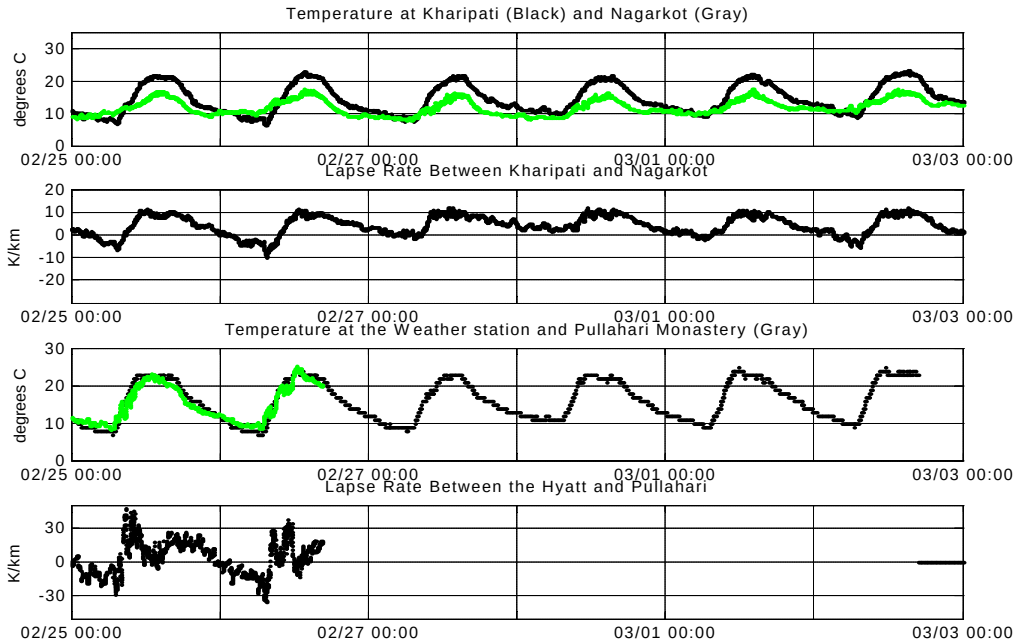

Figure 3.25: (From top to bottom): Temperature at Kharipati and Nagarkot; lapserate between Kharipati and Nagarkot; temperature at the Hyatt weather station and at Pullahari monastery; lapse rate between the Hyatt and Pullahari.

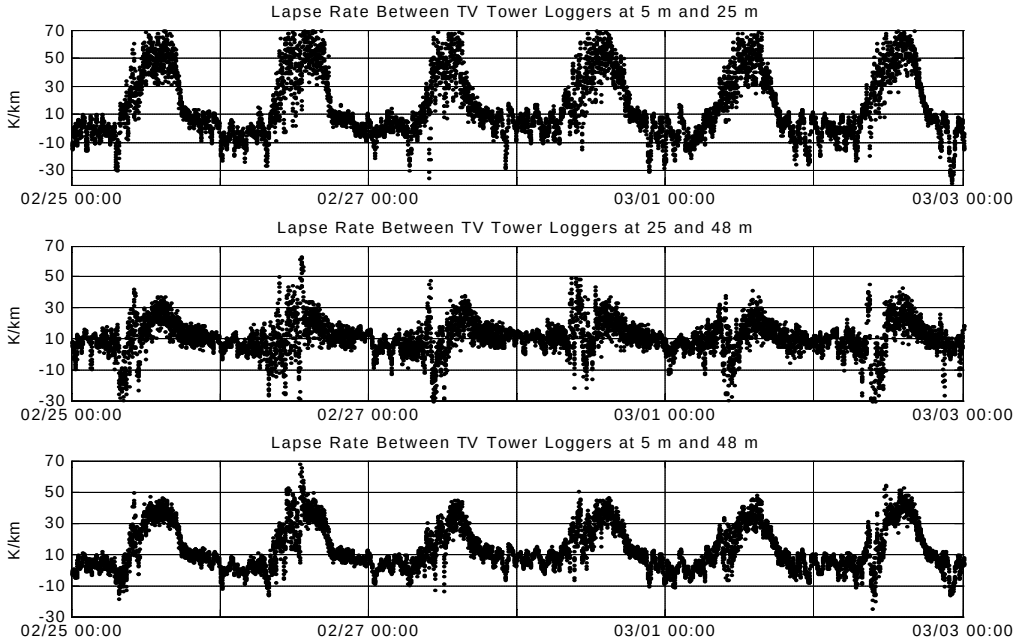

Figure 3.26: Lapse rates between different temperature loggers on the TV tower.

3.8 A Week in April

Figure 3.27 and Figure 3.28 provide a brief glimpse at a week in April. Only plots showing noteworthy differences from earlier cases are reproduced here. In Figure 3.27 we see a high-pollution event recorded on April 12-14, the cause of which has not been identified. Ozone exceeded 100 ppb the only time we measured ozone. CO showed nighttime values that never dropped below 1 ppm. The weather station shows the switch on Friday from hourly to 1 minute average data; it is noteworthy that the hourly averages were lower than the apparent average when looking at densely plotted 1 minute data.

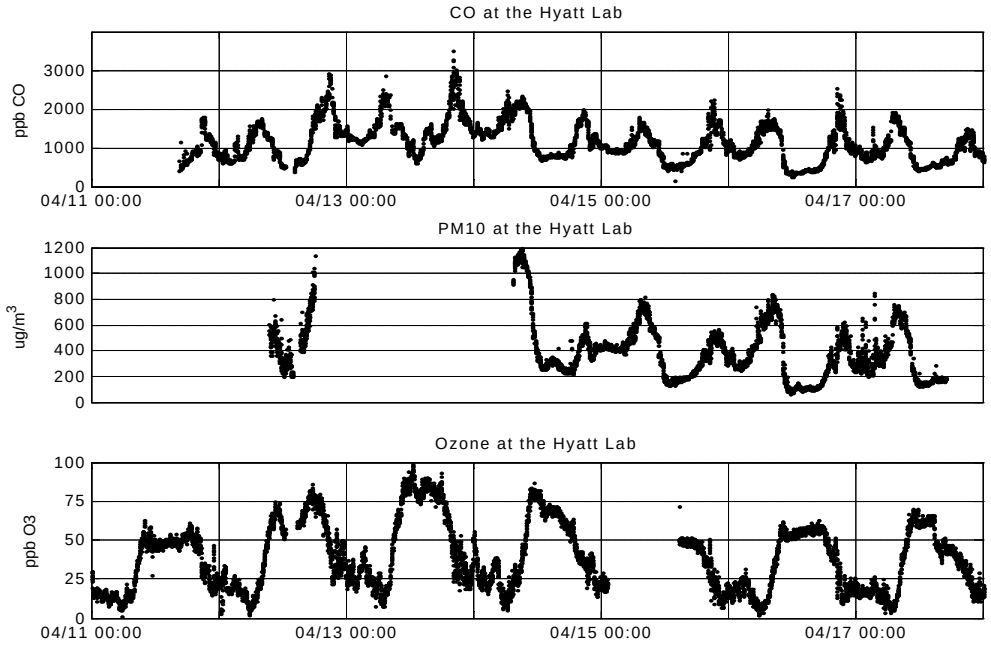

Figure 3.27: CO, PM_{10}, and ozone measurements at the Hyatt lab from February 25 through the end of the week of April 11, 2005.

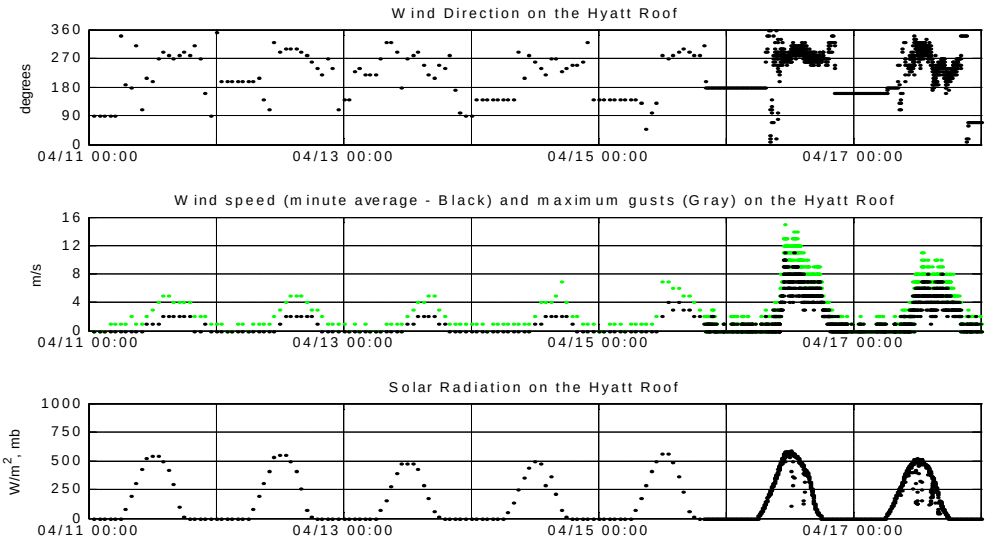

Figure 3.28: Wind direction, wind speed and solar radiation measured by the weather station on the Hyatt roof during the week of April 11, 2005. Note that the weather station was switched from hour to minute average logging during the evening of Friday, April 15, 2005.

3.9 Atmospheric Soundings Using the Sodar

This section describes mixed layer height and wind speed data from the repaired sodar.

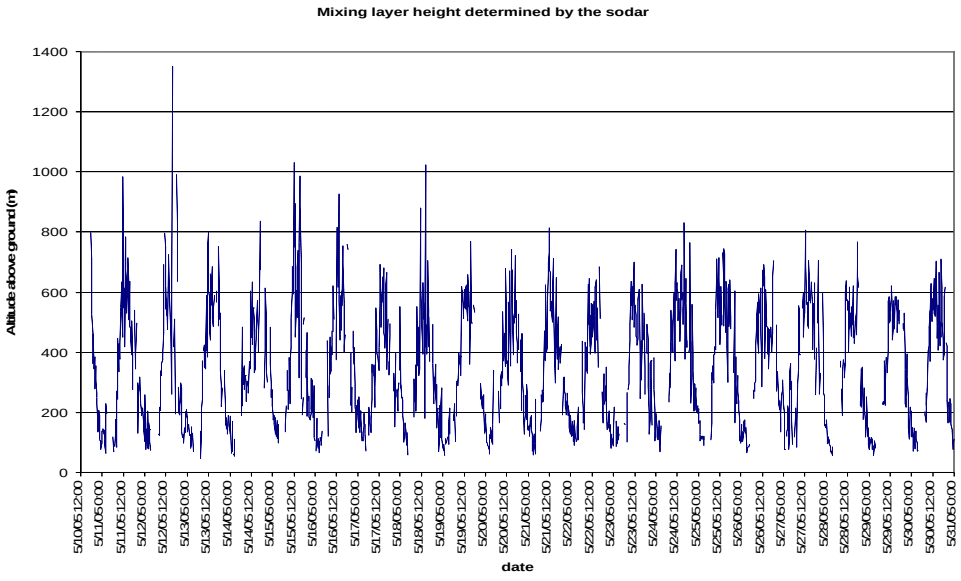

Figure 3.29: Mixed layer height measured by the sodar over a three week period.

Figure 3.29 shows that the mixed layer height measured by the sodar was very regular from day to day, varying between 600-1000 meters on most days during the early afternoon, and dropping to less than 50 meters at night. Note that a sodar's accuracy for calculating the mixed layer height is better during the day than during the night, as discussed in Section 2.6. At night the sodar tends to over-estimate the mixed layer height; it was also limited by the 50 meter cut-off of the lowest measurement bin. Aspects of the sodar measurements that are consistent with our other observations: specifically, during the day the mixed layer did grow at least to the height of Nagarkot. Its rise in the morning was very rapid. At night it *was* less than 50 meters above ground, consistent with temperature logger data showing an inversion almost down to the ground level.

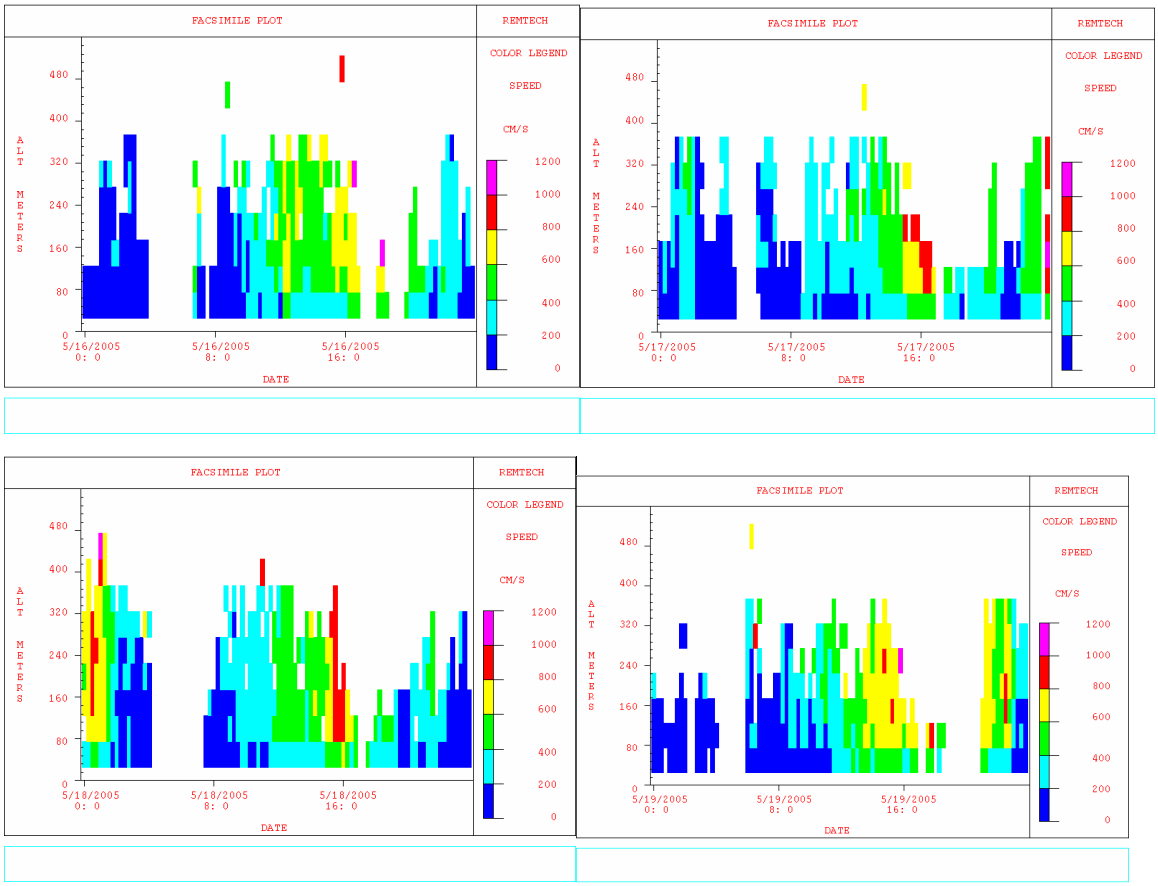

Figure 3.30: Vertical wind speed profiles measured by the sodar at CTEVT on four consecutive days.

The afternoon and evening mixed layer data must be interpreted with caution. The sodar shows the mixed layer height to be slowly decreasing from an early afternoon peak. In mountain basins, inversions usually begin with cold air pooling at the valley bottom: specifically, the inversion cuts the mixed layer rapidly to zero, and then grows from the bottom up, with a basin surface that is cut off from the air above by a lid that grows thicker over time, and NOT, as the sodar suggests, by a lid that slowly descends over time. Remembering that the sodar determines the mixed layer height by estimating the size of the largest eddies from vertical wind speed measurements at several elevations, there is the possibility that in the late afternoon and evenings, the sodar may have seen eddies in the entrainment zone above a growing near-surface inversion. It is also possible that the cold pool in the Kathmandu Valley does not form according to theory.

Figure 3.30 shows vertical profiles of wind speeds measured by the sodar over four consecutive days, running from midnight to midnight. We see that nights and early mornings were calm to altitudes of several hundred meters. On May 17 and 18 there were winds aloft that were experienced on the ground only weakly. Each day, in the late morning, high wind speeds from aloft started to penetrate downwards, reaching the surface around noon. This is consistent with the wind speeds that were measured by the weather station at the Hyatt, as well as with the expectation that winds aloft penetrate into basin bottoms over the course of the day, as the basin inversion disappears.

3.10 A 48 Hour Period in May

To compare and contrast with Section 3.6, this section zooms in on data plots from a 48 hour period in May centered around May 11. That day had good data from the sodar as well as from the temperature loggers on the TV tower. Figure 3.32 shows that CO and PM_{10} still had their morning and evening peaks, although lower than in winter. Ozone's daily peak was wider, reflecting longer daylight hours; also nocturnal ozone values didn't drop to zero until shortly before dawn. Other figures show that at mid-day there was still a shift from weak easterly to strong westerly winds; at night there was no wind, and also no fog. There was a haze and some high clouds throughout May, somewhat reducing

solar radiation. The TV tower again was colder in the morning than the Hyatt, and it showed the same inversion pattern as we had seen before.

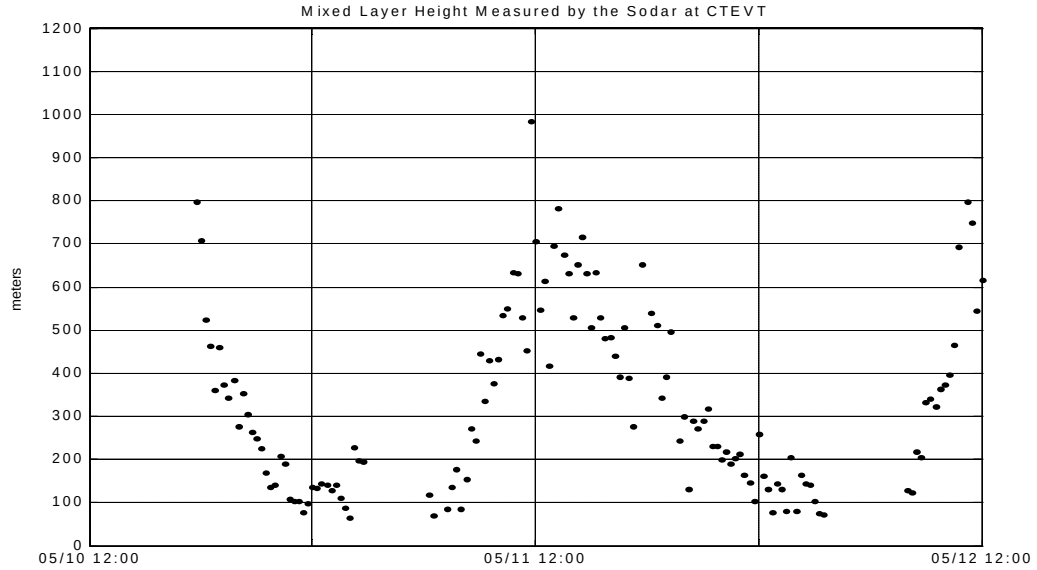

Figure 3.31: The mixed layer height measured by the SODAR at CTEVT.

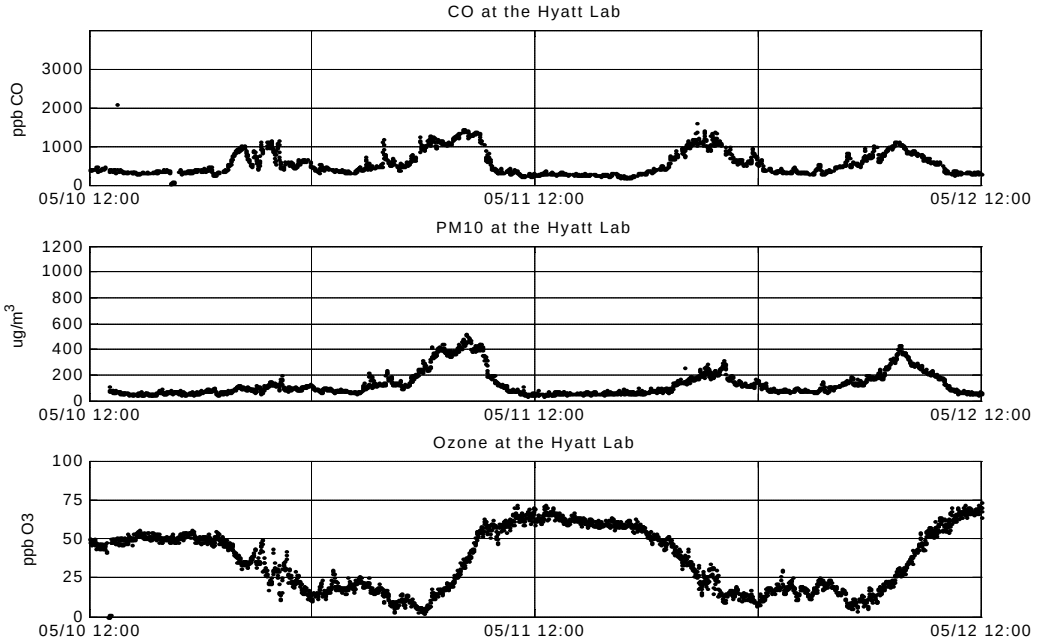

Figure 3.32: CO, PM_{10}, and ozone measurements at the Hyatt lab during a 48 hour period in May, 2005.

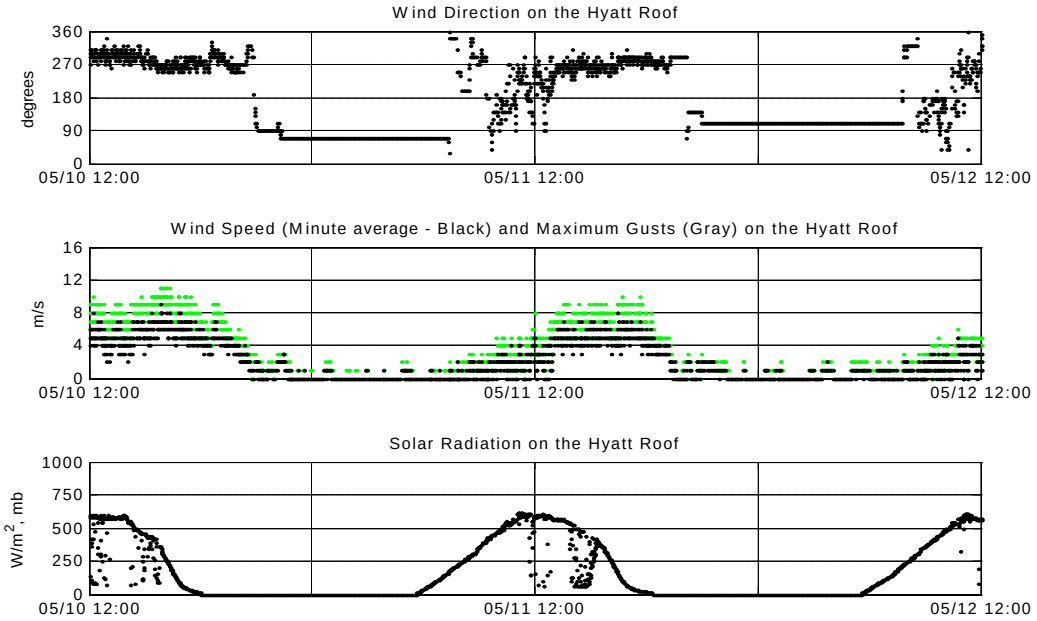

Figure 3.33: Wind direction, wind speed and solar radiation measured by the weather station on the Hyatt roof during a 48 hour period in May, 2005.

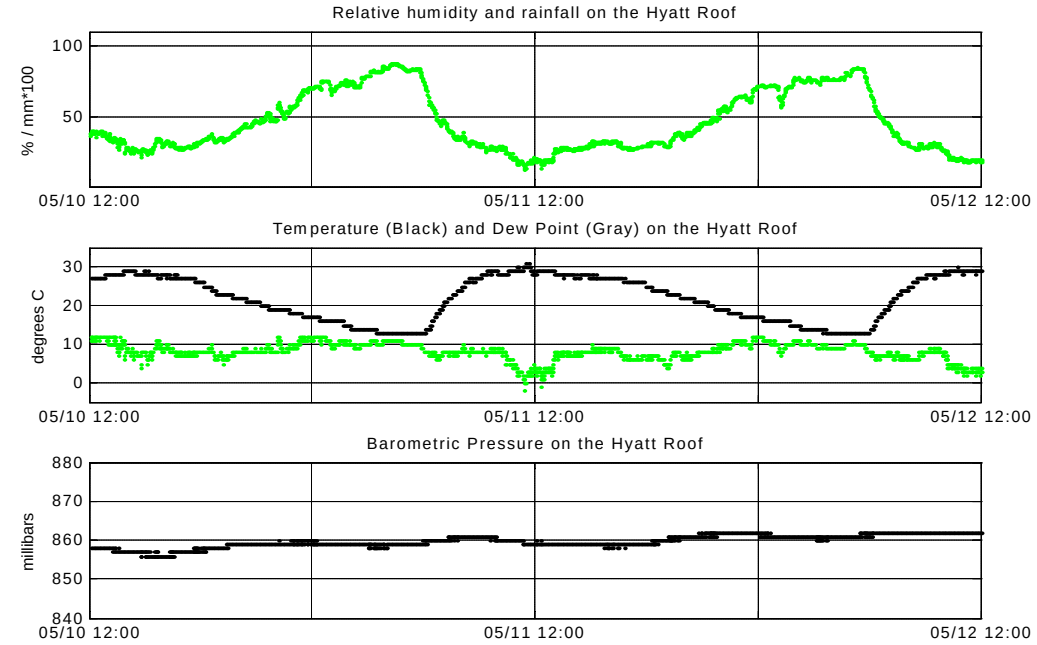

Figure 3.34: Relative humidity, temperature, dew point, and barometric pressure from the weather station on the Hyatt roof during the same time period.

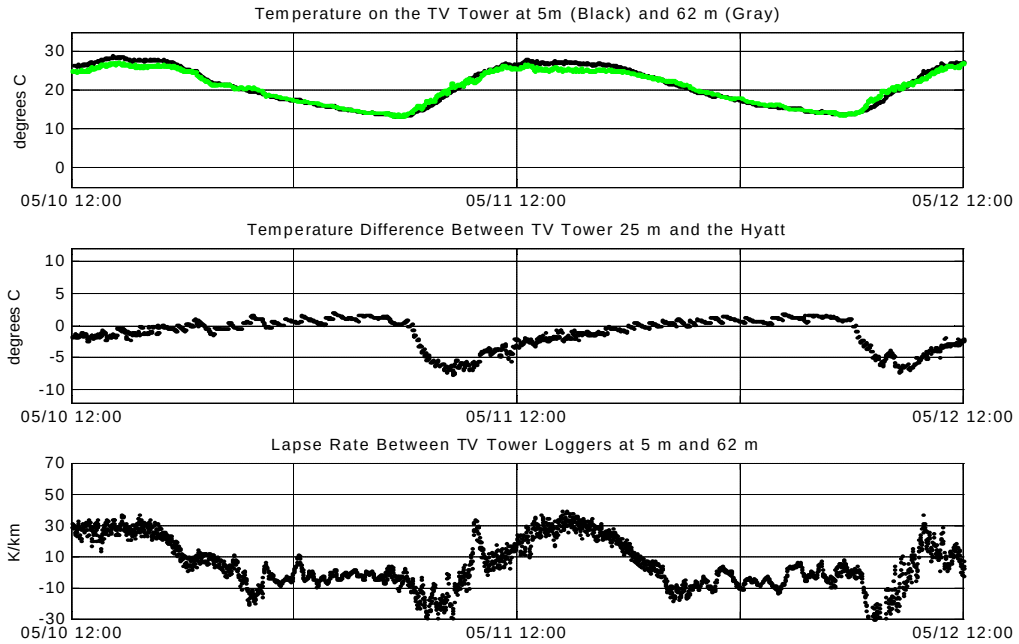

Figure 3.35: (From top to bottom) Temperature at the TV tower top and bottom; temperature difference between the TV tower and the Hyatt; lapse rate between the TV tower top and bottom.

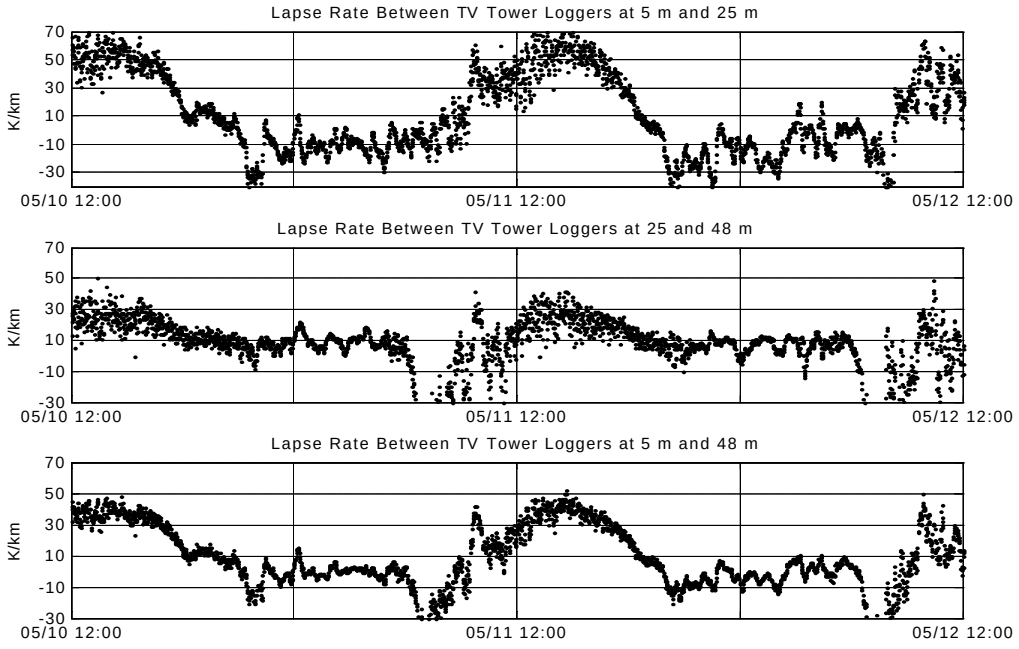

Figure 3.36: Lapse rates between different temperature loggers on the TV tower.

3.11 Spring 2005 Bag Sampling Results

Having seen results from the Hyatt lab and fixed temperature loggers spanning much of the dry season from October through May, we note the high degree of day-to-day similarity and the relatively small changes between seasons. This gives confidence that one-day measurements in other locations can be representative of many days. The next three sections present results of short-term measurements around the valley. We start off by looking at the CO bag sampling data collected during the rest of the spring. To check the representative-ness of measurements taken on and near the Dharahara tower, simultaneous bag samples were collected at various locations on and around the tower a week later. Figure 3.37 shows CO mixing ratios at different locations on and around the Dharahara.

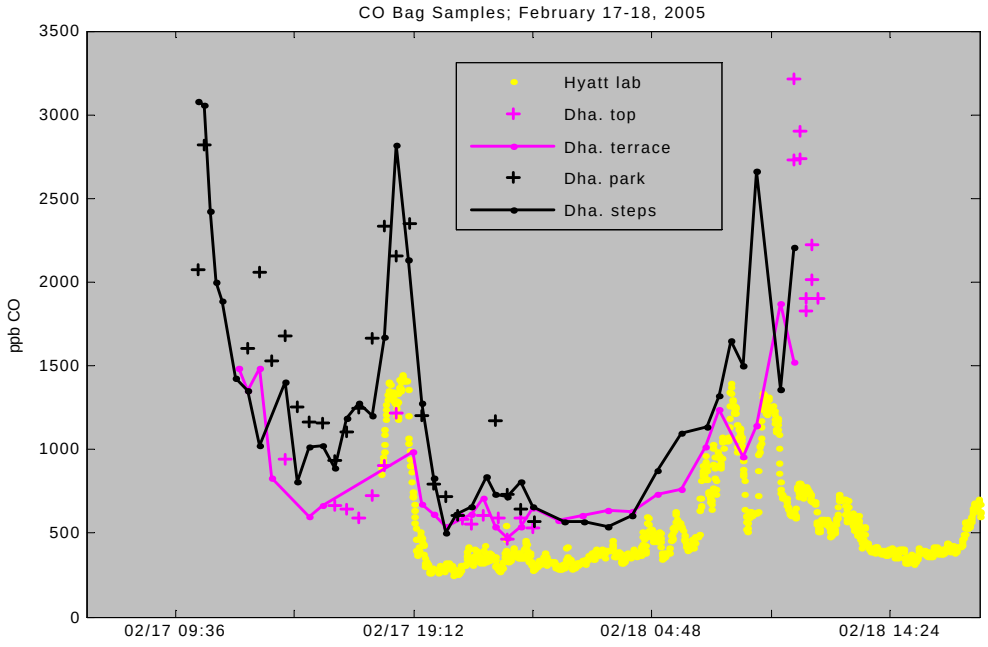

Figure 3.37: Bag sampling at various places on and around Dharahara on February 17-18, 2005. The yellow line shows CO measurements at the Hyatt lab during the same time period.

The solid black dots show samples collected at the tower's entrance steps, and the black crosses show samples taken 40 meters away at the park. They show reasonably good agreement despite the many possible local influences at this polluted urban location. It is

not surprising that during the afternoon, the park, which was closer to the road, showed slightly higher CO mixing ratios. There is also good agreement between measurements taken on the terrace at the Dharahara (solid magenta line) and at the top-most window (magenta crosses). The observations show very good agreement with those at the Dharahara a week earlier. Ground-level measurements showed the morning and evening peaks. At the tower top the morning peak had a similar magnitude to the tower base, but again the evening peak was much lower. The timing of the rise and fall of the peaks corresponded well with the CO measurements at the Hyatt, although the Hyatt showed lower peaks and lower troughs – again not surprising given the Hyatt's location further away from pollution sources.

Figure 3.38 shows that the afternoon low at CTEVT was very similar to that at the Hyatt, and that the evening peak at CTEVT was almost identical to that at the Hyatt. During the night time, though, the CTEVT site had several points with higher CO values that were are likely due to sources that did not reach the Hyatt (perhaps the brick factories east of the city). At the Dharahara nighttime values at both the top and the bottom dropped less than a few weeks earlier, and the top experienced a higher evening peak as well. In the morning the peak was less pronounced, appearing instead as a series of fluctuations. The latter was probably just a result of fluctuations in nearby sources.

Figure 3.39 shows data from hourly bag sampling at six locations in mid-March. CO at Nagarkot and Hattiban had the same, almost constant nocturnal low as found on February 10. At Tribhuvan University, near the base of Hattiban, CO showed an afternoon low, but then an evening high that declined only slowly, persisting through much of the night. CTEVT data showed the same twin-peak diurnal pattern with one exception: starting around 4 am, the night-time values suddenly jumped to a higher stable level. The Dharahara base data had the same overall pattern but with some wilder fluctuations, including an additional peak at 1 am. The top of the tower had an afternoon high corresponding to a peak at Hattiban at the same time, and it had additional fluctuations at night as well.

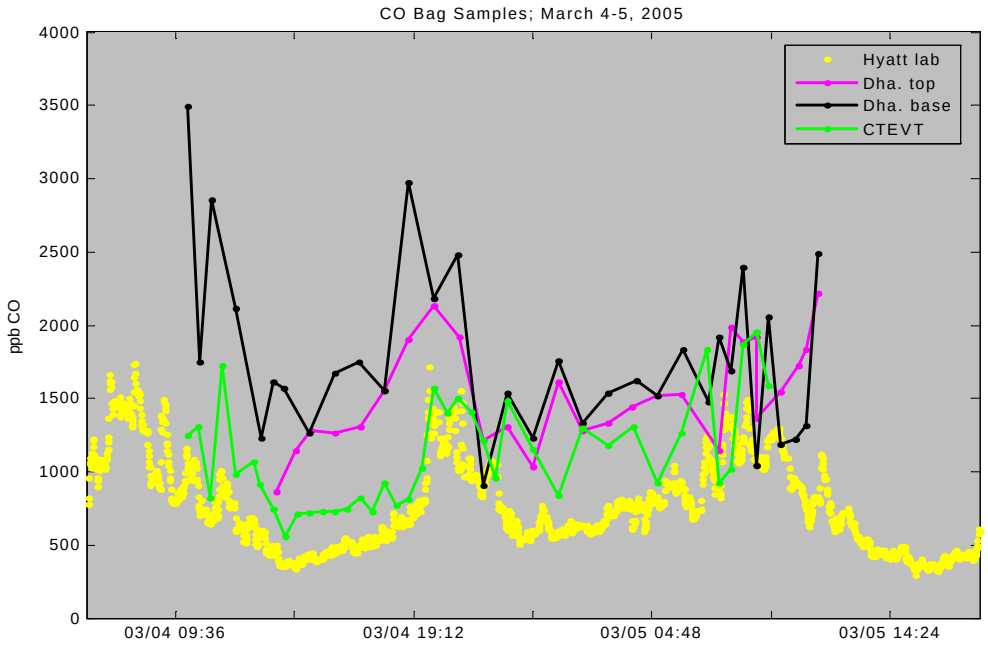

Figure 3.38: CO from bag sampling on March 4-5, 2005. The yellow line shows CO measurements at the Hyatt lab during the same time period.

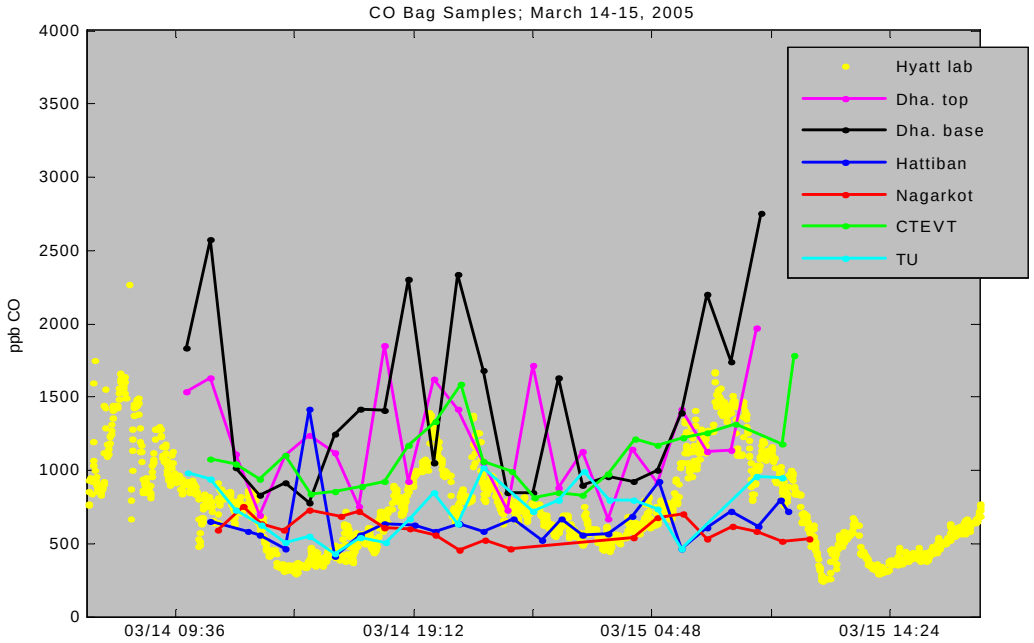

Figure 3.39 CO from bag sampling on March 14-15. The yellow line shows CO measurements at the Hyatt lab during the same time period.

Figure.3.40 shows bag sampling data on a very hazy day (the visibility from the valley rim peaks into the valley was almost zero). Here Hattiban and Nagarkot measurements

did not show the expected low values at night, instead showing considerable fluctuations. The same was true for the Dharahara data at night, although the Dharahara base data still showed a clear evening high. The Dharahara top and base measurements both show the usual morning peak. Pullahari, on a hilltop overlooking the Hyatt lab, had rapidly fluctuating CO values without clear peaks.

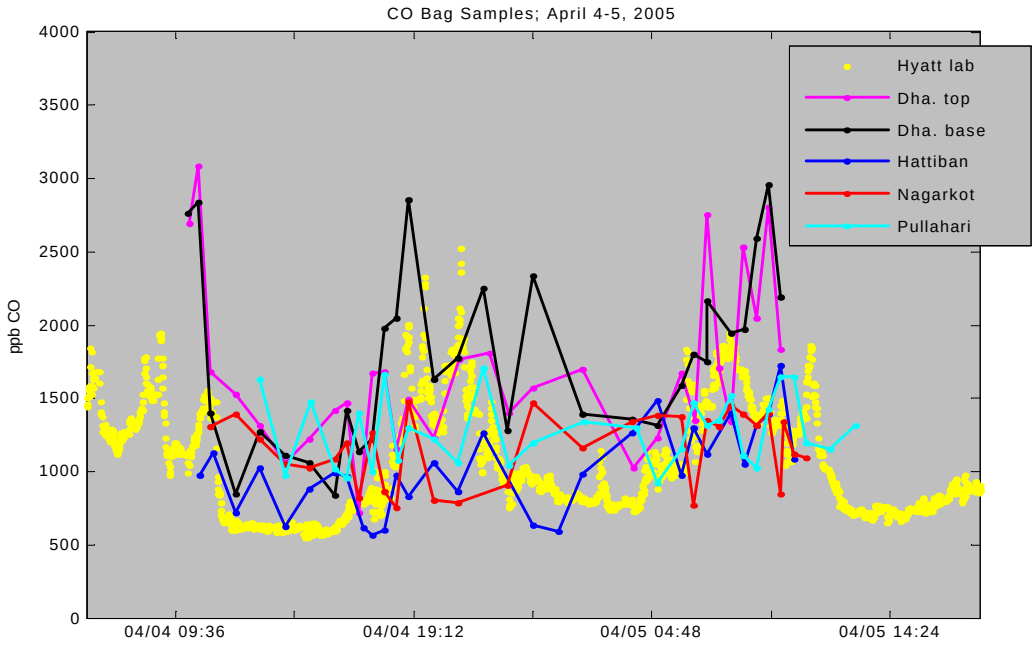

Figure.3.40: CO from bag sampling on April 4-5, 2005. The yellow line shows CO measurements at the Hyatt lab during the same time period.

Clearly the low values at Hattiban still represented background air; in fact they correspond to the afternoon values measured at the Hyatt. But from time to time Hattiban and Nagarkot received more polluted air masses than they did in February. At Pullahari Monastery there also seemed to be a baseline level throughout the afternoon and evening, which was punctuated at times by the arrival of more polluted air. The most interesting observation at Pullahari was at night, when CO levels gradually increased until 4 am during a perfectly calm night. At 5 am, during a light breeze from the mountains to the north, CO dropped once more. The next three figures show bag sampling results from Bhimdhunga Pass on the western valley rim and at Nagarkot on the eastern Valley rim, again superimposed upon data from the Hyatt lab. Figure 3.42 has additional data from CTEVT, east of the city, and Figure 3.43 has measurements at Lubhu as well, which is

east of both the city and an area with brick factories. Expecting the valley to be ventilated by clean air blowing in across the western passes, we expected the afternoon data at Bhimdhunga to show low background values, while east of the city we expected to see added pollution. On Figure 3.41 and Figure 3.42 we see that on both April 18-19 and April 28-29, CO values at Bhimdhunga were higher than at the Hyatt lab in the afternoon. On April 28-29, evening values dropped at night until about 1 am. On May 16-17 (Figure 3.42) CO remained low at Bhimdhunga Pass during the afternoon as well as most of the night, while Lubhu and CTEVT measurements showed a variety of peaks, probably caused by local pollution events. Surprisingly the Nagarkot data no longer show the constant low nocturnal values that they did earlier in the Spring. On May 16-17, the Nagarkot CO values did occasionally drop down to around 500 ppb, interspersed with higher values. The fact that Bhimdhunga Pass often had higher afternoon pollution levels than the Hyatt came as a surprise, since we expected the western entrance to the valley to be the source of clean air brought by the westerlies. Wind data from the weather station at the pass improves our understanding of when and how CO measurements at Bhimdhunga were contaminated by polluted air masses.

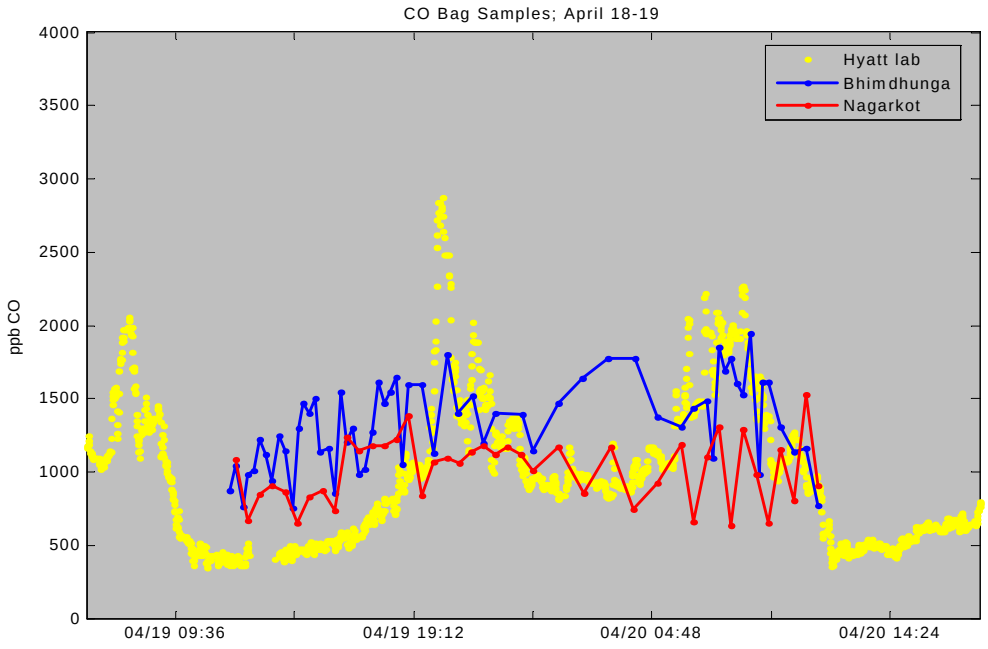

Figure 3.41: Bag sampling results from April 18-19, 2005. The yellow line shows CO measurements at the Hyatt lab during the same time period.

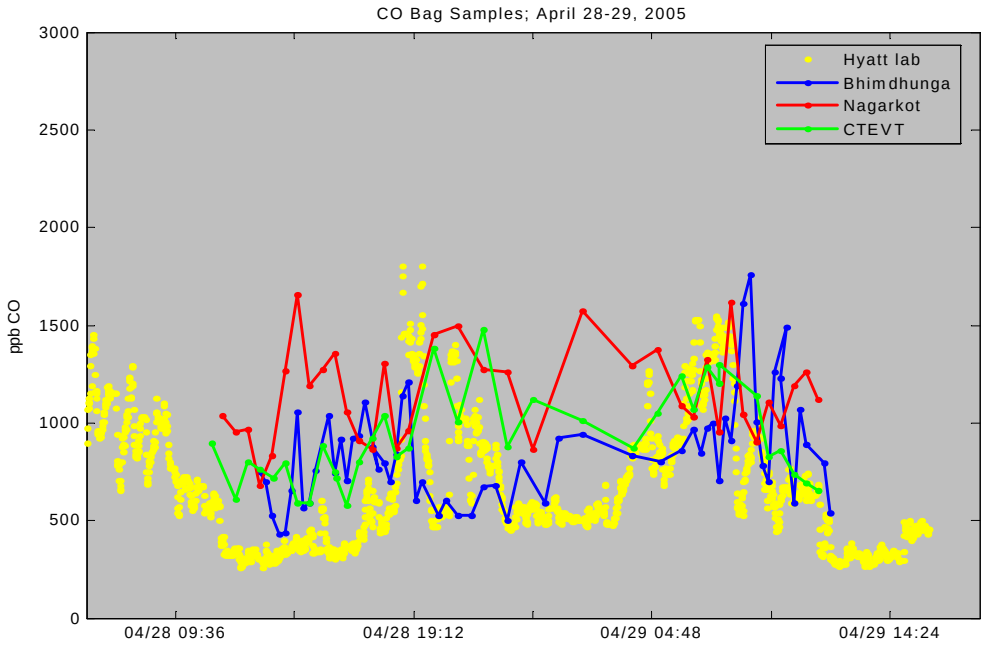

Figure 3.42: Bag sampling results from April 28-29, 2005. The yellow line shows CO measurements at the Hyatt lab during the same time period.

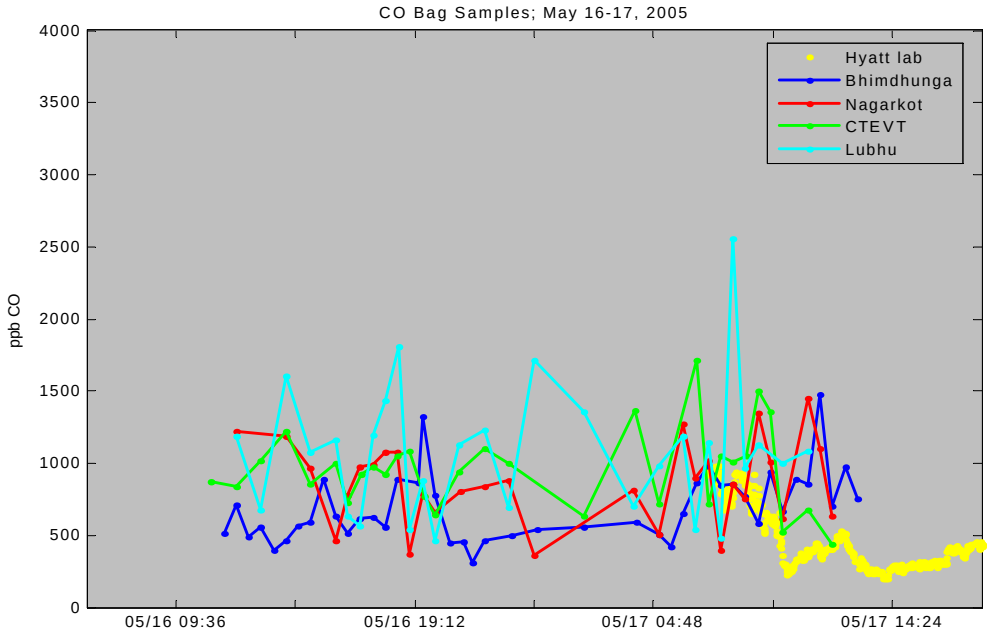

Figure 3.43: Bag sampling results from May 16-17, 2005. The yellow line shows CO measurements at the Hyatt lab during the same time period.

3.12 The Weather Station on Bhimdhunga Pass

Figure 3.45 and Figure 3.46 show weather station measurements on Bhimdhunga Pass over a two-and-a-half day period. We see that there was strong wind all day at the pass, but it flipped direction twice each day, blowing from the west (into the valley) from shortly before noon until dusk, and blowing from the east (out of the valley) from dusk until late morning. These measurements were consistent with the experience of soldiers guarding the pass every day. At the time of the switch to westerly winds, we also saw a sharp drop in relative humidity and in dew point temperature. The switching wind direction shows that during the day the pass was a source of air flowing into the valley, while at nights and early mornings valley air flowed out across the pass, consistent with observations of fog dripping out from the pass into the lower outside valley (Figure 3.44).

Figure 3.47 and Figure 3.48 relate the bag sampling data on Bhimdhunga Pass to the wind data. On April 18 (a sunny day), CO values on the pass fluctuated more strongly in the afternoon, when westerly winds were entering the valley from outside. After the wind direction switched to easterly, CO stayed lower for a while, before creeping up. It is possible that initially the air exiting the valley did not come from the city, but from higher layers. The CO values were found to rise slowly between midnight and 4 am, and then to drop again as the wind speeds increased around 5 am. However the bag sampling frequency at night was less than in the afternoon and morning, and thus we would not see if at night there was as much fluctuation as in the afternoon.

April 28 (Figure 3.48) was a cloudy afternoon that saw the wind direction switching several times. We found noisier CO data until 7 pm, but not correlated to wind direction. In the morning the CO mixing ratio grew before the wind direction switched.

Figure 3.44: Air photo of fog at Nagdhunga Pass from the northwest. The fog-covered Kathmandu Valley is in the left half of the middle ground. Bhimdhunga Pass is in the lower left of the picture. The Bagmati outflow valley is in the upper right, and fog-covered Ganges Plains in the background.

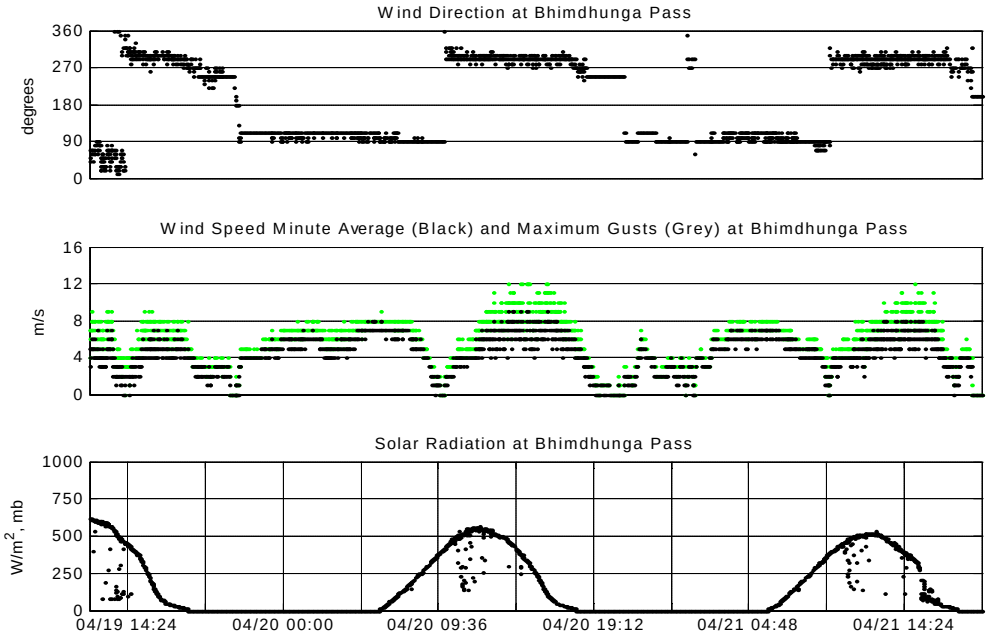

Figure 3.45: Wind direction, wind speed, and solar radiation at Bhimdhunga Pass.

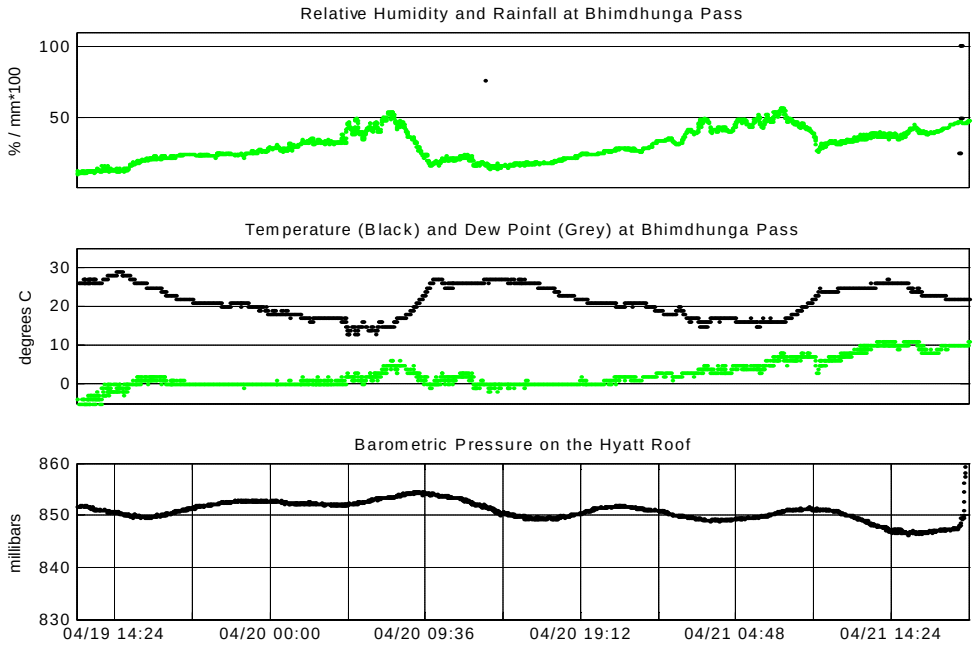

Figure 3.46: Relative humidity, temperature, dew point, and barometric pressure on Bhimdhunga Pass.

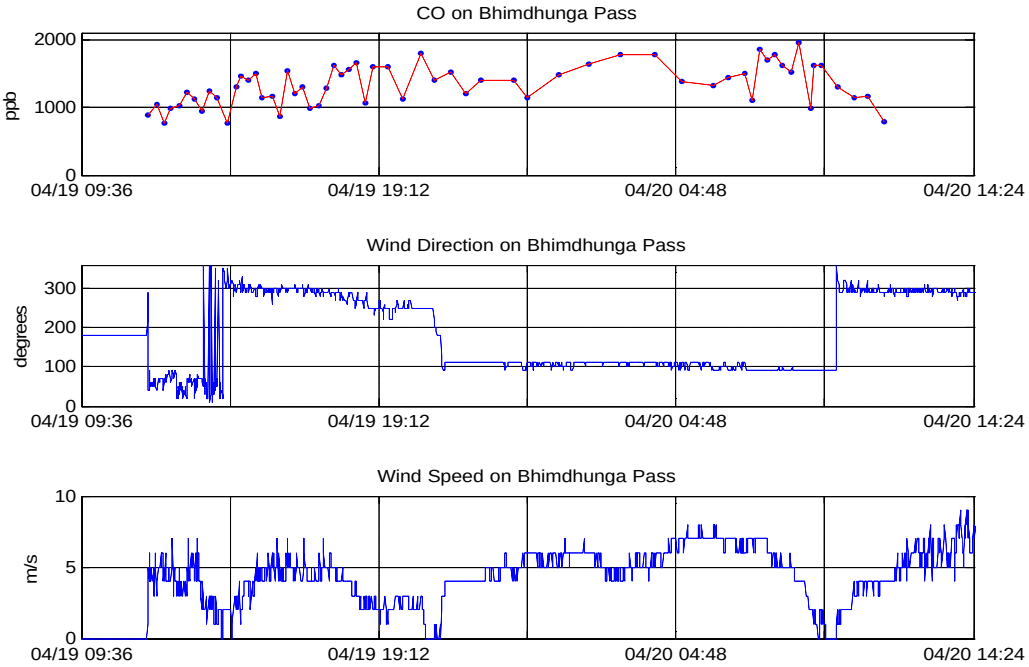

Figure 3.47 Bag samples and weather station data on Bhimdhunga Pass on April 18-19, 2005.

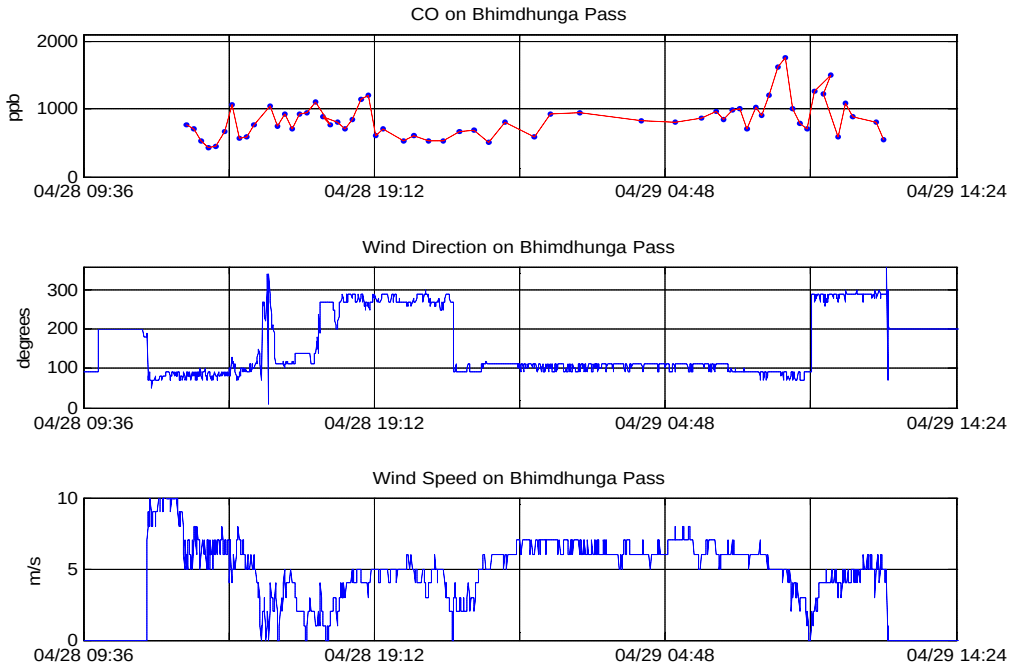

Figure 3.48 Bag samples and weather station data on Bhimdhunga Pass on April 18-19, 2005.

As mentioned earlier, the high values of CO found at Bhimdhunga during westerly wind conditions were unexpected. The fluctuations indicate that we were picking up local pollution sources. It is possible that wood fires at a number of farm houses on either side of the pass contaminated the measurements. It is also possible that we were just unlucky with the choice of days when we were able to collect samples at the pass, since they turned out to be fairly hazy days in April and May. The late dry season is known for forest fires on the hills surrounding the Kathmandu Valley and nearby valleys. Although we did not see actual fires, it is possible that we were measuring CO from them. Had we had access to the pass in early February we may have been able to find flat low afternoon CO values that we expected. It is also possible that the bottoms of the western passes are *not* the places where the clean afternoon air enters the valley, and that the clean afternoon air in the valley reflects air entering at a higher elevation, across the ridges, and then descending. Such hypotheses are investigated in later chapters.

3.13 Ozone in Nagarkot

As mentioned in Section 2.2, on several occasions the ozone instrument was moved to the top of Nagarkot peak. Figure 3.49 shows the results from those time periods (in black), along with adjacent times when it was run at the Hyatt lab in Kathmandu (in gray). In the top subplot, the Nagarkot measurements were carried out from early afternoon on December 30 until shortly after noon on December 31. On the second plot, the instrument was run from the evening of January 24 through the night of January 25. On the final plot, it was moved from Kathmandu to Nagarkot at mid-day on April 19 and run there for several days. The most striking observation is that at Nagarkot, ozone levels did not go down to zero at night. This is consistent with ozone observations on remote mountain tops in Arizona [*Fast et al.*, 2000], Taiwan [*Gao et al.*, 2005] and Thailand [*Pochanart et al.*, 2001]. Mountain-top locations not lack the nocturnal ozone loss mechanism through reaction with NO, but often they have access to a fresh supply of ozone from the free troposphere, while the valleys below are isolated by stable air at night [*Baltensperger et al.*, 1997].

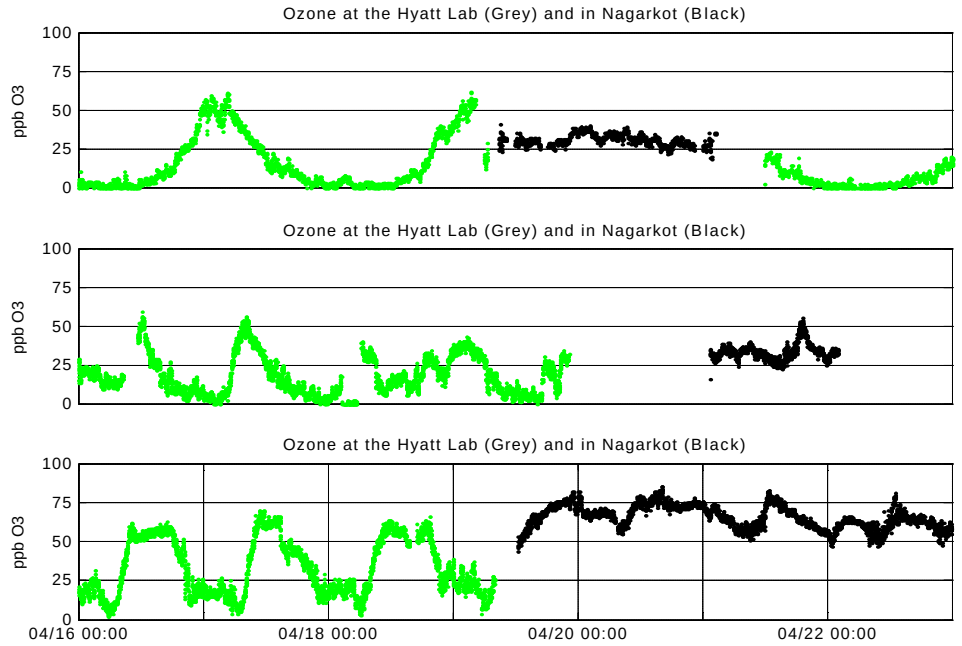

Figure 3.49: Ozone measurements before and after the instrument was moved from the Hyatt to Nagarkot.

In fact, ozone at Nagarkot showed only minor perturbations from its mean value, which was higher in April than in winter. It showed slight decreases during the nights, and increases in the afternoons. Keeping in mind that during the afternoon Nagarkot was downwind of Kathmandu, we can expect that the fluctuations may be a result of some night-time loss, coupled with advection of ozone precursors and ozone to Nagarkot during the afternoons.

3.14 Chapter Summary and Conclusion

The chapter has provided a tour of the highlights of the field data collected in Kathmandu during the 2004-2005 dry season. To illustrate the diurnal cycle across seasons, Figure 3.50 and Figure 3.51 show CO, wind speed, and ozone at the Hyatt lab on February 10 and May 11, 2005. We see that the patterns were remarkably similar, although May had a longer clean period during the day, and a broader ozone peak.

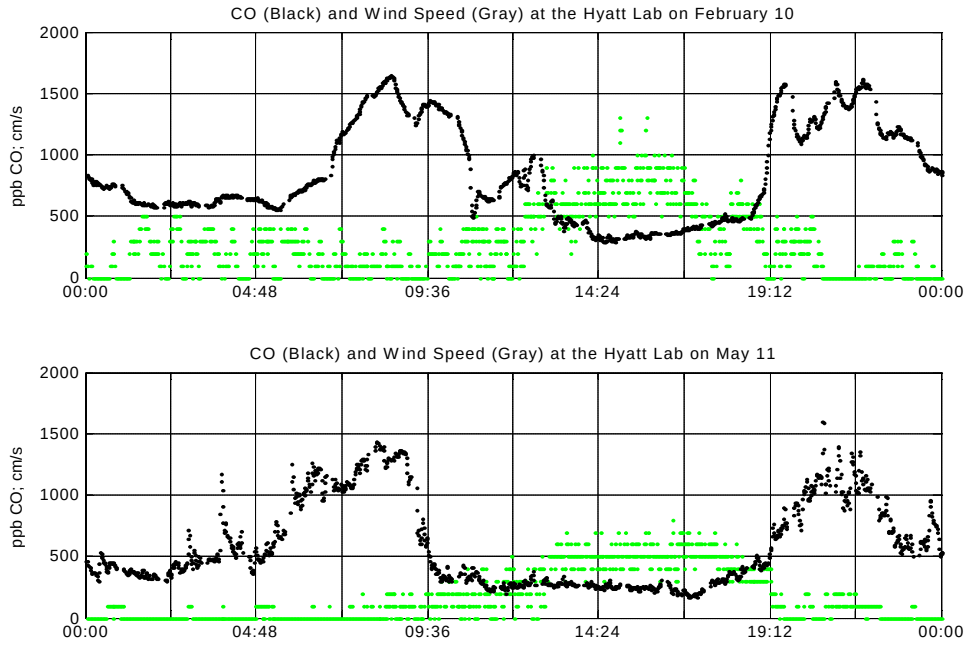

Figure 3.50: CO and wind speed at the Hyatt lab February 10, 2005, and May 11, 2005.

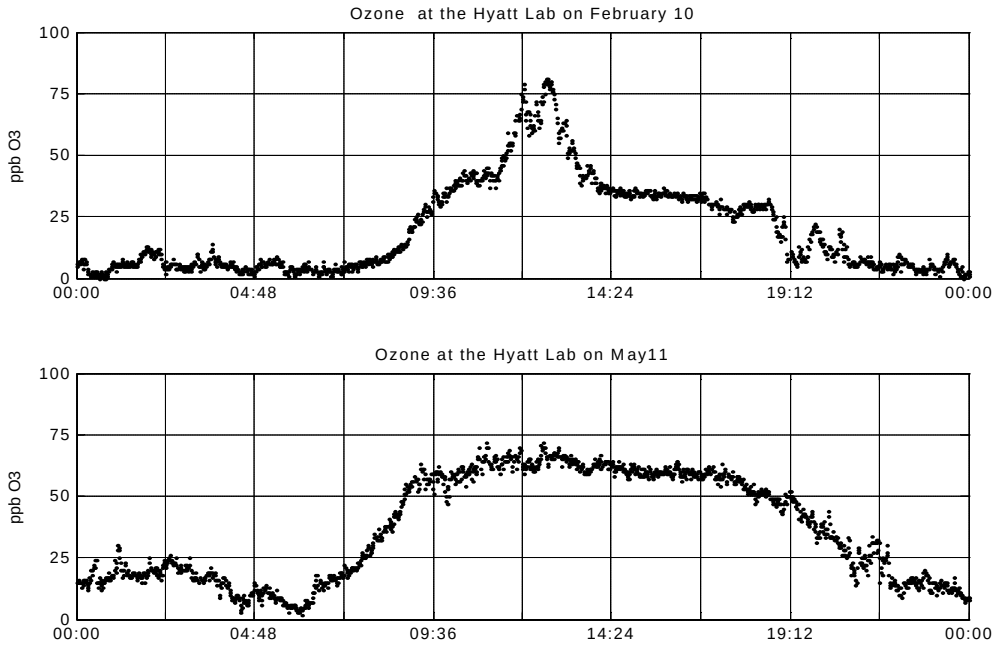

Figure 3.51: Ozone at the Hyatt lab on February 10, 2005, and May 11, 2005.

The major findings described the chapter are summarized here as a numbered list of statements.

1. **At the Hyatt lab** consecutive days had CO, PM_{10} and ozone patterns that were very similar to each other, provided that the weather remained similar.
2. CO showed a peak in the morning and a peak in the evening every day.
3. CO pollution was high.
4. CO and PM_{10} were highly correlated.
5. Ozone showed daily maxima near 40-50 ppb in winter and near 75 ppb in early summer, while its night-time values were near zero.
6. Ozone rose rapidly every morning.
7. While the low CO values during the afternoons and late at night were similar throughout the dry season (~400-450 ppb), the morning and evening peaks were 2-3 times higher in winter than in the fall and spring.
8. Winter mornings usually had fog that lasted several few hours starting about an hour before sunrise.

9. From the wind data and solar radiation data we see that winds were weakest at night, and reached their highest speeds in the mid-afternoon.
10. On sunny winter days (such as January 3-6) the strong westerly or northwesterly winds in the afternoons were often preceded by weaker easterly or southeasterly winds.
11. On cloudy days (such as January 8, 9) the afternoon wind speeds were less, and the wind directions showed less distinct afternoon westerly winds.
12. On a rainy day, there were gusty winds from multiple directions during the day and night.
13. From the temperature logger data, we see that a temperature inversion formed on nights following clear days, but that the valley air mass was well mixed during the day.
14. On all sunny days the air was least stable during the afternoon, a time corresponding to the time of high wind speeds.
15. An ozone spike often seen around noon corresponded to the onset of westerly winds (coming from over the city) and correlated with a spike in CO and PM_{10} concentrations, indicated the transit of a polluted air mass.
16. **From the temperature loggers** we found that the diurnal amplitude of temperature was smaller on Nagarkot peak than inside the valley, with lower day-time maxima and higher night-time minima on the peak.
17. AT dusk the temperature dropped much more rapidly at Kharipati than it did at loggers closer to the center of the valley.
18. The night-time surface cooling was almost linear, at a rate of approximately 1°C per hour.
19. A nocturnal temperature inversion was detected even in the 5-25m layer on the TV tower. The inversion was strongest in the lowest (5-25 m) layer.
20. Around Nagarkot and Kharipati, the air appears to have been neutrally buoyant during the day time.
21. The temperature at 48 meters on the TV tower and at 48 meters on the Dharahara were the same during the afternoon and night. But during the late morning the Dharahara warmed much faster than the TV tower.
22. During the morning, the temperature at Pullahari and Dharahara oscillated.

23. **From the time-lapse** photography we found that the morning fog was confined to altitudes below about 1550 meters.
24. Over the course of the morning the fog became more uniformly mixed.
25. The fog dissipated from the west.
26. In the night and early morning, smoke plumes were seen blowing down the Bagmati Valley, but reversing direction about half an hour before sunrise.
27. The mixed layer depth measured by **the sodar** was very regular from day to day, peaking between 600 and 1000 meters in the early afternoons on most days, and then dropping to less than 50 meters at night.
28. The sodar saw winds from aloft penetrating to the valley bottom over the course of the late morning.
29. **Bag sampling** showed that in the early Spring Nagarkot and Hattiban had constant nocturnal CO values of around 450-500 ppb, probably reflecting regional pollution. These values were similar to the minima found within the valley during afternoons.
30. The diurnal twin-peak in CO was observed at most sites on the valley bottom, and was most pronounced at the Dharahara base, inside the city.
31. Sites close to the brick factories did not show low CO values at night.
32. CO observations at Bhimdhunga did NOT show the predicted low afternoon values. In fact they were quite a bit higher than what was observed at the Hyatt, within the valley.
33. Bhimdhunga Pass experienced strong winds all day, but it flipped direction several times. At the time of the switch to westerly winds, there is a sharp drop in relative humidity and dew point temperature.
34. At Nagarkot, the ozone level did not drop to zero at night. In fact, it showed only minor perturbations from its mean value, which was higher in April than in winter.

Next, Chapter 4, will pull together the individual findings summarized here, drawing an overall picture of how pollution levels in the valley appear to be controlled by anthropogenic emissions and various ventilation mechanisms. It will then summarize the uncertainties in the picture, leading to a set of research questions and hypotheses that will guide the modeling exercises described in subsequent chapters.

CHAPTER 4: QUESTIONS FROM THE DATA : A DISCUSSION

4.1 Chapter Introduction

Chapter 2 described the instrumentation and field measurement set-up, and Chapter 3 presented the raw results of field observations in the Kathmandu Valley during the dry season of 2004-2005. This chapter discusses further the knowledge gained from the field results, summarizing the observed diurnal cycle, and identifying questions that could not be answered directly from the data, and that needed modeling work to address. Section 4.2 presents a chronological narration of a typical diurnal cycle in the Kathmandu Valley on a clear-weather winter day. This is followed in Section 4.3 by a more detailed discussion of the possible causes of the morning and evening peaks of CO. These two sections create the context for a set of research questions to be discussed in the rest of the chapter, and analyzed through modeling in the chapter that follows. Section 4.4 describes these questions, while Section 4.5 discusses hypotheses for each.

4.2 A Typical Diurnal Cycle in the Kathmandu Valley

The data presented in Chapter 3 showed remarkable day-to-day similarities, allowing the simplification of our analysis by considering a typical day that is representative of a large number of days: a winter day with clear skies, no rainfall, and no unusual synoptic-scale activity. During the fifty-nine days of January-February 2005, there were 32 such days: January 3-7, 10-15, 20-21, 27, 29, February 2-3, 5-6, 9-14, 19, and 23-28.[17] Other, non-typical days during that period had high clouds, patchy clouds, rain, or other short-term meteorological conditions that affected the buildup and ventilation of air pollutants. In the discussion that follows, we focus upon the above typical days; complexity introduced

[17] These days were identified from Hyatt lab weather station data (particularly solar radiation and temperature data), as well as records of cloud cover and visibility kept by research assistants at the lab. There were many such "typical" days in December 2004 as well; however, since the weather station was not functioning during much of that month, we cannot verify the weather log kept at the lab.

by other meteorological conditions can only be addressed once this simpler case is understood. We first summarize observations from Chapter 3 in the form of a chronological narrative of events taking place over a typical 24 hour period.

We begin the narrative of the typical day at 2 pm. At this time the sky is clear, with direct sun (550-600 W/m^2) illuminating the entire valley.[18] The temperature is near the winter daytime maximum (~20ºC), while the relative humidity is near the day's minimum (~ 25%). Ground level ozone mixing ratios downwind of the city are around 40 ppb. A persistent westerly wind of several meters per second is blowing into the Kathmandu Valley through the Nagdhunga, Bhimdhunga, and Mudku passes on its western valley rim, and sweeping across the city. Despite ongoing traffic emissions, ambient CO and PM_{10} concentrations at the Hyatt lab are at their minimum of the day, as newly emitted pollutants are rapidly carried east-wards out of the city by winds that are bringing in cleaner replacement air from outside the valley.

As the afternoon progresses, the temperature and solar radiation start to decrease and the relative humidity to increase, while the ozone mixing ratio decreases towards 25 ppb. The westerly wind remains strong, with little directional variation. The CO and PM_{10} levels remain low, even as school buses clog roads after 4 pm, and the full rush hour traffic snarls up most streets after 5 pm. Once the sun sets between 5 and 6 pm, rapid changes take place: the mountains surrounding the valley cool off, and katabatic winds carry cold air down their slopes and towards the valley center. A temperature inversion develops while the surface westerly winds cease. The inversion cuts off downward transport of ozone from higher altitude sources to the surface. Because surface air is also no longer replenished by ozone from local photochemical production, ground-level ozone decreases to zero due to the combined effects of surface deposition and NO titration. Meanwhile, CO and PM_{10} emitted by traffic and evening cooking, and confined by the reduced horizontal and vertical transport, accumulate rapidly in the near-surface air over the city.

[18] On some days solar radiation is reduced a regional haze from the Ganges plains extending to several kilometers above sea level [*Ramana et al.*, 2005].

As the evening progresses, ozone levels remain close to zero. CO and PM_{10} concentrations rise to peak values, and before midnight they start to decrease again down to stable nocturnal values that are the same or slightly higher than they were in the afternoon. Throughout the night, the temperature in the valley drops slowly until sunrise (at a rate close to -1^{o}C/hr), reaching colder temperatures than on the ridges surrounding the valley. Down-slope winds continue throughout the night; in particular, a down-valley wind blows south down the Bagmati river outlet valley. At Bhimdhunga Pass on the western valley rim, a strong easterly wind blows out of the valley. Higher up, on the peaks and ridges surrounding the valley, ozone, CO, and PM_{10} acquire constant, stable concentrations throughout the night.

The surface air temperature at the valley bottom drops to the dew point around 5 am, and a fog begins to form. Generally the Chobhar-Kirtipur ridge (which runs southeast-northwest along the southern end of the valley) divides the near-surface valley air mass into two parts. The air mass south of the ridge has heavy morning fog from earlier in December and until later in February. The air mass over the city, north of the ridge generally has heavy morning fog mainly in January, while at other times experiences a thinner haze layer that remains confined below ~1550 meters above sea levels (250 meters above ground). On either side of the ridge the air is stable, with smoke plumes spreading horizontally. Near the Bagmati valley outlet, smoke plumes from brick kilns blow horizontally down-valley, carried by drainage winds traveling down the valley.

Shortly before sunrise, the smoke plume blowing down the Bagmati valley reverses its direction. As the morning progresses, traffic and cooking start emitting fresh pollutants into the city air. The surface begins to warm and the near-surface inversion starts to break down. The top of the haze layer over the city remains unchanged, but within the haze layer there is increasing mixing, as seen from smoke plumes that rise higher and higher within the layer. The fog south of the Kirtipur-Chobhar ridge dissipates by 8:30 am, while a strong breeze blows up the slope to Hattiban, just to its south. By 10-11 am, polluted air starts arriving at the mountain tops, while within the valley, ozone increases rapidly from near zero to around 40 ppb. Ambient CO and PM_{10} concentrations drop simultaneously. Surface winds within the valley change from southeasterly to strong

westerlies, which then persist throughout the afternoon. The westerlies blow into the valley through the three passes on the western rim of the valley, where the wind direction has switched abruptly from easterly to westerly. Just after noon at the Hyatt lab, the CO, ozone, and PM_{10} concentrations show concurrent peaks (smaller CO and PM_{10} peaks than in the morning, but the highest ozone values of the day, up to 75 ppb), which lasts at most one hour. As the afternoon progresses, the haze confined below 1550 meters is diluted upwards; a new haze top may be seen a kilometer or more above the valley bottom which is often connected to a regional haze layer that has moved up the valleys from the Ganges plains.

We have just seen that the data presented in Chapter 3 is able to inform a detailed narration of the diurnal cycle of air pollution and meteorology in the Kathmandu Valley. A first examination of the data also revealed some hints about the physical and meteorological processes that might be responsible for the particular patterns observed. However, establishing a more definitive understanding requires further analysis of the data, as well as modeling work.

4.3 Discussion: Causes of the Daily Twin Peaks of CO

We saw in Chapter 3 that almost all days showed distinct morning and evening peaks of CO[19]. The bag sample data further showed that the twin peak pattern was not unique to the Hyatt lab location; it was also observed at the Dharahara tower, within the city, as well as at CTEVT, east of the city. Traffic is the biggest source of CO within the Kathmandu Valley [*Kitada and Regmi*, 2003; *Shrestha and Malla*, 1996]; rush hour *is* responsible for distinct morning and evening peaks in traffic and in congestion. At the same time, most of the valley's population cooks one large meal in the morning, and one in the evening, ostly using fuel sources that produce CO (LPG, kerosene, and firewood). The third major source of CO, namely industries (especially brick kilns), do not have emissions that vary distinctly over the course of the day. Let us hypothesize for a

[19] PM_{10} usually had peaks that correlated very well with CO, and likely caused by the same processes. For clarity of the discussion we focus here upon CO, keeping in mind that the answers apply to PM_{10} as well.

moment that the morning and evening peaks in Kathmandu were due to temporal emission patterns in traffic and cooking.

Morning and evening peaks in primary pollutant concentrations due to rush hour traffic have been observed in numerous cities. Already in 1959-1960, excellent correlations were found between hourly traffic count and hourly road-side CO measurements in Nashville and Cincinnati [*McCormick*, 1962]. In Bangkok, vehicular traffic is responsible for 71% of the city's CO emissions, and most measurement stations around the city showed distinct morning and evening peaks in CO [*Zhang and Oanh*, 2002]. On calm clear days in New York and Houston, aerosols were found to show peak values during the morning and evening rush hours [*Jin et al.*, 2005]. In a study in southern California, CO showed pronounced morning peaks on weekdays, and no such peaks on weekends when traffic was much lighter [*Qin et al.*, 2004].

If the diurnal cycle in Kathmandu, including the morning and evening peaks of primary pollutants, were dominated by variations in traffic, then we would expect to find smaller or no peaks on days with less traffic, such as on weekends and festival days. As mentioned in Chapter 1, a flask sampling study of hydrocarbons [*Sharma*, 2000] *did* find street-side concentrations of ethene and acetylene emitted by traffic to be factors of 3-5 lower on weekend mornings and evenings compared to weekdays. A similar three-fold decrease in ethene from weekday to weekend has also been found in Mexico City [*Altuzar et al.*, 2005]. Testing our hypothesis about CO, therefore requires checking whether variations in emissions can account for the observed variation in ambient CO.

Section 3.2 showed that in Kathmandu, distinct morning and evening peaks of CO took place even on festival days that had no morning and evening rush-hours and different cooking patterns. We also saw that Kathmandu's lowest ambient CO values happened between late morning and late afternoons, despite the fact that traffic was much heavier in the afternoon than at night. There are additional reasons to believe that the morning and evening peaks in Kathmandu were not primarily a result of morning and evening peaks in emission: Figure 4.1 shows the CO diurnal cycle on select sunny weekdays in January 2005, while Figure 4.2 shows the same in February. Each day had an early

morning rise in CO, a late morning drop, an afternoon low, an evening rise, and a night-time drop.

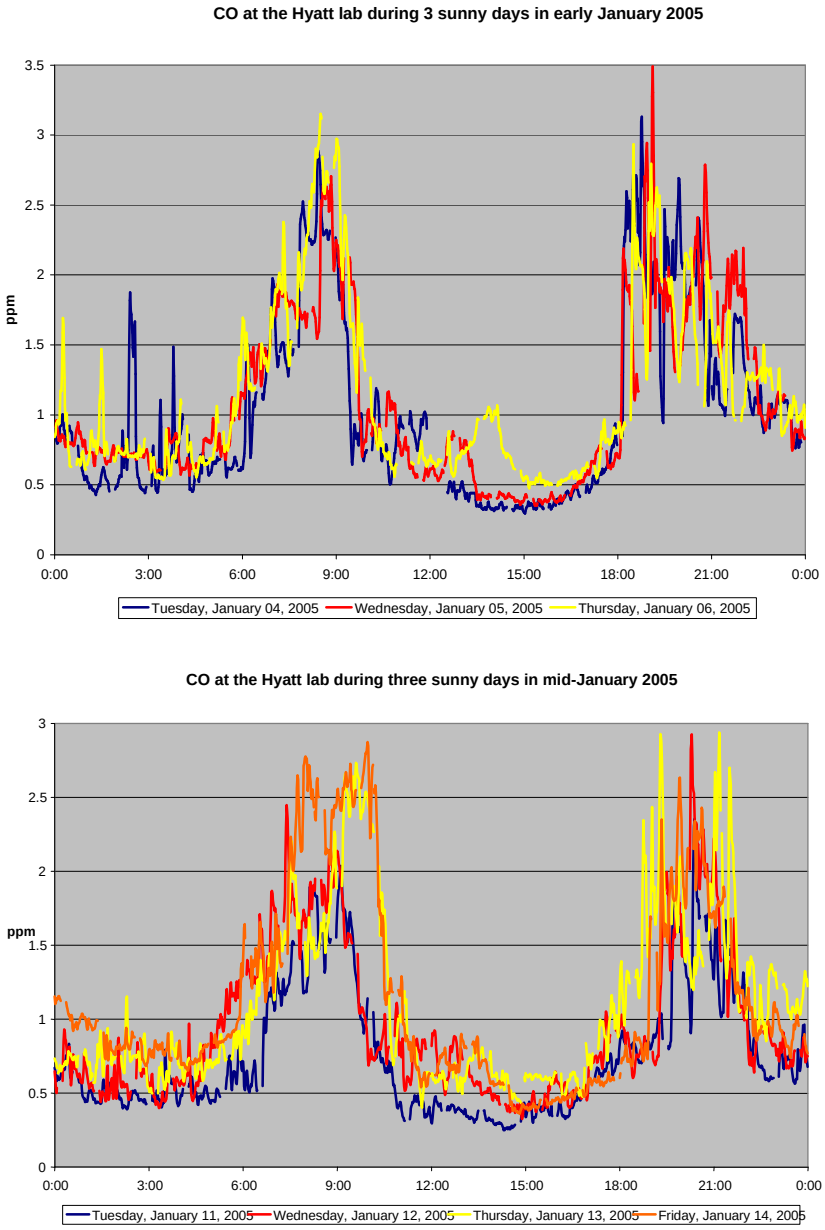

Figure 4.1: CO at the Hyatt lab on selected sunny days in January.

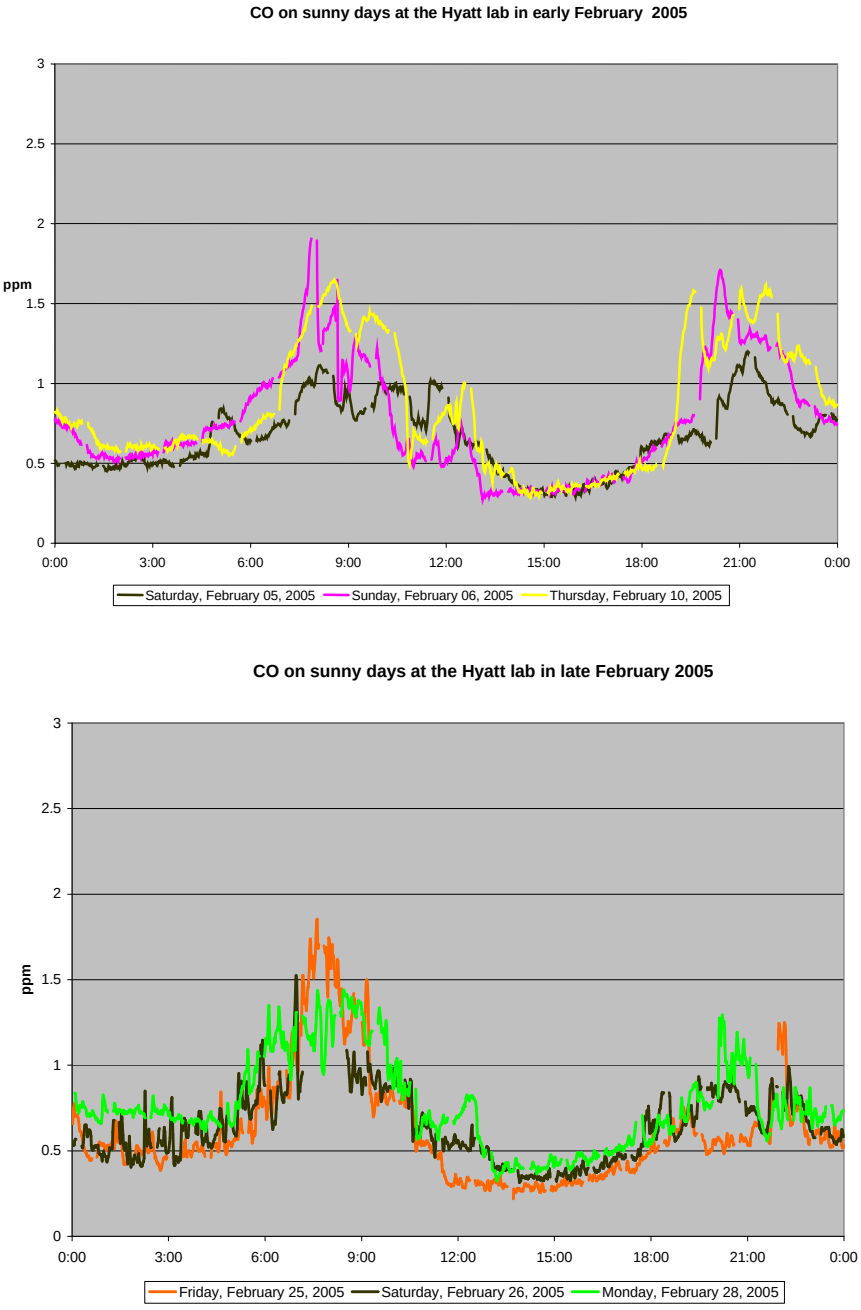

Figure 4.2: CO at the Hyatt lab on selected sunny days in February.

Looking more closely, we see that the evening CO peaks began at or after 6 pm, even though the heaviest evening rush-hour traffic always took place just after 5 pm. In addition, on the bottom panel of Figure 4.1, we can see that on Tuesday and Wednesday, January 11 and 12, the morning peak dropped off sharply at 9 am, while on Thursday and Friday, January 13 and 14, the morning peak reached a maximum shortly after 9 am and

did not drop off until 10 am. In January 2005 most offices started at 9 am, and rush hour traffic had already ebbed off by 10 am. We see similar variations in termination of the morning peaks and the onset of the evening peaks in February (Figure 4.2). Office and school start and end-times did *not* vary from one day to the next, and neither did most of the rush-hour traffic patterns. It is thus clear that the CO peaks did not correspond directly to peaks in the largest emissions source (traffic), allowing us to reject the hypothesis that the peaks were solely due to temporal variations in the input of CO into the near-surface air mass in the Kathmandu Valley.

Could the peaks be solely due to variations in ventilation – in the rate of removal of CO from the near-surface air mass in Kathmandu? Let us hypothesize for a moment that the time-variations in ambient CO in the valley-bottom air mass were only due to time-variations in the rate of the valley's ventilation. In other words, we would get the same patterns regardless of variations in emissions. Is such a hypothesis plausible?

Morning and evening peaks of CO, with an afternoon minimum and a slow night-time decrease have also been found in Pusan, South Korea [*Lee et al.*, 2005]. An experiment in Pusan highlights the importance of ventilation changes: During the Asian Games in Fall 2002, motor vehicle traffic was restricted to help improve air quality [*Lee et al.*, 2005]. Ironically, air quality was worse despite reduced emissions, with higher CO concentrations throughout the day. This was due to changed meteorological conditions, with a maximum mixed layer height averaging 1100 meters above ground during the Games, compared to 1800 meters in the days before. Meanwhile, in Mexico City it was found that, while traffic emissions stayed the same, ethane concentrations were much higher in November than in March; the difference was attributed to November's lower mixing layer height associated with lower temperatures [*Altuzar et al.*, 2005]. Similar patterns with similar explanations were found in Taiwan as well [*Yang et al.*, 2005].

In the literature, examples of situations where ambient pollution was strongly influenced by atmospheric transport processes usually came from remote sites located far from the emissions sources. For example, at the mountain-top observatory at Jungfraujoch in Switzerland, high CO concentrations with late afternoon peaks were found at times of

strong thermally induced transport of air up from nearby valleys [*Forrer and Ruttimann*, 2000]. Downwind of cities, CO and ozone peaks often correlate with each other, as was, for example, found on Mt. Tai in Taiwan [*Gao et al.*, 2005]. Similar correlation was found in Okinawa, Japan, when receiving Chinese emissions; however, when local emissions reached the measurement site high CO measurements were not accompanied by high ozone concentrations [*Kato et al.*, 2004]. At rural sites in the Yangtze Delta in China [*Cheung and Wang*, 2001] and at Srinakarin in western Thailand [*Pochanart et al.*, 2003], CO and ozone also showed coincident peaks at times when the sites were receiving polluted urban air. At Srinakarin, when nearby biomass fires (which burned all night) were responsible for the CO emissions, the ambient CO levels stayed high at night, only dropping during daytime when there was more vertical mixing and convective ventilation.

We saw in Section 3.6 that CO and PM_{10} measurements at the Hyatt lab showed a small secondary peak around noon, coinciding with a sharp peak in ozone shortly after the westerly winds began. Figure 4.3 shows ozone plots for the days corresponding to the bottom panels of Figure 4.1 and Figure 4.2. We see in Figure 4.3 that each day had a distinct mid-day ozone peak lasting about an hour, with values that were 15-25 ppb higher than during the rest of the afternoons. Comparing to Figure 4.1 and Figure 4.2, we see that these ozone peaks occurred at the same times as the smaller CO peaks. We have discussed in Chapter 3 that these simultaneous peaks were likely the result of the transit past the measurement site of an air mass that had been stagnant over the city during the morning. During the rest of the afternoon the Hyatt lab sat downwind of the city, with strong westerly winds blowing fresh urban emissions past the lab within a short time. We would expect emissions from the congested Chabahil intersection, 1 km upwind of the Hyatt lab, to be detected at the Hyatt lab within minutes. Yet the peak in evening rush-hour emissions does not show up in the data; the pollution level does not rise rapidly until around 6 pm when the westerly winds ceased.

The data thus shows clearly that the time variation in the ventilation rate played a significant role in shaping the diurnal twin peaks of CO. It appears to account for the

timing of the abrupt end of the morning peak, the brief concurrent peak with ozone, as well as for the onset of the evening peak.

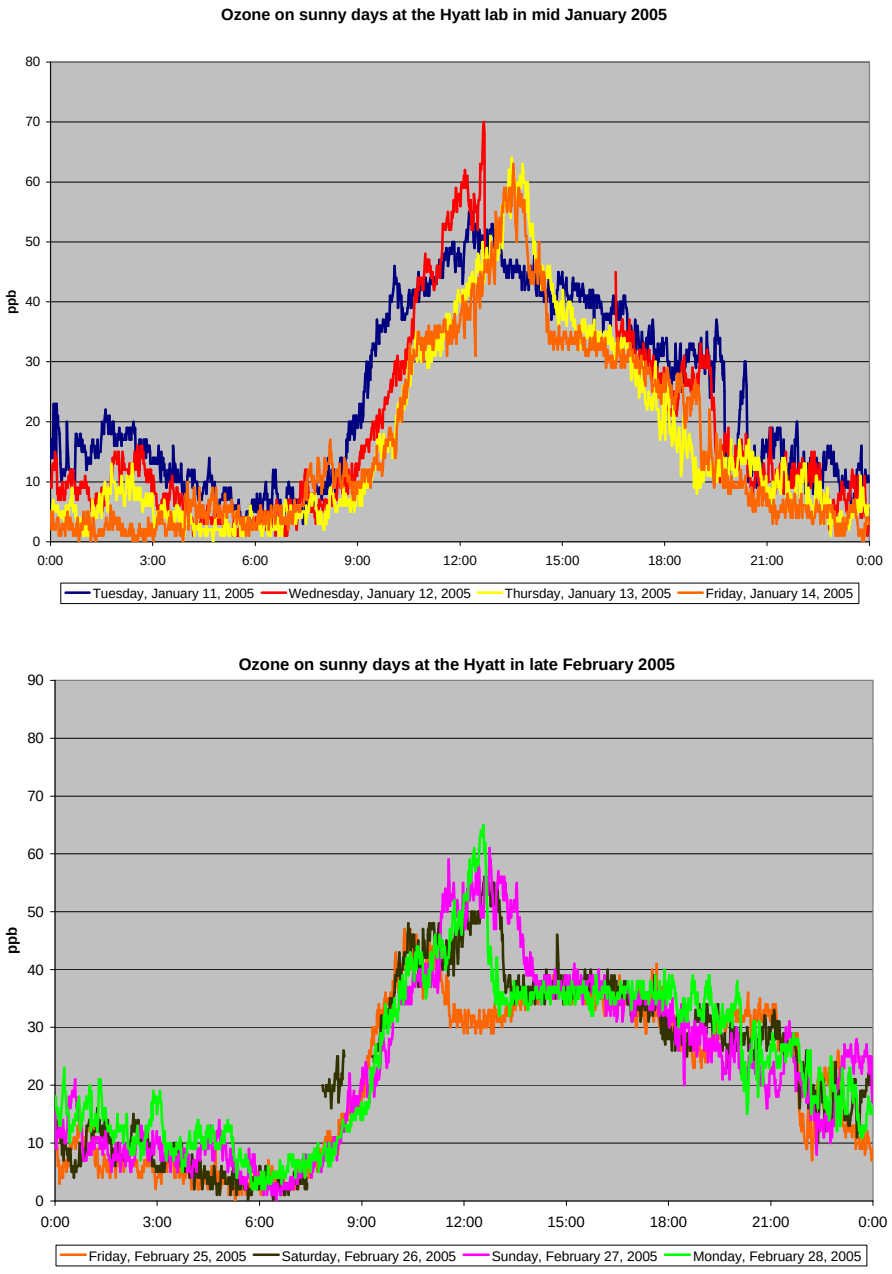

Figure 4.3: Ozone at the Hyatt lab in mid January and late February.

Changes in ventilation do not, however, account for variations in the height of the peaks. We saw in Section 3.2 that on the holidays of the Dashain festival, CO peaks were lower

while there was much less traffic compared to normal week days. Similarly, Figure 4.2 as well as many figures in Chapter 3 show that Saturday[20] peaks were shorter than on adjacent days with similar weather. The timing of the afternoon low appears to be the result of changes in ventilation, but the ventilation rate alone does not fully explain the shape of the CO diurnal profile.

It is clear from the discussion so far that the diurnal pattern of CO in the Kathmandu valley is influenced by the temporal patterns of *both* emissions and ventilation. Let us consider then the hypothesis that the diurnal profile of ambient CO, with the distinct twin-peaks, is shaped by the difference between emission and ventilation rates, both of which vary over time. In other words, ambient levels rise at times when emissions exceed the rate of CO ventilation, and they drop at times when the ventilation rate exceeds the emission rate.

This interpretation fits well with our observations of wind speed, stability, and human activities and is able to qualitatively capture the observed diurnal cycle. In the morning, when the city residents wake up, cook meals, and travel to work, the air is calm and stable, rapidly accumulating pollution near the source. The CO levels measured at the Hyatt lab would be affected by traffic on the nearby Chabahil-Bouddha road and by residential sources. Once the westerly winds start at the valley bottom, they quickly advect eastwards the previously stagnant Chabahil-Bouddha Road air mass containing high concentrations of pollutants as measured at the lab. Then a second peak is observed when the bulk of the air sitting over the more distant city arrives (this peak is lower than the morning peak, since, by now, that air mass has been vertically diluted). All afternoon and into the evening rush-hour, strong westerly winds sweep away CO as it is emitted, maintaining low concentrations at the Hyatt lab. As the inversion rebuilds in the evening and ventilation is once again reduced, pollution from ongoing evening activities begins to be accumulated in the near-surface air mass. Once the city goes to sleep (around 9 or 10

[20] Saturday in Nepal is equivalent to Sunday in the West, with everything shut down. On Sundays generally schools and many private organizations are closed, while banks, stores and many government offices are open.

pm) and emissions from traffic, cooking, and heating die down, a slow nocturnal ventilation is able to gradually clean up the night-time near-surface air mass.

The hypothesis that ambient CO concentrations in the Kathmandu Valley are a result of interplay between rates of emission and ventilation fits with findings at many other places described in the literature. A study of monthly CO data over a period of eight years in fifteen cities around the United States found that information about emissions, wind speed, and mixing height were necessary and sufficient to predict ambient CO concentrations [*Glen et al.*, 1996]. During a year of street-side measurements in Buenos Aires, Argentina [*Bogo et al.*, 2001a], morning and evening CO peaks were found to coincide with peaks in traffic flow. However, during summer months, when average wind speeds were higher, average street-side CO concentrations were lower. Days with no wind had higher night-time values of CO, and higher morning peaks. Meanwhile, at measurement stations downwind of Bangkok, Thailand, the height of the morning CO peaks were also found to be strongly dependent upon wind direction [*Zhang and Oanh*, 2002]. In Santiago de Chile, a field campaign was organized in Spring 2002 to collect CO canister samples upwind, within, and downwind of the city at 2 hour intervals over the course of three days [*Rappenglück et al.*, 2005]. Within the city there were distinct morning and evening peaks, with a minimum value at noon, like we found in Kathmandu. The authors found that the CO time series reflected influences of both meteorology and emissions. An earlier study in the same city found that during the summer there were no evening CO peaks because, at the time of rush hour, there was still strong ventilation [*Rappenglück et al.*, 2000].

So far we have assumed that pollutants, once "ventilated" are permanently removed from the Kathmandu Valley. What if they are not? It is possible to consider that the evening CO peak occurs due to an abrupt slowing down of CO transport away from the near-surface air, but that part of the morning peak is created by re-circulation of polluted air that is stored aloft over-night and that returns to the surface in the morning. Stable nocturnal temperature inversions near the surface grow from the bottom upwards. Pollutants that were, say, 100 meters above the city at dusk, would likely be trapped at

aloft and remain there until either horizontal winds move them or vertical mixing resumes. When the inversion dissolves in the morning, the pollutants can mix back down to the surface, a process known as re-circulation.

In cities near mountains, slope winds at night have been found to affect pollutant storage and re-circulation. In Freiburg, Germany, well developed mountain wind systems were able to remove pollutants during the day, while katabatic winds brought in clean air during the following night. If wind speeds were low and the atmosphere was stable, then the pollutants that were carried into the neighboring black forest mountains during the day were returned back to the city at night [*Baumbach and Vogt*, 1999]. At a mountain-side station 400 meters above southwestern Mexico City, high concentrations of ozone and PM_{10} were often observed at night, in elevated layers that would re-circulate downward the next morning [*Baumgardner et al.*, 2000]. In Phoenix, Arizona, sharp vertical gradients in elevated layers of CO were also found at night and at the time of sunrise [*Berkowitz et al.*, 2005].

In Chapter 5 we shall study further whether pollutants are permanently removed from the near-surface air in the Kathmandu Valley, or whether they re-circulate, by conducting tracer transport modeling with a meso-scale meteorological model, releasing tracers around the Kathmandu valley in the evening, and watching whether they are re-circulated the next morning. But before doing so, we can already find some hints by examining data from a special case: the festival of Shivaratri, when bonfires were lit around the valley during the evening of March 8, 2005. Unfortunately the CO instrument did not work properly that night, but the Dusttrak recorded PM_{10} continuously from March 7 through 10[21]. This PM_{10} data is shown in Figure 3.4.

Not surprisingly, we find that PM_{10} had a very high peak during the evening of March 8th. By late evening most of the fires and thus the source of pollutants had come to an end, and by midnight the PM_{10} concentrations had started to decrease as well. However, we see that in the morning of the 9th, PM_{10} concentrations grew to a second unusually high peak. There was no unusual new source of PM_{10} on the morning of March 9th, so we

[21] Recall from Chapter Two that PM_{10} and CO are almost always well correlated.

appear to have seen particles that were emitted the night before, and were then re-circulated in the morning. Of course one night's data from one location is not sufficient to conclude that re-circulation plays a significant role valley-wide, each day. It does, however suggest the importance of further study of what happens once pollutants depart from the near-surface air.

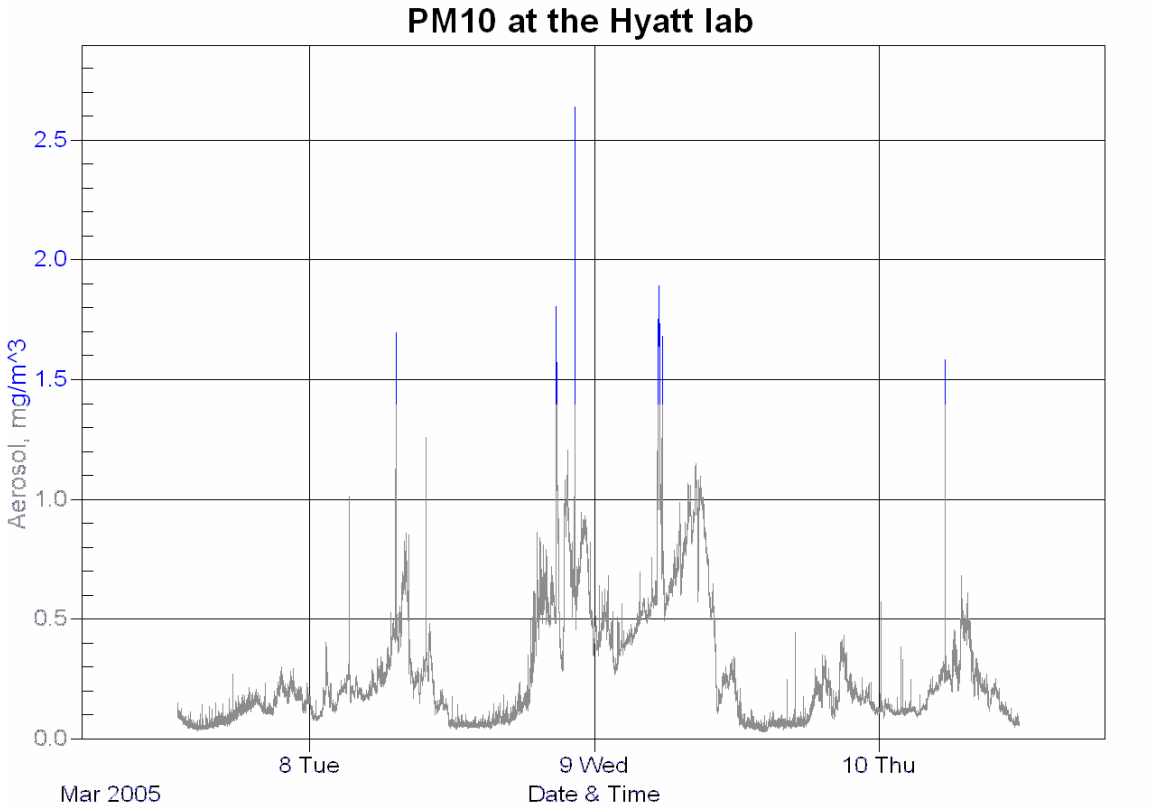

Figure 4.4: PM_{10} at the Hyatt lab at the time of and following the Shivaratri bonfires (evening of March 8).

To summarize, we have concluded in this section that the twin peaks in CO observed in Kathmandu each day are a result of the interplay between ventilation patterns and emissions. But what are the ventilation patterns? We saw in Chapter 3 that that the late-morning drop in CO levels took place at the time when the mixed layer grew and the westerly surface winds picked up speed. We saw that the afternoon drop in pollution corresponded to an eastward transport of the polluted air mass that had been sitting over

the city. We also found, to our surprise, that night-time values of CO usually dropped to near-background levels despite strongly suppressed horizontal and vertical mixing.

4.4 The Questions

In this section we introduce three specific questions whose aggregate answers will help us understand the mechanisms responsible for the observed daily twin peaks of CO, while also addressing the broader question that initially guided the design of the dissertation: How do emission patterns and ventilation mechanisms interact to determine the accumulation and ventilation of pollutants from the Kathmandu Valley? The rest of this chapter, as well as the two chapters that follow, focus upon addressing these specific questions.

Question 1. What is the mechanism of the break-up of the nocturnal inversion, in the Kathmandu Valley on winter mornings, which lets the mixed layer grow? Studies elsewhere have found a variety of mechanisms responsible for the break-up of inversions in valleys and basins. These range from surface heating and convection (as on open plains), to side-wall warming and up-slope flows along the valley edges, to basin-center subsidence warming, to turbulent erosion by winds aloft. The existence, efficiency, and interactions of the individual mechanisms depend upon a valley's size, geometry and orientation, the surrounding topography and land surfaces, the season, synoptic weather conditions, and the moisture budget. The answer is thus not trivially obvious from a glance at the map.

Question 2. How are pollutants ventilated from the Kathmandu Valley in the afternoon? The drop in surface CO and PM_{10} concentrations every afternoon, despite their continued emissions, indicates that they are efficiently removed from the near-surface air. But are they merely lifted up to be re-circulated in the evening? Or are they lifted and then transported away by upper-level winds? Are they blown out of the valley through the eastern passes? Are they carried up the slopes to the valley rim peaks? There are a variety of plausible pathways of pollutant ventilation that need further study.

Question 3. Why do night-time concentrations of CO (and PM_{10}) drop almost to regional background levels? This remains a mystery, since we would expect the lack of surface winds and the suppressed vertical mixing at night to lead to the continued accumulation near the surface of species emitted during the evening and night. We had expected high and growing pollution levels throughout the night.

The next section describes in detail the hypotheses for each of these questions, using knowledge gained from the literature of research done elsewhere. The questions are addressed again Chapter 5.

4.5 The Hypotheses

This section presents a menu of hypotheses that could plausibly answer each question, discussing their likelihood, and describing the model results needed to support or reject each hypothesis.

To facilitate discussion, we shall frequently refer to figures containing a diagram showing one or two schematic vertical cross-sections through the valley (Figure 4.5). This diagram was designed to capture in the simplest possible way the relevant terrain features. The east-west cross-section (top) shows a representative western valley-rim pass (there are three total) and a mountain on the western side (there are two between the three passes); it also shows a representative pass on the eastern side (out of two), the higher Banepa-Dhulikhel valley (with the city of Dhulikhel labeled), the terrain drop beyond the Dhulikhel ridge, as well as a representative eastern valley-rim mountain (such as Nagarkot). The north-south cross section shows the low Likhu Valley to the north, the Shivapuri range on the northern rim of the valley, the cities of Kathmandu and Lalitpur, the small Chobhar-Kirtipur ridge (cut through by the Bagmati river), the Bagmati outflow valley to the south, and the Champadevi and Phulchoki mountains on either side of the Bagmati valley. For some of the hypotheses, time-series of one cross section are shown instead of both a west-east and a north-south cross section.

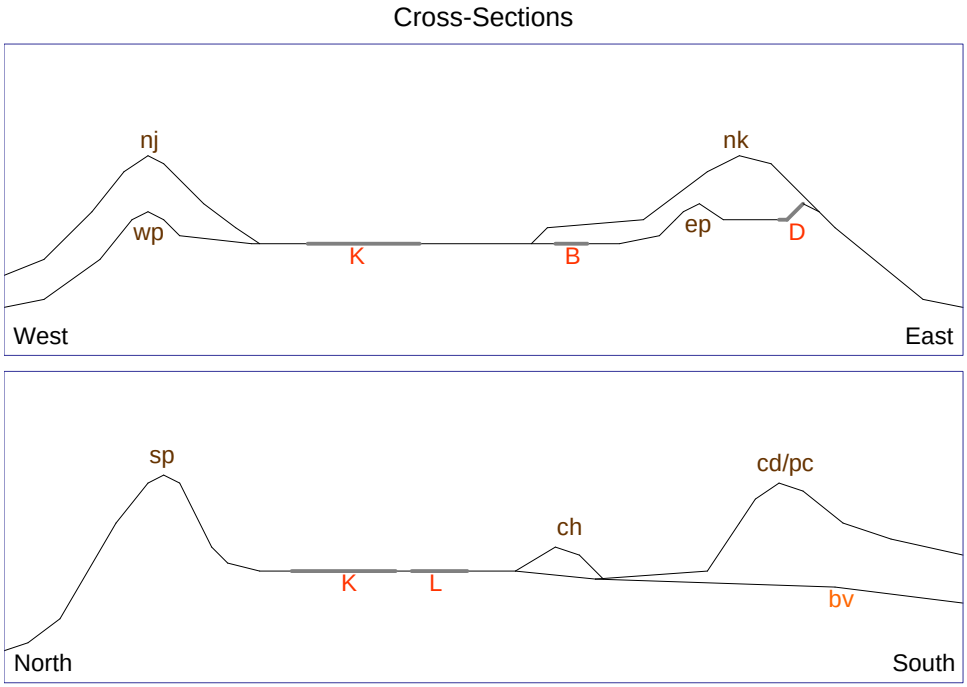

Figure 4.5: Schematic cross-sections through the valley showing the cities Kathmandu (K), Bhaktapur (B), Dhulikhel (D), and Lalitpur (L), the valley-rim mountains and passes, and the Bagmati river out-flow valley (bv). Also labelled in brown in this diagram (but not subsequently) are the western valley rim passes (wp), the eastern passes (ep), Chobhar hill (ch), as well as the Shivapuri massive (sp) on the northern side of the valley, the Champadevi and Phulchoki mountains on the south side (cd/sp), the Nagarjun (nj) mountain on the west, and the Nagarkot (nk) ridge on the east.

4.5.1 Question 1: Mechanism of the breakup of the nocturnal inversion.

We begin with four hypotheses that could plausibly explain the inversion break-up. The first assumes that the valley behaves as if it were a flat plain. The next three discuss three different mechanisms of inversion break-up and mixed layer growth that have commonly been found in mountain valleys and basins.

The first hypothesis (H1A) is that the Kathmandu Valley's inversion breaks up in the morning with the same mechanism as inversions break up over flat plains. The Kathmandu Valley has a ratio of vertical relief (altitude difference from the bottom to the rim) to horizontal expanse on the order of 1:30. It is not a narrow river valley, and it has a large flat center.

Over flat land, inversion break-ups are driven by surface heating and follow a pattern that has been well studied [*Angevine et al.*, 2001; *Garcia et al.*, 2002; *Stull*, 1988; *Young et al.*, 2000]: Once the sun has risen and started to warm the surface, a convective mixed layer grows upward from the surface. The bottom heating creates unstable conditions, which allow thermals of warm air to rise, chipping away at the inversion above. The mixed layer grows by entraining (mixing in) air that was previously isolated from the surface by the inversion. Entrainment of such air containing ozone is often the cause of the rapid rise in surface ozone in the morning observed in many locations. The mixed layer continues to grow until the late afternoon, breaking through the upper-most remnants of the inversion, and then entraining air from the less stable residual layer that spent the night above the inversion. Over land, the mixed layer can often grow to a thickness of 2000 meters or more [*Berman et al.*, 1999]. At times the mixed layer has been observed to grow faster over cities due to enhanced convection driven by additional heat sources [*Kallistratova and Coulter*, 2004]; it has also been found to be affected by soil moisture content [*Santanello et al.*, 2005].

Temperature inversions in mountain valleys tend to be deeper, but to have weaker average stability than inversions over plains [*Whiteman*, 2000]. They also tend to be eroded not just from the bottom up, but also from the top down.

The second hypothesis (H1B) is that the inversion breakup is dominated by mountain - valley wind processes that are normally found in narrow valleys: As the sun's rays in the morning hit the upper slopes first, those start to heat up first, creating up-slope flows that pulls air up from the valley bottom. The air in the valley bottom is then replaced by air coming up the river valley. For much of the day, a strong wind blows up the river valley, while a shallow layer of air blows up the side walls perpendicular to the valley axis [*Atkinson*, 1981; *Li and Atkinson*, 1999; *Prévôt*, 1994; *Prévôt et al.*, 2000b; *Whiteman*, 1990; *Whiteman*, 2000]. As mentioned in Chapter 1, strong up-valley winds driven by the warming of the Mustang Basin were found in the Kali Gandaki Valley in northern Nepal [*Egger et al.*, 2000; *Egger et al.*, 2002].

Figure 4.6 shows that morning fog on the southern edge of the valley disappeared long before the fog lifted over the city at the valley center (in the background). While fog was disappearing below, a strong wind was felt blowing up the slope at the camera location. But what replaced the air that blew up the slopes? Figure 4.7 illustrates the process of the inversion break-up according to hypothesis H1B, with a wind blowing up the Bagmati Valley (red arrow) to replace valley bottom air that is removed up the slope.

Figure 4.6: The Kathmandu Valley from Hattiban on the morning of December 8, 2005. The picture on the left was taken at 7:52 am, and the picture on the right at 8:30 am. The little hill at the center is part of the low Chobhar-Kirtipur ridge.

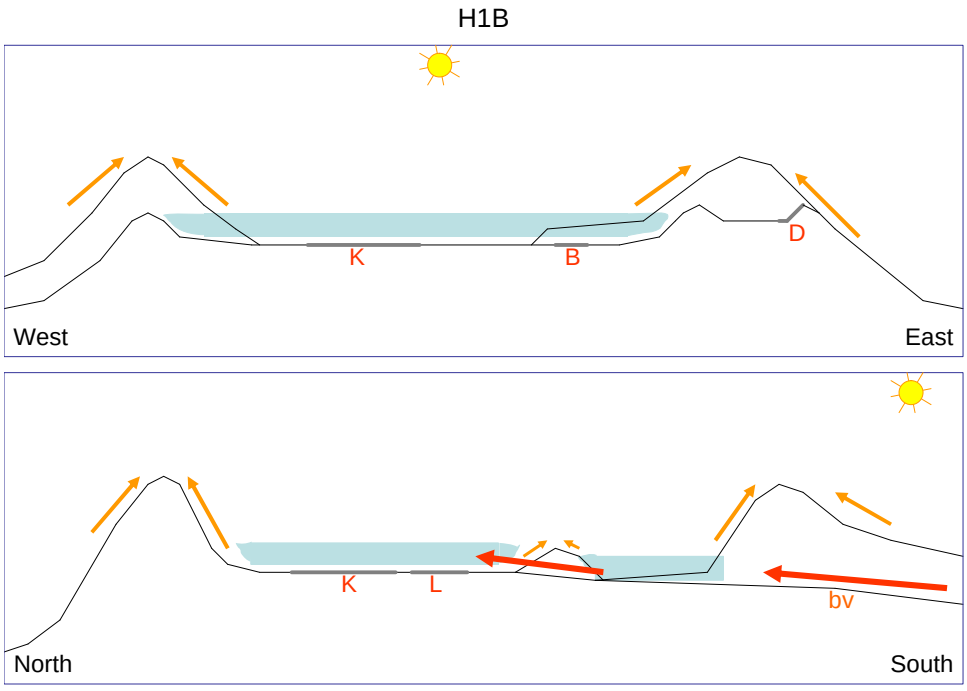

Figure 4.7: Illustration of hypothesis H1B, showing the cold air pool / inversion, slope flows, and flow up the Bagmati River Valley.

The third hypothesis (H1C), described in Figure 4.8, asserts that the break up of the Kathmandu Valley's inversion occurs according to a pattern first described for large basins and wide valleys [*Whiteman*, 1982]: warming side-walls generate upslope flows as in H1B. However, rather than generating a strong replacement flow up the river valley, the diverging air mass at the valley center is replaced by subsidence over the valley center.

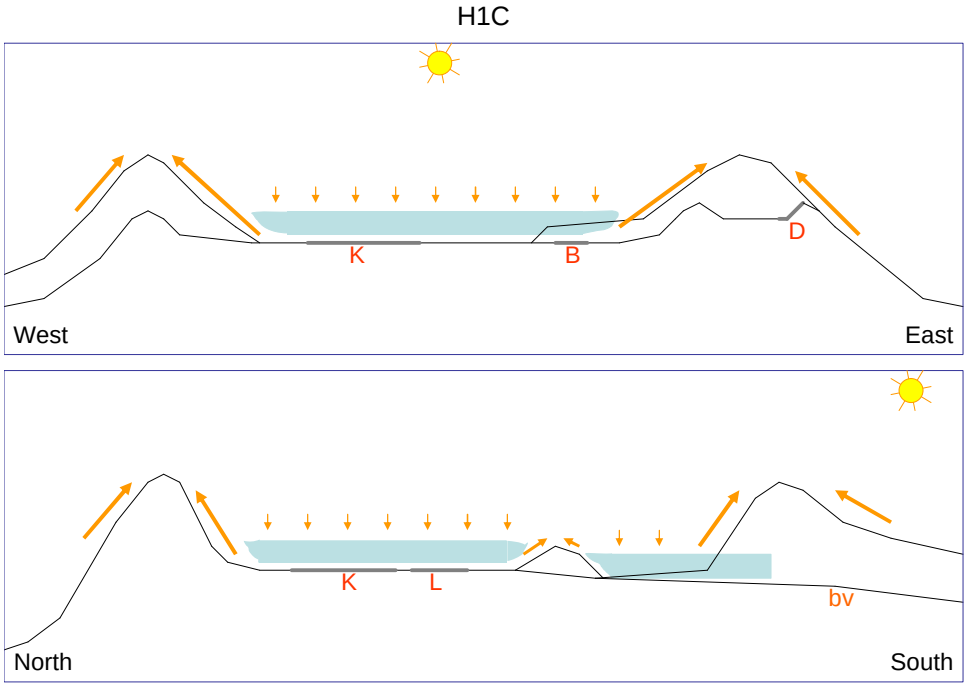

Figure 4.8: Illustration of Hypothesis H1C, showing up-slope winds in the morning creating subsidence over the cold-pool at the bottom of the Kathmandu Valley.

A by-product is that subsidence heating over the basin center erodes the inversion from the top as well. This process of inversion break-up has been observed in basins without river outlets measuring just one kilometer across [*Whiteman et al.*, 2004b] as well as in large basins measuring several hundred kilometers across [*Banta and Cotton*, 1981; *Kondo et al.*, 1989; *Whiteman et al.*, 1999; *Zhong et al.*, 2001]. If a basin is wide enough, then the slope-flows and inversion erosion might begin first on the east-facing west side of the basin [*Kelly*, 1988].

The fourth hypothesis (H1D) is that the inversion is dissipated by turbulent erosion from winds blowing across the top – specifically that momentum from winds aloft propagates downwards through the cold air pool at the basin bottom [*Whiteman and Doran*, 1993]. Dissipation of the cold air pool by winds aloft has been studied in the basin of Ljubljana, Slovenia, using MM5 meso-scale model simulations [*Rakovec et al.*, 2002]; the study found that wind speeds aloft must exceed a certain threshold to begin eroding the cold air pool, and must increase over time to be able to completely remove the pool. In the basin of the Colorado Plateau, deep persistent temperature inversions can be removed rapidly when cold air passes over the plateau, reducing the inversion strength [*Whiteman et al.*, 1999]. In the ASCOT field experiment in western Colorado, it was found that night-time drainage winds in deep valleys can be eroded when above-valley and along-valley winds are blowing in the opposite direction [*Orgill et al.*, 1992]. The authors of a field study in the South Park Basin in Colorado [*Banta and Cotton*, 1981] described three wind regimes in the basin: down-slope, up-slope (both of which take places in narrow valleys as well), and afternoon winds in the same the direction as the wind above the basin (something usually not found in narrow valleys). In the wide Kathmandu Valley the afternoon westerlies did correspond to the large-scale westerly winds blowing above the ridge top. In fact, at the altitude of the tallest Himalayan peaks lining the southern edge of the Tibetan plateau, the westerly jetstream has an average speed of 43 meters per second [*Moore*, 2004]. The vertical cross sections of wind velocity measured by the sodar (Figure 3.30) shows westerly winds penetrating down towards the surface over the course of the afternoon. At the Hyatt lab they were usually seen arriving around noon. It is unclear from the data alone whether these winds penetrated down to the surface as a result of the disappearance of the temperature inversion, or whether they were actively involved in dissipating the cold air pool.

The field data does not provide sufficient information to confirm or reject any of the hypotheses for Question 1. We know that smoke plumes blow up the Bagmati River valley in the morning, but does that provide the primary flux of air into the valley to offset the up-slope flows? We do not have a measure of subsidence heating, or even of the time-evolution of the altitude of the inversion top. We know that by noon of each

day, westerly winds were usually found at the western passes and they then penetrated down to the valley bottom. But do they penetrate down by helping break down the inversion, or because the inversion is gone?

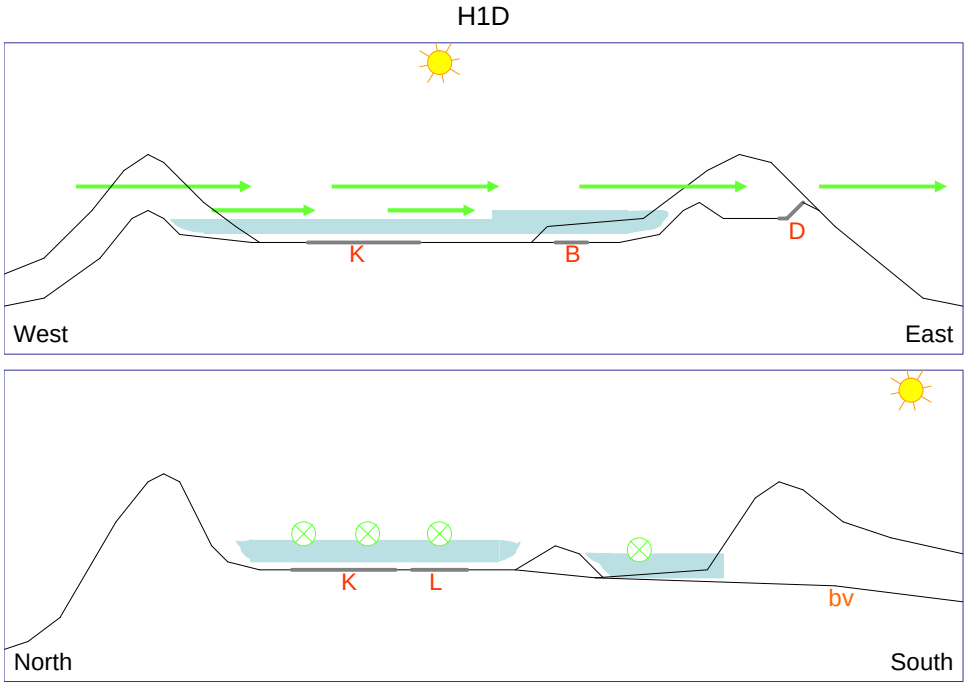

Figure 4.9: Illustration of Hypothesis H1D: The nocturnal inversion is dissipated by turbulent erosion by westerly winds aloft.

Careful analysis of the vertical profiles of wind and potential temperature in meso-scale model runs is needed to determine which hypothesis is correct. Looking at the time evolution over the course of the morning of vertical cross sections of potential temperature and winds, we expect to be able to see whether the mixed layer under the inversion grows horizontally uniformly up from the ground, without any descent of potential temperature surfaces (H1A); whether it grows faster near the valley edges (H1B or H1C); or whether the flux up the Bagmati valley (calculated from the wind speeds) can account for the flux of air up mountain slopes (H1B). Cross sections of vertical wind velocity can show whether there is subsidence over the valley center (H1C). Confirming hypothesis H1D would require not only rejection of the first three hypotheses, but finding that the inversion break-up propagates from west to east.

4.5.2 Question 2: Pathways of pollutant ventilation from the Kathmandu Valley

Section 4.5.1 discussed hypotheses for the dissipation of the nocturnal cold air pool and the break-up of the inversion in the morning. As the inversion breaks up and the mixed layer grows, upper level air is entrained into the mixed layer, and ground-level pollution is diluted. But what are the actual mechanisms for the removal of pollutants from the valley bottom? Most likely, several mechanisms operate over the course of the day, removing a fraction of the pollutants each. Here the hypotheses are presented as if they were mutually exclusive; Chapter 5 will return to discuss the individual contribution of each mechanism over time.

We saw earlier that the afternoon low in CO in the Kathmandu Valley corresponded to a time of ongoing emissions, but with a tall mixed layer and high wind speeds that allowed quick removal of fresh emissions from the source region. The night-time low corresponded to a time of low emissions and low ventilation, and a mystery of why stored evening emissions did not maintain high concentrations through the night. Here we discuss the ways that pollutants could be removed from the valley air during the day time; the night-time low is the subject of the next sub-section.

The **first hypothesis (H2A)** to explain the afternoon low in pollution is that the pollutants are not actually ventilated from the valley, but merely re-circulated, as illustrated in Figure 4.10. This implies that the evening peak is a result of both evening emissions and the return of pollutants that had been stored elsewhere during the afternoon. Re-circulation of pollutants has been found to take place in Freiburg, Germany, during low-wind situations [*Baumbach and Vogt*, 1999]. In British Columbia pollutants flowing up slopes were found to return again in the evening, trapped in a closed circulation [*Reuten et al.*, 2005]. Closed local circulation cells have also been found over Athens [*Asimakopoulos et al.*, 1992]. Depending on the wind speed and other meteorological conditions, air pollutants in Mexico City can be vented out of the basin or re-circulated to add to the next day's pollution [*Fast and Zhong*, 1998].

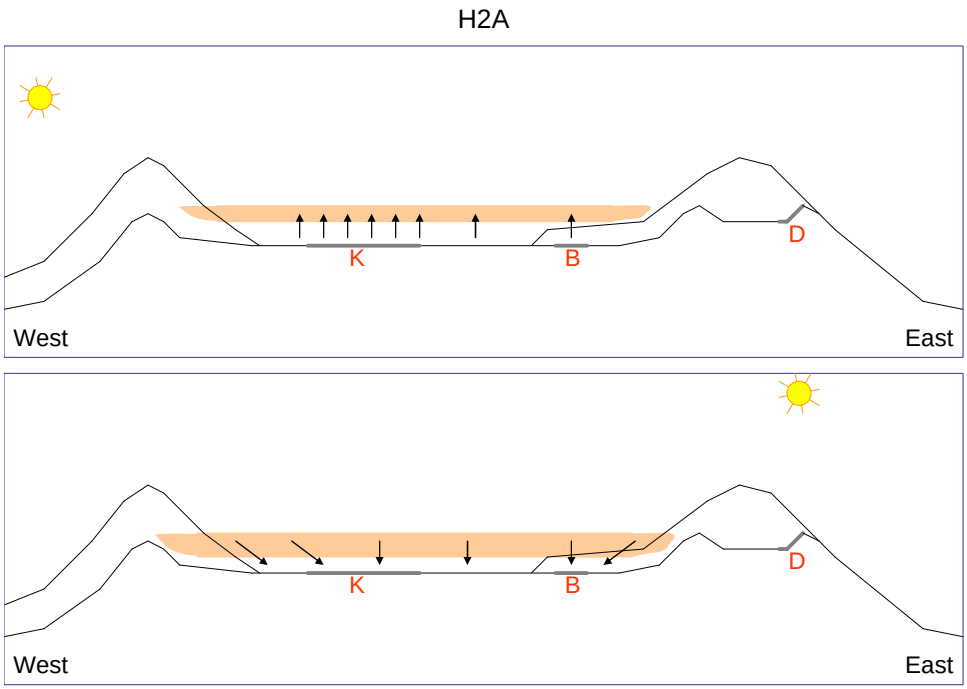

Figure 4.10: Time-series illustration of hypothesis H2A on west-to-east cross sections over time. The storage of pollutants in higher layers in the evening (top), and subsequent re-circulation the next morning (bottom).

Section 4.3 showed evidence from the *Shivaratri* bonfires that in the Kathmandu Valley pollutants emitted in the evening might be stored at night in air masses away from the surface and then re-circulated back to the city in the morning. Is that possible during the afternoon as well? We hypothesize here that even during the afternoon low in surface air pollution, a large fraction of the pollutants were merely stored elsewhere for re-circulation in the evening, rather than being removed from the valley system.

The second hypothesis (H2B) is that the pollutants are ventilated from the valley because the daytime mixed layer rises above the height of the surrounding peaks, to altitudes where strong winds can blow the pollutants out beyond the valley, as illustrated in Figure 4.11. Such behavior has been observed and modeled in Mexico City [*Bossert*, 1996; *Bossert*, 1997; *Fast and Zhong*, 1998]. During the TRACT experiment over the Black Forest in southern Germany, it was found that the altitude of the mixed layer top is higher over mountains than over surrounding flat land, and that the mixed layer top rises and falls with underlying topography [*Kalthoff et al.*, 1998; *Kossmann et al.*, 1998]. In

other words, the top of a fully formed mixed layer over the Kathmandu Valley would be flat over the valley center, and not only rise as it approached the valley rim mountains, but also rise higher than the mountain tops. Sodar data at CTEVT, at the valley center, had already indicated a mixed layer height approaching or exceeding the height of the surrounding mountains. Once mixed to heights above the surrounding mountains, the pollutants could then easily be carried eastwards by the strong westerly winds that in winter blow continuously over the top of the valley.

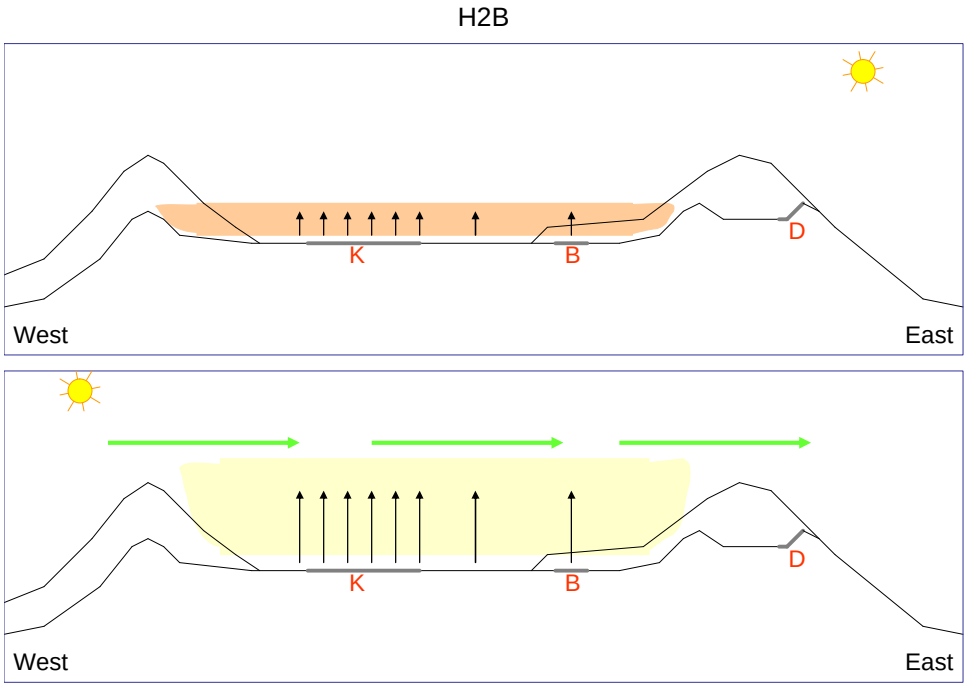

Figure 4.11: Time sequence illustration of hypothesis H2B on west-to-east cross sections over time. The ventilation of pollutants from the Kathmandu Valley through the growth of the mixed layer above the height of the surrounding mountains.

The third hypothesis (H2C) is that the pollutants are removed from the valley by relatively clean air blowing in through the western valley rim passes and out the eastern passes. In other words, the existence of low passes on the west side allows strong westerly winds to penetrate into the valley that would not be able to if there were a high wall of mountains without passes. The hypothesis is illustrated in Figure 4.12. In a field study in South Park basin in Colorado [*Banta and Cotton*, 1981], it was found that an inversion in the morning prevented upper-level westerly winds from penetrating to the

surface; once the inversion was gone the westerlies reached down to the surface. Another study did idealized modeling of flows up valleys that terminated at the edge of a plateau [*Egger*, 1987], similar to the valleys to the west of Kathmandu Valley that terminate at Nagdhunga, Bhimdhunga, and Mudku Passes (see Section 1.3). That study showed that such valleys were able to contribute to the wind intensity above the plateau. It also showed that the wind intensity up the valleys was determined by the difference in elevation of the plateau heat source (1300 meters in the Kathmandu Valley's case), and the lowland heat source (~500-600 meters in the valleys west of Kathmandu). Tracers passing from a lowland area over a mountain ridge into a basin have also been studied before *[Kimura and Kuwagata*, 1993].

In the case of the western rim of the Kathmandu Valley, the flow can enter through the gaps created by the mountain passes. Flows through gaps have been studied downwind of Athens [*Asimakopoulos et al.*, 1992] and the Brenner Pass in the Austrian Alps [*Mayr et al.*, 2002]. Often wind speeds accelerate as air passes through a gap [*Whiteman*, 2000]. In winter, Mexico City regularly experiences a low-level jet exceeding 10 m/s entering the basin through a pass to the southeast [*Doran and Zhong*, 2000]. Tracer transport modeling has shown that the flow through this pass plays an important role in flushing pollutants out of Mexico City [*Bossert*, 1997]. A July and August 2003 field campaign studying the diurnal circulation of the Bolivian Altiplano (an elevated plateau surrounded by mountains) carried out vertical soundings at the in-flow passes [*Egger et al.*, 2005]. Inflow was found to start a few hours after sunrise, at the time when the stable nighttime layer over the Altiplano had heated up to become neutrally buoyant. In Chapter 3, we saw that, in the Kathmandu Valley, CO concentrations dropped down from the morning peak (indicating dilution) at the time when westerly inflow through the Bhimdhunga Pass commenced.

To examine the plausibility of this hypothesis, let us divide it into two parts: first, that the western passes allow winds to enter the valley to flush out pollutants, and, second, the eastern passes provide an exit route for the pollutants. As discussed in the paragraph above, we have found support for the first part in both the literature and in our data. But

do the eastern passes play a major role? In Mexico city, the flushing can happen by inflow through the pass in the southeast and outflow through wider gaps in the north [*Bossert*, 1997]. In the Kathmandu Valley the mountain passes on the east side are no wider than the ones on the west side; yet anecdotal evidence suggests that during the afternoons, the eastern passes, unlike the western passes, do not experience strong westerly winds. The in-flux of air through the western passes does not appear to be matched by the out-flux through the eastern passes. Unfortunately no air samples were collected in the Dhulikhel region. If the Kathmandu Valley were flushed out through the eastern passes then Dhulikhel should experience a sharp rise in pollution in the afternoon. Anecdotal evidence as well as unpublished hydrocarbon flask sampling by the author in 2000-2001, suggest that Dhulikhel has cleaner air throughout the afternoon. Bag sampling did show an afternoon rise in pollution in Lubhu, southeast of Kathmandu city at the base of Phulchoki Mountain. Could it be that flushing air enters the Kathmandu valley through the western passes (and perhaps up the Bagmati Valley), but that the exit takes place up the mountains rather than through the eastern passes?

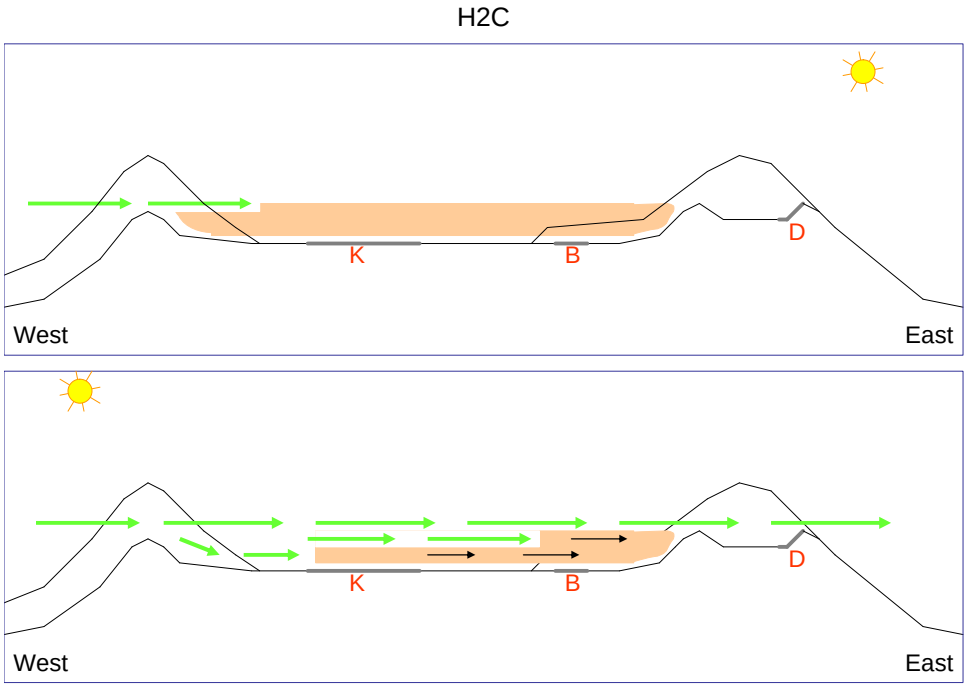

Figure 4.12: Time sequence illustration of Hypothesis H2C on west-to-east cross sections over time. Pollutants are ventilated from the valley over the course of the day by westerly winds entering through the western passes and exiting through the eastern passes.

The fourth hypothesis (H2D) is that pollutants are vented out the top of the valley rim by up-slope flows. Specifically, pollutants are transported out of the valley bottom by up-slope flows all along the valley rim mountains (as well as by up-valley flows in the steep stream valleys cascading down from the valley rim) and vented into the rapidly flowing air aloft at the peaks and ridges. This is illustrated in Figure 4.13.

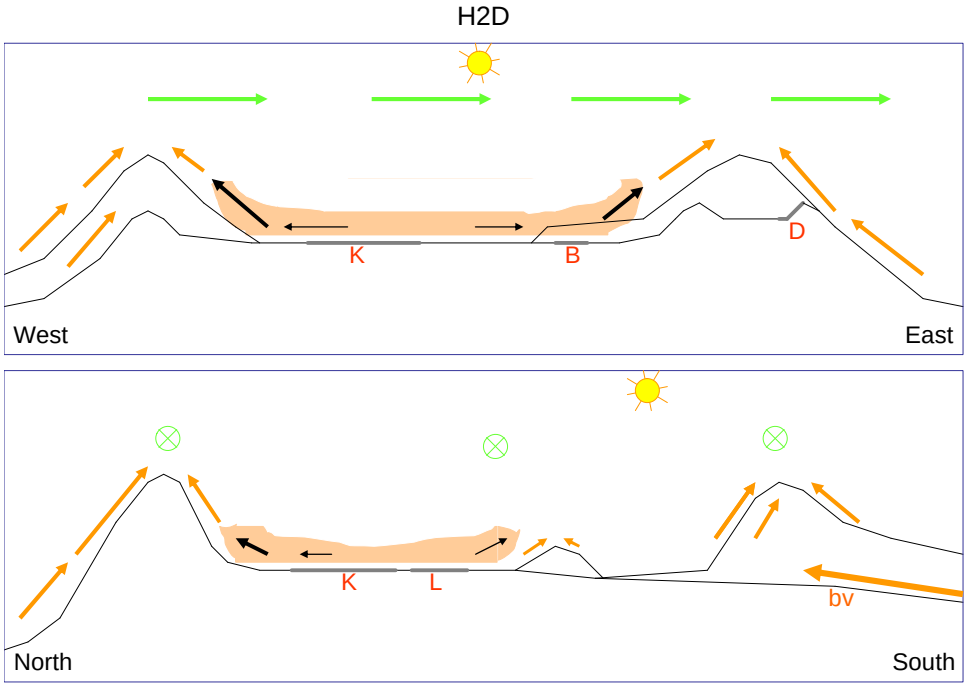

Figure 4.13: Illustration of hypothesis H3D: the venting of pollutants by upslope flows into the westerlies aloft.

Thermally driven flows up slopes and valleys have been studied in many places and have been found to be efficient ways of removing air pollutants from lower altitudes and venting them into fast-flowing upper-level winds that can transport them long distances. At the Jungfraujoch mountain observatory in Switzerland, pollutants are seen arriving from the valleys during warm afternoons [*Baltensperger et al.*, 1997]. Winds blowing up valleys of the Black Forest mountains have been found to transport tracers out of Freiburg city to be vented above the mountains [*Kalthoff et al.*, 2000]. Polluted air has has also been observed traveling up the Yahagi River valley in Japan [*Kitada et al.*,

1986]. Modeling studies in Santiago de Chile have found pollutant export above mountain peaks through convergence of upslope flows [*Schmitz,* 2005]. Mountains near Phoenix, Arizona vent the city enough that there is no multiple-day build up of ozone from local emission sources [*Fast et al.*, 2000]. Up-valley flows in the Ticino area of southern Switzerland have been found to carry pollutants upwards from industrial northern Italy to the crest of the Alps [*Prévôt et al.*, 2000b]; transporting several times the valley volume over the course of a day [*Henne et al.*, 2004]. Such topographic venting has been quantified in the form of "net vertical air mass export" [*Henne et al.*, 2004] as well as a dimensionless "ventilation rate" [*Allwine,* 1993].

Determining which of the four hypotheses of pollutant ventilation from the Kathmandu Valley is correct during clear dry-season days will require using model-generated wind fields to advect tracers released on the Valley floor during the afternoon. Hypothesis H1A can be rejected if it can be shown that pollutants removed from the valley floor in the afternoon are not re-circulated back into the city in the evening. We will be able to distinguish between hypotheses H2B, H2C, and H2D by checking whether tracers rise into the upper level westerlies while still over the valley, whether they blow out the eastern passes, or whether they go up the slopes.

4.5.3 Question 3: What is the cause of the night-time low in CO concentrations?

As mentioned in Chapter 3, one of the mysteries in the field data is the question why CO levels drop to low values at night, only to rebound again around 6 am. One would expect the lack of surface winds and the suppressed vertical mixing at night to lead to the continued accumulation of evening and night-time emissions near the surface. For example, at a measurement site in the Yangtze Delta in rural China, CO remained high throughout the night if the site was experiencing local pollution, and only dipped low during the afternoons [*Cheung and Wang*, 2001]. A similar persistent night-time high in CO and a low during the daytime was found on biomass burning generated CO in

Thailand [*Pochanart et al.*, 2003]. We discuss here four hypotheses to explain the nocturnal low in CO found in Kathmandu.

The first hypothesis (H3A) is that polluted city air is carried down the Bagmati Valley by katabatic winds (cold drainage winds) at night, and then returns up the Bagmati valley in the morning, as illustrated in Figure 4.14. Tracer release studies have demonstrated the ability of drainage flows in deep river valleys to transport pollutants down-valley [*Allwine*, 1993]. Interviews with residents of the Bagmati valley have shown a regular pattern of down-valley winds at night. As a further piece of evidence, the timing of the morning increase in pollution coincided with the observation of the smoke plume's direction reversal in the Bagmati outflow valley, as illustrated by the time-lapse photography in Chapter 3.

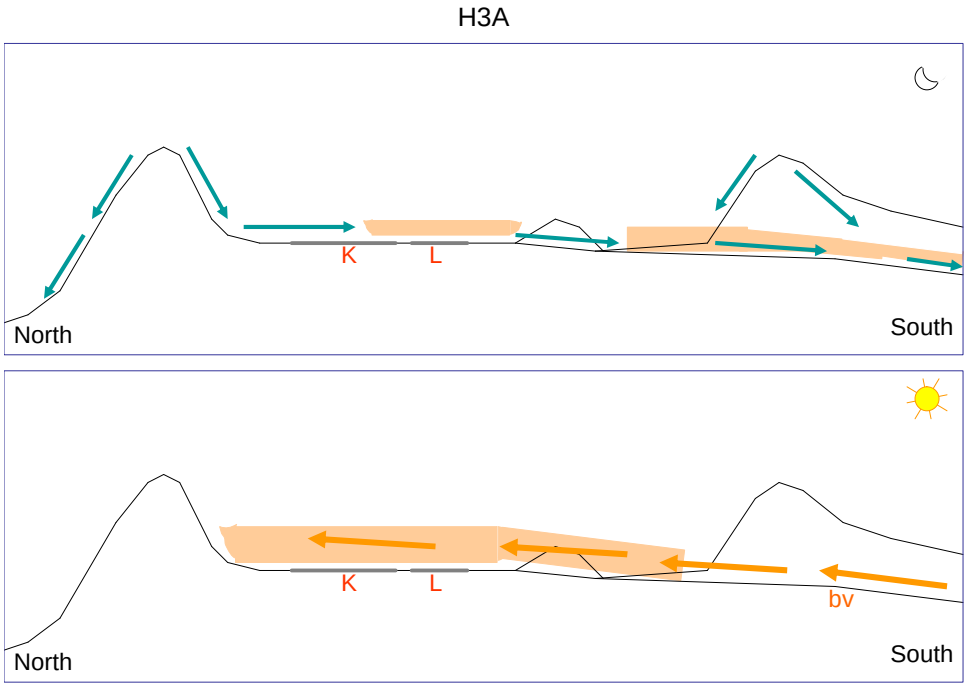

Figure 4.14: Time sequence illustration of a north-to-south cross section for hypothesis H3A: the export of pollution down the Bagmati Valley at night (top), and its return in the morning (bottom).

Geometric considerations, however, make this hypothesis highly implausible for the entire Kathmandu Valley. Cold drainage winds travel at the bottoms of valleys only a

few meters above the river water. The Chobhar-Kirtipur ridge (~150 meters tall) runs along the southeast side of the Kathmandu Valley, and the Bagmati river crosses this ridge through a narrow gorge that is only about 30 meters wide at the bottom and no more than 100 meters wide at the top. For drainage flows to be able to transport the entire polluted air mass from over the city down the Bagmati River valley, about 20 cubic kilometers of air would have to pass through that gorge within a span of about six hours. This would require wind speeds in the Chobhar Gorge that are several times the speed of sound! It is possible that a small fraction of the polluted air from south of Chobhar does travel partly down the Bagmati exit valley, and that the return of this air might be responsible for some of the morning pollution at the upper end of the Bagmati exit valley, but on the scale of the entire Kathmandu Valley this cannot be the dominant mechanism.

The second hypothesis (H3B) is that layers of polluted city air are lifted at night as colder katabatic winds converging over the city. In the morning, pollutants accumulated in these layers are mixed downwards as the growing mixed layer entrains the elevated layers. This is illustrated in Figure 4.15. Chapter 3 showed that at dusk the temperature dropped first at the edge of the valley, and later at the valley center, as well as that it continued to drop all night long. It is possible that the decrease in temperature in the valley over the course of the night was not only due to radiative cooling of the surface, but also due to the continuous arrival of katabatic winds bringing increasingly colder temperatures. Given that dense katabatic winds travel nearest to the surface, it is plausible that they arrived at the Hyatt without showing a clear signal in the data recorded by weather station 22 meters above ground. Parcels of colder air arriving at the city would flow underneath the less cold, less dense air parcels already there, lifting the latter up along with the pollutants they contain.

High pollution loads have also been found in Mexico City at times of strong surface confluence [*Jazcilevich et al.*, 2005]. Elevated night-time layers of pollutants have been found through measurements at the top of skyscrapers in Phoenix [*Berkowitz et al.*, 2005] and Milan [*Rubino et al.*, 1998], and through air sampling with a customized tethersonde

in Japan [*Sahashi et al.*, 1996]. Elevated layers of aerosols have also been found over the Rhine Valley [*Frioud et al.*, 2003]. The frequent existence of elevated polluted layers over the Kathmandu Valley has been confirmed through photography from Hattiban and Pullahari.[22] Bag sampling data on the Dharahara tower and at Pullahari gave some indication but no proof of possible upward transport of pollutants at night. A tower located further from local pollution sources might have given a clearer picture.

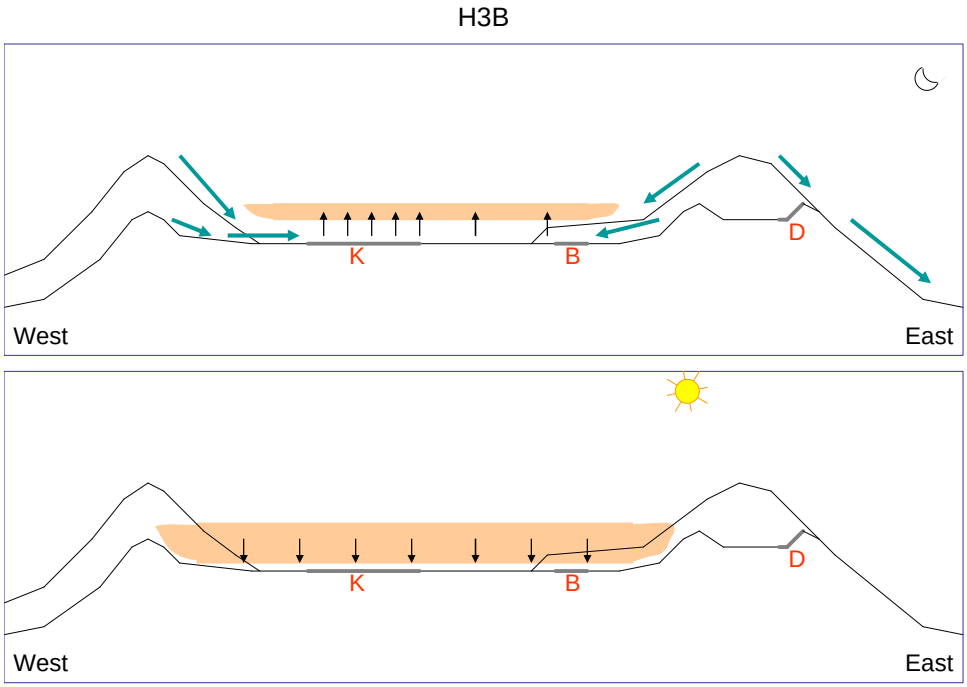

Figure 4.15: Time sequence illustration of hypothesis H3B, showing the night-time lifting (top) and morning downward mixing (bottom) of layers of polluted air.

The third hypothesis (H3C) for the night-time drop in CO concentrations is turbulent diffusion upwards and transport out by slow winds, as illustrated in Figure 4.16. Wind measurements from towers have shown that there can be significant mechanical turbulence even during stable conditions [*Mahrt and Vickers*, 2002]. The validity of this hypothesis requires establishing that pollutants are not re-circulated in the morning. We already saw hints of re-circulation in the Shivaratri data earlier. In addition, high peaks

[22] However, the photographed layers did not extend across the entire valley; they appeared close to the slopes, in the vicinity of farm houses that might have served as an elevated source of smoke in a stratified air mass. The photographed layers do not confirm the lifting of pollution layers.

of CO have also been found during the mornings (but not evenings) of a general strike on February 4, and on a number of Saturdays.

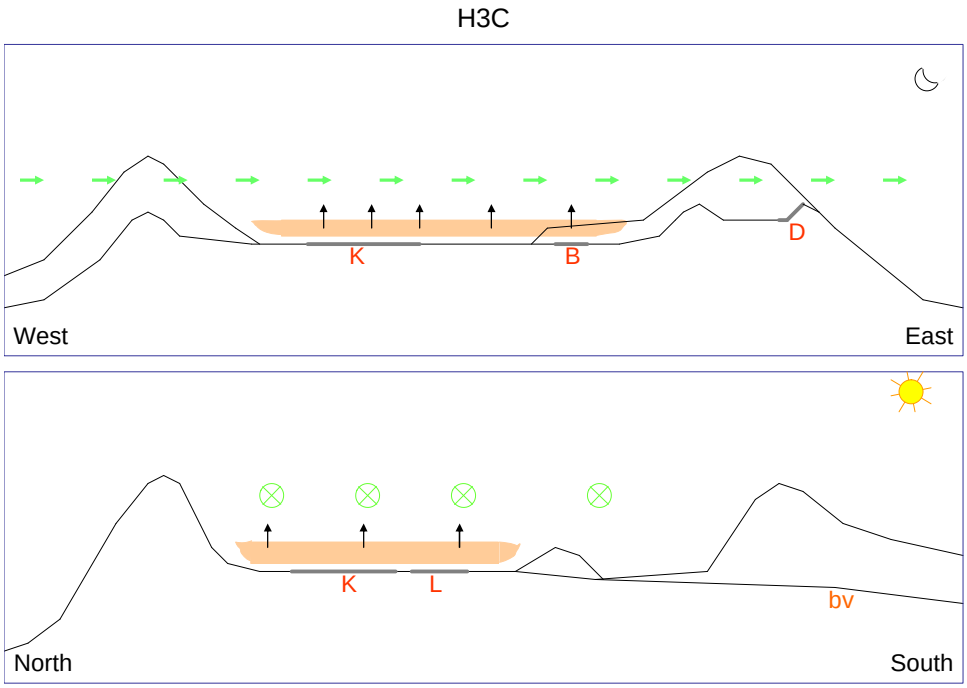

Figure 4.16: Illustration of Hypothesis H3C: the turbulent transport upward of pollutants at night.

A fourth hypothesis (H3D) combines parts of H3B and H3C: nonzero turbulence at night, rather than convergence of katabatic winds is responsible for gradually lifting pollution layers above the city (as in hypothesis H3C), but these lifted layers, instead of being removed from the valley, are re-circulated back the next morning (as in hypothesis H3B).

To summarize, hypothesis H3A might play a role in the southern parts of the valley, but appears unlikely to be dominant for the entire valley due to wind speed requirements in the Chobhar gorge. Sorting among the remaining three hypotheses requires modeling trajectories of tracers at night. Forward and back trajectories of tracers can show whether air parcels remain suspended somewhere over the valley during the night, and whether they are re-circulated in the morning (H3B or H3D), or whether they are transported out of the valley (H3C). Wind fields and trajectories of tracers released on the valley rim

slopes can show whether katabatic winds are able to penetrate to the valley center (H3B). Confirming hypothesis H3B would require passing an additional test: if the CO low recorded in the basin bottom were due to a continuous supply of clean air from the valley rim brought by katabatic winds, then there would also be a continuous supply of ozone from aloft. Yet ozone concentrations were found to be near zero in the basin bottom during the late night, despite the absence of new NO emissions. Passing the test would thus require demonstrating that the katabatic winds traveled slowly enough to allow dry-deposition of the ozone in them onto vegetation surfaces en-route.

4.6 Chapter Summary and Conclusion

This chapter described a typical diurnal cycle in the Kathmandu valley and discussed how the daily twin peaks in CO are the result of interaction between emissions patterns and ventilation. It then listed three questions whose answers help us understand the details of this interaction, followed by hypotheses for each question. The next two chapters describe the modeling work that was done to answer how the valley's nocturnal inversion breaks up, how pollutants are ventilated from the valley, and what happens to them at night. Next, Chapter 5 presents a meso-scale meteorological frame-work to address each of the questions, while Chapter 6 tries to understand the valley's CO budget using an eulerian model.

CHAPTER 5: MM5 METEOROLOGICAL MODELING

5.1 Chapter Introduction

The previous chapters reviewed the literature about past research in the Kathmandu Valley, described the field measurement set-up and field results, and discussed questions and hypotheses arising from the data. This chapter describes the set-up and validation of the meteorological modeling system used to simulate the diurnal cycle of the Kathmandu Valley's air pollution meteorology and to address the questions posed in Chapter 4. Section 5.2 briefly describes the MM5 meso-scale meteorological model and Section 5.3 describes the modeling domain, nesting, and boundary values, and simulation times that were chosen. Section 5.4 demonstrates the validity of the model runs by comparing model output to field observations. Sections 5.5 through 5.7 address the questions about the inversion break-up, the pollutant ventilation pathways, and the nocturnal CO low. Section 5.8 discusses additional findings about the observed diurnal cycle.

5.2 The MM5 Meso-scale Meteorological Model

MM5 is a non-hydrostatic limited area meteorological model using terrain following sigma-pressure coordinates [*Dudhia*, 1989; *Dudhia*, 1993; *Grell et al.*, 1994]. The model uses an Arakawa-Lamb-B grid, with scalars defined at the centers of grid cells, and velocity components defined at the corners. In the vertical direction, all variables except vertical velocities are calculated at layer centers; the latter is calculated at the layer interfaces ("levels"). Simulations are integrated forward through time using second-order leapfrog finite-differencing. MM5's vertical sigma coordinate is defined as [*Grell et al.*, 1994]:

$$s = \frac{p - p_t}{p_s - p_t}$$

where p_s is the surface pressure, p_t is a constant pressure at the top of the model domain. The value of s is 1 at the surface and 0 at the model top. In the terrain-following coordinates (x,y, s), MM5 solves the following [*Dudhia et al.*, 2005] equations:

The pressure equation:

$$\frac{\partial p'}{\partial t} = -r_o g w + g p \nabla \cdot \mathbf{V} = - \mathbf{V} \cdot \nabla \mathrm{p}'$$

The horizontal momentum equations:

$$\frac{\partial u}{\partial t} + \frac{m}{p}\left(\frac{\partial p'}{\partial x} - \frac{s}{p^*}\frac{\partial p^*}{\partial x}\frac{\partial p'}{\partial s} \right) = -\mathbf{V} \cdot \nabla u + v\left(f + u\frac{\partial m}{\partial y} - v\frac{\partial m}{\partial x} \right) - ew\cos a - \frac{\mathrm{uw}}{\mathrm{r_{earth}}} + D_u$$

$$\frac{\partial v}{\partial t} + \frac{m}{p}\left(\frac{\partial p'}{\partial y} - \frac{s}{p^*}\frac{\partial p^*}{\partial y}\frac{\partial p'}{\partial s} \right) = -\mathbf{V} \cdot \nabla v - u\left(f + u\frac{\partial m}{\partial y} - v\frac{\partial m}{\partial x} \right) - ew\sin a - \frac{\mathrm{vw}}{\mathrm{r_{earth}}} + D_v$$

The vertical momentum equation:

$$\frac{\partial w}{\partial t} - \frac{r_o}{r}\frac{g}{p^*}\frac{\partial p'}{\partial s} + \frac{gp'}{gp} = -\mathbf{V} \cdot \nabla w + g\frac{p_o}{p}\frac{T'}{T_o} - g\frac{R_d}{c_p}\frac{p'}{p} - e(u\cos a - v\sin a) + \frac{\mathrm{u}^2 + \mathrm{v}^2}{\mathrm{r_{earth}}} + D_w$$

The thermodynamics equation:

$$\frac{\partial T}{\partial t} = -\mathbf{V} \cdot \nabla T + \frac{1}{r c_p}\left(\frac{\partial p'}{\partial t} + \mathbf{V} \cdot \nabla p' - r_o g w \right) + \frac{Q}{c_p} + \frac{T_o}{q_o} D_q$$

where m is the map scale factor, e=2Wcos$l$, α=f - f_c, l is the latitude, f is the longitude, f_c is the central longitude, $p^* = p_s - p_t$, D represents horizontal and vertical diffusion and turbulent mixing terms, and c_p is the heat capacity of dry air. The pressure equation neglects an additional term expressing increased pressure due to heating [*Dudhia et al.*, 2005]. There are additional equations for water vapor, and for the microphysical variables included in particular simulations, such as cloud liquid water, graupel, or ice.

MM5 was initially developed by researchers at Pennsylvania State University and the National Center for Atmospheric Research (NCAR) for weather forecasting purposes. Over the years it has seen contributions from numerous collaborating researchers around the world, and has become one of the most widely used and best documented meso-scale models. Allowing a high degree of choice and customization in its grid structure,

nesting, boundary conditions, and physics parameterization, the model has been used in a large range of applications.

MM5 has been used to study air pollution meteorology in numerous situations and locations around the world, including for driving prognostic air quality models in Mexico City [*Jazcilevich et al.*, 2005], to study pollutant re-circulation in Phoenix, Arizona [*Fernando et al.*, 2001; *Lee et al.*, 2003b], and to study valley wind systems in the Austrian Alps [*Gohm et al.*, 2004; *Zaengl*, 2004]. In Hong Kong MM5 has been used to drive an urban boundary layer model [*Tong et al.*, 2005]. In Santiago de Chile, it was used to create the meteorological fields needed to drive a transport model for a study of the diurnal cycle of carbon monoxide [*Schmitz*, 2005]. Chapter 1's literature review noted that MM5 has been used twice before for studies in Nepal. The first time was for an investigation of diurnal winds in the Kali Gandaki Valley [*Zängl et al.*, 2001], particularly focusing on studying the driving mechanism of high-speed up-valley winds in the Kali Gandaki Valley by running a series of experiments with idealized, smoothed, and realistic topography. During its second application in Nepal, the model was run for a 4 day period in the Kathmandu Valley [*Regmi et al.*, 2003] , but with no field data from that period to verify the run. In this chapter the model is first validated against our detailed observations, and then applied to answer the questions described in Chapter 4.

Several comparably capable alternative models [*Cox et al.*, 1998] could have been used for the modeling work instead of MM5, including RAMS [*Pielke et al.*, 1992] and the German Lokal-Modell (LM) [*Doms and Schättler*, 1999]. MM5's successor, NCAR's Weather Research and Forecast (WRF) model, was not ready for nested runs at the time work started on modeling Kathmandu for this dissertation, in Summer 2003. MM5 was chosen for its easy availability and user support, because it was already used in MIT's Mexico City Project, and because it had been applied to cases in Nepal in the past.

5.3 MM5 Domain, Boundary Conditions, Parameterizations, and Choice of Runs

For the meso-scale meteorological modeling part of the dissertation research, the latest version 3 of the MM5 model was used. This section describes how MM5 was set up and customized. Initial and boundary conditions were taken from NCEP FNL global analyses, available online at 1 degree resolution every 6 hours from the National Center for Environmental Prediction. The MM5 modeling domain was set up using Lambert conformal projection, with four levels of two-way nesting, stepping down in resolution from the NCEP FNL boundary while maintaining a 1:3 grid resolution ratio. The four nested domains had grid resolutions of 27, 9, 3, and 1 km from the outermost to the innermost. The domains were all centered at 27.7°N, 85.3°E, corresponding to a point in central Kathmandu City, close to the Dharahara tower. This was deliberately chosen to match with the domain center used in the earlier MM5 simulation for Kathmandu [*Regmi et al.*, 2003]. It is common to use concentric nests in MM5 [*Tong et al.*, 2005]. Figure 5.1 illustrates the four nested domains. The outer two domains had horizontal dimensions of 50 by 50 grid cells, while the inner two domains measured 75 by 75 grid cells. The outermost nest spanned much of the Ganges Plains and a big part of the Tibetan Plateau, while the innermost domain spanned approximately three times the horizontal extent of Kathmandu valley, reaching into neighboring valleys.

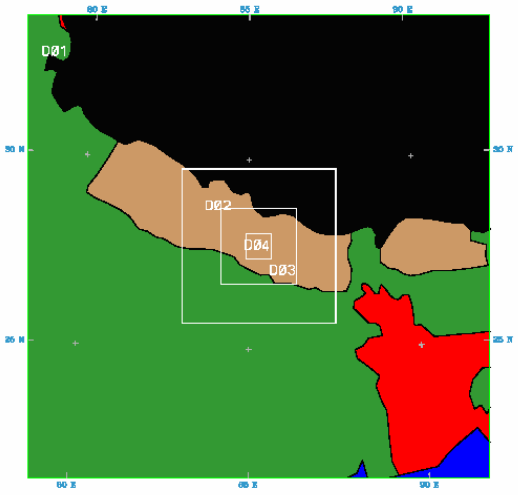

Figure 5.1: The four nest levels used in our MM5 simulations. The outer domain spanned from the Bay of Bengal to Kashmir. Political boundaries are approximate.

Surface land use and vegetation for the simulations were taken from the public USGS 25-category 30 arc-second database downloadable via the MM5 homepage (ftp://ftp.ucar.edu/mesouser/MM5V3/TERRAIN_DATA/), while underlying topography was taken from the USGS GTOPO-30 (global 30-arcsecond) database and smoothed appropriately for each nest level. At the 1 km grid resolution of the innermost nest, the model topography was able to capture the essential features of the Kathmandu Valley, including the surrounding mountains, passes, and relatively flat basin bottom. It did *not* capture smaller-scale features within the valley bottom, such as Chobhar hill, Chobhar Gorge, Swayambhu hill, Pullahari –Kapan ridge, and Changu Narayan hill or any of the river channels. These features would require horizontal resolutions of a few tens to a hundred meters to capture properly.

Modeling the Kathmandu Valley at a finer resolution than the set-up described would require not just higher resolution terrain and landuse datasets that are not available publicly, but would also require switching from MM5 to a different modeling system. MM5 is not designed to be run at resolutions much finer than 1 km. In the literature, the finest grid spacing for a successful MM5 simulation (but with modified source code) was found with 267 meter inner-most grid resolution for a study of valley winds in Austria [*Gohm et al.*, 2004]. But even that resolution would not be able to capture the shapes and sizes of the geographic features listed above, and thus would not be able to capture their influences on air flow within the Kathmandu Valley.

The model runs were each initialized with NCEP analyses at 0600 UTC, corresponding to 11:45 am Nepal Standard Time. Initialization at mid-day rather than at mid-night was chosen because, during the night, mountain valleys often contain stably stratified air masses that are disconnected from overlying regional flows. The model runs were then allowed to spin up for 36 hours before the results were used.[23] Experimental runs with various configurations led to a final set up having 40 vertical layers that extended from

[23] Surprisingly we found the results after 12 hours to be already sufficiently reliable; these were used for the studies of May 11, 2006.

the surface to 100 mb[24]. The bottom-most five layers were 15 meters thick each (corresponding to 0.006 *s* levels).[25] Above those, the layers were gradually were thickened. An MM5 simulation studying valley wind systems in the Alps [*Zaengl*, 2004] used a similar number of layers and also a 15 meter vertical resolution in the bottom layers. At the top of the model domain, boundary conditions were chosen to allow radiation of internal gravity waves according to [*Klemp and Durran*, 1983]. Simulation time steps were chosen to be 60 seconds in the outer-most domain with 27 km resolution; this produced a ~1 second time step in the innermost domain.

The simulations' physics parameterizations were chosen from a menu of available in MM5: for moisture, the Simple Ice parameterization [*Dudhia*, 1989] was used. This used explicit microphysics calculations to simulate cloud and rain water and cloud ice. MM5 was allowed to calculate cumulus clouds explicitly in the 1 and 3 kilometer-resolution inner two domains, while in the coarser domains cumulus clouds were parameterized using the updated Kain-Fritsch scheme [*Kain*, 2004]. The boundary layer was parameterized using the MRF scheme [*Hong and Pan*, 1996], which is suitable for fine resolution runs while maintaining computational efficiency. Solar and terrestrial radiation were recalculated every 30 minutes, using a parameterization [*Dudhia*, 1989] that included long and short-wave radiation interacting with clear air, clouds, precipitation and the ground. For the surface energy budget, a 5-layer soil model was used [*Dudhia*, 1993]. For the analysis needed to address the questions outlined in Chapter 4, simulations were carried out from the days before until the days after the representative late winter and early summer days that were introduced in Chapter 3, and that had the highest quality field data available: February 10 and May 11, 2005. The MM5-customized interpolation and plotting package RIP (ftp://ftp.ucar.edu/mesouser/MM5V3/RIP.TAR.gz) was used to generate plots and to calculate forward and backward trajectories. The trajectories used half-hourly MM5 output files, but computed trajectories at 1 minute intervals.

[24] MM5 does *not* have the capability of changing the vertical resolution between nest levels.
[25] Finer vertical resolution required time steps that created impractically large demands on computing time to avoid CFL stability problems. The 15 meter surface layer thickness was considered satisfactorily fine given that the Hyatt lab sample inlet was 12 meters above ground, and the weather station was about 22 meters above ground.

5.4 MM5 Model Validation

Regardless of their complexity, all atmospheric models contain physics that is vastly simplified compared to what takes place in nature. Simplifications imply choices made to exclude certain processes, time scales, and spatial scales from consideration. Choosing to run MM5 with the set-up described in Section 5.3 provided us with a state-of-art tool to address our research questions. However, MM5 can only be trusted to answer the questions if it reproduces reality, as measured in the field, sufficiently well. Meso-scale models have been inter-compared with each other and with field data in great detail; MM5 has a proven track record in many locations and situations [*Castelli et al.*, 2004; *Chandrasekar et al.*, 2003; *Chandrasekar et al.*, 2004; *Cox et al.*, 1998; *Dudhia*, 1993; *Hogrefe et al.*, 2001a; *Hogrefe et al.*, 2001b; *Lena and Desiato*, 1999; *Zamora et al.*, 2003]. In this section our MM5 runs are tested by comparing their output to field observations in Kathmandu on the same days.

Figure 5.2 and Figure 5.3 show the wind fields computed by MM5 in the lowest model layer (between s = 1 and s = 0.994) before dawn and in the afternoon on February 10, 2005. Note that the center of this terrain-following layer is approximately 7.5 meters above the ground throughout the domain. For visual clarity, wind vectors have only been plotted every second grid-cell. Their length is proportional to the wind speed; a length of two grid cells corresponds to a speed of 10 m/s. The two figures show an overall pattern that matches fairly well the field results from Chapter 3, while showing nothing that contradicts the field observations. At dawn (Figure 5.2) the valley center had almost no surface winds. Katabatic winds descended from mountain ridges; drainage flows traveled down both the Bagmati river valley (32,20)[26] and the river valleys outside of the Kathmandu Valley. We also see that easterly winds crossed the passes on the western edge of the Kathmandu Valley, such as Bhimdhunga Pass (31,42).

[26] Coordinates correspond to the scales along the figure edge. Because of the innermost nest's grid resolution, a unit is both one grid cell and one kilometer. The domain's origin is at the southwest corner.

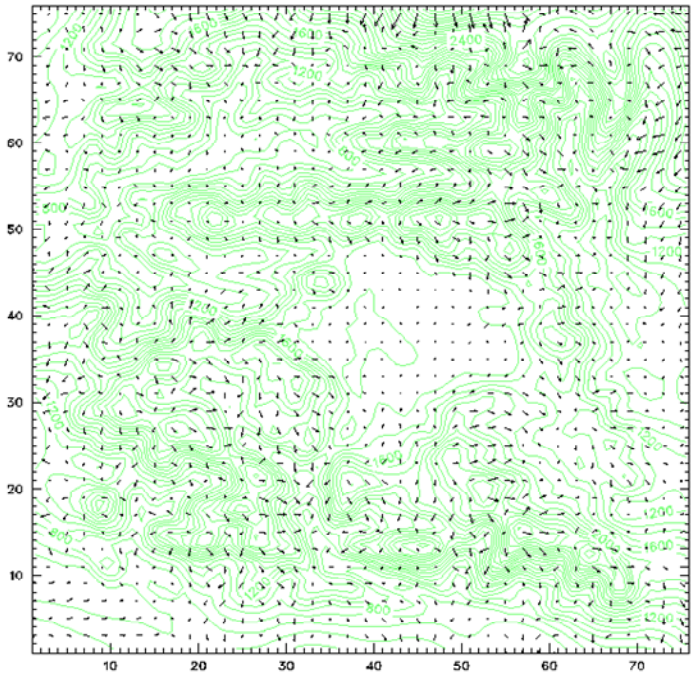

Figure 5.2: Surface wind vectors (black) superimposed upon contour lines of topography (green) at 5:45 am on February 10, 2005. The Kathmandu Valley is the flat (contour-free) area at the center of the frame.

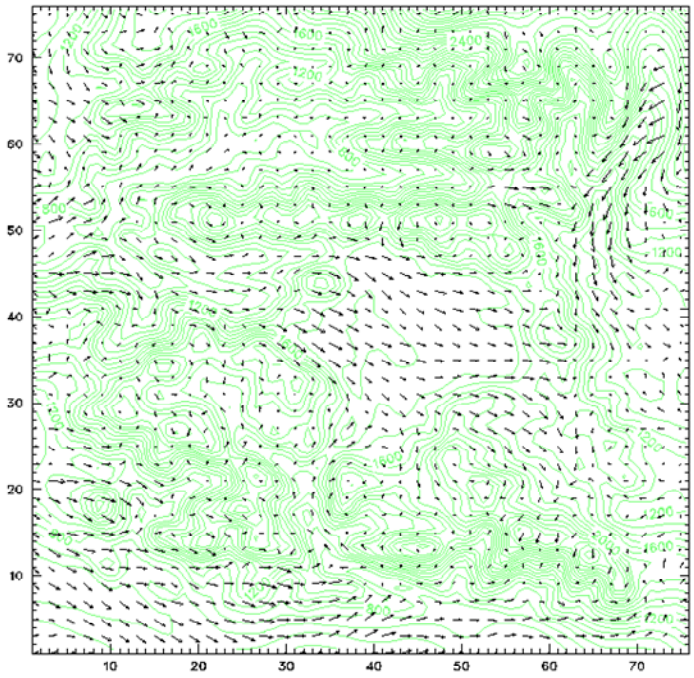

Figure 5.3: Same as the previous figure, but at 4:15 pm local time.

In Figure 5.3 we see that in the afternoon, strong winds traveled up the river valleys, while the Kathmandu Valley was swept by westerly/northwesterly winds entering through the western passes. Afternoon wind speeds on the order of 5-6 km/s over the valley were close to the average afternoon wind speeds measured at the Hyatt. We also see in the same plot that up-valley winds traveling up the Bagmati River valley were able to enter the southern part of the valley, but were pushed east-wards by the stronger westerlies entering from the western passes. An earlier MM5 simulation of the Kathmandu Valley for March 2002 [*Regmi et al.*, 2003] also found interactions between westerlies entering the valley through the western passes and southerlies arriving up the Bagmati Valley, with the cooler arriving air masses pushing underneath the warmer air already in the valley. This resulted in vertical mixing being suppressed during the afternoons. This topic will be revisited several times in this chapter while answering questions about the mixed layer dynamics and the pollutant ventilation pathways.

Figure 5.4 and Figure 5.5 illustrate the temperature of the lowest layer of air over the Kathmandu Valley at dawn and in the afternoon. They show that at dawn, the entire bottom of the basin was filled with a pool of cold air whose temperature did not exceed that of the highest (and coldest) peaks on the valley rim. We also see that surrounding river valleys (for example in the upper left quadrant of the figure) did not contain cold pools. In contrast to the Kathmandu Valley's confined basin shape, these river valleys are long and open along the valley axis, allowing drainage flows to travel down-valley unimpeded. In the afternoon (Figure 5.5) the Kathmandu Valley's center was warmer than its edges, while that temperatures showed a monotonic decrease with elevation throughout the domain. MM5 appears to simulate the observed temperature pattern reasonably well. Later, Figure 5.13 through Figure 5.15 will show that MM5 indeed was able to simulate the measured diurnal temperature cycle in several locations.

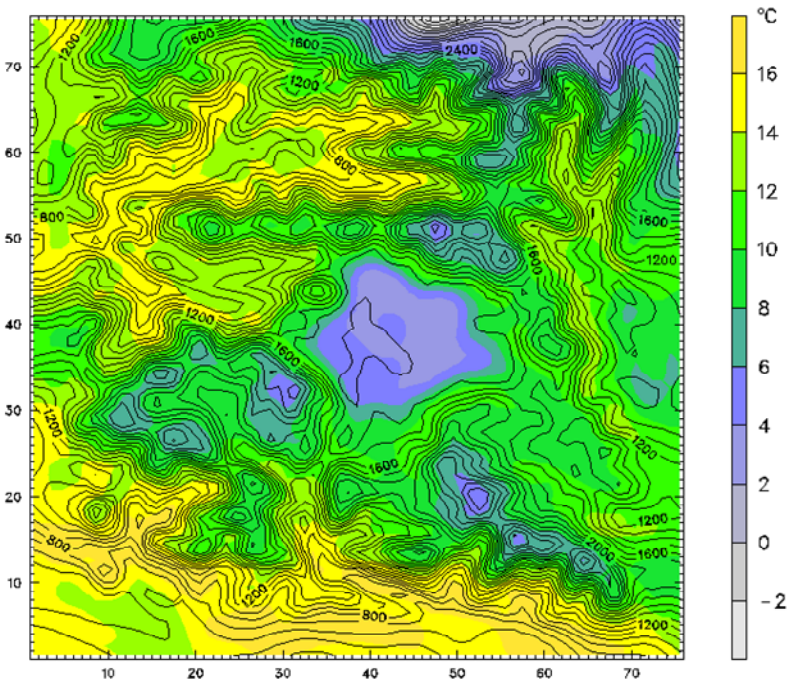

Figure 5.4: Air temperature in the lowest layer (color shading) at 5:45 am on February 10, 2005. The underlying topography is indicated by contour lines with a contour interval of 100 meters.

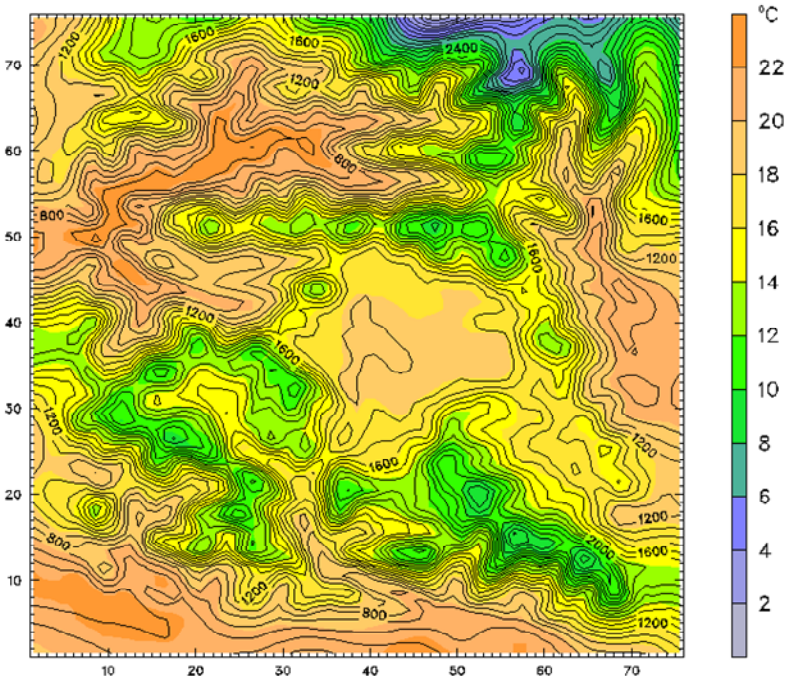

Figure 5.5 Air temperature in the lowest layer at 2:45 pm on February 10, 2005.

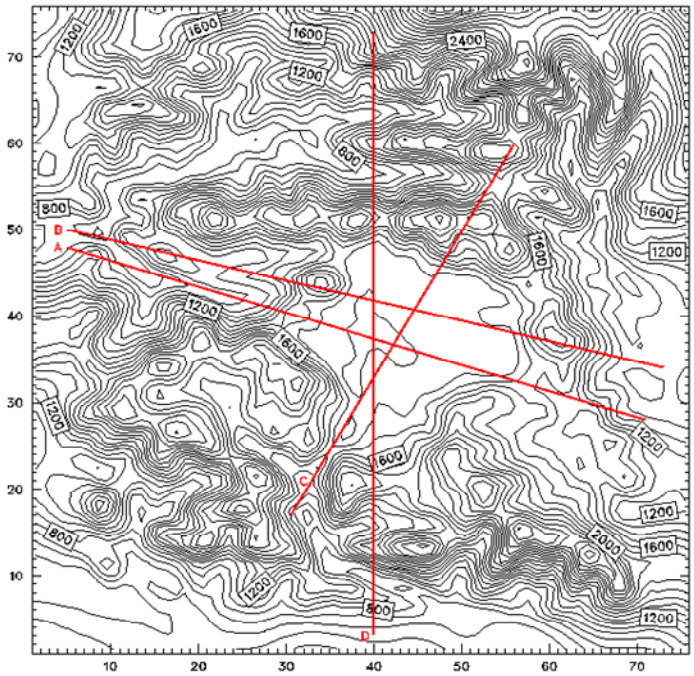

Figure 5.6 Locations of 4 cross-sections through the Kathmandu Valley used for various displays of model output. Cross-section A cuts across a western valley rim Pass and Sanga Pass and Dhulikhel in the east, Cross-section B cuts across Nagarjun and Nagarkot peaks. C runs down the Bagmati Valley outflow, and D runs due north-south.

Figure 5.6 shows locations of four vertical cross sections (A,B,C,D) through the model domain that will be referred to frequently. The next four figures give a sequence of west-to-east vertical cross-sections through the Kathmandu Valley, showing the topography and potential temperature. They show that, at dawn (Figure 5.7), the cold pool in the Kathmandu Valley created a more stable situation than what was found in neighboring lower valleys. Also visible (looking from right to left) are isentropes which crossed the valley at the level of the eastern passes, skimmed along the top of the cold air pool, rose slightly over the western valley rim and then fell steeply and continued at a lower elevation outside the valley: the valley-rim ridge on the west side obviously confined the cold air pool, preventing it from draining out. Recall that we had observed the top of the fog level corresponding to the altitude of the western passes. Figure 5.8 (10:15 am) shows the evolution of the mixed layer height. It grew first along the edge of the valley, with the cold air pool surviving and suppressing vertical mixing for the longest time over the valley center. This matches with our observations during time lapse photography of the morning fog ablating first along the edges of the valley.

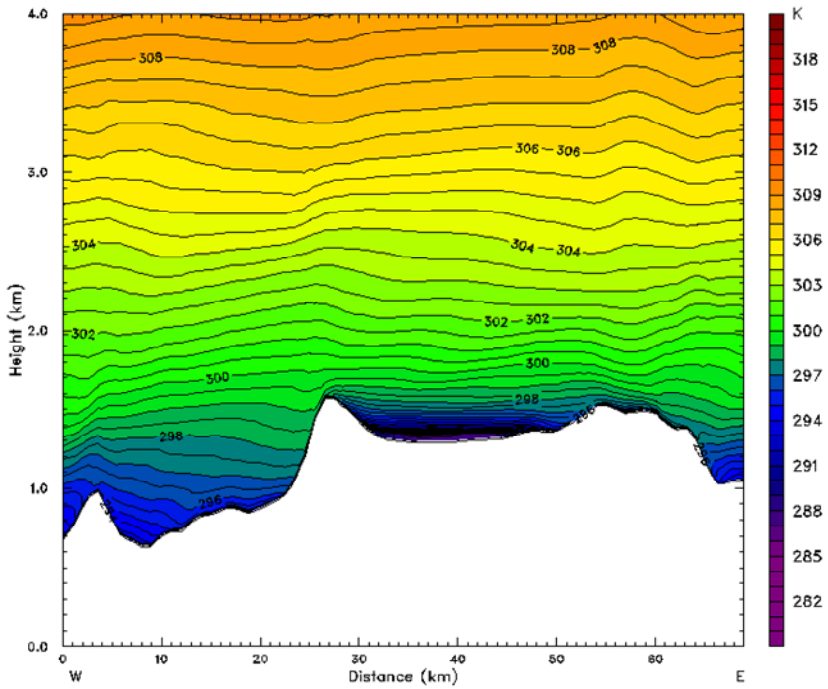

Figure 5.7: West to east vertical cross section A through the Kathmandu Valley, showing in sequence, the Trisuli River's low tributary valleys, (west of Kathmandu) the ridge with passes on the western valley rim, the elevated flat basin of the Kathmandu Valley, the eastern Sanga Pass and shallow elevated Banepa Valley, and the drop-off from Dhulikhel to the low Panchkhal Valley east of Kathmandu. Color shading and contours indicate potential temperature. Note that the vertical scale is in kilometers, with a vertical to horizontal exaggeration of about 15:1. Local time is 5:45 am.

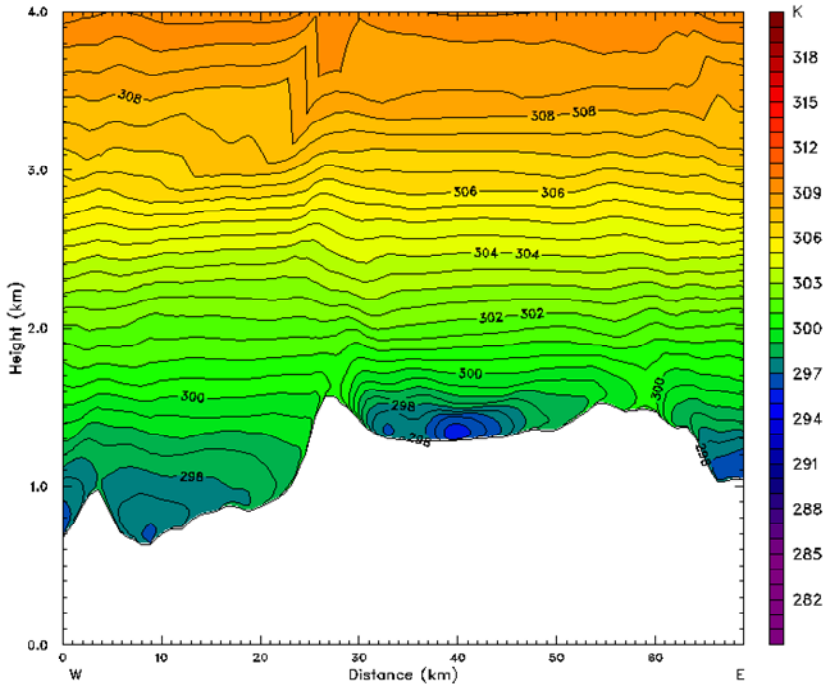

Figure 5.8: Potential temperature on cross section A (as in previous figure), but at 10:15 am.

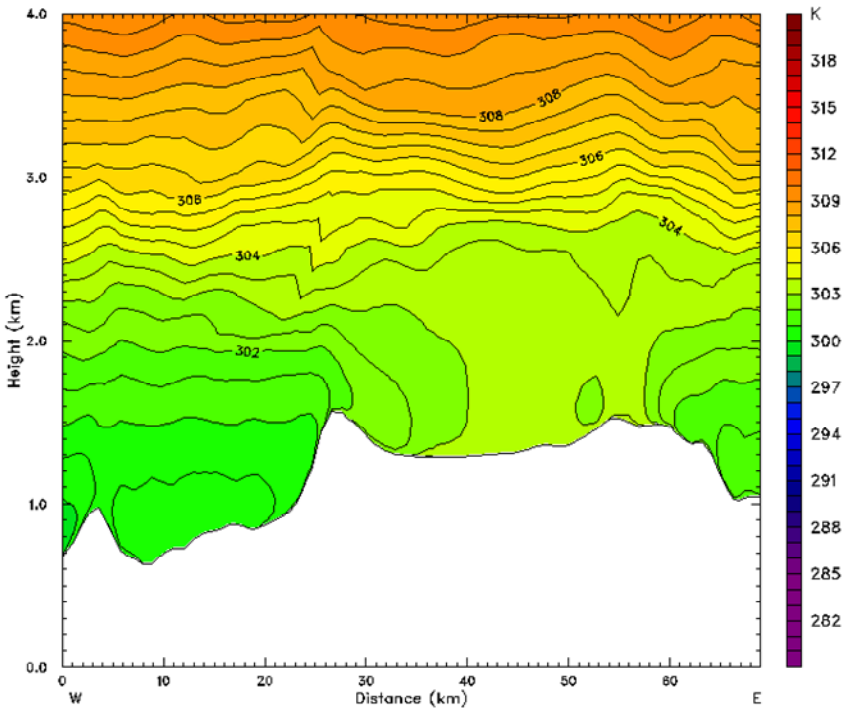

Figure 5.9: Same as in the previous two figures, but at 2:45 pm local time.

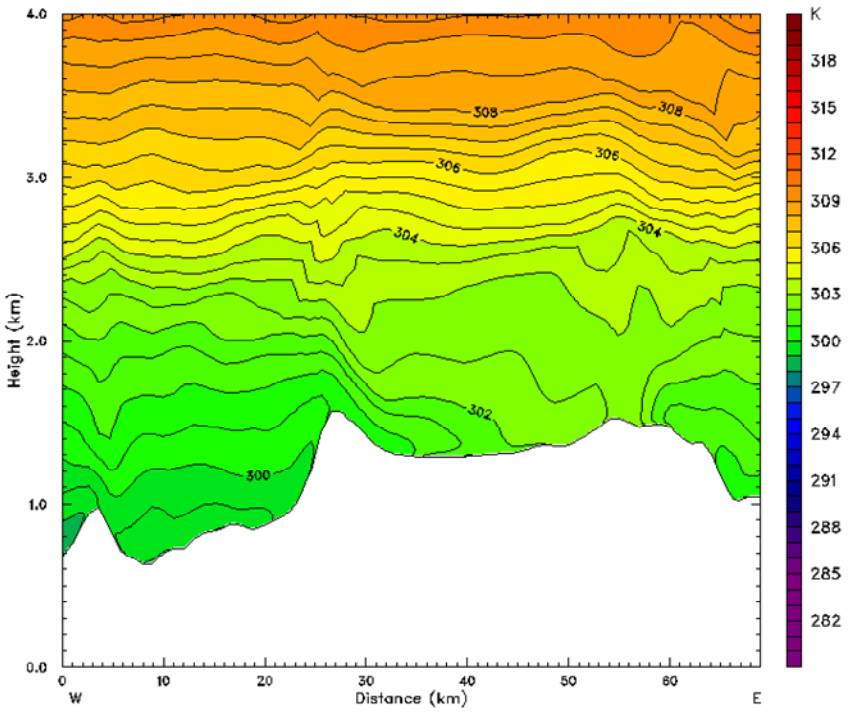

Figure 5.10: Same as in the previous three figures, but at 4:15 pm local time.

By 2:45 pm (Figure 5.9) a fully developed mixed layer[27] extended up to a kilometer above the valley bottom; the Kathmandu Valley had a taller mixed layer than its neighboring valleys. An air mass with colder potential temperature appeared to be advecting into the valley across the western valley rim. By 4:45 pm (Figure 5.10) this air mass had indeed pushed in along the bottom of the valley, creating vertical stratification that confined vertical mixing to far lower heights than was possible just two hours earlier. We had no sodar observations in February; in May sodar measurements showed that the mixed layer height indeed started dropping shortly after noon, rather than remaining high throughout the afternoon as is common in many parts of the world [*Arya*, 1999]. This again matches the results of the earlier MM5 simulation of the Kathmandu Valley [*Regmi et al.*, 2003] which found cooler air from above the neighboring valleys to the west and from the Bagmati Valley to the south pushing underneath the air mass already in the valley.

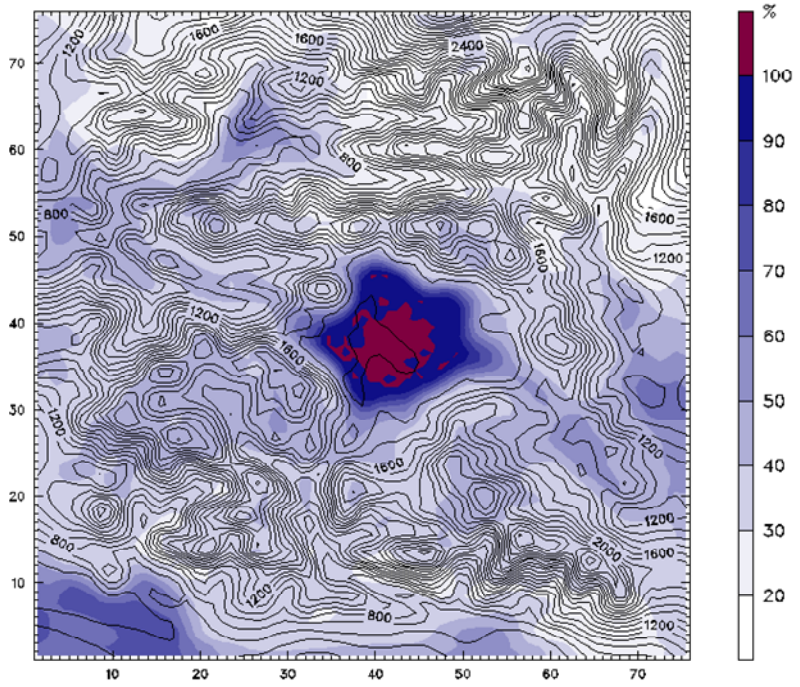

Figure 5.11: Relative humidity in the surface layer at 5:45 am. Note that the color scale goes from white (0%) to dark blue (99.9%). Red indicates the threshold value of 100%. As in the surface temperature plots, the underlying topography is shown in black contour lines (interval 100m).

[27] Indicated by the lack of vertical gradient in potential temperature.

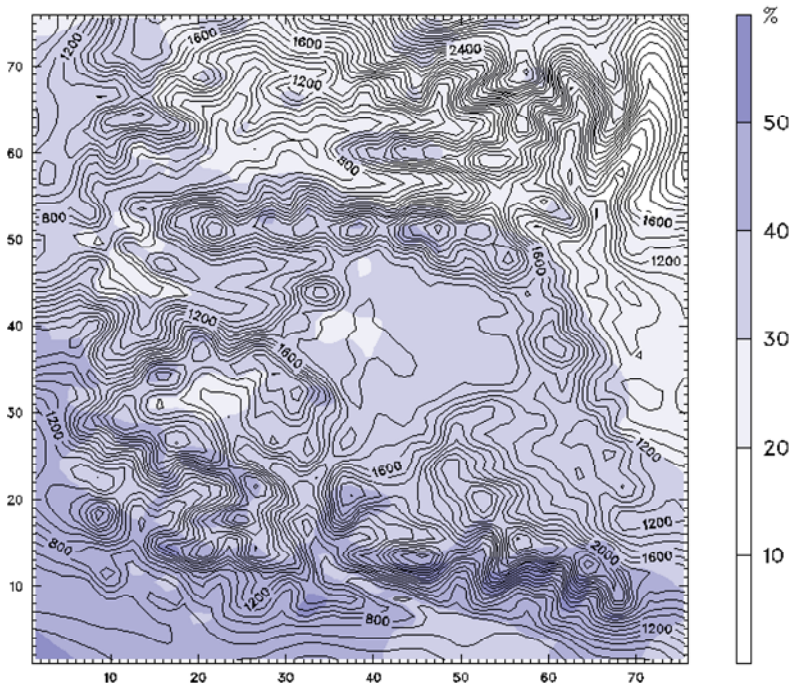

Figure 5.12: Same is the figure above, but at 11:45 am.

Figure 5.11 shows the relative humidity in the surface layer at dawn, and Figure 5.12 shows it shortly before noon on February 10, 2005. At dawn a large part of the valley center had 100% relative humidity, and the rest of the valley floor had relative humidity exceeding 90%. In fact, during the early morning hours the simulation showed frequent fluctuations in the locations of area reaching the 100% threshold, indicating that many of the areas shown in dark blue actually had relative humidity close to 100% as well. Indeed at dawn that morning we photographed a thin fog layer covering much of the valley (Figure 3.19). The photography had shown that over the course of the morning the fog layer thickened, and then disappeared by late morning. The MM5 simulation confirms that by 11:45 am the relative humidity was below 40% in the entire valley.

So far we have shown that the MM5 simulation is capable of correctly describing the valley-wide patterns seen in the field on February 10, 2005. How does it compared quantitatively with measurements? The next two figures show time series of MM5 simulations and field observations over a two-day period. Figure 5.13 shows that, at the Hyatt weather station, MM5 accurately captured the night-time temperature, but under-

estimated the day-time temperature. It also shows that MM5 accurately captured the day-time relative humidity minimum, but that it over-estimated the relative humidity at night, while also over-estimating the duration of 100% relative humidity and thus of fog.

Part of the differences seen here might have explanations other than model error. First, the weather station was located 22 meters above ground, and the MM5 simulation's layer center was 7.5 meters above ground. Fog tends to develop from the ground up, so it is indeed possible that there was fog near the ground earlier in the morning than the time when 100% relative humidity was reached at the weather station. Second, it is plausible that during the daytime the temperature sensor at the Hyatt weather station was slightly contaminated by local infrared radiation from the tile roof underneath it, while the MM5 results represent an average over a grid cell of 1 km by 1 km. The weather station was set up at the best compromise location that was available. Third, unlike the Hobo and Gemini temperature loggers used elsewhere, the weather station at the Hyatt had a rather crude temperature probe (see Table 2.1) that may have caused measurement inaccuracies.

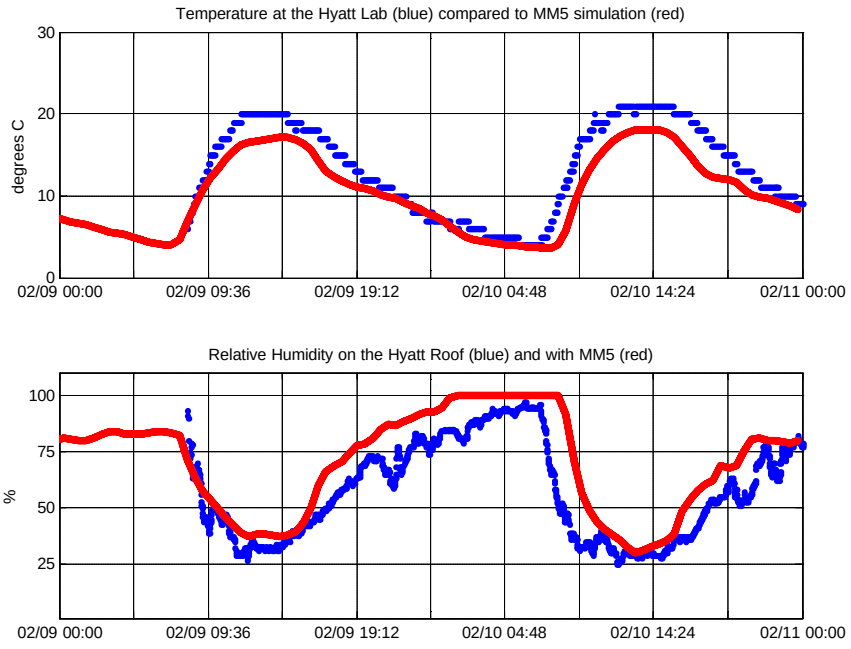

Figure 5.13: Intercomparison of measurements by the weather station on the Hyatt roof (blue) on February 9 and 10, 2005 with MM5 simulation for the same time period at the grid cell containing the Hyatt (red). The top panel shows air temperature, and the bottom panel shows relative humidity.

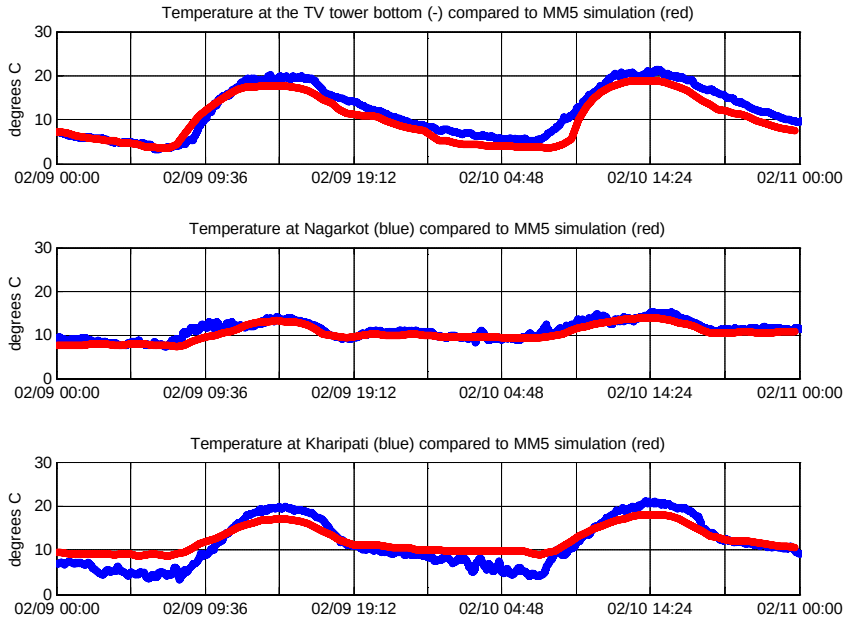

Figure 5.14: Intercomparison of air temperature measurements by Hobo loggers (blue) at three locations on February 9 and 10, 2005 with MM5 simulations (green) for the same time period at grid cells containing the logger sites. From top to bottom: TV tower bottom (5 meters above ground), Nagarkot, and Kharipati.

Figure 5.14 top and middle show that MM5 captured the diurnal temperature cycle at the TV tower and at Nagarkot Peak remarkably well. At Kharipati (bottom) it slightly under-estimated the day-time temperature, while overestimating it at night. The source of error at Kharipati appears to be MM5's crude 1 km grid resolution, which cannot properly capture the topographic geometry of the sensor's location in Kharipati. The sensor was located within the valley, just beyond the base of the mountain slope. If MM5 placed the Kharipati location even slightly up the slope, the site would not capture the cold air pool properly.

From the comparison of MM5 to field observations, we can conclude that the MM5 simulation for February 10, 2005, was indeed able to simulate the Kathmandu Valley's meteorology, within the limited accuracy expected from the limits of its horizontal and vertical grid resolution. We can thus expect this simulation to be able to provide

reasonable transport input for the pollution modeling discussed in chapter 6. The next figures examine the validity of the simulation for May 11, 2005.

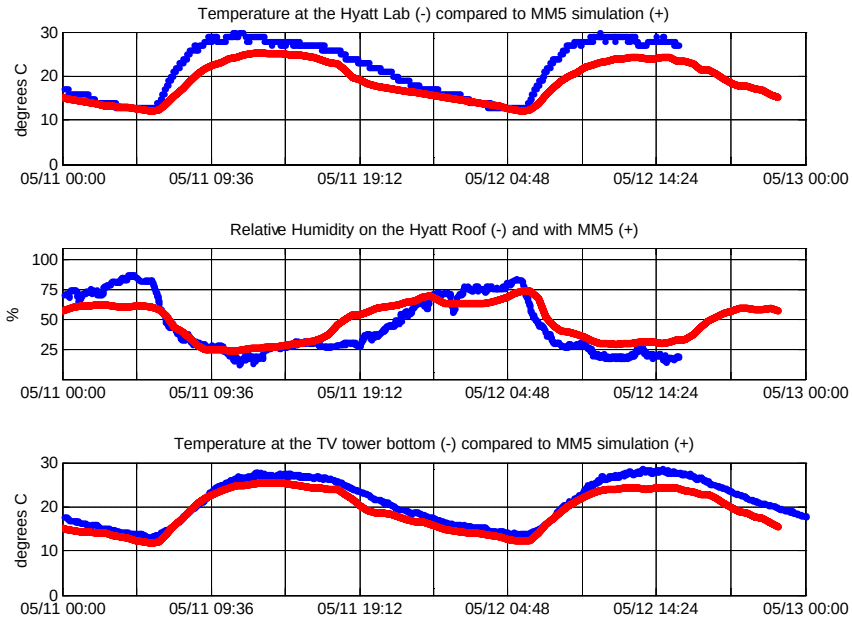

Figure 5.15: Intercomparison of field measurements (blue) and MM5 simulations (green) on May 11 and 12, 2005. From top to bottom: temperature at the Hyatt weather station, relative humidity at the Hyatt weather station, and temperature at the bottom TV tower logger.

In Figure 5.15 we see that the May simulation was also able to reasonably capture the diurnal cycles of temperature and relative humidity. It again slightly under-estimated the day-time temperature measured at the Hyatt, while it under-estimated the relative humidity on May 11 in the early morning and over-estimated it that evening.

The surface wind fields from May look very similar to the ones in Figure 5.2 and Figure 5.3, and thus are not reproduced here. Figure 5.16 and Figure 5.17 show the air temperature in the lowest model layer. Although the average temperatures were significantly higher, we see the same patterns as on February 10, with a cold pool in the Kathmandu Valley at dawn, with temperatures corresponding to those of the tallest nearby peaks, and no cold pool in the surrounding river valleys. During the day, the temperature in the Kathmandu Valley was warmer than the surrounding mountains, but still cooler than nearby lower valleys.

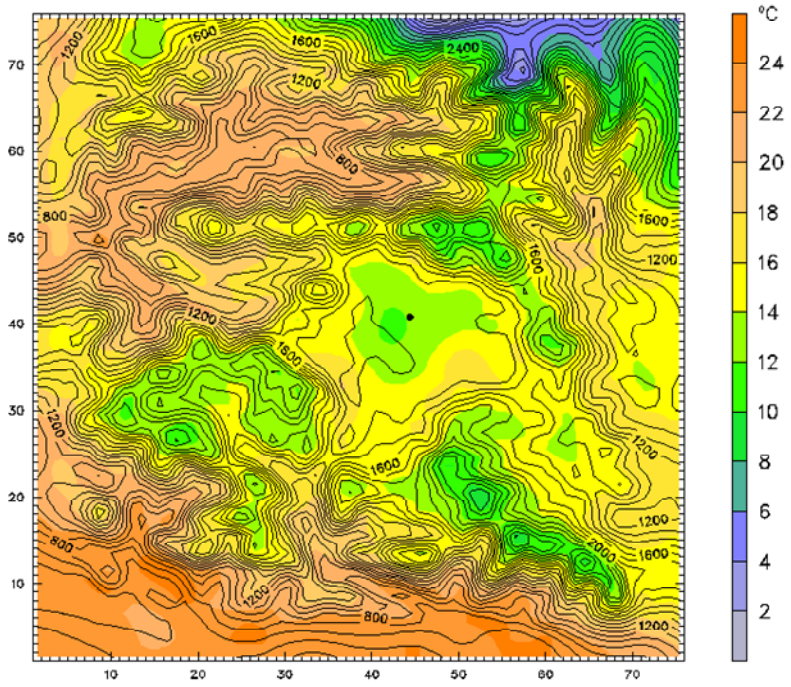

Figure 5.16: Surface temperature at 5:45 am on May 11, 2005.

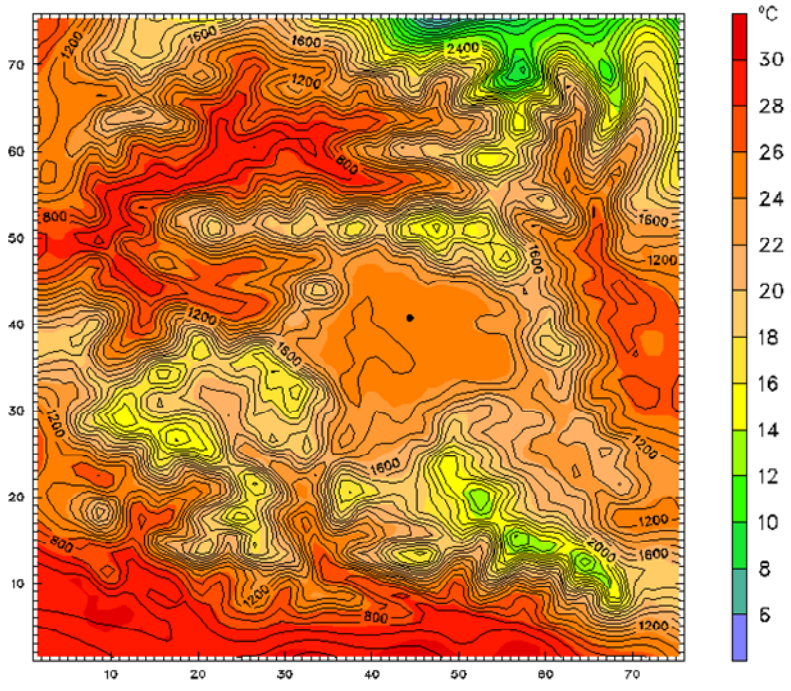

Figure 5.17: Surface temperature at 11:45 am on May 11, 2005.

The next two figures show west-to-east cross sections on May 11, 2005, showing potential temperature contours and as well as wind vectors parallel to the cross-section surface. Figure 5.18 shows a cold pool over the valley at 5:45 am, and easterly winds traveling across the top of that cold pool and out the western passes, descending quickly into the neighboring valleys to the west. Close examination of the cross sections every half an hour showed that the easterlies started crossing the passes and descending just after midnight – the time when we recorded the switch in wind direction at Bhimdhunga Pass. MM5 correctly calculated the timing of the switch from easterlies to westerlies at the pass. In Figure 5.19 we see again the afternoon mixed layer being under-cut by air with lower potential temperature crossing the western ridge and descending into the valley, carried forward by the high speed afternoon westerly winds. The February 10 and May 11 simulations are used in the next few sections to help address the questions from Chapter 4.

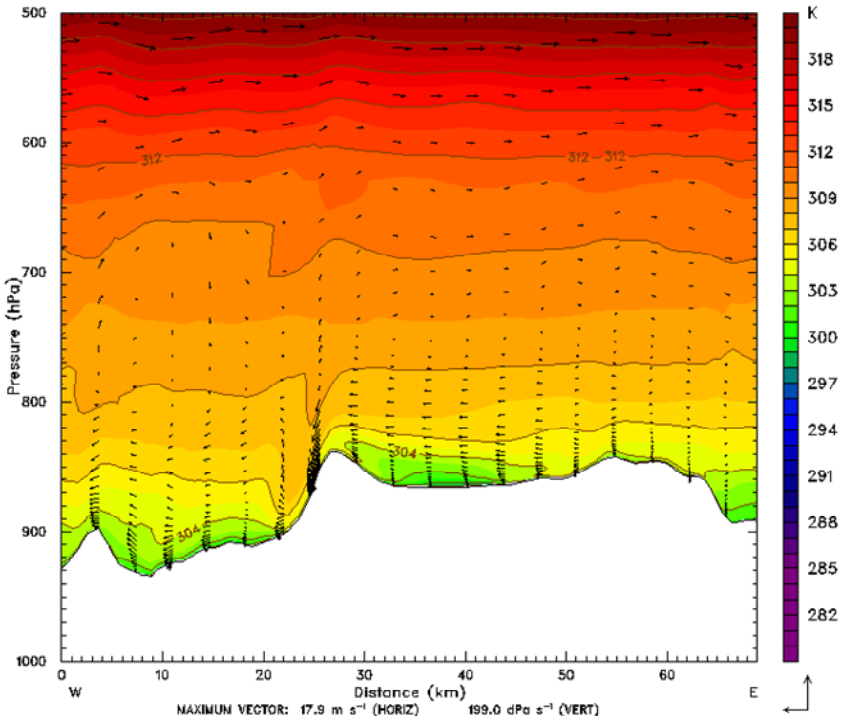

Figure 5.18: West-to-east cross section and potential temperature on May 11, 2005 at 5:45 am. Same cross section as Figure 5.7,but with vertical coordinates in pressure-scale, and with addition of wind vectors in the plane parallel to the cross section.

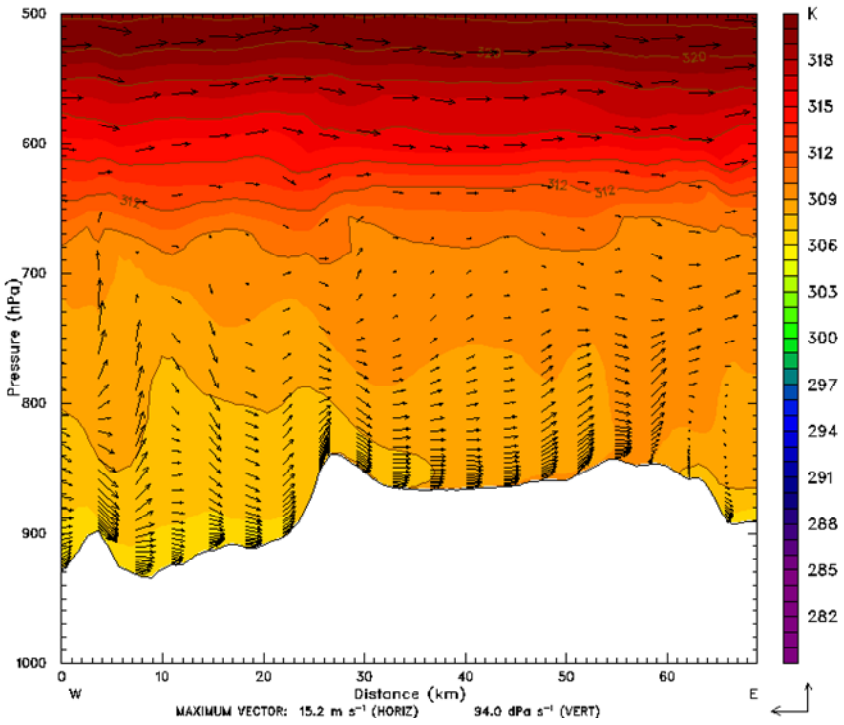

Figure 5.19: Same as previous figure, but for 5:45 pm on May 11, 2005.

5.5 Answering Question 1, the Inversion Break-up Mechanism

Chapter 4 described four hypotheses of possible mechanisms of the Kathmandu Valley's nocturnal inversion break-up in the morning that allows the mixed layer to grow. Our MM5 simulations found strong evidence pointing towards hypothesis H1C: that the inversion breaks up through the combined effect of up-slope flows along the valley edge, and subsidence over the valley center. The potential temperature contours in Figure 5.20 and Figure 5.21 show that on the morning of February 10, 2005, a mixed layer characterized by constant potential temperatures first grew at the valley edge, while the valley center remained stably stratified. A zoomed-in view confirmed that near the surface the winds were indeed blowing upslope everywhere, as expected from Hypothesis H1B or H1C. The downward dip in potential contours over the valley center seen in both figures suggests sinking air over the center. Indeed, a zoomed view shows that wind vectors over the valley center had a down-ward component.

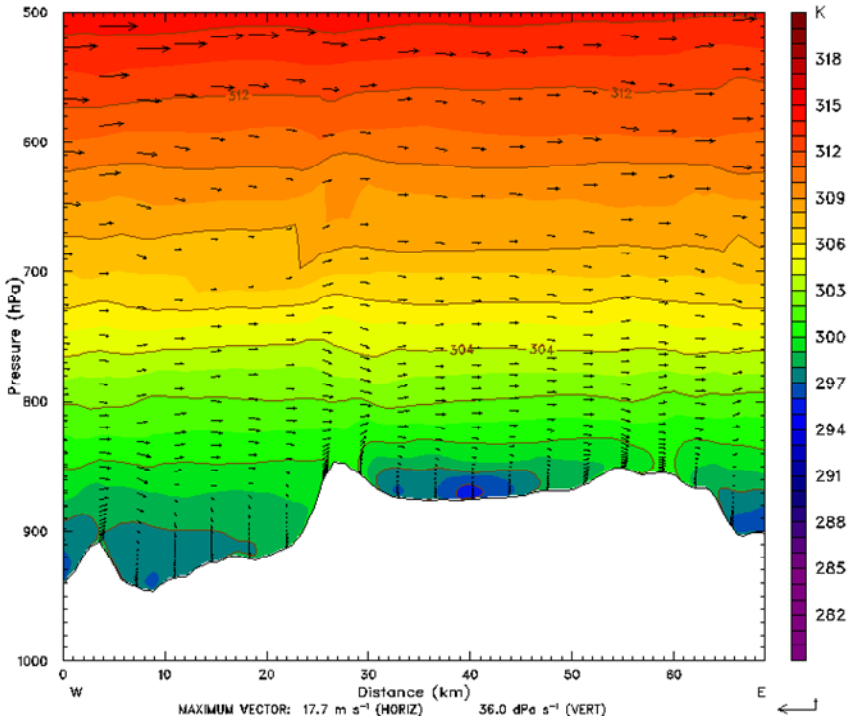

Figure 5.20: Cross Section A at 10:15 am on February 10, 2005, showing potential temperature in color and contours, as well as wind vectors parallel to the plane of the cross section .

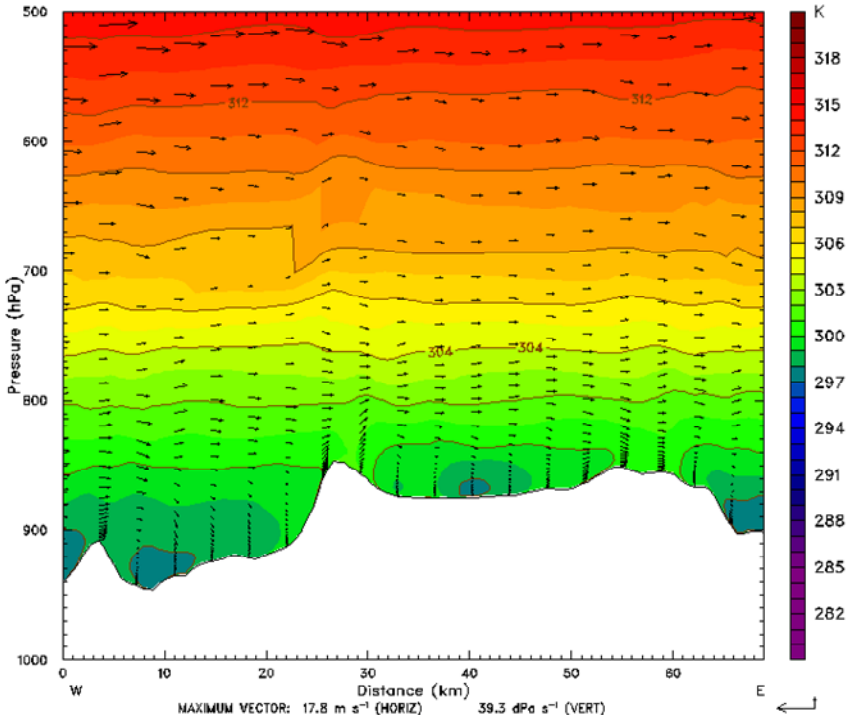

Figure 5.21: Same as the previous figure, but at 10:45 am.

According to hypothesis H1C, subsidence over the basin center replenishes air removed from the basin by upslope flows, while according to hypothesis H1B, the replenishment would take place by flows up the Bagmati River valley. Given the narrowness of the Bagmati Valley compared to the length of the basin perimeter experiencing up-slope flows, hypothesis H1B would require wind speeds up the Bagmati valley ~ 50 times the upslope flows. That was not seen in the MM5 simulation (nor found in real life). Thus it appears that during the time studied, winds up the Bagmati Valley played at most a minor role in basin air replenishment during morning up-slope flows, compared to the role played by subsidence over the basin center. Figure 5.22 shows potential temperature contours and wind vectors on cross section B (through the eastern and western valley rim peaks) at 11:45 am. By this time there was a uniform mixed layer over the valley (the valley-center stratification is gone), but there continued to be higher potential temperatures over the peaks, driving up-slope flows, while allowing air parcels reaching the peaks to mix to higher elevations than ones rising straight up from the basin floor.

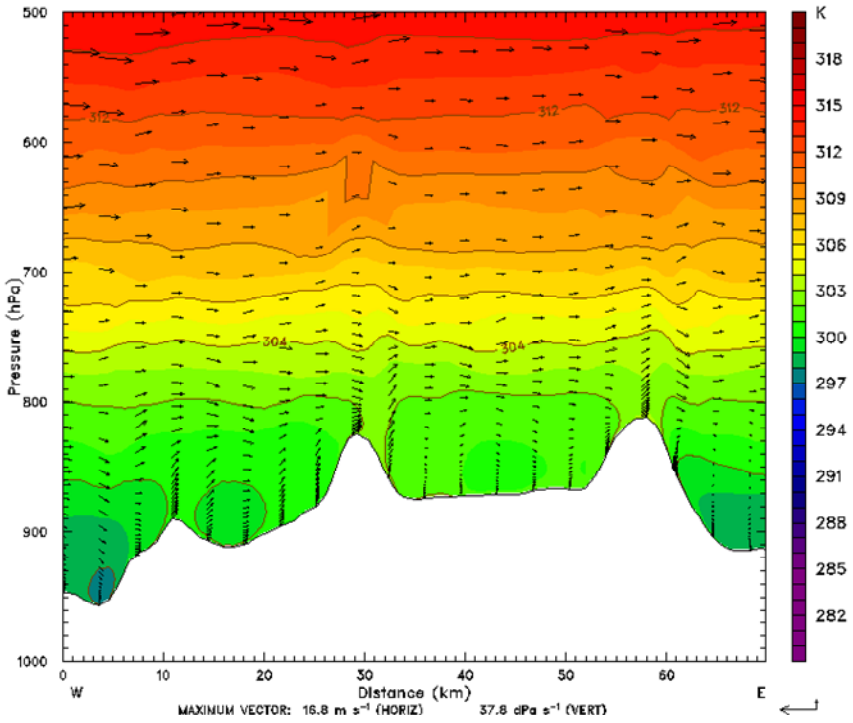

Figure 5.22: Potential temperature and wind vectors on cross section B at 11:45 am on February 10, 2005.

Figure 5.23 shows Cross Section A at 9:45 am on May 11, 2005. There was again stronger vertical mixing over the peaks than over the basin center, and there were flows up the slopes; these were found, that day, to initiate the mixed layer growth around the basin perimeter as early as 7 am, with a tall mixed layer already existing by 9:45 am. We see in the figure that the land surface over the basin bottom was heating as well, with an unstable near-surface region of higher potential temperature than in the air above. Indeed this was only seen briefly; by 10:15 am the air over the entire valley was well mixed.

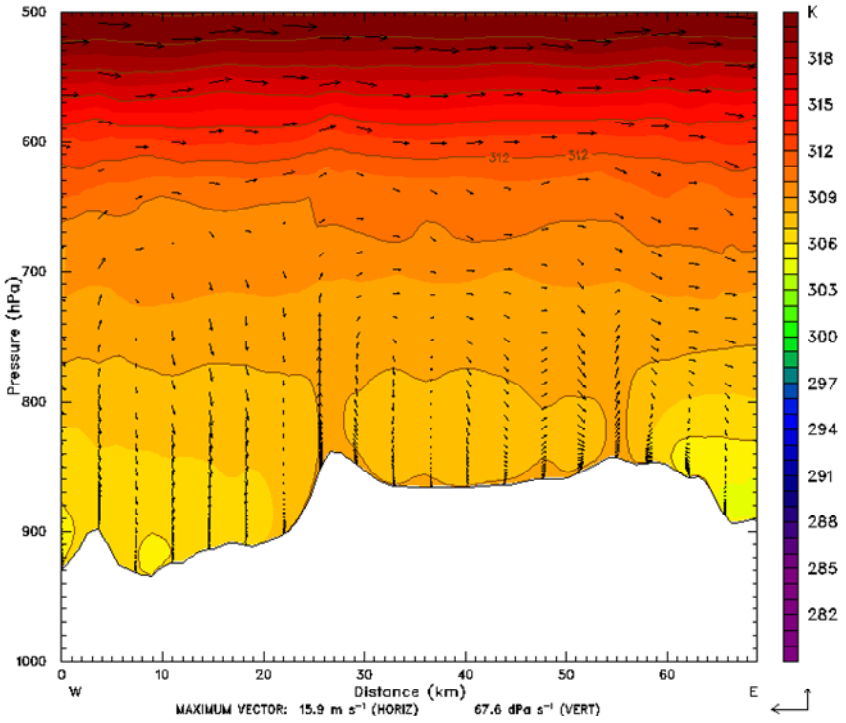

Figure 5.23: Potential temperature and wind vectors on cross section A at 9:45 am on May 11, 2005.

The simulations suggest that in May the mechanisms described by two hypotheses play a major role in the growth of the mixed layer. Shortly after dawn, upslope flows begin, at least on sun-lit slopes, eroding the nocturnal stable stratification as described in hypothesis H1C. However, as the sun rises higher, the basin bottom generates thermals that let the mixed layer grow from below. This is the mechanism that describes the mixed layer growth over flat plains (hypothesis H1A). A likely reason that this mechanism was seen in May but not in February was the fact that the basin bottom was covered in fog in February, which reduced the surface heating.

No evidence was found in support of hypothesis H1D (turbulent erosion by winds flowing across the top of the cold air pool) playing a dominant role in the removal of the Kathmandu Valley's nocturnal inversion. The break-up of the inversion did not propagate from west to east, and strong winds were found to penetrate into the valley only after the mixed layer had risen above the height of the western passes.

Thus, in summary, in February the Kathmandu Valley's nocturnal inversion break-up and mixed layer growth took place following a mechanism observed in large basins (hypothesis H1C), while in May, it started with that mechanism, but then received contributions from the mechanism observed over flat plains (hypothesis H1A). As noted in Chapter 5, the valley's mixed layer did not remain high throughout the afternoon as is usually the case over flat plains. Instead it was affected by the arrival of cooler air from the western valleys and up the Bagmati valley, which reduced vertical mixing. Figure 5.24 shows the two centers of the westerlies (north and south of Nagarjun Peak) confined to the surface. The southerlies entering up the Bagmati valley have even colder potential temperature.

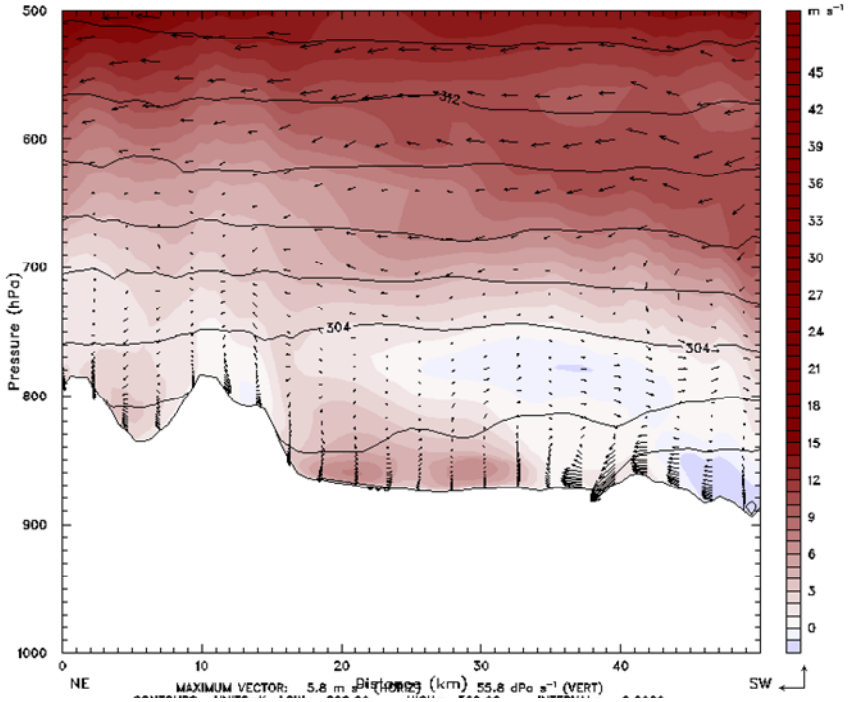

Figure 5.24: Cross-section C, showing potential temperature contours, wind vectors parallel to the plane of the cross-section, and shaded wind velocities perpendicular to the cross section (red shading indicates westerlies, while blue shading indicates easterlies)

5.6 Answering Question 2, the Pollutant Ventilation Pathways

Chapter 4 examined various pathways by which pollutants emitted within the Kathmandu Valley could leave the valley. Plausible pathways included vertical mixing to the top of the mixed layer, followed by transport out by strong westerly winds aloft (H2B), transport out the eastern passes by westerly winds (H2C), and transport up valley rim slopes to the strong westerly winds aloft (H2D). The pollution transport pathways were studied using lagrangian forward trajectories of tracers released on the valley floor over the time period corresponding to the February 9-10 bag sampling campaign. The tracers were released along a north-south line running through the MM5 inner nest domain center. For visual clarity, only release points at 2 km intervals are shown; these are a small selection of hundreds of plots that were examined to draw conclusions. Throughout all the trajectory plots, the positions are color coded by time: from 11:45 pm to 3:45 am they are black, from 3:45 am to 7:45 am blue, from 7:45 am to 11:45 am green, from 11:45 am to 3:45 pm red, from 3:45 pm to 7:45 pm orange, and from 7:45 pm to 11:45 pm brown. To illustrate this, Figure 5.25 shows a map view and a projection onto the west-to-east cross section B of the trajectory of one tracer that was released shortly before midnight. We see that it lingered in the valley overnight, traveled up the valley rim slope in the morning and crossed the valley at the new elevation around noon, before traveling up and over the eastern valley rim.

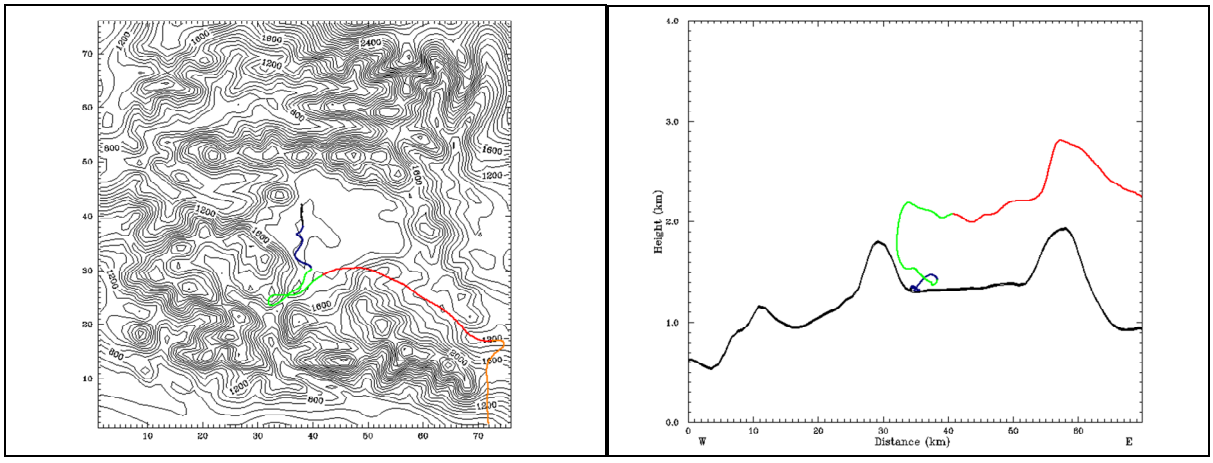

Figure 5.25: Sample trajectory released at 11:45 pm viewed on a contour map (left) and cross section (right)

Figure 5.26 shows 11 tracers released at 11:45 pm along the north-south line. We see that the southern-most ones left the Kathmandu Valley along the Bagmati River valley during the night (black and blue), while the northern-most ones crossed a pass and traveled down a neighboring valley to the west before rising up in the morning (green) and traveling eastward on the north-side of the valley-rim mountains. Tracers released closer to the center of the valley lingered within the valley over-night, then traveled up valley rim slopes in the morning (green) before exiting the valley to the east.

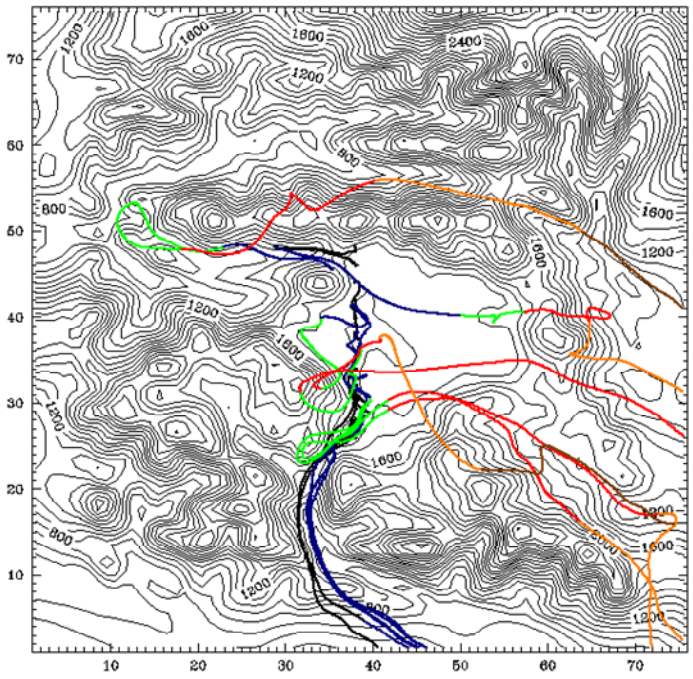

Figure 5.26: Trajectories of tracers released at 11:45 pm at a line running north-south at between (38,26 and 38,46).

Tracers released during the rest of the night continued along similar trajectories. The ones at the southern end of the Kathmandu Valley traveled down the Bagmati river valley. Most tracers released within the Kathmandu Valley lingered close to their point of origin. Tracers released near the western valley-rim passes rose and crossed over the passes, and traveled down the western valleys until the morning, when up-slope and up-valley winds carried them back up. Cross-sections have shown strong nocturnal drainage winds in those valleys; these appear able to create a sufficient pressure gradient to force some Kathmandu Valley air up and over the western passes during the night. This

explains the strong easterly winds observed at Bhimdhunga Pass during the night. Likely the drainage winds in the neighboring valleys were also responsible for driving the light easterly winds that were found traveling along the top of the Kathmandu Valley's cold pool at night and that were seen in sodar soundings at night as well.

Figure 5.27 shows the trajectories of tracers released at 7:45 am. They are plotted in green until 11:45 am, in red until 3:45 pm, and in orange until 7:45 pm. It is clear that over the course of the morning, most of the tracers traveled towards the nearest valley rim slope, and then traveled up the slope to a height of 500-1000 meters above the basin bottom. Then, before 11:45 they started to travel eastwards, crossing the Kathmandu Valley at high elevation. Detailed study of individual tracers showed that, upon arriving at the eastern valley rim, trajectories which passed over passes or low ridge regions maintained their altitude, whereas trajectories passing over the eastern mountain peaks experienced a step-like gain in altitude that was driven by the convergence of up-slope flows at the peaks. Heating of the highest peaks was able to lift air parcels another kilometer.

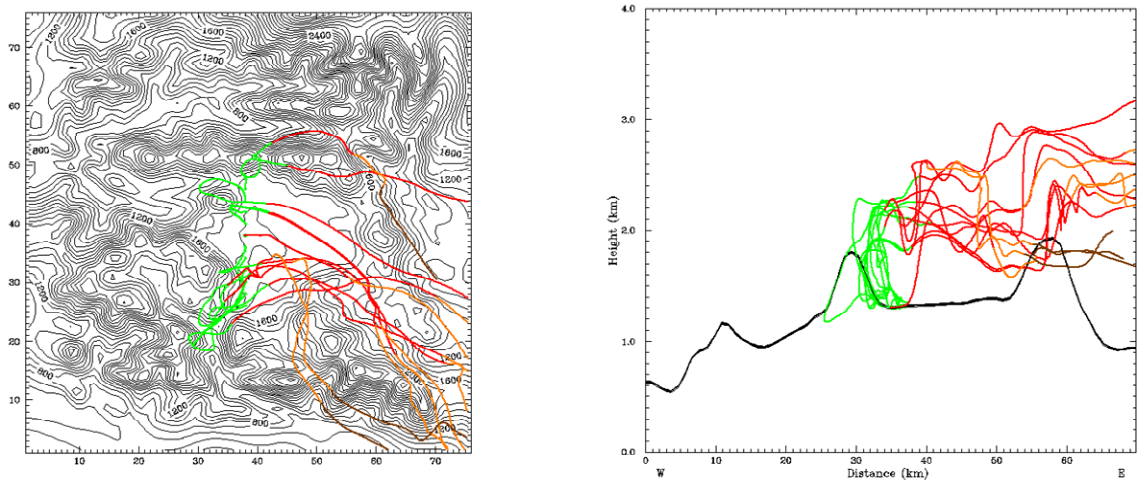

Figure 5.27: Tracers released at 7:45 am on February 10, 2005, shown on a contour map (left) and on cross-section B (right).

By early afternoon, once the cooler air masses from the neighboring valleys and the strong westerly winds had swept into the Kathmandu Valley, tracers released in the

valley traveled straight to the east. Some trajectories released around noon were able to travel up and over the eastern valley rim mountains, such as Nagarkot peak. As the afternoon progressed, most trajectories converged to flow through passes: the Sanga and Nala passes on the eastern valley rim, and a much higher pass on the southern valley rim, above the town of Tika Bhairav, which had not been expected to play a significant role. Figure 5.28 shows the trajectories of tracers that were released along the north-south line on the valley floor at 3:45 pm on February 9, 2005.[28] We see that of the eleven released tracers, the southern-most four traveled south, across the high pass. Of the remaining seven, five left via the eastern passes, and two lingered in the valley about 400 meters above ground before departing via the eastern passes around midnight.

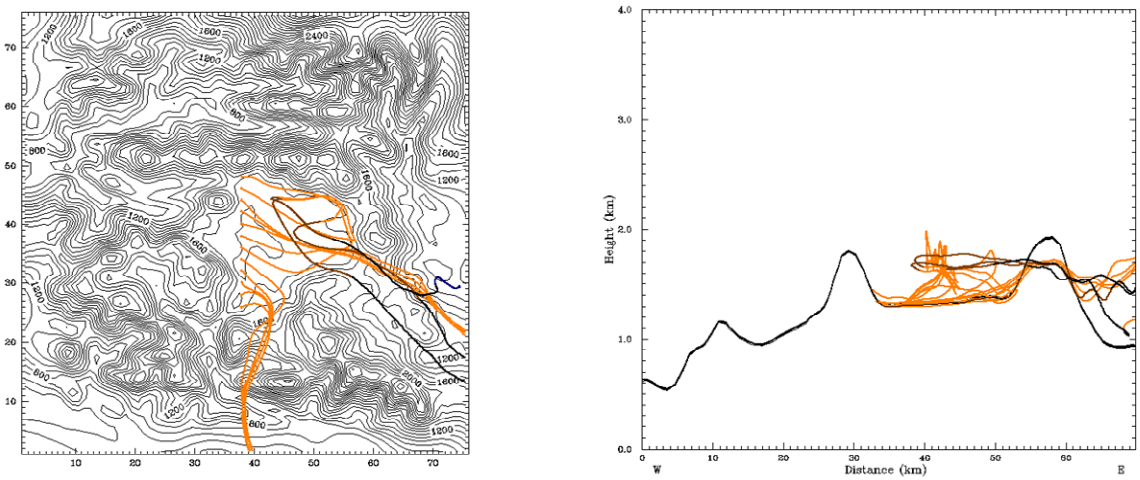

Figure 5.28: Tracers released at 3:45 pm on February 10, 2005, shown on a contour map (left) and on cross-section B (right).

In Chapter 4 we discussed three pathways for pollutant ventilation from the Kathmandu Valley. We have found here that the dominant pathway depended upon the time of day. On the February day studied, we found that during the morning, tracers were advected out of the valley by transport up the slopes of the valley rim mountains whence they were carried east by the upper-level westerly winds (hypothesis H2D); during the afternoons, when the valley air mass was stratified again, tracers were found to be removed from the

[28] The tracer studied focused upon the time period corresponding to the bag sampling campaign from late morning on February 9 through late morning on February 10. The afternoon of February 10 showed comparable patterns to the afternoon of February 10.

valley through mountain passes, both to the east (hypothesis H2C) and to the south. During the night some tracers near the Bagmati River left down the river valley, and near the western passes some tracers were able to escape from the Kathmandu Valley via drainage flows. On the February day studied, unlike in May, little evidence was found of tracers rising vertically over the valley center to sufficient heights to be carried out of the valley (hypothesis H2B). The previous section described how stronger surface warming produced rising thermals over the valley center in May, so that the mixed layer growth took place not only at the edges. Indeed tracers released in May showed that, during the mornings, both hypotheses H2B (buoyant rise over the valley center into the upper level westerlies) and H2D (transport up the valley rim slopes) played an important role. During May afternoons, transport out the passes (H2C) remained the dominant mechanism of pollutant ventilation from the Kathmandu Valley.

5.7 Answering Question 3, the Causes of Nocturnal Pollution Low

Chapter 4 presented four hypotheses suggesting why high concentrations of CO and PM_{10} emitted in the evening did not persist throughout the night in the measurements of near-surface air. The first hypothesis (H3A) considered the possibility of the polluted airmass draining down the Bagmati Valley to be re-circulated in the morning. The second hypothesis discussed the possibility of the polluted air mass over the city being lifted by katabatic winds converging underneath, to be re-circulated later. The third hypothesis considered whether turbulence could transport the pollutants high enough so as to be carried away by winds aloft, while the fourth hypothesis considered whether turbulence could dilute the pollutants by upward transport sufficiently to cause a drop in concentrations near the surface.

Figure 5.26 showed that tracers released just before midnight in the southern parts of the valley could indeed depart down the Bagmati Valley at night. However, these tracers were not found to return to the Kathmandu Valley. After dawn most were found to travel up the nearest slopes into stronger winds aloft, as illustrated for one typical tracer in

Figure 5.29. The tracer studies alone would indicate that cold air draining down the Bagmati Valley could carry out a substantial part of the polluted air mass from the southern half of the Kathmandu Valley. However, it is important to keep in mind that the model did not resolve surface features smaller than 1 km across, thereby entirely missing the Chobhar Gorge which would be the biggest hindrance to the down-valley drainage of cold air starting off over the city. Thus it is likely that the mechanism in hypothesis H3A can only remove pollution in the small fraction of the Kathmandu Valley that sits south of the Kirtipur-Chobhar-Bhaisepati ridge.

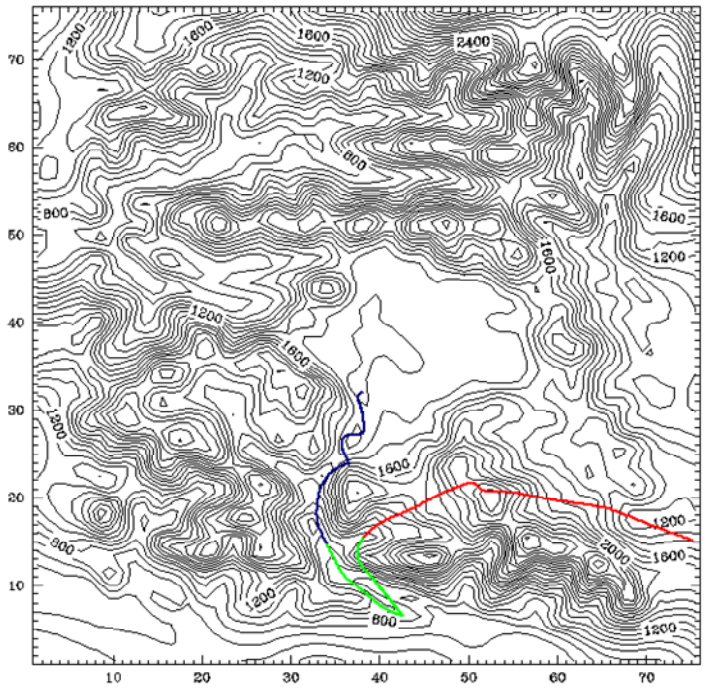

Figure 5.29: One tracer released at the southern end of the Kathmandu Valley at 3:45 am on February 10, 2005.

Confirming hypothesis H3B (lifting of polluted air by convergence of katabatic winds) would require several tests. First, if the katabatic winds were transporting air from the valley rim mountains to basin bottom, they would also be bringing a fresh supply of ozone. A continuous supply of ozone, but zero ozone levels at night (observed), would require an efficient ozone removal mechanism. NOx emissions are small during the night, after most vehicles stop operating; thus for the hypothesis to hold, it would need to

be plausible for dry deposition to remove the ozone before it arrived at the measurement location. Even with the low night-time wind-speeds, converging katabatic winds would arriving at the Hyatt sensors from the valley rim base in at most a few hours. Is that sufficient time for dry-deposition of ozone? The katabatic flows would be following the surface, traveling underneath layers of air from which ozone would already have been removed. Thus they would not have any en-route replenishment. A quick survey of the literature [*Lagzi et al.*, 2004; *Matsuda et al.*, 2005; *Sorimachi et al.*, 2003; *Zhang et al.*, 2002] suggests that agricultural land-use as found between the valley-rim slope and the Hyatt sensors experience ozone dry-deposition velocities on the order of 0.2 cm/s, or 7.2 meters/hour. Given that katabatic flows are only a few meters thick, and this does sound like a reasonable mechanism for the removal of ozone from air masses arriving at the Hyatt measurement station at night.

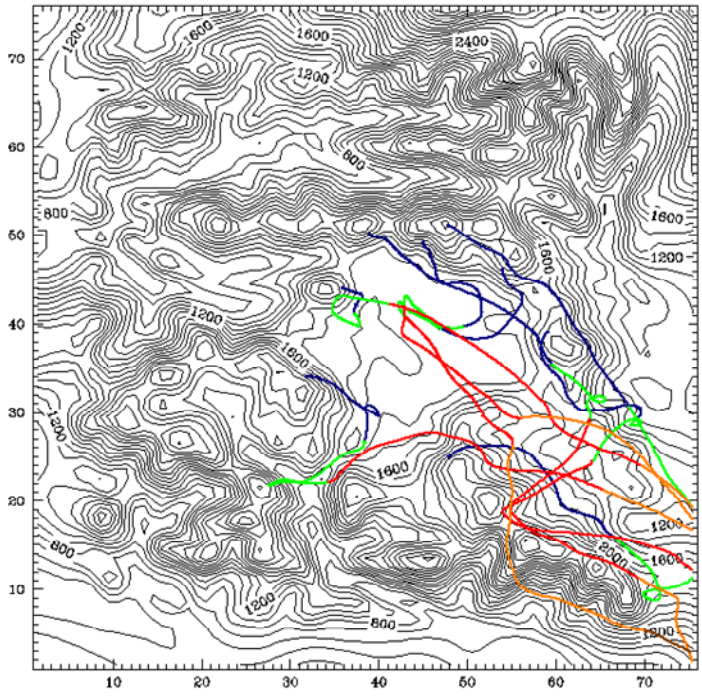

Figure 5.30: Forward trajectories of tracers released on valley rim peaks and along the Kathmandu-valley facing slopes of the valley rim at 3:45 am on February 10, 2005.

Second, confirming the hypothesis would require confirming that katabatic winds did indeed arrive at the valley center. Simulated wind fields in the lowest MM5 sigma layer (for example in Figure 5.2) indicate down-slope winds along the basin rim, but calm

conditions over the basin center. Indeed, forward trajectories of tracers released around the valley rim (for example, in Figure 5.30) indicated that most tracers did not arrive on the valley bottom. Tracers released on Shivapuri, Nagarkot, and Phulchoki Peaks were all carried eastwards at elevations close to their release point by the strong westerly winds found at those altitudes. Tracers released lower down on Nagarjun, Hattiban and Shivapuri arrived at the base of the slope, but did not converge at the valley center.

At a first glance this suggests a rejection of the hypothesis; however we must keep in mind the limitations of MM5's ability to properly capture katabatic flows given its horizontal and vertical resolution. Our lowest layer was 15 meters thick – far thicker than typical katabatic flows [*Mahrt et al.*, 2001]. Meanwhile, Katabatic flows tend to travel along gullies and river valleys; the horizontal resolution of MM5's terrain data did not capture the fine-scale topography of the Kathmandu Valley's basin bottom, which is dominated by flat plateaus interrupted by floodplains, a few hundred meters wide, that sit 10-30 meters lower. The hypothesis can neither be rejected nor confirmed because the model lacked the precision needed to do so.

Let us discuss the remaining two hypothesis: vertical turbulent transport followed by transport out (H3C) or re-circulation (H3D). Except for the tracers released in the northwest corner of the valley that crossed a pass and traveled down the neighboring valleys to the west, no tracer was found to be transported out of the valley after being lifted at night. Hypothesis H3C thus appears to apply only in limited situations. What about hypothesis H3D?

In the MM5 simulation, some of the tracers originating in the city at night were found to rise slightly then to sink back down. The sample trajectory released at night (Figure 5.25, right) shows the tracer rising 150 meters above ground at night, and then sinking back down in the morning. Two more examples of re-circulating tracers released at 11:45 pm are shown in Figure 5.31. Some tracers that rose up at night did not return to the surface before traveling up nearby slopes in the morning; only a fraction of pollutants lifted during the evening were re-circulated down to the surface in the morning.

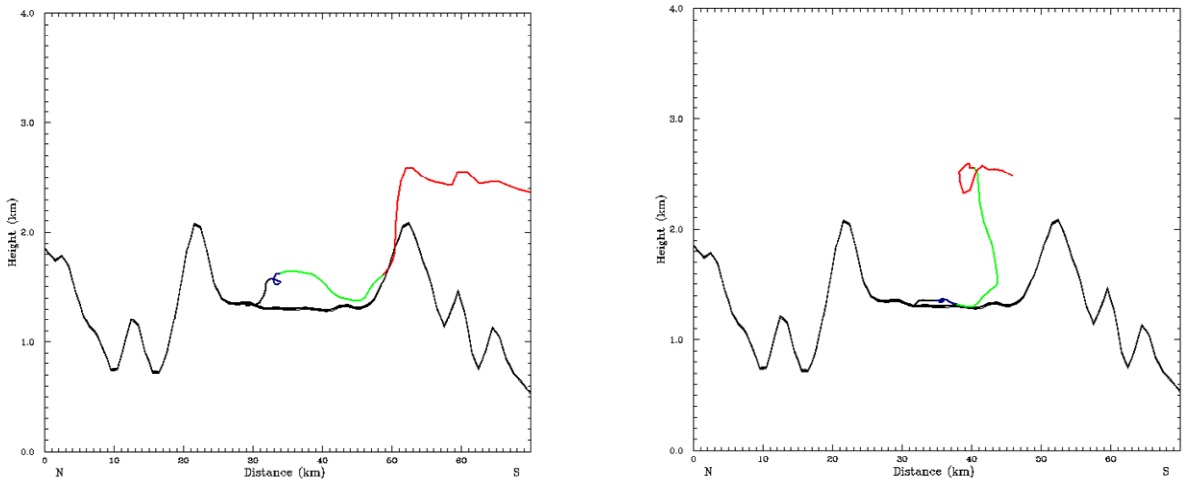

Figure 5.31: Cross-section D, showing re-circulation exhibited by tracers released at 11:45 pm on February 9, 2005.

But is vertical transport by turbulence plausible at the bottom of a stratified cold air pool? A review of the literature suggests that could be. Turbulence in stable nocturnal boundary layers is generally not caused by surface heating, but by shear in the nocturnal jet. A field study involving a 60m instrumented tower found turbulence in the stable nocturnal boundary layer created by wind shear increasing with height [*Mahrt and Vickers*, 2002]. In addition to shear-generated turbulence, substantial vertical mixing is also possible within the stable layers by internal gravity waves [*Monti et al.*, 2002; *Stull*, 1988]. The temperature oscillations in the TV tower data (Figure 3.15) are possibly due to the presence of such gravity waves. These oscillations are dependent upon the wind profile at the time of sunset [*Singh et al.*, 1997]. In Phoenix, Arizona, pollutants were found to mix vertically two hours before sunrise due to the arrival of a density current [*Shaw et al.*, 2005]. CO_2 measurements on a tall tower in North Carolina found night-time oscillations at the 123m level that were not seen at 51 or 496 meters above ground; similar oscillations have also been seen on data collected on a tower in Wisconsin [*Bakwin*, 1995; *Bakwin et al.*, 1998]. WE thus have to conclude that either hypothesis H3B or H3D remain plausible, and cannot be resolved with the MM5 modeling. A future project will involve calculation of vertical turbulence from the tower data.

5.8 The Diurnal Cycle Revisited

Studying back trajectories of air masses arriving at the three locations where bag sampling and measurements established an unambigious twin-peak pattern (the Hyatt, CTEVT, and Dharahara) as well as at higher elevation locations where the twin-peak diurnal cycle was absent (Nagarkot, Hattiban, and Bhimdhunga Pass) we are able to fill additional gaps in our understanding of the complete diurnal cycle.

Figure 5.32 shows back-trajectories arriving at the three valley-bottom locations at 11:45 pm. We see why bag sampling at the Dharahara and CTEVT showed a higher night-time low than at the Hyatt: during the last four hours the tracers arriving at the first two places traveled only 2-3 km over urban areas, while the tracers arriving at the Hyatt swept a long arc over the rural eastern edges of the valley. Four hours later, patterns were still similar. Around mid-day, back-trajectories started indicating air arriving at a high speed from west of the Kathmandu Valley (red line extending back-trajectory out of the valley), arriving first at Dharahara, then at the Hyatt, and finally at CTEVT (two hours later than at the Dharahara). During the afternoon, all three sites received air coming directly from west of the Kathmandu Valley, from an elevation higher than the Kathmandu Valley (Figure 5.33).

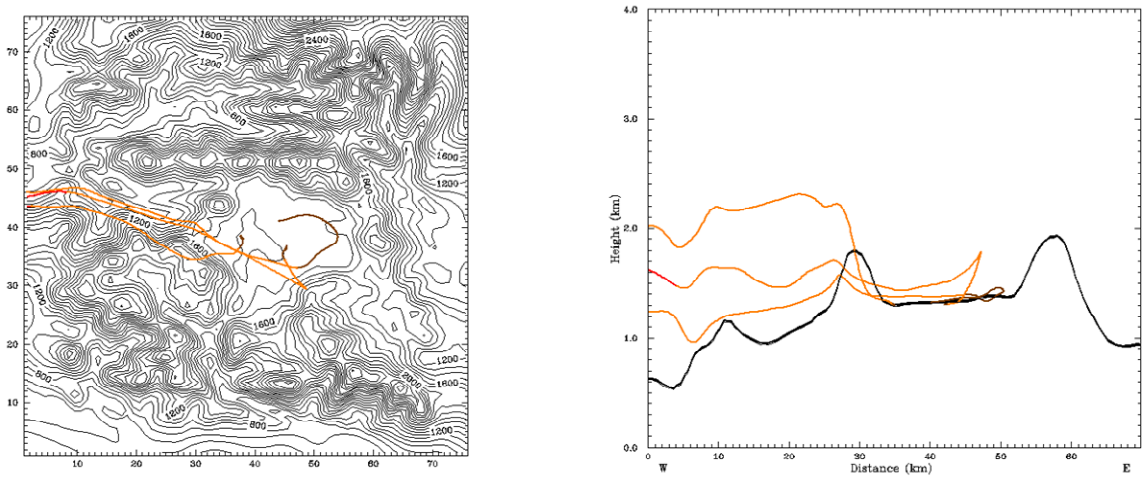

Figure 5.32: Back trajectories of tracers arriving at 11:45 pm at Dharahara (38,38), CTEVT(45,36) and the Hyatt (44,41).

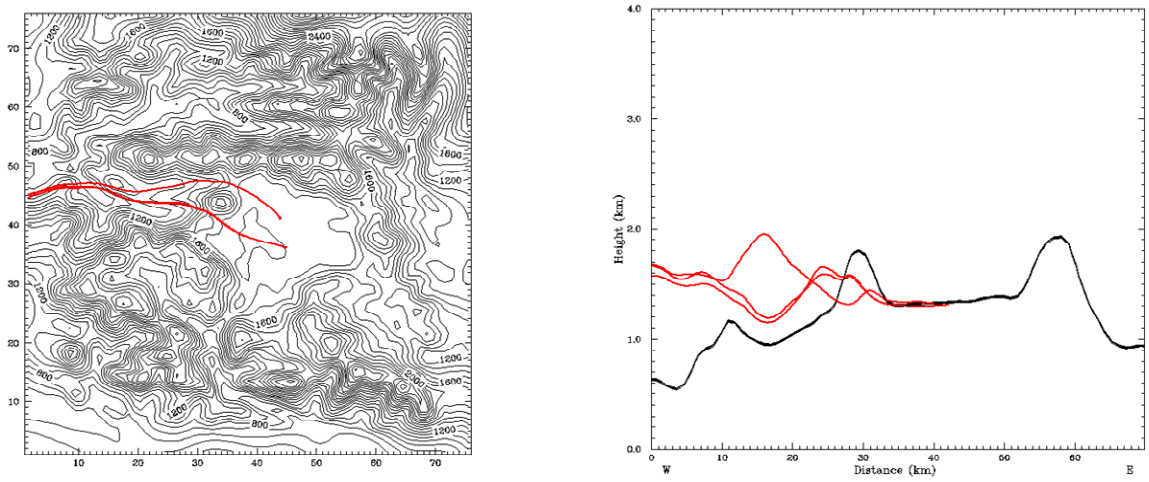

Figure 5.33: Back trajectories of tracers arriving at 3:45 pm at Dharahara, CTEVT and the Hyatt.

Meanwhile, back trajectories have confirmed that during the night, the valley rim locations received air that never passed through the bottom of the Kathmandu Valley. Hattiban and Bhimdhunga Pass received air parcels arriving horizontally from the west and northwest. Nagarkot received air that originated northwest of the Kathmandu Valley, and traveled across the northern part of the Kathmandu Valley at high elevation. By late morning Nagarkot and Hattiban were receiving air that had crossed the bottom of the Kathmandu Valley, while Bhimdhunga received air that had swept up the bottom of the neighboring western valley. We thus have confirmation that during the night of February 9-10, Nagarkot and Hattiban did indeed measure relatively unpolluted "background" air. Although bag sampling was not carried out at Bhimdhunga Pass on the days that were modeled, the regularity of the wind patterns at the pass suggest that model results may be able to help interpret the surprising result of finding rapidly fluctuating pollution levels at the pass where we expected to find clean background air. The day-time fluctuations in CO at Bhimdhunga were a result of minor shifts in the trajectories of air parcels arriving from up the western valleys traveling among farm houses and other rural point sources of pollution. At night the pressure gradient created by the drainage flow descending down the western valleys forced polluted air from Kathmandu City up and over the pass.

5.9 Chapter Summary and Conclusion

This chapter introduced a meso-scale modeling framework to interpret our field observations and that will be used to the questions posed in Chapter 4. It described how MM5 was set up, and showed some MM5 results that demonstrated the model's ability to accurately capture the observed meteorology in the Kathmandu Valley.

The chapter addressed the three large questions introduced Chapter 4. It showed that in February, the Kathmandu Valley's nocturnal inversion is eroded and its mixed layer grows according to the mechanism first described by *Whiteman* [1982], with up-slope winds along the edges, and subsidence at the center. In May, the same mechanism begins the process, but then is overwhelmed by the mechanism usually found on flat plain, with surface heating of the basin bottom creating thermals that travel increasingly high. The chapter also showed that pollutants are ventilated up the slopes during the morning, and out the passes in the afternoon. It also showed that the night-time minimum in pollution was not a result of most of the polluted air draining down the Bagmati valley, but of it being lifted above the surface, either lifted by undercutting katabatic winds, or by slow turbulent mixing to heights of 100-200 meters above the surface, followed by re-circulation in the morning. Finally the chapter explained why the Hyatt had a lower night-time low in CO values than other observation sites, and it showed model results which confirmed that Hattiban and Nagarkot did indeed provide locations to sample background CO levels at night.

CHAPTER 6: TOWARDS EULERIAN MODELING OF CARBON MONOXIDE IN THE KATHMANDU VALLEY

6.1 Chapter Introduction

Chapter 5 used the meso-scale meteorological model MM5 to explain the processes responsible for a number of patterns observed in field data, thereby significantly increasing the understanding the valley's physical processes. We understand better when and where pollutants accumulate in the Kathmandu Valley, and how they leave. But that understanding alone is not sufficient to address many of the questions posed by policy makers, who would like to know more directly how various policy choices would impact air quality. That requires directly relating changes in anthropogenic emissions patterns to ambient air quality, forecasting the consequences of various emissions scenarios.

This needs a different modeling framework from the tracer trajectories described so far. It needs to take information about pollution emissions taking place at each time and place, and calculate their transport around the valley; it needs a eulerian transport model which takes as inputs both spatially and temporally resolved emissions, and the temporal evolution of wind fields. This chapter presents an attempt to put together such a model, while assessing current bottlenecks and shortcomings. It addresses the first step of using the model to try to reproduce field observations. Section 6.2 describes the CAMx eulerian transport model, which was adapted to compute the time-evolution of CO in the Kathmandu Valley, using meteorology from MM5 and an emissions database described in Section 6.3. In Section 6.4 the CAMx model is tested by comparison to field measurements of CO, while making necessary adjustments to the emissions assumptions.

6.2 The CAMx Model

The "Chemistry Transport Model with Extensions", or CAMx [*ENVIRON*, 2005], is one of the newest chemistry transport models. It is designed in a modular way and is capable

of using a wide variety of meteorological inputs, chemistry mechanisms, and integration algorithms [*Chock et al.*, 2005]; it can be applied to a wide range of research questions. Essentially it solves the continuity equation for each species considered, computing, at each time step, the local rate of change in a grid cell as the sum of changes due to emissions, horizontal and vertical advection, horizontal and vertical diffusion, and, depending on the species, dry deposition, wet scavenging, and chemical production and loss. The model has recently been used for studies of secondary aerosol formation and impacts upon photochemistry by wildfires in eastern Texas [*Junquera et al.*, 2005; *Russel and Allen*, 2005], for studies of tropospheric chlorine chemistry [*Chang and Allen*, 2006], and for a study of the impact of shifting NOx sources [*Mauzerall et al.*, 2000]. CAMx has also been used for a detailed statistical inter-comparison with observations in Europe [*Riccio et al.*, 2006]. For the purpose of this dissertation, only a small fraction of the model's capabilities were used.

There are numerous choices of chemistry transport models driven by MM5 meteorology [*Grell et al.*, 2000; *Grell et al.*, 2005; *Jazcilevich et al.*, 2005; *Schmitz*, 2005]. CAMx was chosen because it is already in use in the Prinn Group [*Jason Cohen*, 2006, personal communication], because it is being used in the Mexico City Project [*Ben de Foy*, 2006, personal communication], and because it will very likely be used in post-doctoral research that Arnico Panday will be doing at MIT immediately following dissertation completion [*Ronald Prinn*, 2006, personal communication].

The model domain was set up to correspond to a cropped part of MM5's inner-most domain, with a grid spacing of 1 km. The domain spanned 38 by 30 cells in the horizontal direction, with an origin off-set of (+25, +23) . The domain is illustrated in Figure 6.1. Its location and size were chosen to correspond exactly with the emissions inventory available for the Kathmandu Valley on a 1 km grid resolution [*Kitada and Regmi*, 2003]. In the vertical direction, CAMx was set up with 14 layers, corresponding to MM5 layers as follows: layers 1-8 corresponded to MM5's bottom eight layers; layers 9-14 corresponded to the two MM5 layers each, taking the CAMx model domain to a height corresponding to the 20th MM5 layer. MM5 meteorology was fed to a CAMx

preprocessor [*ENVIRON*, 2005], which then wrote out files for each time period containing information on winds, humidity, temperature, pressure, vertical eddy diffusivity and clouds. Advection was calculated using the BOTT solver. The model was run using only one chemical species, CO. Chemistry, wet deposition, dry deposition, the plume-in-grid tool and the probing tool were turned off. The point source emission module was also turned off, since emissions were available as grid-averages. The model was run numerous times for a 48 hour period from noon on February 9 and through noon on February 11, 2005, using a variety of emissions scenarios.

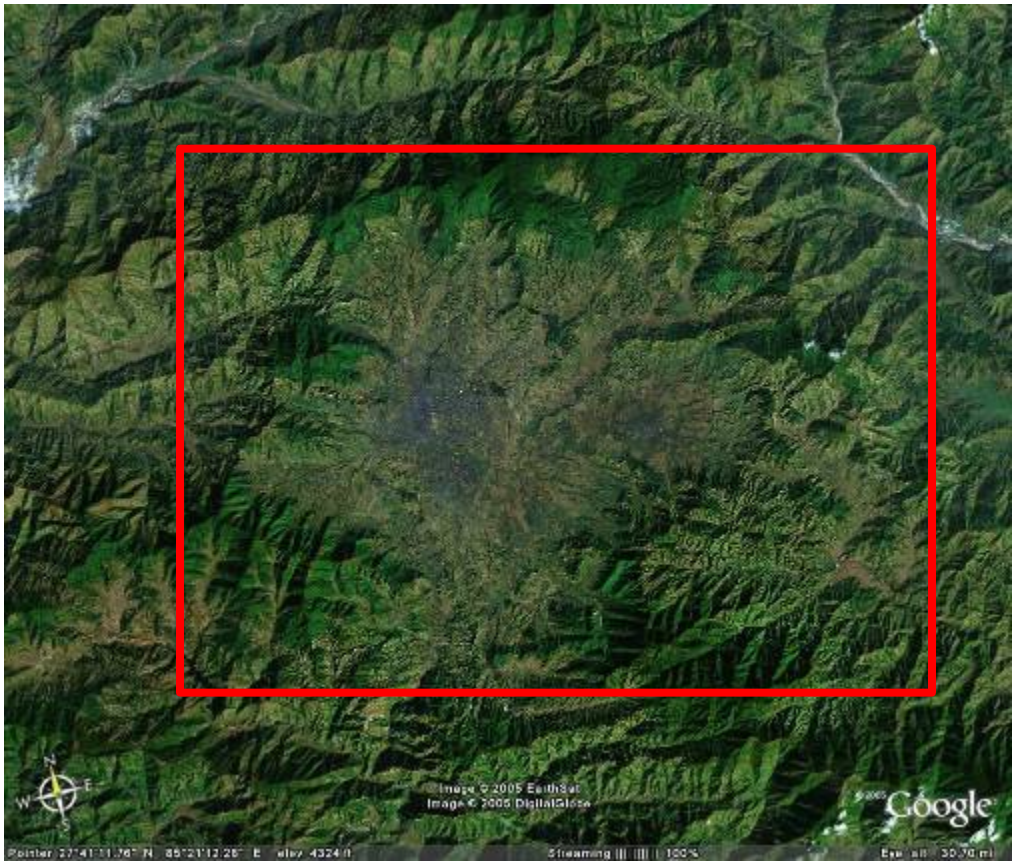

Figure 6.1: The CAMx domain (red square) super-imposed upon a Google Earth ® image of the Kathmandu Valley. Note that the inner domain of MM5 extends beyond the edges.

6.3 The Emissions Inventory

Several past studies have computed Kathamandu Valley-wide annual or average daily emissions of air pollutants [*Devkota*, 1992; *Dhakal*, 2003; *Malla*, 1993; *Shrestha and*

Malla, 1996]. However, only one past study attempted to quantify the spatial distribution of emissions with the valley [*Kitada and Regmi*, 2003].

That last study published a NO_2 and SO_2 emissions inventory for the Kathmandu Valley and surrounding regions on a 1 km grid resolution for the year 2000-2001. In the process of putting together those emissions inventories, the authors had also compiled an unpublished CO emissions inventory [*Regmi*, 2004, personal communication]. This was made available to us, and became the starting point for the work reported here. It had gridded annual average daily emissions of CO on a 38 by 30 km grid, divided among three sectors: traffic, household, and industrial. Traffic emission data was based on traffic distributions calculated in 1992 [*JICA*, 1992][29] and 1997, but adjusted for the vehicle numbers and fleet composition of 2000, and using emissions factors from the literature. The domestic fuel consumption data was calculated using earlier per capital urban and rural consumption data [*Shrestha and Malla*, 1996], with 2001 population census data for individual city wards and villages within the Kathmandu Valley, assigned to individual grid cells on the basis of built-up area distribution. Industrial emissions were based upon fuel consumption and source distribution surveys carried out by the researchers [*Kitada and Regmi*, 2003]. CO emissions factors were used from earlier studies in Nepal [*Bradley et al.*, 1999; *Jha*, 2001; *Shrestha and Malla*, 1996; *Zhang et al.*, 1995]. The emissions inventory was calculated using the following summations:

Transport emissions = (sum over vehicle types) of

(% vehicle type) x (grid vehicle kilometers) x (emission factor per km of travel).

Household emissions for each grid cell = (sum over fuel types) of

(fuel per capita) x (grid population) x (emission factor)

Industrial emission = (sum over fuel types) of

(grid fuel consumption) x (emission factor).

[29] Although traffic volume has grown in the valley, no major new roads have been built between 1992 and the present.

Taking Regmi's emissions database as a starting point appeared to save several months of labor. Before it could be used, it had to be checked, and updated. The spatial distribution of emissions were checked against the distribution of roads, industries, and settlements on Kathmandu Valley maps. With the exception of some unexplained industrial emissions in a rural area south of the Kathmandu Valley, which were removed from the data, the spatial distributions of sources matched with expectations based on the maps. As a second check, Regmi's estimates were summed up over all grid cells, yielding annual emissions of 10,560.5 tons from vehicles, 7652 tons from industries, and 12,150 tons from households.

These total industrial and domestic emissions were found to be within the range calculated by other researchers. For example, [*Malla*, 1993; *Shrestha and Malla*, 1996] calculated 1992-93 industrial and domestic emissions of 5220 and 9867 tons of CO respectively. However, Regmi's vehicular CO emissions were smaller than that of other researchers. A detailed field study [*Dhakal*, 2003], which surveyed vehicle distances traveled and fuel consumption rates for different vehicle types in 2000, found annual vehicular CO emissions to be a factor of two higher, at 21,125 tons/year. This was closer to earlier estimates [*Shrestha and Malla*, 1996]. During the 4 years, from 2001 to 2005, traffic in the Kathmandu Valley grew rapidly, as reflected in the estimated vehicle fleet growth of 63.7% from 165,264 to 270,631 vehicles registered in Bagmati Zone, most of which are within the Kathmandu Valley. It was thus decided to multiply the corrected numbers from Regmi by an additional factor of 1.637, so that his original vehicular emissions (in each grid cell) needed to be multiplied by a factor of 2 x 1.637 = **3.274.** Similarly, the population of the Kathmandu Valley grew rapidly from 2001 to 2005, partly due to the influx of internally displaced people fleeing the government-maoist civil war. The population is estimated to have grown from 1.64 million to 2 million during that period, i.e. a 21.9% growth. It was thus decided that the gridded domestic emissions be multiplied by a factor of **1.219**. Industries have not substantially changed in the time period, so it was decided to keep Regmi's industrial emissions estimates constant. Thus the final numbers for the annual emissions used in the modeling work were: vehicles 33,992 tons, industries 7652 tons, households, 14811 tons.

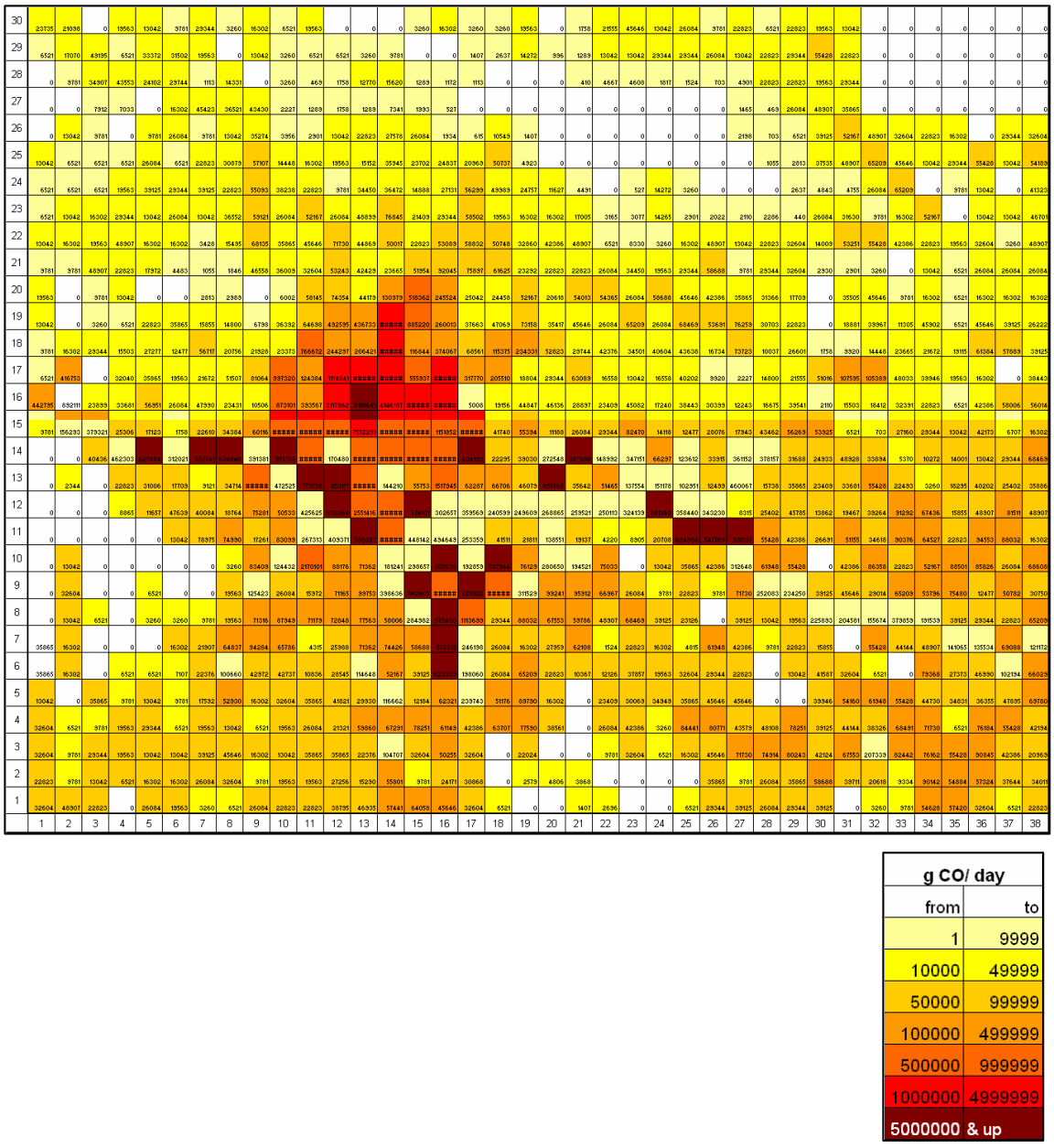

Figure 6.2: Map of CO emissions in gram CO per grid cell per day, updated from [*Regmi et al.*, 2003]. The high emissions in the Kathmandu city center, as well as along highways to the west and to the southeast are clearly visible.

These "updated" emissions in each grid cell were taken as the starting point for our simulations. Since this study focuses upon the diurnal cycle, and since CAMx needed hourly emissions estimates, we had to compose a function for each sector that described the fraction of the daily emission taking place during each hour. Figure 6.3 shows the

best-guess diurnal cycle of emissions for the Kathmandu Valley based upon local knowledge of meal times, traffic counts at several locations, and extensive driving around the Kathmandu Valley at all hours of the day. Traffic shows a morning peak just before offices start, and a slightly more diffuse evening peak. Most households cook a warm meal in the morning and in the evening; industries are divided among ones that run 24 hours and ones that run just during office hours.

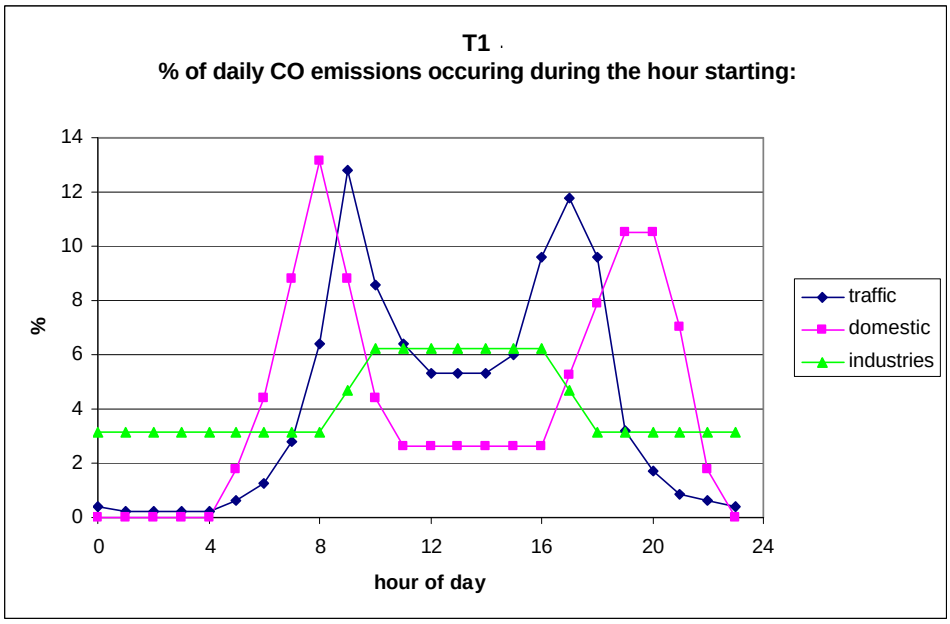

Figure 6.3: Best guess time functions of emissions for the Kathmandu Valley ("T1")

There are several sources of potential error in the emissions database as used. First, the spatial distributions were based upon old distributions of traffic and homes. Over the years the city has grown outwards, greatly increasing both traffic and household emissions in areas outside of the Ring Road. Second, the same time function was applied across all grid cells. Not only is there considerable uncertainty in this less-than-scientific time function, but it represents a rough valley-wide average that does not describe spatial variations. Brick factories on the southeast side of the valley run 24 hours a day; industries on the west end of Kathmandu mostly shut down for the night. The roads on the outskirts of the valley have virtually no traffic after 8 pm, while there is still considerable traffic in entertainment parts of Kathmandu until past 11 pm.

6.4 CAMx Simulations of CO at the Hyatt

This section describes "trial-and-error" adjustments to the reference emission in order to make CAMx simulate CO concentrations in the grid cell containing the Hyatt hotel. The simulation was carried out from noon on February 9, 2005 through noon on February 11, 2005. The top plot in Figure 6.4 shows the results using the "T1" emissions described in the previous section. We see that the simulation succeeded in reproducing a twin-peak diurnal cycle, and it managed to correctly capture the night-time decline in CO. However, it greatly over-estimated the morning peaks, showing CO values as high as 9 ppm. It also expected the evening peaks to take place earlier than found in the measurements. Assuming that the MM5 meteorology inputs were correct, there are three possible sources of error in the CAMx simulation: the total emissions might have been wrong; the time function might have been wrong; or the spatial distribution might have been wrong.

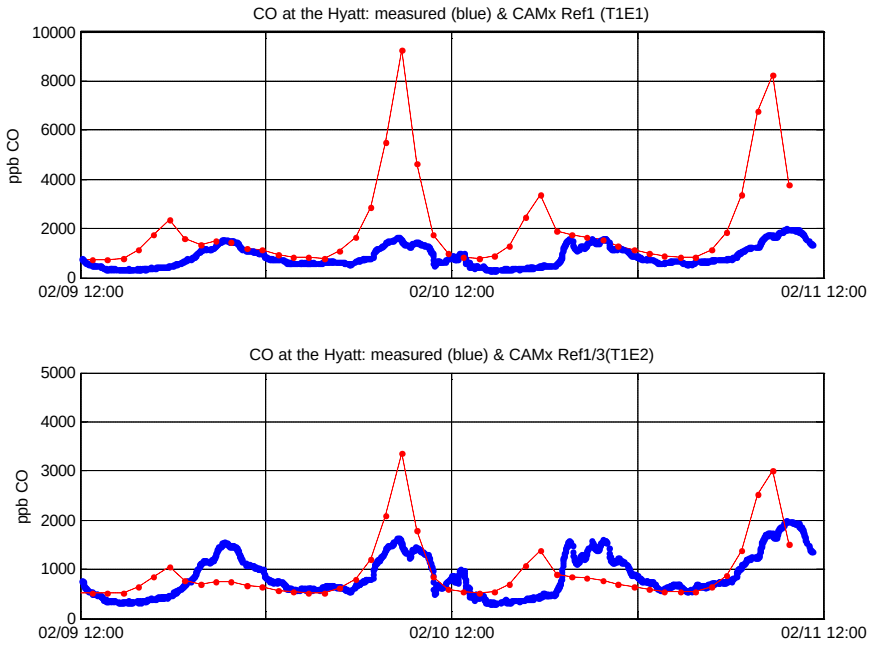

Figure 6.4: CO measured at the Hyatt (blue), and simulated with CAMx (red), using T1E1 scenario and T1E2 scenario (1/3 of normal emissions).

To investigate the first possibility, we divided the total emissions each hour by a factor of 3. It is worth noting that our reference E1 emissions had multiplied Regmi's traffic emissions by a factor of 3.274 and his domestic emissions by 1.219. The results with the same time function T1, but with only 1/3 of the total emissions are shown in the bottom plot (Emissions scenario E2). We see that the morning peaks were still over estimated, while the evening peaks, although more reasonably sized, still took place too early. Night-time values of CO were now slightly under-estimated.

A plausible alternative hypothesis for the over-estimate of the morning peak puts the cause not on problems with the emissions, but on the possibility that the model might be under-estimating the turbulent transport of CO away from the surface during the stable morning hours, creating a larger-than-real vertical gradient in CO, with insufficient flux of CO away from the surface. This was tested in the next run, which used a time function, T2, that keeps emissions constant in time: each sector emitted 1/24 of its daily emissions during each hour. This scenario obviously never took place in Kathmandu, but its results help improve our understanding. We see in Figure 6.5 that CO concentrations stayed high throughout the night (close to 6 ppm), and only dropped from late morning through early evening. We see that the model captured an afternoon low in pollution even without an afternoon low in traffic and cooking emissions, indicating the strong role played by ventilation.

With constant emissions and suppressed ventilation, we would have expected CO concentrations to increase throughout the night. If the hypothesis of under-estimated vertical mixing in the early morning were true, we would have expected an especially large increase in CO concentrations towards the morning. Instead we found the opposite. Initially in the evenings, CO concentrations did increase rapidly, but then they flattened out for the rest of the night starting around 10 pm – the time when we saw the evening peak beginning to disappear in the field observations. Thus it appears that from 10 pm onwards the model did *not* over-estimate the vertical flux of CO; the surface concentrations barely kept up with the constant emissions.

We just saw that with constant CO emissions at night, there is no nocturnal low in CO. We can say with confidence that the nocturnal CO low discussed in earlier chapters owes its existence to the slowing down of emissions at night. However, the fact that in the constant emissions scenario T2E1, CO did not accumulate fast after 10 pm does indicate that from around 10 pm to dawn, at least one other process is responsible for preventing CO from accumulating within the grid cell containing the Hyatt measurement station.

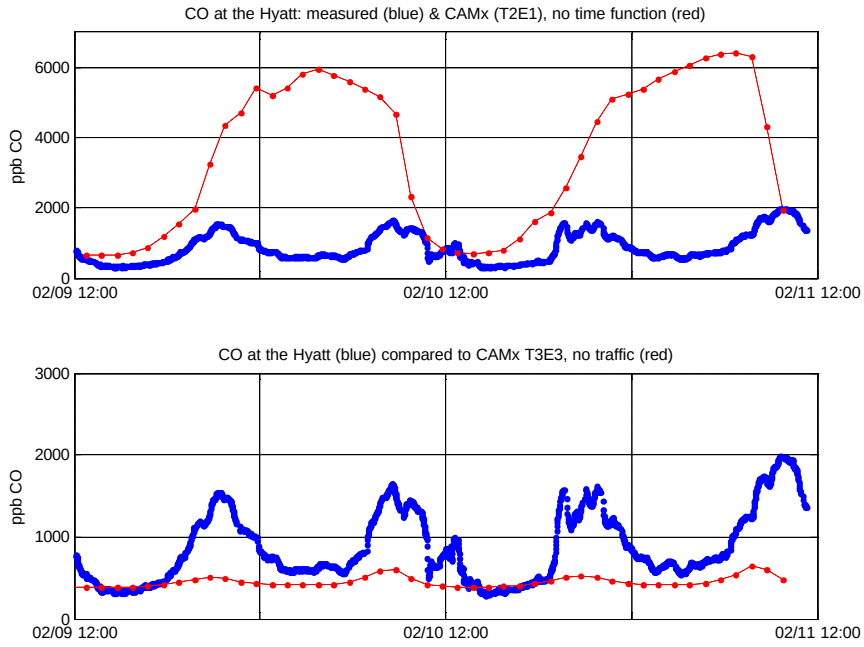

Figure 6.5: Comparison of CO from CAMx runs (red) and measurements at the Hyatt using constant emissions(T2E1)" and scenario with no traffic emissions (T3E3).

The bottom panel of Figure 6.5 shows a run using another idealized emissions scenario "T3E3". This uses the same total emissions and time functions for households and industries as in Scenario T1E1, but it assumes zero traffic emissions. Here we clearly see that, with the loss of the largest source of CO, much of the diurnal cycle disappeared, and the simulation underestimated CO concentrations at most times. This highlights the importance of the magnitude and timing of traffic emissions.

Could it be that the time functions were wrong and that they concentrated the morning emissions into too narrow a time frame, while starting the evening emissions too early?

We examine here the consequences of changing time functions while maintaining the emissions at 1/3 of the database estimate. First, we consider time-function "T4", as illustrated in Figure 6.5. This makes the morning peaks in cooking and traffic less sharp, while allowing the evening peak traffic to persist longer. It thus adjusts the initial best-guess time function (T1E1), reducing the morning peak, and allow the evening peak to last longer, while staying within the bounds of realistic traffic counts and experiences.

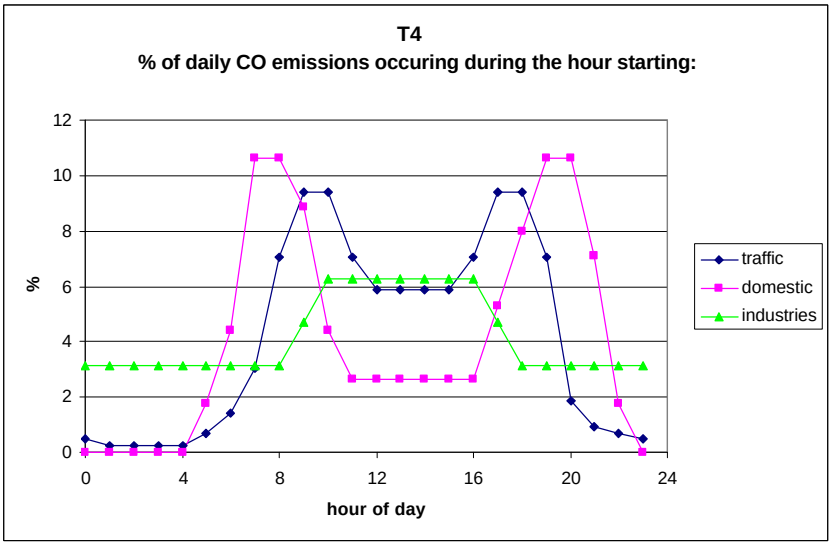

Figure 6.6: Time function "T4": flatter morning peak and more persistent evening traffic.

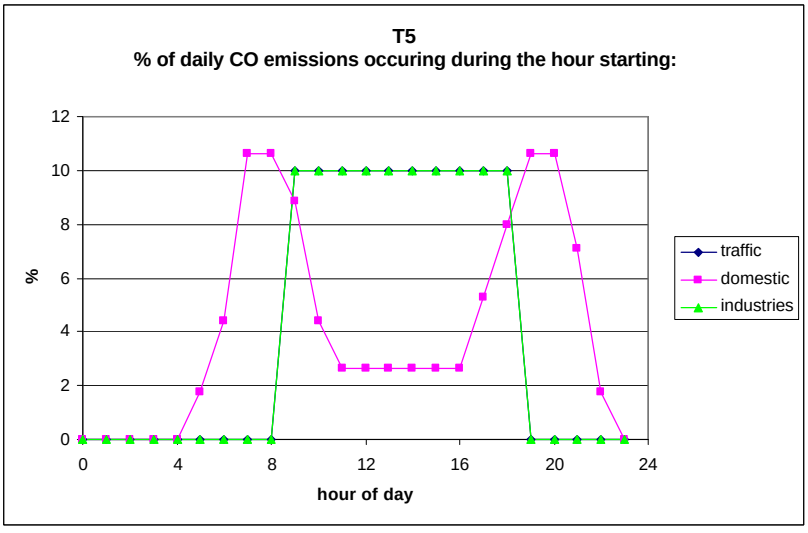

Figure 6.7: Time function T5: Traffic and industries only between 9 am and 6 pm.

Emission time function T5 (Figure 6.7) considers the radical scenario of traffic and industries being allowed only between 9 am and 7 pm. The results of both scenarios are shown in Figure 6.8. We see that time function T4 managed to reduce the CO over-estimate in the morning, but it did not move the evening peak sufficiently late. Time function T5, meanwhile, managed to reduce pollution to a minimum throughout the night, but still morning and evening peaks and an afternoon low, despite high day-time emissions. Presumably the morning and evening peaks occured because the emissions start off before the valley is well ventilated, and persist beyond the time when it is well ventilated.

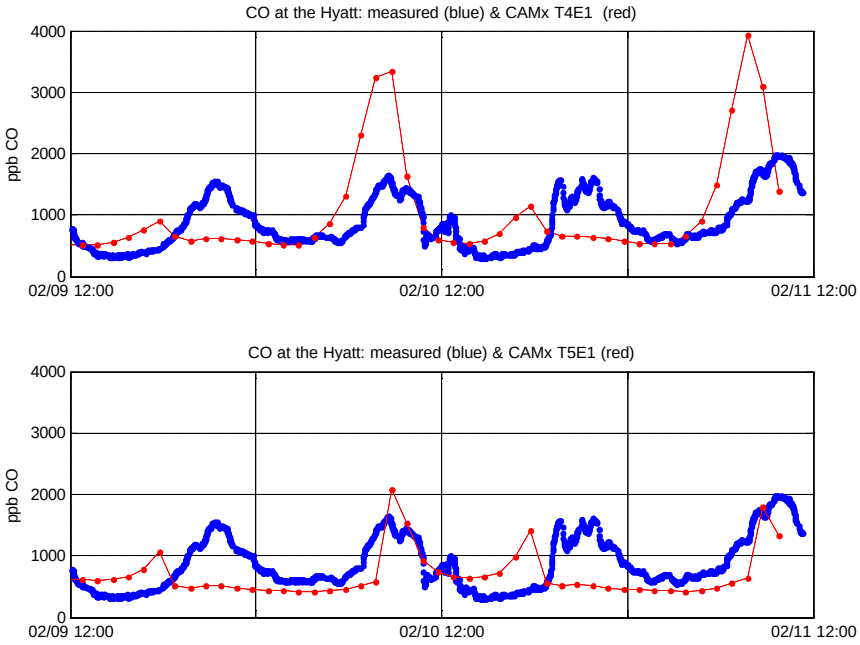

Figure 6.8: CO at the Hyatt as measured (blue) and simulated (red) using the T4 emissions scenario (top) and the T5 scenario (bottom), while .

Time function T7 (Figure 6.9) was composed by putting together the knowledge gained up to this point in order to recreate observed CO at the Hyatt as closely as possible. This was achieved by adjusting household emissions, further flattening the morning traffic peak, while moving the evening traffic peak to a much later time than observed traffic patterns in the valley would suggest. The resulting CO concentrations at the Hyatt station are shown in the top panel of Figure 6.10. With these adjustments to the emission time

function it was possible to correct the timing of the evening peak, as well as correctly estimate the night-time and afternoon values of CO. However the peak values of CO were still over-estimated.

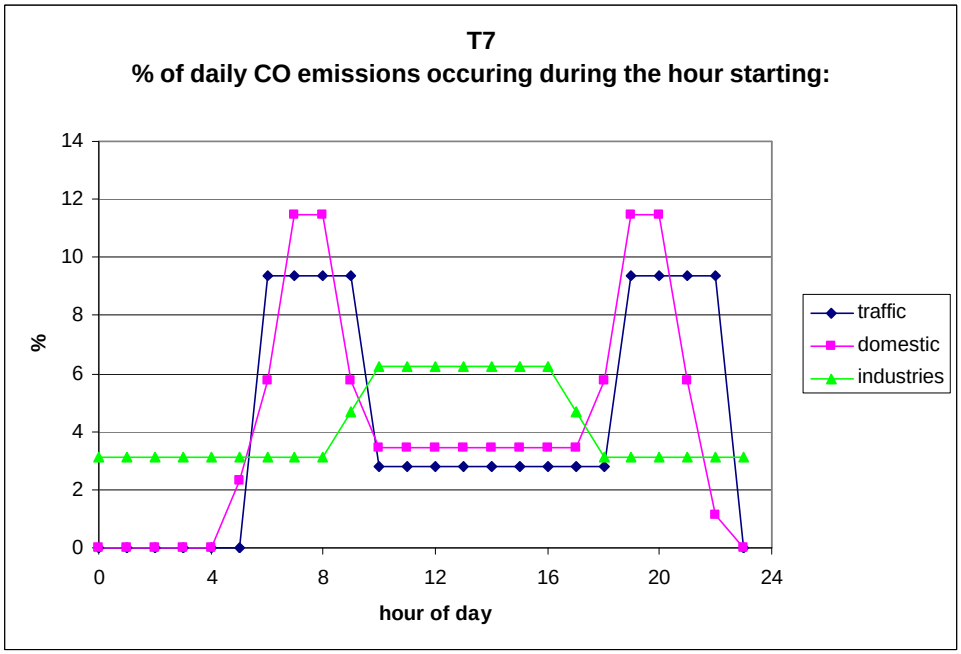

Figure 6.9: Emission time function T7.

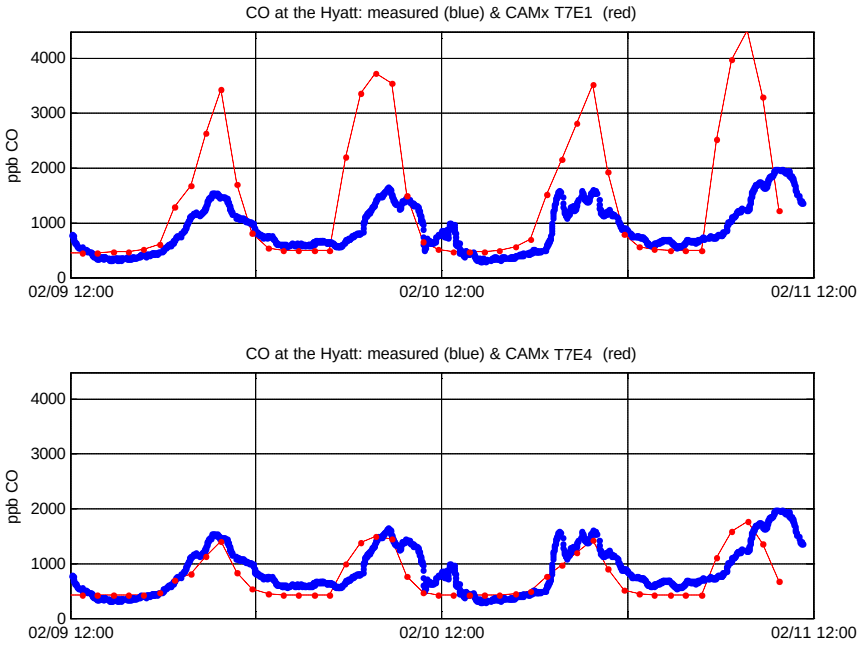

Figure 6.10: Simulation using time function T7 and 1/3 of reference emissions (top) and 1/6 (bottom).

The bottom panel divided the total emissions by another factor of 2: i.e. using only 1/6th of the reference total emissions. We see that this simulation came close to matching the observations. However, the extent of adjustments needed in both the valley-average time function and in the total emissions don't appear plausible. In fact, looking at CAMx results from bag sampling locations, it appears that the model under-estimated CO at those locations (Figure 6.11), especially at times of peak values.

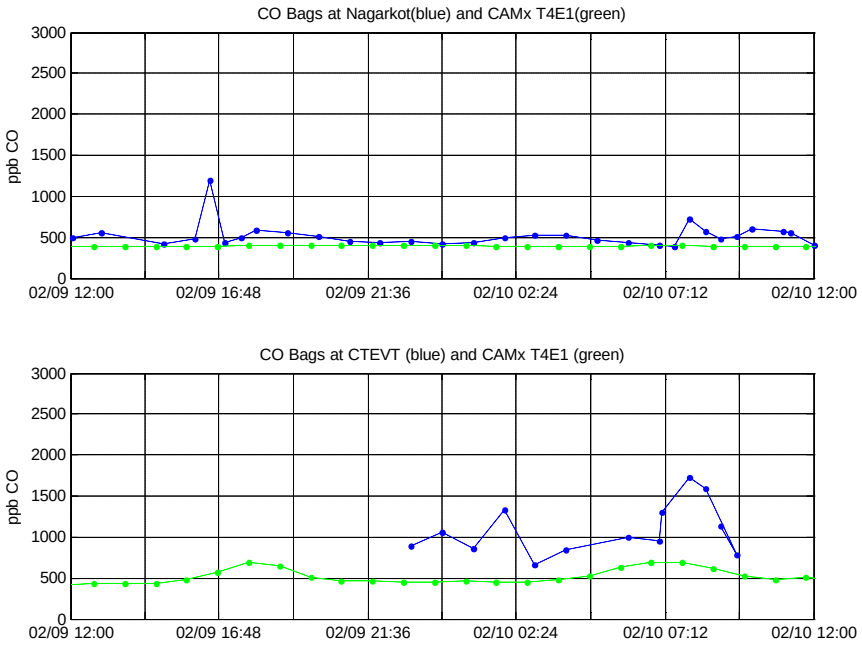

Figure 6.11: CAMx simulations (green) and bag-sampled observations (blue) at Nagarkot (top) and CTEVT (bottom) for scenari T1E4.

Thus we have several clues about the origin of the differences between observation and model results in Figure 6.4. As already mentioned, it is likely that the spatial distributions of emissions used in the simulation were outdated. For example, they would cause model air parcels arriving at the Hyatt in the evening from outside of the city to pick up less pollution than in reality. Another possible source of error might be the assumption of a spatially invariant emission time function. For example, the Chabahil-Bouddha road passing by the Hyatt had heavier traffic until later in the evening than the Kathmandu to Bhaktapur road. The measurements indicate larger pollution levels until

later in the evening than the model first-guess emissions scenario was capable of capturing.

Other sources of error are possible as well. Inadequate vertical fluxes were dismissed earlier, and no problems were found in mass conservation in the model, but there might still be some yet undiscovered problems in CAMx's handling of the tracer. Errors might be introduced by the low frequency of ingesting MM5 meteorology into CAMx. CAMx was used with the default setting, reading hourly meteorology files. Given the large diurnal variation in wind speeds and directions, as well as the large variations in emissions between adjacent grid cells, it might have been necessary to increase the frequency at which CAMx received updated meteorology.

From the discussion it is not entirely clear what the ranking among possible sources of error might be, but given the over-estimates at the Hyatt and the under-estimates at the bag sampling locations, it appears that the spatial distribution of the emissions might be a large problem needing further field research to address. A related source of error, as already mentioned, might be the assumption of a single time function for all grid cells.

6.5 Chapter Conclusion

This chapter described the set-up of CAMx as a tracer transport model, described the emissions inventory used, and showed some CAMx modeling results, adjusting emissions to reproduce observations, and discussing possible sources of error in the simulations. It appears that the biggest weakness in the modeling system was the uncertainties associated with the original emissions inventory, especially its spatial distribution.

CHAPTER 7: DISSERTATION CONCLUSION

7.1 Summary of Major Findings

The results from the field measurements and modeling described in this dissertation together provide a surprisingly complete picture of the diurnal cycle of carbon monoxide in the Kathmandu Valley during the dry season. Almost every day, CO in the valley bottom was found to exhibit a morning peak, a sharp drop in the late morning, low concentrations throughout the afternoon, and a sharp rise to a second peak in the evening, followed by a gradual decline overnight. PM_{10} was found to be well correlated with CO, while ozone concentrations remained close to zero at night, growing in the morning, and peeking around noon.

This diurnal cycle was explained as follows. During the morning, pollutants were emitted into a cold stable air mass sitting in the valley bottom. A mixed layer grew first along the edges (driven by up-slope flows) and gradually over the center, finally reaching heights that were above the valley rim mountain peaks. A fraction of the pollutants were able to escape up the slopes in the morning, but the valley was well ventilated only after the inversion was completely gone, and strong westerly winds, which penetrated down to the surface, transported pollutants out through the eastern passes. The formation of the cold air pool at dusk suppressed the vertical motion, cut off the westerly winds from the surface, and allowed a second peak of CO to occur near the ground. Once the city residents fell asleep and emissions ceased, the near-surface CO levels were able to gradually decrease as air parcels from the surface were transported upwards within the cold pool to be re-circulated after entrainment into the morning's mixed layer. A small fraction of the pollutants were able to escape down the Bagmati outlet valley and over the western passes, forced by pressure gradients generated by drainage winds in neighboring valleys. This contributed to high pollution levels seen at Bhimdhunga Pass at night. Meanwhile, on top of the valley rim mountains, CO levels dropped to regional background levels at night, but grew again when upslope winds arrived in the morning.

7.2 Contributions to Science and to the Public in Kathmandu

Chapter 1 mentioned geographical comparisons to the basin of Mexico City, a bowl-shaped urban that has been studied in much greater depth. Looking at the literature from Mexico City, we see that Kathmandu and Mexico City both have strong temperature inversions in winter and complex circulations affecting the ventilation of air pollutants [*Fast and Zhong*, 1998]. The mountain passes connecting to nearby valleys play crucial roles in both places, with thermally driven gap winds bringing highest wind speeds in the afternoon [*Doran and Zhong*, 2000]. Mexico City often has a much higher mixed layer (2-3 km above ground) [*Bossert*, 1997], while Kathmandu's mixed layer growth is interrupted in the early afternoon by the arrival of cooler air from neighboring valleys. Both have high particulate levels during much of the year [*Villasenor et al.*, 2003]. Unlike Mexico City [*Molina and Molina*, 2002], the Kathmandu Valley usually does not have health-threatening ozone levels, and it has 3 months a year of "clean" air during the summer monsoon (not studied in this project). The research findings highlight the fact that surrounding mountains introduce complexities in air pollution meteorology that need to be studied locally, and that cannot be understood solely based on what was learned elsewhere.

Section 7.1 summarized what has been learned in this study of air pollution in the Kathmandu Valley. The dissertation also makes several additional contributions to science. Research for it involved collecting a high temporal resolution dataset of CO, PM_{10}, ozone, wind and vertical temperature structure for an interesting place with no similar past data. This dataset will be available to future researchers interested in studying air pollution and meteorology in the Kathmandu Valley. Its collection has also shown that it is possible to carry out field measurements during political instability and a military coup, and that, given the right approach, it is possible in Kathmandu to attach sensors in highly unusual places with restricted access.

The field research has demonstrated that reasonable understanding of air pollution in a mountain basin can be gained with only a handful of sensors. The necessary components

for such studies include the continuous measurement of pollutants in at least one place, the ability to collect air samples elsewhere, the measurement of wind speed and direction in as many places as possible, as well as the measurement of temperature inversions and the mixed layer using temperature loggers and vertical acoustic sounders. In addition, unconventional research methods like time lapse photography and watching smoke stacks can provide valuable insights into processes for which no data exists.

Meanwhile, the dataset from Kathmandu has demonstrated the strong influence of thermally driven circulations in the Himalaya during the dry season, which were responsible for the day-to-day similarity observed in both meteorology and air pollution. Such day-to-day similarity can be exploited by future researchers to study a larger area by moving sensors around.

The meso-scale meteorological modeling has answered questions about the processes responsible for the observed diurnal pattern in air pollution in Kathmandu. It has also demonstrated MM5's ability to capture remarkably well the meteorology over a very complex landscape with just surface topographic and land use data and global winds at the edges. The eulerian modeling exercises have highlighted the sensitivity of air pollution simulation to the accuracy of emission databases.

The dissertation will also be able to make several contributions to the interested general public and to policy makers in Kathmandu. Section 7.4 will describe how an improved emissions database would allow reliable eulerian modeling of the impact of emissions scenarios on air quality. It would be good to know what impact changing the timing of rush hour, or of the operating hours of factories, would have on air quality at different places around the valley. However, even without this additional work, several statements can be made now, with some confidence.

First, because ventilation of pollutants from much of the valley is limited to the late-morning and afternoon hours, any polluting activity whose timing can be chosen should

be scheduled during those times. This includes garbage incineration, and non-commuting automobile trips. Second, early morning walks are probably not as healthy as most residents assume; outdoor exercise in the afternoon would expose people to less air pollution. Third, the Kathmandu Valley's stagnant nocturnal air mass makes the valley very vulnerable to much more serious future air pollution problems if its urban population and economy continue to grow without strong air quality management policies. Infrastructure projects to accommodate and promote urban growth, such as pumping drinking water from Melamchi Valley and building a second ring road around the city would worsen the Kathmandu Valley's air quality by attracting economic activities that would not otherwise have come to the valley, had the money been invested in infrastructure elsewhere in Nepal. Fourth, if polluting industries absolutely have to be sited within the Kathmandu Valley, then the best location would be where pollutants have a chance to depart even during the night, specifically south of Chobhar, at the head of the Bagmati River outflow valley.

7.3 Limitations of the Dissertation

Three sets of shortcomings have limited the scope of the research presented in this dissertation. These were lack of experience, resource constraints in the field, and limited time for modeling.

Setting up and running field experiments in Nepal provided many diverse learning opportunities. Based on the experience gained, it should be possible to set up future such experiments more efficiently, with a clearer sense of required steps, better protection against vulnerabilities, and a more reliable data flow. An indicator of new learning is also the thought that one should have done certain things differently. Two issues stand out: first, greater generosity to oneself in terms of time allowed would have made it possible to set things up more carefully at the outset, with less need for repair and repetition. That was the case with both field measurements and modeling. Second, a re-allocation of funds from shipping to instrument purchasing would have provided a better

data set. Choosing cheaper, slower shipping options, and shipping fewer non-essential items back to MIT would have freed up enough funds to purchase several additional sensors. In particular, a second weather station for moving around the valley, as well as recording anemometers to install on the TV tower would have provided a wealth of useful data about the valley's air pollution meteorology.

Resource constraints (rather than misallocations) contributed to several other limitations in the scope of the work. The limited availability of enthusiastic students to help with bag sampling limited the number of sites that could be sampled each time, as well as the frequency of bag sampling. Similarly, limits in time and manpower prevented a complete bottom-up rebuilding and field verification of the emissions inventory, thereby limiting the scope of the eulerian modeling possible in this dissertation. Uncertainties in the database have restricted the ability to investigate policy scenarios within this dissertation. Limits in time and manpower also did not allow the measurement of hydrocarbons and NOx, which would have provided a means to verify MM5/CAMx model runs with full photochemistry.

Measurements of CO away from the laboratory at the Hyatt were limited to bag sampling due to the difficulty of transporting the instrument and its calibration gases; a second CO instrument set would have provided a better understanding of spatial patterns, but attempts to get Tribhuvan University's stored CO instrument running did not succeed. Meanwhile, it turned out that political instability brought to Kathmandu many more transportation strikes, riots, tire burnings and curfews during the dry season 2005-2006. Had the instruments been kept running in Kathmandu a year longer, they would have collected a fascinating data set containing many more "experiments" of selectively turning off (or on) individual pollution sources.

The MM5 modeling work was carried out within the span of a few months, under significant time pressure. Only a fraction of the many possibly interesting model runs were completed and analyzed. In the future, many additional questions can be addressed with the combination of the collected field data and modeling.

7.4 Future Research

As described, this dissertation has significantly improved the scientific understanding of the diurnal cycle of air pollution in the Kathmandu Valley during the dry season, describing the mechanism of the valley's mixed layer growth, discovering the pathways of pollutant ventilation from the valley, and clarifying the nocturnal lows in pollution. It sets the stage for several directions of future investigation about air pollution in the Kathmandu Valley.

One question eager to be addressed with additional modeling is what limits the cold air pool formation at night? It is very common for enclosed basins to experience accumulating cold pools during winter nights [*Whiteman*, 2000]. What is not clear is how deep the Kathmandu Valley's cold pool becomes over night, and whether the accumulation of cold air is limited solely by the length of the night (interrupted by surface heating after sunrise), or by other factors as well. The temperature and the depth of the cold air pool affect how rapidly the mixed layer can grow in the morning, and thus the vertical transport of pollutants out of the valley.

Night time temperatures on Hattiban ridge and on Nagarkot peak were significantly warmer than temperatures in the valley bottom[30], indicating that the valley's cold pool was confined to lower elevations. But what limits the overnight accumulation of cold air in the valley? Is it limited by the rate and duration of surface cooling due to fog formation? Does Kathmandu City's nocturnal urban heat island erode the cold pool while it is forming? Or is the cold pool limited by the rate of outflow of cold air down the Bagmati Valley, and out the western passes? A modeling exercise to address this question could take two complementary approaches. It could build a surface energy budget for the slopes and the basin bottom, calibrated with actual temperature measurements. This can be used to study the rates of cold air formation. MM5 could then be used to study the fluxes across passes and the river outlet. Using a different approach,

[30] Found from temperature records collected while filling bags with air samples.

sensitivity studies could be used to investigate the effects of artificially changing the pass heights and geometry on cold pool depth.

Future research should also focus on pollution transport modeling using an improved emissions inventory. Even without traveling to Kathmandu, the spatial distribution of domestic emissions sources could be updated with new air photos outlining the extent of sprawling new areas of urbanization. In Kathmandu, an updated household energy survey could bring the fractional distribution of cooking fuels up to date, checked against economic figures of total fuel imports. Day-long traffic counts on different roads could provide location-specific time functions of traffic. Locations of shifting brick factories could be updated with site visits and a GPS. Industrial emission time functions could be adjusted with surveys of individual factories' operating hours.

The new spatial distributions and time functions of emissions can easily be inserted into the MM5-CAMx modeling framework that is already set up. It can then be used for further study of the sensitivity of ambient air quality to changes in the quantity and timing of emissions. Such knowledge is useful for the design of policies aimed at reducing people's exposure to unhealthy levels of air pollutants: it is worth noting that human health is affected more by peak pollution values than by long-term averages. An initial analysis of pollution exposure maps [*Regmi and Kitada*, 2003] found that 8% of the valley's population lives in areas with very unhealthy air pollution. Model runs with altered total emissions or emission time functions can be used to explore sub-questions, such as: what happens to morning and evening peak values of CO when the daily total CO emissions are increased or decreased, without changing the proportions emitted at each time of day? What happens to the afternoon and night-time low values of CO when the total amount of CO emissions in the valley is increased or decreased, without changing the proportions emitted at each time of day? Does shifting the rush hour earlier or later affect peak values? One could sort between the hypotheses by comparing a reference run with runs containing altered time-functions of emissions, moving just the peak traffic portions of the time functions earlier and later. What is the effect of spreading out or compressing rush hours? The Kathmandu Valley's particular patterns of

suppressed ventilation during much of the day, and vigorous ventilation during the afternoons provides policy makers with interesting opportunities to improve air quality by merely shifting the timing of emissions without having to reduce the totals. Since the air quality is sensitive to small changes in the timing of emissions, an accurate modeling framework is necessary for the analysis of policy scenarios.

The analysis in this dissertation was limited to clear-weather days in the dry season. There is much more to study on other days of the year, including an alternative pathway of pollution ventilation from the valley. This is a variation of the second and the fourth hypothesis in Chapter 4: when vertical mixing over the valley or up-slope flows converging over peaks cool air down to the dew point, then clouds form. If air parcels are lifted beyond the level of free convection, cumulus clouds form, which are able to carry pollutants even higher up due to the vertical motion generated by latent heat release. Transport of pollutants into the upper troposphere by convective clouds is a well known pathway for the export of boundary layer air, and a well known way to extend the atmospheric lifetime of pollutants so that they can be transported long distances [*Cotton et al.*, 1995; *Donnell et al.*, 2001; *Wang and Prinn*, 1998].

Indeed, cumulus clouds were often seen forming over Kathmandu Valley rim peaks in the afternoons of Fall and Spring (Figure 7.1), and at times over the valley center as well (Figure 7.2). Visiting Kathmandu, meteorologist Edward Hindman of City College, New York described the clouds over the valley center as an opportunity for soaring with gliders planes [*Hindman*, 1999], and later hypothesized that they might play an important role in venting pollutants from the valley [*Hindman and Upadhyay*, 2002], calling them the “Kathmandu Chimney”. This cloud venting pathway can be studied using MM5.

Additional field measurements in the valley could focus upon a better understanding of the spatial distribution of pollutants: studying the fluxes of air across valley rim passes using a sodar; using weather stations to study katabatic winds on the valley rim slopes and in the Bagmati River valley; as well as carrying out chemical measurements to study the full photochemistry. There is a need for more field measurements of exported

pollution downwind of the Kathmandu Valley, as well as better understanding of the regional pollution upwind of the valley. It is hoped that this dissertation has planted the seeds for many more research projects about air pollution in an interesting valley where air quality plays a major role in people's welfare.

Figure 7.1: Cumulus cloud over Shivapuri Peak in October, observed from the eastern end of the Kathmandu Valley.

Figure 7.2: Cumulus clouds observed over the south-central Kathmandu Valley and over Phulchoki Peak, as seen from Hattiban.

REFERENCES

Allwine, K.J., Atmospheric Dispersion and Tracer Ventilation in a Deep Mountain Valley, *J. Applied Meteorol.*, *32*, 1017 - 1032, 1993.

Altuzar, V., S.A. Tomás, O. Zelaya-Angel, F. Sánchez-Sinencio, and J.L. Arriaga, Atmospheric ethene concentrations in Mexico City: Indications of strong diurnal and seasonal dependences, *Atmospheric Environment*, *39*, 5219 - 5225, 2005.

Angevine, W.M., H. Klein Baltink, and F.C. Bosveld, Observations of the Morning Transition of the Convective Boundary Layer, *Boundary-Layer Meteorology*, *101*, 209 - 227, 2001.

Argentini, Editorial: Special issue on ISARS 2002. Internatinoal symposium on acoustic remote sensing and associated techniques, *Meteorol. Atmos. Phys.*, *85*, 1-2, 2004.

Arya, S.P., *Air Pollution Meteorology and Dispersion*, Oxford University Press, New York, 1999.

Asimakopoulos, D., D. Deligiorgi, C. Drakopoulos, C. Helmis, K. Kokkori, D. Lalas, D. Sikiotis, and C. Varotsos, An experimental study of nighttime air pollutant transport over complex terrain in Athens, *Atmos. Environ., 26B* (1), 59-71, 1992.

Asimakopoulos, D.N., C.G. Helmis, and J. Michopolous, Evaluation of SODAR methods for determination of the atmospheric boundary layer mixing height, *Meorol. Atmos. Phys.*, *85*, 85 - 92, 2004.

Atimtay, A.T., S. Emri, T. Bagci, and A.U. Demir, Urban CO Exposure and Its Health Effects on Traffic Policement in Ankara, *Environmental Research Section A*, *82* (222-230), 2000.

Atkinson, B.W., *Meso-scale Atmospheric Circulations*, Academic Press, London, 1981.

Badr, O., and S.D. Probert, Sinks and Environmental Impacts for Atmospheric Carbon Monoxide, *Applied Energy*, *50*, 339 - 372, 1995.

Baek, S.-O., Y.-S. Kim, and R. Perry, Indoor air quality in homes, offices, and restaurants in Korean Urban Areas -- Indoor/Outdoor Relationship, *Atmospheric Environment*, *31* (4), 529 - 544, 1997.

Bakwin, P.S., Measurements of carbon dioxide on a very tall tower, *Tellus, 47B*, 535-549, 1995.

Bakwin, P.S., P.P. Tans, D.F. Hurst, and C. Zhao, Measurements of carbon dioxide on very tall towers: results of the NOAA/CMDL program, *Tellus, 50B*, 401- 415, 1998.

Baltensperger, U., H.W. Gäggeler, D.T. Jost, M. Lugauer, M. Schwikowski, P. Seibert, and E. Weigartner, Aerosol climatology at the high-alpine site Jungfraujoch, Switzerland, *J. Geophys. Res.*, *102* (D16), 19707-19715., 1997.

Banta, R., and W.R. Cotton, An Analysis of the Structure of Local Wind Systems in a Broad Mountain Basin, *J. Applied. Meteorol.*, *20* (11), 1255 - 1266, 1981.

Barnes, D.H., S.C. Wofsy, B.P. Fehlau, E.W. Gottlieb, J.W. Elkins, G.S. Dutton, and S.A. Montzka, Urban/industrial pollution for the New York City - Washington, D. C., corridor 1996-1998: 1. Providing independent verification of CO and PCE emissions inventories, *J. Geophys. Res.*, *108* (D6), 4185, doi:10.1029/2001JD001116, 2003.

Barros, A.P., and T.J. Lang, Monitoring the Monsoon in the Himalayas: Observations in Central Nepal, June 2001, *Monthly Weather Review, 131*, 1408 - 1427, 2003.

Baumbach, G., and U. Vogt, Experimental determination of the effect of mountain-valley breeze circulation on air pollution in the vicinity of Freiburg, *Atmos. Environ., 33*, 4019-4027, 1999.

Baumgardner, D., G.B. Raga, G. Kok, J. Ogren, I. Rosas, A. Báez, and T. Novakov, On the evolution of aerosol properties at a mountain site above Mexico City, *J. Geophys. Res., 105*, 22,243-22, 253, 2000.

Berkowitz, C.M., J.C. Doran, W.J. Shaw, S.R. Springston, and C.W. Spicer, Trace-gas mixing in isolated urban boundary layers: Results from the 2001 Phoenix sunrise experiment, *Atmospheric Environment*, in press, 2005.

Berman, S., J.-Y. Ku, and S.T. Rao, Spatial and Temporal Variation in the Mixing Depth over the Northeastern United States during the Summer of 1995, *Journal of Applied Meteorology, 38*, 1661 - 1673, 1999.

Bertschi, I., and D.A. Jaffe, Long-range transport of ozone, carbon monoxide, and aerosols to the NE Pacific troposphere during the summer of 2003: Observations of smoke plumes from Asian boreal fires, *J. Geophys. Res., 110* (D05303), doi:10.1029/2004JD005135, 2005.

Beyrich, F., Mixing height estimation from sodar data -- a critical discussion, *Atmos. Environ., 31* (23), 3941-3953, 1997.

Bhatt, B.C., and K. Nakamura, Characteristics of Monsoon Rainfall around the Himalayas Revealed by TRMM Precipitation Radar, *Monthly Weather Review, 133*, 149 - 165, 2005.

Boddy, J.W.D., R.J. Smalley, P.S. Goodman, J.E. Tate, M.C. Bell, and A.S. Tomlin, The spatial variability in concentrations of a traffic-related pollutant in two street canyons in York, UK -- Part II: The influence of traffic characteristics, *Atmospheric Environment, 39*, 3163 - 3176, 2005.

Bogo, H., D.R. Gómez, S.L. Reich, R.M. Negri, and E. San Román, Traffic pollution in a downtown site of Buenos Aires City, *Atmos. Environ., 35*, 1717 - 1727, 2001a.

Bogo, H., D.R. Gómez, S.L. Reich, R.M. Negri, and E. San Román, Traffic pollution in a downtown site of Buenos Aires City, *Atmospheric Environment, 35*, 1717 - 1727, 2001b.

Bogo, H., R.M. Negri, and E. San Roman, Continuous measurement of gaseous pollutants in Buenos Aires, *Atmos. Environ., 33*, 25-87-2598, 1999.

Bossert, J.E., An investigation of flow regimes affecting the Mexico City region, in *7th Conf. on Mountain Met.*, pp. 371 - 376, 1996.

Bossert, J.E., An Investigation of Flow Regimes Affecting the Mexico City Region, *J. Applied. Meteorol., 36*, 119 - 140, 1997.

Bradley, K.S., D.H. Stedman, and G.A. Bishop, A global inventory of carbon monoxide emissions from motor vehicles, *Chemosphere: Global Change Science, 1* (1), 65-72, 1999.

Brasseur, G.P., J.T. Kiehl, F.-J. Mueller, T. Schneider, C. Granier, X. Tie, and D. Hauglustaine, Past and future changes in global tropospheric ozone: impact on radiative forcing, *Geophys. Res. Let., 25* (20), 3807-3810, 1998.

Brasseur, G.P., R.G. Prinn, and A.A.P. Pszenny, *Atmospheric Chemistry in a Changing World: An Integration and Synthesis of a Decade of Tropospheric Chemistry Research*, Springer Verlag, Berlin, 2003.

Brühl, C., and P.J. Crutzen, Reductions in the anthropogenic emissions of CO and their effect on CH_4, *Chemosphere: Global Change Science*, *1* (1), 249 - 254, 1999.

Castelli, S.T., S. Morelli, D. Anfossi, J. Carvalho, and S. Zauli Sajani, Intercomparison of Two Models, ETA and RAMS with TRACT Field Campaign Data, *Environmental Fluid Mechanics*, *4*, 157 - 196, 2004.

Chandrasekar, A., C.R. Philbrick, R. Clark, B. Doddridge, and P. Georgopoulos, Evaluating the performance of a computationally efficient MM5/CALMET system for developing wind field inputs to air quality models, *Atmospheric Environment*, *37*, 3267 - 3276, 2003.

Chandrasekar, A., C.R. Philbrick, B. Doddridge, R. Clark, and P. Georgopoulos, A Comparative Study of Prognostic MM5 Meteorological Modeling with Aircraft, Wind Profiler, Lidar, Tethered Balloon, and RASS Data over Philadelphia during a 1999 Summer Episode, *Environmental Fluid Mechanics*, *4*, 339 - 365, 2004.

Chang, S., and D.T. Allen, Atmospheric Chlorine Chemistry in Southeast Texas: Impacts on Ozone Formation and Control, *Environ. Sci. Technol.*, *40*, 251 - 262, 2006.

Chen, T.-Y., D.R. Blake, J.P. Lopez, and S. Rowland, Estimation of global vehicular methyl bromide emissions: Extrapolation from a case study in Santiago, Chile, *Geophys. Res. Let.*, *26* (3), 283-286, 1999.

Cheung, V.T.F., and T. Wang, Observational study of ozone pollution at a rural site in the Yangtze Delta of China, *Atmos. Environ.*, *35*, 4947 - 4958, 2001.

Chock, D.P., M.J. Whalen, S.L. Winkler, and P. Sun, Implementing the trajectory-grid transport algorithm in an air quality model, *Atmospheric Environment*, *39*, 4015 - 4023, 2005.

Cotton, W.R., G.D. Alexander, R. Hertenstein, R.L. Walko, R.L. McAnnely, and M. Nicholls, Cloud venting -- a review and some new global annual estimates, *Earth-Science Reviews*, *39*, 169 - 206, 1995.

Coulter, R.L., M.S. Pekour, and M.T. J., Elevanted stratified layers observed with SODAR during VTMX, *Meorol. Atmos. Phys.*, *85*, 115 - 123, 2004.

Cox, R., B.L. Bauer, and T. Smith, A Mesoscale Model Intercomparison, *Bulletin of the American Meteorological Society*, *79* (2), 265 - 283, 1998.

Davidson, C.I., Saw-Feng Lin, and James F. Osborn., Indoor and outdoor air pollution in the Himalayas, *Environ. Sci. Technol.*, *20* (6), 561-566, 1986.

Derwent, R.G., D.B. Ryall, S.G. Jennings, T.G. Spain, and P.G. Simmonds, Black carbon aerosol and carbon monoxide in European regionally polluted air masses at Mace Head, Ireland during 1995-1998., *Atmos. Environ.*, *35*, 6371 - 6378, 2001.

Derwent, R.G., P.G. Simmonds, S. Seuring, and C. Dimmer, Observation and interpretation of the seasonal cycles in the surface concentrations of ozone and carbon monoxide at Mace Head, Ireland, from 1990 to 1994, *Atmos. Environ.*, *32* (2), 145 - 157, 1998.

Desiato, F., S. Finardi, G. Brusasca, and M.G. Morselli, TRANSALP 1989 Experimental Campaign -- I. Simulation of 3D flow with diagnostic wind and field models, *Atmos. Environ.*, *32* (7), 1141- 1156, 1998.

Devkota, S.R., Energy Utiliation and Air Pollution in Kathmandu Valley, Nepal, Master of Science thesis, Asian Institute of Technology, Bangkok, 1992.

Dhakal, S., Implications of transportation policies on energy and environment in Kathmandu Valley, Nepal, *Energy Policy*, *31*, 1493 - 1507, 2003.

Dickerson, R.R., and A.C. Delaney, Modification of a Commercial Gas Filter Correlation CO Detector for Enhanced Sensitivity, *J. Atmos. Oceanic Technol.*, *5*, 424 - 431, 1988.

Dommen, J., A.S.H. Prevot, A.M. Hering, T. Staffelbach, G.L. Kok, and R.D. Schillawski, Photochemical production and aging of an urban air mass, *J. Geophys. Res.*, *104* (D5), 5493-5506, 1999.

Doms, G., and U. Schättler, The Nonhydrostatic Limited-Area Model LM (Lokal-Modell)of DWD. Part I: Scientific Documentation, pp. 172, Deutscher Wetterdienst, Offenburg, 1999.

Donnell, E.A., D.J. Fish, E.M. Dicks, and A.J. Thorpe, Mechanism for pollutant transport between the boundary layer and the free troposphere, *J. Geophys. Res.*, *106* (D8), 7847 - 7856, 2001.

Doran, J.C., S. Abbott, J. Archuleta, X. Bian, J. Chow, R.L. Coulter, S.F.J. de Wekker, S. Edgerton, S. Elliott, A. Fernandez, J.D. Fast, J.M. Hubbe, C. King, D. Langley, J. Leach, J.T. Lee, T.J. Martin, D. Martinez, J.L. Martinez, G. Mercado, V. Mora, M. Mulhearn, J.L. Pena, R. Petty, W. Porch, C. Russell, R. Salas, J.D. Shannon, W.J. Shaw, G. Sosa, L. Tellier, B. Templeman, J.G. Watson, R. White, C.D. Whiteman, and D. Wolfe, The IMADA-AVER Boundary Layer Experiment in the Mexico City Area, *Bull. Am. Meterol Soc.*, *79* (11), 2497-2508, 1998.

Doran, J.C., C.M. Berkowitz, R.L. Coulter, G.E. Shaw, and C.W. Spicer, The 2001 Phoenix Sunrise experiment: vertical mixing and chemistry during the morning transition in Phoenix, *Atmospheric Environment*, *37*, 2365 - 2377, 2003.

Doran, J.C., and S. Zhong, Thermally driven gap winds into the Mexico City Basin, *Journal of Applied Meteorology*, *39*, 1330 - 1340, 2000.

Dudhia, J., Numerical Study of Convection Observed During the Winter Monsoon Experiment Using a Mesoscale Two-Dimensional Model, *Journal of Atmospheric Sciences*, *46* (20), 3077 - 3107, 1989.

Dudhia, J., A Nonhydrostatic version of the Penn-State-NCAR Mesoscale model: Validation Tests and Simulation of an Atlantic Cyclone and Cold Front, *Monthly Weather Review*, *121*, 1493 - 1513, 1993.

Dudhia, J., D. Gill, K. Manning, W. Wang, and C. Bruyere, PSU/NCAR Mesoscale Modeling System: Tutorial Class Notes and User's Gude: MM5 Modeling System Version 3, National Center for Atmospheric Research, Boulder, CO, 2005.

Egger, J., Valley winds and diurnal circulation over plateaus, *Monthly Weather Review*, *115*, 2177 - 2185, 1987.

Egger, J., S. Bajracharya, U. Egger, R. Heinrich, J. Reuder, P. Shakya, H. Wendt, and V. Wirth, Diurnal Winds in the Himalayan Kali Gandaki Valley. Part I: Observations, *Monthly Weather Review*, *128*, 1106-1122, 2000.

Egger, J., S. Bajracharya, R. Heinrich, P. Kolb, S. Laemmlein, M. Mech, J. Reuder, W. Schaeper, P. Shakya, J. Schween, and H. Wendt, Diurnal Winds in the Himalayan Kali Gandaki Valley. Part III: Remotely Piloted Aircraft Soundings, *Monthly Weather Review*, *130*, 2042 - 2058, 2002.

Egger, J., L. Blacutt, F. Ghezzi, R. Heinrich, P. Kolb, S. Laemmlein, M. Leeb, S. Mayer, E. Palenque, J. Reuder, W. Schaeper, J. Schween, R. Torrez, and F. Zaratti, Diurnal Circulation of the Bolivian Altiplano. Part I: Observations, *Monthly Weather Review*, *133*, 911 - 924, 2005.

Emeis, S., C. Muenkel, S. Vogt, W. Mueller, and K. Schaefer, Atmospheric boundary-layer structure from simultaneous SODAR, RASS and ceilometer measurements, *Atmospheric Environment*, *38*, 273 - 286, 2004.

ENVIRON, *User's Guide: CAMx Comprehensive Air Quality Model with Extensions Version 4.20*, Environ International Corporation, Novato, CA, 2005.

Fan, C.-W., and J.J. Zhang, Characterization of emissions from portable household combustion devices: particle size distributions, emission rates and factors, and potential exposures, *Atmospheric Environment*, *35*, 1281 - 1290, 2001.

Fast, J.D., J.C. Doran, S.W. J., R.L. Coulter, and T.J. Martin, The evolution of the boundary layer and its effect on air chemistry in the Phoenix area, *J .Geophys. Res.*, *105* (D18), 22833-22848, 2000.

Fast, J.D., and S. Zhong, Meteorological factors associated with inhomogeneous ozone concentrations within the Mexico City basin, *J. Geophys. Res.*, *103* (D15), 181927-18946, 1998.

Fernandez-Bremauntz, A.A., and M.R. Ashmore, Exposure of Commuters to Carbon Monoxide in Mexico City -- I. Measurement of In-Vehicle Concentrations, *Atmospheric Environment*, *29* (4), 525 - 532, 1995.

Fernando, H.J.S., S.M. Lee, J. Anderson, M. Princevac, E. Pardyjak, and S. Grossman-Clarke, Urban Fluid Mechanics: Air Circulation and Contamination in cities, *Environmental Fluid Mechanics*, *1*, 107 - 164, 2001.

Finlayson-Pitts, B.J., and J.N. Pitts, Jr., *Chemistry of the Upper and Lower Atmosphere*, Academic Press, San Diego, 2000.

Forrer, J., and R. Ruttimann, Variability of trace gases at the high-Alpine site Jungfraujoch caused by meteorological transport processes, *J. Geophys. Res.*, *105*, 12,241-12,251, 2000.

Frioud, M., V. Mitev, R. Matthey, C. Häberli, H. Richner, R. Werner, and U. Vogt, Elevated aerosol stratification above the Rhine Valley under strong anticyclonic conditions, *Atmospheric Environment*, *2003*, 1785 - 1797, 2003.

Furger, M., J. Dommen, W.K. Graber, L. Poggio, A. Prévôt, S. Emeis, G. Grell, T. Trickl, B. Gomiscek, B. Neininger, and G. Wotawa, The VOTALP Mesolcina Valley Campaign 1996 -- concept, background and and some highlights, *Atmos. Environ.*, *2000*, 1395 - 1412, 2000.

Gao, J., T. Wang, A. Ding, and C. Liu, Observational study of ozone and carbon monoxide at the summit of mount Tai (1534m a.s.l.) in central-eastern China, *Atmospheric Environment*, *39*, 4779-4791, 2005.

Garcia, J.A., M.L. Cancillo, and J.L. Cano, A Case Study of the Morning Evolution of the Covective Boundary Layer Depth, *Journal of Applied Meteorology*, *41*, 1053 - 1059, 2002.

Gehrman, E., Ana Barros chases the monsoon, *Harvard University Gazette* (Oct. 4, 2001), 2001.

Gillies, J.A., V. Etyemezian, H. Kuhns, D. Nikolic, and D.A. Gillette, Effect of vehicle characteristics on unpaved road dust emissions, *Atmospheric Environment*, *39*, 2341 - 2347, 2005.

Glen, W.G., M.P. Zelenka, and R.C. Graham, Relating meteorological variables and trends in motor vehicle emissions to monthly urban carbon monoxide concentrations, *Atmospheric Environment*, *30* (24), 4225 - 4232, 1996.

Gohm, A., G. Zängl, and G.J. Mayr, South Foehn in the Wipp Valley on 24 October 1999 (MAP IOP 10): Verification of High Resolution Numerical Simulations with Observations, *Monthly Weather Review*, *132*, 78 - 102, 2004.

Greenberg, J.P., D. Helmig, and P.R. Zimmerman, Seasonal measurements of nonmethane hydrocarbons and carbon monoxide at the Mauna Loa Observatory during the Mauna Loa Observatory Photochemistry Experiment 2, *J. Geophys. Res.*, *101* (D9), 14,581 - 14598, 1996.

Grell, G.A., J. Dudhia, and D.R. Stauffer, A Description of the Fifth-Generation Penn State/NCAR Mesoscale Model (MM5), NCAR Mesoscale and Meteorological Division, Boulder, 1994.

Grell, G.A., S. Erneis, W.R. Stockwell, T. Scheonemeyer, R. Forkel, J. Michalakes, R. Knoche, and W. Seidl, Application of a multiscale, coupled MM5/chemistry model to the complexs terrain of the VOTALP valley campaign, *Atmos. Environ.*, *34*, 1435 - 1453, 2000.

Grell, G.A., S.E. Peckham, R. Schmitz, S.A. McKeen, G. Frost, W.C. Skamarock, and B. Eder, Fully coupled "online" chemistry within the WRF model, *Atmospheric Environment*, *39*, 6957 - 6975, 2005.

Gros, V., B. Bonsang, and R.S. Esteve, Atmospheric carbon monoxide 'in situ' monitoring by automatic gas chromatography, *Chemosphere: Global Change Science*, *1* (1), 153-161, 1999.

Gros, V., K. Tsigaridis, B. Bonsang, M. Kanakidou, and C. Pio, Factors controlling the diurnal variation of CO above a forested area in southeast Europe, *Atmospheric Environment*, *36*, 3127 - 3135, 2002.

Güsten, H., G. Heinrich, and D. Sprung, Nocturnal depletion of ozone in the upper Rhine valley, *Atmos. Environ.*, *32* (7), 1195-1202, 1998.

Guttikunda, S.K., Y. Tang, G.R. Carmichael, G. Kurata, L. Pan, D.G. Streets, J.-H. Woo, N. Thongboonchoo, and A. Fried, Impacts of Asian megacity emissions on regional air quality during spring 2001, *J. Geophys. Res.*, *110*, D20301, doi:10,1029/2004JD004921, 2005.

Han, X., and L.P. Naeher, A review of traffic-related air pollution exposure assessment studies in the developing world, *Environment International*, *xx*, xxx-xxx (in press), 2005.

Harley, R.A., A.G. Russell, G.J. McRae, G.R. Cass, and J.H. Seinfeld, Photochemical modeling of the southern California air quality study, *Environ. Sci. Technol.*, *27*, 378-388, 1993.

Henne, S., M. Furger, S. Nyeki, M. Steinbacher, B. Neininger, S.F.J. de Wekker, J. Dommen, N. Spichtinger, A. Stohl, and A.S.H. Prévôt, Quantification of topographic venting of boundary layer air to the free troposphere, *Atmos. Chem. Phys.*, *0000*, 0001-12, 2004.

Hindman, E.E., Soaring Weather at the Top of the World, *Technical Soaring*, *XXIII* (2), 52 - 57, 1999.

Hindman, E.E., and B.P. Upadhyay, Air pollution transport in the Himalayas of Nepal and Tibet during the 1995-1996 dry season, *Atmos. Environ.*, *36*, 727 - 739, 2002.

Hodson, E., Elke Hodson's General Exam Paper, pp. 32, MIT, Cambridge, 2003.

Hogrefe, C., S.T. Rao, P. Kasibhatla, W. Hao, G. Sistla, R. Mathur, and J. McHenry, Evaluating the performance of regional-scale photochemical modeling systems: Part II -- ozone predictions, *Atmos. Environ.*, *35*, 4175 - 4188, 2001a.

Hogrefe, C., S.T. Rao, P. Kasibhatla, G. Kallos, C.J. Tremback, W. Hao, D. Olerud, A. Xiu, J. McHenry, and K. Alapaty, Evaluating the performance of regional-scale photochemical modeling systems: Part I -- meteorological predictions, *Atmos. Environ.*, *35*, 4159 - 4174, 2001b.

Holmes, N.S., L. Marawska, K. Mengersen, and E.R. Jayaratne, Spatial distribution of submicrometre particles and CO in an urban microscale environment, *Atmospheric Environment*, *39*, 3977 - 3988, 2005.

Hong, S.-Y., and H.-L. Pan, Nonlocal Boundary Layer Vertical Diffusion in a Medium-Range Forecast Model, *Monthly Weather Review*, *124*, 2322 - 2339, 1996.

Horvath, H., L. Catalan, and A. Trier, A study of the aerosol of Santiago de Chile III: Light absorption measurements, *Atmospheric Environment*, *31* (22), 3737-3744, 1997.

Hünerbein, S.v., and H. Richner, A Doppler Sodar Case Study of Top-Down Convection and Convective Dissipation of Stratus, *J. Atmos. Oceanic Technol.*, *19*, 1170 - 1180, 2002.

Idso, S., C.D. Idso, and R.C. Balling, Jr., Seasonal and diurnal variations of near-surface atmospheric CO_2 concentration within a residential sector of the urban CO_2 dome of Phoenix, AZ, USA, *Atmospheric Environment*, *36*, 1655 - 1660, 2002.

Jacobson, M.Z., Studying the effects of aerosols on vertical photolysis rate coefficint and temperature profiles over an urban airshed, *J. Geophys. Res.*, *103* (D9), 10,593 - 10,604, 1998.

Jazcilevich, A.D., A.R. Garciá, and E. Caetano, Locally induced surface air confluence by complex terrain and its effects on air pollution in the valley of Mexico, *Atmospheric Environment*, *39*, 5481 - 5489, 2005.

Jha, P.K., Transport Sector Technocal Inspection System in Nepal, in *Asia worksop on I&M Policy*, ESCAP Global Initiative on Transport Emissions, Bangkok, 2001.

Jin, M., J.M. Shepherd, and M.D. King, Urban aerosols and their variations with clouds and rainfall: A case study for New York and Houston, *J. Geophys. Res.*, *110*, D10S20, doi:10.1029/2004JD005081, 2005.

Jorquera, H., R. Perez, a. Cipriano, A. Espejo, M.V. Letelier, and G. Acuña, Forecasting ozone daily maximum levels at Santiago, Chile, *Atmos. Environ.*, *32* (20), 3415 - 3424, 1998.

Junquera, V., M.M. Russell, W. Vizuete, Y. Kimura, and D. Allen, Wildfires in eastern Texas in August and September 2000: Emissions, aircraft measurements, and impact on photochemistry, *Atmospheric Environment*, *39*, 4983 - 4996, 2005.

Kain, J.S., The Kain-Fritsch Convective Parameterization: An Update, *Journal of Applied Meteorology*, *43*, 170 - 181, 2004.

Kallistratova, M.A., and R.L. Coulter, Appliation of SODARs in the study and monitoring of the environment, *Meteorol. Atmos. Phys.*, *85*, 21 - 37, 2004.

Kalthoff, N., H.J. Binder, M. Kossmann, R. Voegtlin, U. Corsmeier, F. Fiedler, and H. Schlager, Temporal evolution and spatial variation of the boundary layer over complex terrain, *Atmos. Environ.*, *32* (7), 1179-1194, 1998.

Kalthoff, N., V. Horlacher, U. Corsmeier, A. volz-Thomas, B. Kolahger, H. Geib, M. Mollmann-Coers, and A. Knaps, Influence of valley winds on transport and dispersion of airborne pollutants in the Freiburg-Schauinsland area, *J. Geophys. Res.*, *105*, 1585-1597, 2000.

Kanakidou, M., and P.J. Crutzen, The photochemical source of carbon monoxide: Importance, uncertainties and feedbacks, *Chemosphere: Global Change Science*, *1* (1), 91 - 109, 1999.

Kanda, M., R. Moriwaki, and Y. Kimoto, Temperature Profiles Within And Above An Urban Canopy, *Boundary-Layer Meteorology*, *115*, 499 - 506, 2005.

Kataoka, T., E. Yunoki, M. Shimizu, T. Mori, O. Tsukamoto, Y. Ohashi, K. Sahashi, T. Maitani, K. Miyashita, T. Iwata, Y. Fujikawa, A. Kudo, and R.H. Shaw, A Study of the Atmospheric Boundary-Layer Using radon and Air Pollutants as Tracers, *Boundary-Layer Meteorology*, *101*, 131 - 155, 2001.

Kato, S., Y. Kajii, R. Itokazu, J. Hirokawa, S. Koda, and Y. Kinjo, Transport of atmospheric carbon monoxide, ozone, and hydrocarbons from Chinese coast to Okinawa island in the Western Pacific during winter, *Atmospheric Environment*, *38*, 2975 - 2981, 2004.

Keder, J., M. Strizik, P. Berger, A. Cerny, P. Engst, and I. Nemcova, Remote sensing detection of atmospheric pollutants by differential absorption LIDAR 510M / SODAR PA2 mobile system, *Meorol. Atmos. Phys.*, *85*, 155 - 164, 2004.

Kelly, R.D., Asymmetric Removal of Temperature Inversions in a High Mountain Valley, *Journal of Applied Meteorology*, *27*, 664 - 673, 1988.

Khalil, M.A.K., and R.A. Rasmussen, Global decrease in atmospheric carbon monoxide concentration, *Nature*, *370*, 639 - 641, 1994.

Kimura, F., and T. Kuwagata, Thermally Induced Wind Passing from Plain to Basin over a Mountain Range, *J. Applied. Meteorol.*, *32*, 1538 - 1547, 1993.

King, G.M., Characteristics and significance of atmospheric carbon monoxide consumption by soils, *Chemosphere: Global Change Science, 1* (1), 53-63, 1999.

Kitada, T., K. Igarashi, and M. Owada, Numerical Analysis of Air Pollution in a Combined Field of Land/Sea Breeze and Mountain/Valley Wind, *Journal of Climate and Applied Meteorology*, *25*, 767 - 784, 1986.

Kitada, T., and R.P. Regmi, Dynamics of air pollution transport in late wintertime over Kathmandu Valley, Nepal: as revealed with numerical simulation, *Journal of Applied Meteorology*, *42*, 1770-1798, 2003.

Kleinman, L.I., P.H. Daum, Y.-N. Lee, L.J. Nunnermacker, S.R. Springston, J. Weinstein-Lloyd, P. Hyde, P. Doskey, J. Rudolph, J. Fast, and C. Berkowitz, Photochemical age determination in the Phoenix metropolitan area, *J. Geophys. Res.*, *108* (D3), 4096, doi:10.1029/2002JD002621, 2003.

Klemp, J.B., and D.R. Durran, An Upper Boundary Condition Permitting Internal Gravity Wave Radiation in Numerical Mesoscale Models, *Monthly Weather Review*, *111*, 430 - 444, 1983.

Kondo, J., T. Kuwagata, and S. Haginoya, Heat Budget Analysis of Nocturnal Cooling and Daytime Heating in a Basin, *J. Atmos. Sci., 46* (19), 2917 - 2933, 1989.

Kossmann, M., R. Vögtlin, U. Corsmeier, F. Fiedler, H.J. Binder, N. Kalthoff, and F. Beyrich, Aspects of the convective boundary layer structure over complex terrain, *Atmos. Environ., 32* (7), 1323-1348, 1998.

Kuebler, J., J.-M. Giovannoni, and A.G. Russell, Eulerian modeling of photochemical pollutants over the Swiss Plateau and Control Strategy Analysis, *Atmospheric Environment, 30* (6), 951 - 966, 1996.

Lagzi, I., R. Mészáros, L. Horváth, A. Tomling, T. Weidinger, T. Turányi, F. Ács, and L. Haszpra, Modeling ozone fluxes over Hungary, *Atmospheric Environment, 38*, 6211 - 6222, 2004.

Lal, C.K., The sun will come out tomorrow, in *Nepali Times*, pp. 2, 2002.

Lal, S., Naja, M., Subbaraya, B.H., Seasonal variations in surface ozone and its precursors over an urban site in India, *Atmospheric Environment, 34*, 2713-2724, 2000.

Lang, T.J., and A.P. Barros, An Investigation of the Onsets of the 1999 and 2000 Monsoons in Central Nepal, *Monthly Weather Review, 130*, 1299-1316, 2002.

Larssen, S., F. Gram, I. Haugsbakk, J. Huib, X. Olsthoorn, A.S. Giri, R. Shah, M.L. Shrestha, and B. Shrestha, *Urban Air Quality Management Strategy in Asia: Kathmandu Valley Report*, The World Bank, Washington D. C., 1997.

Law, K.S., Theoretical studies of carbon monoxide distributions, budgets and trends, *Chemosphere: Global Change Science, 1* (1), 19-31, 1999.

Lee, B.-K., N.-Y. Jun, and H.K. Lee, Analysis of impacts on urban air quality by restricting the operation of passenger vehicles during Asian Game events in Busan, Korea, *Atmospheric Environment, 39*, 2323 - 2338, 2005.

Lee, E.H., D.T. Tingey, W.E. Hogsett, and J.A. Laurence, History of tropospheric ozone for the San Bernadino Mountains of Southern California, 1963 - 1999, *Atmospheric Environment, 37*, 2705 - 2717, 2003a.

Lee, S.-M., H.J.S. Fernando, M. Princevac, D. Zajic, M. Sinesi, J.L. McCulley, and J. Anderson, Transport and Diffusion of Ozone in the Nocturnal and Morning Planetary Boundary Layer of the Phoenix Valley, *Environmental Fluid Mechanics, 3*, 331 - 362, 2003b.

Lena, F., and F. Desiato, Intercomparison of nocturnal mixing height estimate methods for urban air pollution modelling, *atmos. Environ., 33*, 2385-2393, 1999.

Li, J.-G., and B.W. Atkinson, Transition Regmies in Valley Airflows, *Boundary-Layer Meteorology, 91*, 385 - 411, 1999.

Lobert, J.M., and J.M. Harris, Trace gases and air mass origin at Kaashidhoo, Indian Ocean, *J. Geophys. Res., 107* (D19), 8013, doi:10.1029/2001JD000731, 2002.

Lu, R., and R.P. Turco, Ozone distributions over the Los Angeles basin: three-dimensional simulations with the smog model, *Atmos. Environ., 30* (24), 4155-4176, 1996.

Mahrt, L., and D. Vickers, Contrasting Vertical Structures of Nocturnal Boundary Layers, *Boundary-Layer Meteorology, 105*, 351 - 363, 2002.

Mahrt, L., D. Vickers, R. Nakamura, M.R. Soler, J. Sun, S. Burns, and D.H. Lenschow, Shallow Drainage Flows, *Boundary-Layer Meteorology, 101*, 243 - 260, 2001.

Malla, S., Urban Energy Use and Environmental Management: The Case of Kathmandu Valley, Master of Engineering thesis, Asian Institute of Technology, Bangkok, 1993.

Marsik, F.J., K.W. Fischer, T.D. McDonald, and P.J. Samson, Comparison of Methods for Estimating Mixing Height Used during the 1992 Atlanta Field Intensive, *Journal of Applied Meteorology*, *34*, 1802 - 1814, 1995.

Martano, P., D. Cava, G. Mastrantonio, S. Argentini, and A. Viola, Sodar Detected Top-Down Convection In a Nocturnal Cloud-Topped Boundary Layer: A Case Study, *Boundary-Layer Meteorology*, *115*, 85 - 103, 2005.

Martilli, A., and G. Graziani, Mesoscale circulation across the Alps: preliminary simulation of TRANSALP 1990 Observations, *Atmos. Environ.*, *32* (7), 1241 - 1255, 1998.

Martin, B.D., H.E. Fuelberg, N.J. Blake, J.H. Crawford, J.A. Logan, D.R. Blake, and G.W. Sachse, Long-range transport of Asian outflow to the equatorial Pacific, *J. Geophys. Res.*, *108* (D2), 8322, doi:10.1029/2001JD001418, 2003.

Matsuda, K., I. Watanabe, V. Wingpud, P. Theramongkol, P. Khummongkol, S. Wangwongwatana, and T. Totsuka, ozone dry deposition over a tropical forest in the dry season in northern Thailand, *Atmospheric Environment*, *39*, 2571 - 2577, 2005.

Mauzerall, D.L., D. Narita, H. Akimoto, L. Horowitz, S. Walters, D.A. Hauglustaine, and G. Brasseur, Seasonal characteristics of tropospheric ozone production and mixing ratios over East Asia: A global three-dimensional chemical transport model analysis, *J. Geophys. Res.*, *105* (D14), 17,895 - 17,910, 2000.

Mayr, G.J., J. Vergeiner, and A. Gohm, An Automobile Platform for the Measurement of Foehn and Gap Flows, *J. Atmos. Oceanic Technol.*, *19*, 1545 - 1556, 2002.

McCormick, R.A., Variation of Carbon Monoxide Concentrations as Related to Sampling Interval, Traffic, and Meteorological Factors, *Journal of Applied Meteorology*, *1*, 237 - 243, 1962.

McRae, G.J., W.R. Goodin, and J.H. Seinfeld, Development of a second-generation mathematical model for urban air pollution -- I. Model Formulation, *Atmospheric Environment*, *16* (4), 679-696, 1982.

Mestayer, P.G., P. Durand, P. Augustin, S. Bastin, J.-M. Bonnefond, B. Bénech, P. Drobinski, A. Druilhet, E. Fréjafon, C.S.B. Grimmond, D. Groleau, M. Irvine, C. Kergomard, S. Kermadi, J.-P. Lagouarde, A. Lomonsu, F. Lohou, N. Long, V. Masson, C. Moppert, J. Noilhan, B. Offerle, T.R. Oke, G. Pigeon, V. Puygrenier, S. Roberts, J.-M. Rosant, S. F., J. Salmond, M. Talbout, and J. Voogt, The Urban Boundary-Layer Field Campaign in Marseille (UBL/CLU-ESCOMPTE): Set-up and First Results, *Boundary-Layer Meteorology*, *114*, 315 - 365, 1005.

Mészáros, T., L. Haszpra, and A. Gelencsér, Tracking changes in carbon monoxide budget over Europe between 1995 and 2000, *Atmospheric Environment*, *39*, 7297 - 7306, 2005.

Milford, J.B., A.G. Russell, and G.J. McRae, A New Approach to Photochemical Pollution-Control - Implications of Spatial Patterns in Pollutant Responses to Reductions in Nitrogen-Oxides and Reactive Organic Gas Emissions, *Environmental Science & Technology*, *23* (10), 1290-1301, 1989.

Molina, L.T., and M.J. Molina, *Air Quality in the Mexico Megacity: An Integrated Assessment*, Kluwer Academic Publishers, Dordrecht, Netherlands, 2002.

Möllman-Coers, M., D. Klemp, K. Mannschreck, and F. Slemr, Statistical study of diurnal variation of modeled and measured NMHC contributions, *Atmospheric Environment, 36 Supplement No. 1*, S109 - S122, 2002.

Monti, P., H.J.S. Fernando, M. Princevac, W.C. Chan, T.A. Kowalewski, and E.R. Pardyjak, Observations of Flow and Turbulence in the Nocturnal Boundary Layer over a Slope, *Journal of Atmospheric Sciences, 59* (17), 2513 - 2534, 2002.

Moore, G.E., S.G. Douglas, R.C. Kessler, and J.P. Killus, Identification and Tracking of Polluted Air Masses in the South-Central Coast Air Basin, *Journal of Applied Meteorology, 30*, 715 - 732, 1991.

Moore, G.W.K., Mount Everest snow plume: A case study, *Geophysical Research Letters, 31*, l22102, doi:10.1029/2004GL021046, 2004.

Morawska, L., E.R. Jayaratne, K. Mengersen, M. Jamriska, and S. Thomas, Differences in airborne particle and gaseous concentrations in urban air between weekdays and weekends, *Atmospheric Environment, 36*, 4375 - 4383, 2002.

Morel, B., S. Yeh, and L. Cifuentes, Statistical distribution for air pollution applied to the study of the particulate problem in Santiago, *Atmos. Environ.*, *33*, 2575 - 2585, 1999.

Moxley, J.M., and K.A. Smith, Factors Affecting Utilisation of Atmospheric Co by Soils, *Soil. Biol. Biochem.*, *30* (1), 65 - 79, 1998.

Mühle, J., A. Zahn, C.A.M. Brenninkmeijer, V. Gros, and P.J. Crutzen, Air mass classification during the INDOEX R/V *Ronald Brown* cruise using measurements of nonmethane hydrocarbon,s CH_4, CO_2, CO, ^{14}CO, and $\delta^{18}O(CO)$, *J. Geophys. Res.*, *107* (D19), 8021, doi:10.1029/2001JD000730, 2002.

Mulholland, M., and J.H. Seinfeld, Inverse air pollution modelling of urban-scale carbon monoxide emissions, *Atmospheric Environment, 29* (4), 497-516, 1995.

Narita, D., P. Pochanart, J. Matsumoto, K. Someno, H. Tanimoto, J. Hirokawa, Y. Kajii, H. Akimoto, M. Nakao, T. Katsuno, and Y. Kinjo, Seasonal variation of carbon monoxide at remote sites in Japan, *Chemosphere: Global Change Science, 1* (1), 137-144, 1999.

NESS, Ambient air quality monitoring of Kathmandu Valley, Nepal Environmental and Scientific Services

Ministry of Population and Environment, HMG Nepal, Kathmandu, 1999.

Novelli, P.C., CO in the atmosphere: measurement techniques and related issues, *Chemosphere: Global Change Science, 1* (1), 115 - 126, 1999.

Novelli, P.C., V.S. Connors, H.G. Reichle, B.E. anderson, C.A.M. Brenninkmeijer, E.G. Brunke, B.G. Doddridge, V.W.J.H. Kirchhoff, K.S. Lam, K.A. Masarie, T. Matsuo, D.D. Parrish, H.E. Scheel, and L.P. Steele, An internally consistent set of globally distributed atmospheric carbon monoxide mixing ratios developed using results from an intercomparison of measurements, *J. Geophys. Res.*, *103* (D15), 19,285 - 19,293, 1998.

Novelli, P.C., K.A. Masarie, P.P. Tans, and P.M. Lang, Recent changes in atmospheric carbon monoxide, *Science, 263*, 1587 - 1590, 1994.

Novelli, P.C., L.P. Steele, and P.P. Tans, Mixing ratios of carbon monoxide in the troposphere, *J. Geophys. Res.*, *97* (D18), 20731 - 20750, 1992.

Orgill, M.M., J.D. Kincheloe, and R.A. Sutherland, Mesoscale Influences on Nocturnal Valley Drainage Winds in Western Colorado Valley, *Journal of Applied Meteorology*, *31*, 121 - 141, 1992.

Pachart, E., J. Lenoble, C. Brogniez, D. Masserot, and J.L. Bocquet, Ultraviolet spectral irradiance in the French Alps: Results of two campaigns, *J. Geophys. Res.*, *104* (D14), 16777-16784, 1999.

Paino, J.H., 1993 Carbon Monoxide Saturation Study in Boston, pp. 36, Air Quality Surveillance Branch, Environmental Protection Agency, Boston, 1993.

Parrish, D.D., and F.C. Fehsenfeld, Methods for gas-phase measurements of ozone, ozone precursors and aerosol precursors, *Atmos. Environ.*, *34*, 2000.

Parrish, D.D., J.S. Holloway, and F.C. Fehsenfeld, Routine, Continuous Measurement of Carbon Monoxide with Parts per Billion Precision, *Environ. Sci. Technol.*, *28*, 1615 - 1618, 1994.

Parrish, D.D., M. Trainer, M.P. Buhr, B.A. Watkins, and F.C. Fehsenfeld, Carbon monoxide concentrations and their relation to concentrations of total reactive oxidized nitrogen at two rural U.S. sites, *J. Geophys. Res.*, *96* (D5), 9309 - 9320, 1991.

Perez, P., and A. Trier, Prediction of NO and NO2 concentrations near a street with heavy traffic in Santiago, Chile, *Atmos. Environ.*, *35*, 1783 - 1789, 2001.

Pielke, R.A., W.R. Cotton, R.L. Walko, C.J. Trembach, M.E. Nicholls, M.D. Moran, D.A. Wesley, T.J. Lee, and J.H. Copeland, A comprehensive meteorological modeling system - RAMS, *Meteorol. Atmos. Phys.*, *49*, 69 - 91., 1992.

Pochanart, P., H. Akimoto, Y. Kajii, and P. Sukasem, Carbon monoxide, regional-scale transport, and biomass burning in tropical continental Southeast Asia: Observations in rural Thailand, *Journal of Geophysical Research*, *108* (D17), 4552, doi:10.1029/2002JD003360, 2003.

Pochanart, P., J. Kreasuwun, P. Sukasem, W. Geeratithadaniyom, M.S. Tabucanon, J. Hirokawa, Y. Kajii, and H. Akomoto, Tropical tropospheric ozone observed in Thailand, *Atmospheric Environment*, *35*, 2657-2668, 2001.

Prévôt, A.S.H., Photooxidantien und Primärluftschadstoffe in der planetaren grenzschicht in der Schweiz nördlich und südlich der Alpen, ETH, Zürich, 1994.

Prévôt, A.S.H., J. Dommen, and M. Bäumle, Influence of road traffic on volatile organic compound concentrations in and above a deep Alpine valley, *Atmospheric Environment*, *34*, 4719 - 4726, 2000a.

Prévôt, A.S.H., J. Dommen, M. Bäumle, and M. Furger, Diurnal variation of volatile organic compounds and local circulation systems in an Alpine valley, *Atmos. Environ.*, *34*, 1413 - 1423, 2000b.

Prévôt, A.S.H., J. Staehelin, G.L. Kok, R.D. Schillawski, B. Neininger, T. Staffelbach, A. Neftel, H. Wernli, and J. Dommen, The Milan photooxidant plume, *J. Geophys. Res.*, *102* (D19), 23,375 - 23,388, 1997.

Qin, Y., G.S. Tonnesen, and Z. Wanng, Weekend/weekday differences of ozone, NO_x, CO, VOCs, PM_{10} and light scatter during ozone season in southern California, *Atmospheric Environment*, *38*, 3069 - 3087, 2004.

Raga, G.B., D. Baumgartner, T. Castro, A. Martínez-Arroyo, and R. Navarro-González, Mexico City air quality: a qualitative review of gas and aerosol measurements (1960-2000), *Atmos. Environ.*, *2001*, 4041 - 4058, 2001.

Rakovec, J., J. Merse, S. Jernej, and B. Paradiz, Turbulent dissipation of the cold-air pool in a basin: comparison of observed and simulated development, *Meteorol. Atmos. Phys.*, *79*, 195 - 213, 2002.

Ramana, M.V., V. Ramanathan, and I.A. Podgorny, The Direct Observations of Large Aerosol Radiative Forcing, *Geophysical Research Letters*, *31* (doi:10.1029/2003GL018824), L0511, 2004.

Ramanathan, V., and M.V. Ramana, Atmospheric Brown Clouds: Long-Range Transport and Climate Impacts, *EM* (December 2003), 28 - 33, 2003.

Rao, P.L.S., Circulation characteristics over the Himalayas durinng winter season, *Meorol. Atmos. Phys.*, *83*, 19 - 33, 2003.

Rappenglück, B., P. Oyola, I. Oleata, and P. Fabian, The evolution of photochemical smog in the metropolitan area of Santiago de Chile, *J. Applied Meteorology*, *39*, 275-290, 2000.

Rappenglück, B., R. Schmitz, M. Bauerfeind, F. Cereceda-Balic, D. von Baer, H. Jorquera, Y. Silva, and P. Oyola, An urban photochemistry study in Santiago de Chile, *Atmospheric Environment*, *39*, 2913 - 2931, 2005.

Raub, J.A., Health effects of exposure to ambient carbon monoxide, *Chemosphere: Global Change Science*, *1* (1), 331 - 351, 1999.

Regmi, R.P., and T. Kitada, Human-Air pollution exposure map of the Kathmandu Valley, Nepal: Assessment based on chemical transport simulation, *Journal of Global Environmental Engineering*, *9*, 2003.

Regmi, R.P., T. Kitada, and G. Kurata, Numerical Simulation of Late Wintertime Local Flows in Kathmandu Valley, Nepal: Implication for Air Pollution Transport, *Journal of Applied Meteorology*, *42*, 389 - 403, 2003.

Reid, S., Hilltop Wind Profiles Using Sodar, *Boundary-Layer Meteorology*, *108*, 305 - 314, 2003.

Remtech, Operation and Maintenance Manual for the PA0, PA1, PA2, PA5, and RASS, Remtech S. A., Velizy Cedex, France, 2003.

Reuten, C., D.G. Steyn, K.B. Strawbridge, and P. Bovis, Observations of the Relation Between Upslope Flows and The Convective Boundary Layer in Steep Terrain, *Boundary-Layer Meteorology*, *116*, 37 - 61, 2005.

Riccio, A., G. Barone, E. Chianese, and G. Giunta, A hierarchical Bayesian approach to the spatio-temporal modeling of air quality data, *Atmospheric Environment*, *40*, 554 - 566, 2006.

Röckmann, T., C.A.M. Brenninkmeijer, M. Hahn, and N.F. Elansky, CO mixing and isotope ratios across Russia; trans-Siberian railroad experiment TROICA 3, April 1997, *Chemosphere: Global Change Science*, *1* (1), 219 - 231, 1999.

Romero, H., M. Ihl, A. Rivera, P. Zalazar, and P. Azocar, Rapid urban growth, land-use changes and air pollution in Santiago, Chile, *Atmos. Environ.*, *33*, 4039 - 4047, 1999.

Röösli, M., G. Theis, N. Künzli, J. Staehelin, P. Mathys, L. Oglesby, M. Camenzind, and C. Braun-Fahrländer, Temporal and spatial variation of the chemical composition of PM10 at urban and rural sites in the Basel area, Switzerland, *Atmos. Environ.*, *35*, 3701 - 3713, 2001.

Rosoff, Y., Himalayan Thunder, in *Weatherwise*, 2003.

Rotach, M.W., S.-E. Gryning, E. Batchvarova, A. Christen, and R. Vogt, Pollutant dispersion close to an urban surface -- the BUBBLE tracer experiment, *Meteorol. Atmos. Phys.*, *87*, 39 - 56, 2004.

Rubino, F.M., L. Floridia, M. Tavazzani, S. Fustinoni, R. Giampiccolo, and A. Colombi, Height profile of some air quality markers in the urban atmosphere surrounding a 100 m tower building, *Atmospheric Environment*, *32* (20), 3569 - 3580, 1998.

Russel, M., and D.T. Allen, Predicting secondary organic aerosol formation rates in southeast Texas, *J. Geophys. Res.*, *110* (D07S17), doi:10.1029/2004D004722, 2005.

Russell, A., and R. Dennis, NARSTO critical review of photochemical models and modeling, *Atmospheric Environment*, *34*, 2283-2324, 2000.

Sachse, G.W., G.F. Hill, L.O. Wade, and M.G. Perry, Fast-response, high-precision carbon monoxide sensor using a tunable diode laser absorption technique`, *J. Geophys. Res.*, *92* (D2), 2071 - 2081, 1987.

Sahashi, K., T. Hieda, and E. Yamashita, Nitrogen-oxide layer over the urban heat island in Okayama City, *Atmos. Environ.*, *30* (3), 531-535, 1996.

Saitoh, T.S., T. Shimada, and H. Hoshi, Modeling and simulation of the Tokyo urban heat island, *Atmos. Environ.*, *30*, 3431 - 3442, 1996.

Santanello, J.A., M.A. Friedl, and K.W. P., Am Empirical Ivestigation of Convective Planetary Boundary Layer Evolution and Its Relationship with the Land Surface, *Journal of Applied Meteorology*, *44*, 917 - 932, 2005.

Sapkota, B., and R. Dhaubadel, Atmospheric turbidity over Kathmandu valley, *Atmospheric Environment*, *36*, 1249-1257, 2002.

Scheel, H.E., E.-G. Brunke, R. Sladkovic, and W. Seiler, In situ CO concentrations at the sites (Zugspitze (47ºN, 11ºE) and Cape Point (34ºS, 19ºE) in April and October 1994, *Journal of Geophysical Research*, *103* (D15), 19,295 - 19,304, 1998.

Schmitz, R., Modelling of air pollution dispersion in Santiago de Chile, *Atmospheric Environment*, *39*, 2035 - 2047, 2005.

Scorer, R.S., *Air Pollution Meteorology*, Horwood Publishing, Chichester, UK, 2002.

Seibert, P., F. Beyrich, S.-E. Gryning, S. Joffre, A. Rasmussen, and P. Tercier, Review and intercomparison of operational methods for the determination of the mixing height, *Atmos. Environ.*, *34*, 1001-1027, 2000.

Seibert, P., H. Kromp-Kolb, A. Kasper, M. Kalina, H. Puxbaum, D.T. Jost, M. Schwikowski, and U. Baltensperger, Transport of polluted boundary layer air from the Po Valley to High Alpine Sites, *Atmos. Environ.*, *34* (23), 3953 - 3965, 1998.

Seiler, W., and J. Fishman, The distribution of carbon monoxide and ozone in the free troposphere, *J. Geophys. Res.*, *86* (C8), 7255 - 7265, 1981.

Seiler, W., and C. Junge, Carbon Monoxide in the Atmosphere, *J. Geophys. Res.*, *75* (12), 2217 - 2226, 1970.

Sharma, C.K., Short Communication: Urban air quality of Kahtmandu Valley, Kingdom of Nepal, *Atmospheric Environment*, *31* (17), 2877-2883, 1997.

Sharma, M., and S. Maloo, Assessment of ambient air PM_{10} and $PM_{2.5}$ and characterization of PM_{10} in the city of Kanpur, India, *Atmospheric Environment*, *39*, 6015 - 6026, 2005.

Sharma, U.K., Kajii, Y., Akimoto, H., Characterization of NMHCs in downtown urban center Kathmandu and rural site Nagarkot in Nepal, *Atmospheric Environment*, *34*, 3297-3307, 2000.

Shaw, W.J., J.C. Doran, and R.L. Coulter, Boundary-layer evolution over Phoenix, Arizona and the premature mixing of pollutants in the early morning, *Atmospheric Environment*, *39*, 773 - 786, 2005.

Shrestha, A.B., C.P. Wake, and J.E. Dibb, Chemical composition of aerosol and snow in the high Himalaya during the summer monsoon season, *Atmospheric Environment*, *31* (17), 2815-2826, 1997.

Shrestha, A.B., C.P. Wake, J.E. Dibb, P.A. Payewski, S.I. Whitlow, G.R. Carmichael, and M. Ferm, Seasonal variations in aerosol concentrations and compositions in the Nepal Himalaya, *Atmos. Environ.*, *34*, 3349 - 3363, 2000.

Shrestha, A.B., C.P. Wake, P.A. Mayewski, and J.E. Dibb, Maximum Temperature Trends in the Himalaya and Its Vicinity: An Analysis Based on Temperature Records from Nepal for the Period 1971-94, *J. Climate*, *12*, 2775 - 2786, 1999.

Shrestha, R.M., and S. Malla, Air pollution from energy use in a developing country city: the case of the Kathmandu Valley, Nepal, *Energy*, *21* (9), 785-794, 1996.

Sillman, S., D. He, C. Cardelinos, and R.E. Imhoff, The use of photochemical indicators to evaluate ozone-NOx-hydrocarbon sensitivity: case studies from Atlanta, New York, and Los Angeles, *J. Air & Waste Manage. Assoc.*, *47*, 1030-1040, 1997.

Silva, C., and A. Quiroz, Optimization of the atmospheric pollution monitoring network at Santiago de Chile, *Atmospheric Environment*, *37*, 2337 - 2345, 2003.

Simmonds, P.G., S. Seuring, G. Nickless, and R.G. Derwent, Segretation and Interpretation of Ozone and Carbon Monoxide Measurements by Air Mass Origin at the TOR Station Mace Head, Ireland from 1987 to 1995, *J. Atmos. Chem.*, *28*, 45-59, 1997.

Singh, M.P., R.T. McNider, R. Meyers, and G. Shekhar, Nocturnal wind structure over land and dispersion of pollutations : an analytical study, *Atmos. Environ.*, *31* (1), 105-115, 1997.

Sorimachi, A., K. Sakamoto, H. Ishihara, T. Fukuyama, M. Utiyama, H. Liu, W. Wang, D. Tang, X. Dong, and H. Quan, Measurements of sulfur dioxide and ozone dry deposition over short vegetation in northern China -- a preliminary study, *Atmospheric Environment*, *37*, 3157 - 3166, 2003.

Staehelin, J., R. Locher, S. Mönkeberg, and W.A. Stahel, Contribution of road traffic emissions to ambient air concentrations of hydrocarbons: the interpretation of mnitoring measurements in Switzerland by Principal Component Analysis and road tunnel measurements, *It. J. Vehicle Design*, *X* (X), 1-12, 2001.

Staffelbach, T., A. Neftel, A. Blatter, A. Gut, M. Fahrni, J. Stähelin, A. Prévôt, A. Hering, M. Lehning, B. Neiniger, M. Bäumle, G.L. Kok, J. Dommen, M. Hutterli, and M. Anklin, Photochemical oxidant formation over southern Swtizerland: 1. Results from summer 1994., *J. Geophys. Res.*, *102* (D19), 23,345 - 23,362, 1997.

Stehr, J.W., W.P. Ball, B.G. Doddridge, C.A. Piety, and J.E. Johnson, Latitudinal gradients in O_3 and CO during INDOEX 1999, *J. Geophys. Res.*, *107* (D19), 8015, doi:10.1029/2001JD000446, 2002.

Stohl, A., S. Eckhardt, C. Forster, P. James, and N. Spichtinger, On the pathways and timescales of intercontinental air pollution transport, *J. Geophys. Res.*, *107* (D23), 4684, doi:10.1029/2001JD001396, 2002.

Straka, J.M., E.N. Rasmussen, and S.E. Fredrickson, A mobile mesonet for finescale meteorological observations, *J. Atmos. Oceanic Technol.*, *13*, 921 - 936., 1996.

Stull, R.B., *An Introduction to Boundary Layer Meteorology*, Kluwer Academic Publishers, Dordrecht, 1988.

Teledyne_API, Instruction Manual: Model 300E Carbon Monoxide Analyzer, pp. 151 - 156, Teledyne Instruments, San Diego, 2003.

Tong, H., A. Walton, J. Sang, and J.C.L. Chan, Numerical simulation of the urban boundary layer over the complex terrain of Hong Kong, *Atmospheric Environment*, *39*, 3549 - 3563, 2005.

Tyler, S.C., G.A. Klouda, G.W. Brailsford, A.C. Manning, J.M. Conny, and A.J.T. Jull, Seasonal snapshots of the isotopic (^{14}C, ^{13}C) composition of tropospheric carbon monoxide at Niwot Ridge, Colorado, *Chemosphere: Global Change Science*, *1* (1), 185-203, 1999.

Ulrickson, B.L., Numerical Investigation of Mesoscale Circulations over the Los Angeles Basin. Part II: Synoptic Influences and Pollutant Transport, *Monthly Weather Review*, *118*, 2162 - 2184, 1990.

Ulrickson, B.L., and C.F. Mass, Numerical Investigation of Mesoscale Circulation over the Los Angeles Basin. Part I: A Verification Study, *Monthly Weather Review*, *118*, 2138 - 2161, 1990.

Venkatesan, R., V. Sitaraman, and M. Manju, Estimation of the atmospheric surface layer parameters and comparison with sodar observations, *Atmospheric Environment*, *29* (22), 3325 - 3331, 1995.

Villasenor, R., López-Villegas, S. Eidels-Dubovoi, A. Quintanar, and J.C. Gallardo, A mesoscale modeling study of wind blown dust on the Mexico City Basin, *Atmospheric Environment*, *37*, 2451 - 2462, 2003.

Waibel, A.E., H. Fischer, F.G. Wienhod, P.C. Siegmung, B. Lee, J. Ström, J. Lelieveld, and P.J. Crutzen, Highly elevated carbon monoxide concentrations in the upper troposphere and lowermost stratosphere at northern midlatitudes during the STREAM II summer campaign in 1994, *Chemosphere: Global Change Science*, *1* (1), 233-248, 1999.

Wake, C.P., J.E. Dibb, P.A. Mayewski, L. Zhongqin, and X. Zichu, The chemical composition of aerosols over the eastern Himalayas and Tibetan Plateau during low dust periods, *Atmospheric Environment*, *28* (4), 695-704, 1994.

Wang, C., and R.G. Prinn, Impact of the horizontal wind profile on the convective transport of chemical species, *Journal of Geophysical Research*, *103* (D17), 22063-2071, 1998.

Wang, T., T.F. Cheung, K.S. Lam, G.L. Kok, and J.M. Harris, The characteristics of ozone and related compounds in the boundary layer of the South China coast: temporal and vertical variations during autumn season, *Atmospheric Environment*, *35*, 2735 - 2746, 2001.

Wang, T., and J.Y.H. Kwok, Measurement and Analysis of a Multiday Photochemical Smog Episode in the Pearl River Delta of China, *Journal of Applied Meteorology*, *42*, 404 - 416, 2003.

Wang, T., C.N. Poon, Y.H. Kwok, and Y.S. Li, Characterizing the temporal variability and emission patterns of pollution plumes in the Pearl River Delta of China, *Atmospheric Environment, 37*, 3539 - 3550, 2003.

Warneck, P., *Chemistry of Natural Atmospheres*, 927 pp., Academic Press, San Diego, 2000.

Whiteman, C.D., Breakup of Temperature Inversions in Deep Mountain Valleys: Part I. Observations, *Journal of Applied Meteorology, 21*, 270 - 289, 1982.

Whiteman, C.D., Chapter 2. Observations of Thermally Developed Wind Systems in Mountainous Terrain, in *Atmospheric Processes in Complex Terrain*, edited by W. Blumen, pp. 5-42, American Meteorologial Society, Boston, 1990.

Whiteman, C.D., *Mountain Meteorology: Fundamentals and Applications*, Oxford University Press, New York, 2000.

Whiteman, C.D., X. Bian, and S. Zhong, Wintertime Evolution of the Temperature Inversion in the Colorado Plateau Basin, *Journal of Applied Meteorology, 38*, 1103 - 1117, 1999.

Whiteman, C.D., and J.C. Doran, The Relationship between Overlying Synoptic-Scale Flows and Winds within a Valley, *J. Applied Meteorol., 32*, 1669 - 1682, 1993.

Whiteman, C.D., S. Eisenbach, B. Pospichal, and R. Steinacker, Comparison of vertical soundings and sidewall air temperature measurements in a small Alpine basin, *Journal of Applied Meteorology, [*[submitted], 2004a.

Whiteman, C.D., J.M. Hubbe, and W.J. Shaw, Evaluation of an Inexpensive Temperature Datalogger for Meteorological Applications, *Journal of Atmospheric and Oceanic Technology, 17*, 77 - 81, 2000a.

Whiteman, C.D., B. Pospichal, S. Eisenbach, P. Weihs, C.B. Clements, R. Steinacker, E. Mursch-Radlgruber, and M. Dorninger, Inversion Breakup in Small Rocky Mountain and Alpine Basins, *Journal of Applied Meteorology, 43*, 1069 - 1082, 2004b.

Whiteman, C.D., S. Zhong, X. Bian, J.D. Fast, and J.C. Doran, Boundary layer evolution and regional-scale diurnal circulations over the Mexico Basin and Mexican plateau, *J. Geophys. Res., 105*, 10,081-10,102, 2000b.

Whiteman, C.D., S. Zhong, W.J. Shaw, J.M. Hubbe, and X. Bian, Cold Pools in the Columbia Basin, *Weather and Forecasting, 16*, 432 - 447, 2001.

Wilson, J.G., S. Kingham, J. Pearce, and A.P. Sturman, A review of intraurban variations in particulate air pollution: Implicationsfor epidemiological studies, *Atmospheric Environment, 39*, 6444-6462, 2005.

Yang, K.-L., C.-C. Ting, J.-L. Wang, O.W. Wingenter, and C.-C. Chan, Diurnal and seasonal cycles of ozone precursors observed from continuous measurement at an urban site in Taiwan, *Atmospheric Environment, 39*, 2829 - 2838, 2005.

Young, G.S., B.K. Cameron, and E.E. Hebble, Observations of the Entrainment Zone in a Rapidly Etraining Boundary Layer, *J. Atmos. Sci., 57*, 3145 - 3160, 2000.

Zaengl, G., A reexamination of the valley wind system in the Alpine Inn Valley with numerical simulation, *Meteorol. Atmos. Phys., 87*, 241 - 256, 2004.

Zahn, A., C.A.M. Brenninkmeijer, W.A.H. Asman, P.J. Crutzen, G. Heinrich, H. Fischer, J.W.M. Cuijpers, and P.F.J. van Velthoven, Budgets of O_3 and CO in the upper troposphere: CARIBIC passenger aircraft results 1997-2001, *J. Geophys. Res., 2002* (D17), 4337, doi:10.1029/2001JD001529, 2002.

Zamora, R.J., S. Solomon, E.G. Dutton, J.W. Bao, M. Trainer, R.W. Portmann, A.B. White, D.W. Nelson, and R.T. McRider, Comparing MM5 radiative fluxes with observations gathered during the 1995 and 1999 Nashville southern oxidants studies, *J. Geophys. Res.*, *108* (D2), 4050, doi:10.1029/2002JD002122, 2003.

Zängl, G., J. Egger, and V. Wirth, Diurnal Winds in the Himalayan Kali Gandaki Valley. Part II: Modeling, *Monthly Weather Review, 129*, 1062 - 1080, 2001.

Zhang, B.-N., and N.T.K. Oanh, Photochemical smog pollution in the Bangkok Metropolitan Region of Thailand in relation to O_3 precursor concentrations and meteorological conditions, *Atmospheric Environment*, *36*, 4211 - 4222, 2002.

Zhang, L., J.R. Brook, and R. Vet, On ozone dry deposition - with emphasis on non-stomatal uptake and wet canopies, *Atmospheric Environment*, *36*, 4787 - 4799, 2002.

Zhang, R., M. Wang, and L. Ren, Long-term trends of carbon monoxide inferred using a two-dimensional model, *Chemosphere: Global Change Science*, *3*, 123-132, 2001.

Zhang, Y., D.H. Stedman, G.A. Bishop, P.L. Guenther, and S. Beaton, Worldwide on-road vehicle exhaust emissions study by remote sensing, *Environ. Sci. Technol.*, *29*, 2286 - 2294, 1995.

Zhong, S., C.D. Whiteman, X. Bian, W.J. Shaw, and J.M. Hubbe, Meteorological Processes Affecting the Evolution of a Wintertime Cold Air Pool in the Columbia Basin, *Monthly Weather Review, 129*, 2600-2613, 2001.